IJOCTA
An International Journal of Optimization and Control: Theories & Applications
2010

ISSN:2146-0957
eISSN:2146-5703

Volume:7 Number:1
January 2017

An International Journal of Optimization and Control:

Theories & Applications

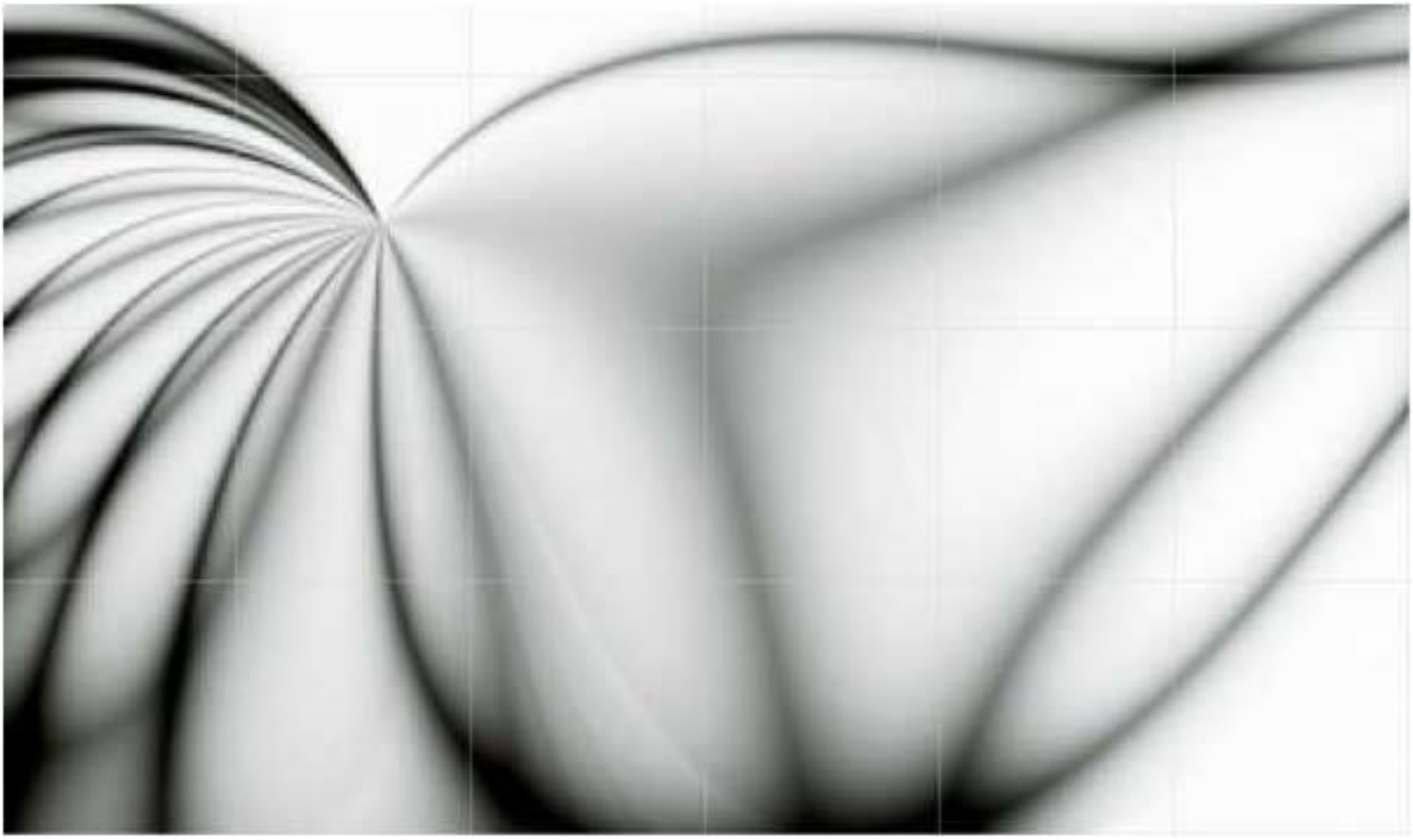

www.ijocta.com

IJOCTA
An International Journal of Optimization and Control: Theories & Applications
2010

www.ijocta.com
info@ijocta.com

An International Journal of Optimization and Control: Theories & Applications

Volume: 7, Number: 1

January 2017

Publisher & Owner *(Yayımcı & Sahibi)*:

Prof. Dr. Ramazan YAMAN
Balikesir University, Faculty of Engineering, Department of Industrial Engineering, Cagis Campus, 10145, Balikesir, Turkey
Balıkesir Üniversitesi, Mühendislik Fakültesi, Endüstri Mühendisliği Bölümü, Çağış Kampüsü, 10145, Balıkesir, Türkiye

ISSN: 2146-0957
eISSN: 2146-5703

Press *(Basımevi)*:

Bizim Dijital Matbaa (SAGE Publishing), Kazım Karabekir Street, Kültür Market, No:7 / 101-102, İskitler, Ankara, Turkey
Bizim Dijital Matbaa (SAGE Yayıncılık), Kazım Karabekir Caddesi, Kültür Çarşısı, No:7 / 101-102, İskitler, Ankara, Türkiye

Date Printed *(Basım Tarihi)*:

March 2017
Mart 2017

Responsible Director (Sorumlu Müdür):

Prof. Dr. Ramazan YAMAN

IJOCTA is an international, bi-annual, and peer-reviewed journal indexed/ abstracted by Cabell's Directories, DOAJ, EBSCO Databases, JournalSeek, Google Scholar, Index Copernicus, International Abstracts in Operations Research, JournalTOCs, Mathematical Reviews (MathSciNet), ProQuest, Ulrich's Periodical Directory, and Zentralblatt Math.

crossref

We Use Plagiarism Detection iThenticate Learn More »

iThenticate and ijocta.balikesir.edu.tr are granted by Balikesir University.

An International Journal of Optimization and Control:

Theories & Applications

Volume: 7 Number: 1
January 2017

CONTENTS

An International Journal of Optimization and Control: Theories & Applications
ISSN: 2146-0957 eISSN: 2146-5703
Vol.7, No.1, pp.1-15 (2017)
https://doi.org/10.11121/ijocta.01.2017.00300

RESEARCH ARTICLE

A stochastic location and allocation model for critical items to response large-scale emergencies: A case of Turkey

Erkan Celik [a], Nezir Aydin [b*], Alev Taskin Gumus [b]

[a] *Department of Industrial Engineering, Munzur University, Turkey*
[b] *Department of Industrial Engineering, Yildiz Technical University, Turkey*
erkancelik@munzur.edu.tr, nzraydin@yildiz.edu.tr, ataskin@yildiz.edu.tr

ARTICLE INFO

Article history:
Received: 31 January 2016
Accepted: 22 July 2016
Available Online: 11 October 2016

Keywords:
Emergency response
facility location
large scale emergencies
two stage stochastic programming

AMS Classification 2010:
91B70, 90B06

ABSTRACT

This paper aims to decide on the number of facilities and their locations, procurement for pre and post-disaster, and allocation to mitigate the effects of large-scale emergencies. A two-stage stochastic mixed integer programming model is proposed that combines facility location- prepositioning, decisions on pre-stocking levels for emergency supplies, and allocation of located distribution centers (DCs) to affected locations and distribution of those supplies to several demand locations after large-scale emergencies with uncertainty in demand. Also, the use of the model is demonstrated through a case study for prepositioning of supplies in probable large-scale emergencies in the eastern and southeastern Anatolian sides of Turkey. The results provide a framework for relief organizations to determine the location and number of DCs in different settings, by using the proposed model considering the main parameters, as; capacity of facilities, probability of being affected for each demand points, severity of events, maximum distance between a demand point and distribution center.

1. Introduction

Large-scale emergency incidents, both natural, such as flood, earthquake, etc., and human made, such as terror (or bio-terror) attacks, can cause a big increment in demand for food, water, medical supplies or protective materials. In the early stage of post-emergencies, the demand for medical supplies and protective materials are the most vital components in reducing the number of injured people and casualties. In case of emergency, the initial supplies are needed to be delivered to the affected regions within 24 hours [1]. Sheu [2] indicates that efficient logistics play a significant role in relieving the impact of emergencies. To be able to deliver supplies on time, the locations of DCs play a critical role in humanitarian relief logistics management.

Prepositioning the DCs is a challenging task in emergency management system. Particularly, this paper addresses the location of facilities which is a critical strategic decision for suchlike systems. One of the most significant applications of location theory is the location of medical and protective supplies. Jia et al. [3, 4] introduce models and solution approaches to determine the facility location of medical supplies in response to large-scale emergencies.

Besides location decisions, capacities of supply providers are key decisions in emergency response management. However, comparatively limited research has been found on the topic of pre-positioning particular supplies [5]. The existing models usually do not consider uncertainty in demand. There has been a few works on pre- positioning first responders for large scale emergencies. Locating first-response commodities is different from locating and stocking supplies, where multiple commodities must be considered, the commodities may have different storage necessities and transportation conditions and costs [5].

In this paper, a mathematical model is proposed that combines facility location- prepositioning, decisions on pre-stocking levels for emergency supplies, and allocation of located DCs to affected locations and distribution of those supplies to several demand locations after large-scale emergencies; with uncertainty in demand and number of affected locations where high demand requirements occur. The proposed mathematical formulation is a two-stage stochastic mixed integer programming (SMIP) model,

*Corresponding author

which is addressed as NP hard problems [6]. In many situations, parameters of the optimization problems cannot be known with certainty [5, 7, 8, 9, 10], in such cases stochastic programming (SP) methodologies are one of the strategies to apply. In two-stage stochastic programming, first-stage decisions are made in the existence of uncertainty for future scenarios. Second-stage decisions are made after the realization of the random parameters are known, and are dependent on the first-stage decisions [5, 11].

In our model, potential locations and severity of the uncertain large scale emergency events are represented via a set of discrete scenarios with probabilities. The first-stage decisions in the SP model involve the DCs' locations and allocation of the located DCs to affected regions, as well as the amount of stocking for multiple types of supplies (medical and protective). In the second-stage, recourse decisions are made including the distribution of available stocked and projected to be bought supplies, after large-scale emergencies occur, to reply particular scenario events.

In the next section, the literature on related topics is reviewed as emergency management, facility location and allocation, and prepositioning. In Section 3, the formulation of the proposed mathematical model is presented. We demonstrate the use of the model through a case study for pre positioning of supplies in probable large-scale emergencies in the eastern and southeastern Anatolian sides of Turkey. Data setup and results and analysis are presented in detail, in Section 4. Section 5 delivers conclusions and directions for future work.

2. Literature review

A survey on general insight to emergency management for operations research and management sciences is presented by Altay and Green [12]. Galindo and Batta [13] also present an extended literature review that covers the years between 2005 and 2010, inspired by Altay and Green's [12] paper. The optimization models in emergency logistics problems are reviewed in detail by Caunhye et al. [14]. In this paper, we present a literature review of the humanitarian relief logistics management taking into account disaster operations, as the facility location, prepositioning, and allocation problems, using deterministic and stochastic programming models.

The facility location problem is determined as one of the main operations of the preparedness in humanitarian relief operations. The early paper on facility location models for humanitarian relief operations are presented by Toregas et al. [15], Psaraftis et al. [16] and Iakovou et al. [17]. Jia et al. [3,4] and Huang et al. [18] presented only the location problem. Murali et al. [1] present locate-allocate heuristic for capacitated facility location to response large-scale emergencies under demand uncertainty. Shui et al. [19] present a mixed integer programming model in order to determine the locations and amounts of the emergency logistics DCs. Yushimito et al. [20] propose a heuristic algorithm based on Voronoi diagrams in order to solve the distribution center location problem.

As a preparation for an emergency, the prepositioning of supplies aims to minimize the response time, enhance emergency response capacity [21], and cover the maximum required inventory. The two-stage stochastic programming models are presented for prepositioning of relief inventory in Rawls and Turnquist [5, 22], Verma and Gaukler [23], Döyen et al. [24], Hong et al. [25], Salmerón and Apte [26], Lodree et al. [27], Campbell and Jones [28]. The relief routing [29] and disruption of network [30] is taken into consideration along with prepositioning.

Location and allocation models enable to decide where to open facilities and determine how to assign demand to facilities to increase the utilization of resources. Mitsakis et al. [31] present an optimal allocation model for emergency response to minimize maximum and average response time using existence resources. Chang et al. [32], Mete and Zabinsky [33,34], and Gunnec and Salman [35] propose two stage stochastic programming model for location and allocation of emergency relief source. Yi and Özdamar [36], Sheu [55], and Rawls and Turnquist [43] presented dynamic allocation model to optimize for preparedness and response activities. A genetic algorithm [56], particle swarm optimization algorithm [38], an epsilon constrained approach [45] are also proposed for location and allocation model for emergency response. The location-allocation plans often fail, because the uncertain and unusual nature of emergencies is not explicitly accounted [41, 57]. Stochastic programming is specified as a suitable optimization tool to plan the humanitarian relief logistics activities, because of reflecting uncertainty by probabilistic scenarios representing disasters and their outcomes [33]. Uncertainty is the nature of natural and man made disasters.

In summary, Table 1 categorizes facility location models according to the problem and data type that use deterministic or stochastic parameters. Firstly, most of the studies consider location but prepositioning. Secondly, most of the studies deal with either pre or post disaster procurements. Almost none of them take into account both procurement types. Bozorgi-Amiri et al. [38] is one of the studies that consider both procurement types. Lastly, approximately half of the studies solves problem with only deterministic parameters. In this study, we propose a two-stage stochastic optimization model to solve the location, prepositioning and allocation and post disaster procurement problem for critical items to be prepared in responding to large scale emergencies. The proposed model aims to support and improve the decisions made at strategic and operational levels for large-scale emergencies. The strategic decisions contain the location of DCs. The operational part

Table 1. Facility location problems and data type

Author	Objective	Location	Location/ Prepositioning	Location/ Allocation	Deterministic	Stochastic	
						Stochastic	Stochastic/Uncertain Parameters
Yi and Ozdamar [36]	Unsatisfied Demand Minimization	✓		✓	✓		
Yushimito and Ukkusuri [28]	Cost Minimization	✓	✓		✓		
Jia et al. [3]	Distance Minimization	✓				✓	Demand
Chang et al. [32]	Distance Minimization	✓		✓		✓	Demand
Jia et al. [4]	Coverage Minimization	✓			✓		
Günneç and Salman [35]	Time and Risk Minimization	✓		✓		✓	Demand
Mete and Zabinsky [33]	Cost and Time Minimization	✓		✓		✓	Demand and time
Balcik and Beamon [11]	Coverage Maximization	✓			✓		
Shui et al. [19]	Cost and Time Minimization	✓			✓		
Mete and Zabinsky [34]	Cost Minimization	✓		✓		✓	Demand time and supply
Rawls and Turnquist [5]	Cost Minimization	✓	✓			✓	Demand and link availability
Salmeron and Apte [26]	Unsatisfied Demand Minimization		✓	✓		✓	Demand and time
Huang et al. [18]	Coverage Maximization/Distance Minimization	✓			✓		
Han et al. [37]	Distance Minimization	✓			✓		
Verma and Gaukler [23]	Distance Minimization	✓	✓			✓	Distance
Campell and Jones [28]	Cost Minimization		✓		✓		
Duran et al. [21]	Time Minimization	✓	✓			✓	Demand/ Supply
Rawls and Turnquist [22]	Cost Minimization	✓	✓			✓	Demand and link availability
Bozorgi-Amiri et al. [38]	Cost Minimization	✓		✓		✓	Procuring cost, demand and inventory
Naji-Azimi et al. [39]	Distance Minimization				✓		
Döyen et al. [24]	Cost Minimization	✓	✓	✓		✓	Demand
Yushimito et al. [20]	Cost Minimization and Coverage Maximization	✓			✓		
Galindo and Batta [30]	Cost Minimization	✓	✓			✓	Demand
Murali et al. [1]	Coverage Maximization	✓				✓	Demand
Lin et al. [40]	Cost Minimization	✓		✓	✓		
Paul and Hariharan [41]	Cost Minimization	✓		✓	✓		
Afshar and Haghani [42]	Unsatisfied Demand Minimization	✓			✓		
Rawls and Turnquist [43]	Cost Minimization	✓		✓		✓	Demand and link availability
Hong et al. [25]	Cost Minimization	✓	✓			✓	Demand and transportation capacity
Lodree et al. [27]	Cost Minimization		✓			✓	Demand
Rath and Gutjahr [44]	Cost Minimization	✓			✓		
Abounacer et al. [45]	Unsatisfied Demand and Time Minimization	✓		✓	✓		
Sheu and Pan [46]	Distance, operational and physiological costs minimization	✓		✓	✓		
Verma and Gaukler [47]	Cost Minimization	✓	✓	✓	✓	✓	Earthquake damage and distances
Salman and Gül [48]	Time Minimization	✓		✓	✓		
Caunhye et al. [49]	Time Minimization	✓		✓	✓		
Renkli and Duran [50]	Distance Minimization		✓	✓		✓	Survivability of infrastructure
Rath et al. [51]	Coverage maximization and cost minimization			✓		✓	Route accessibility cost
Kılcı et al. [52]	Maximization of the minimum weight of open shelter areas	✓			✓		
Aydin [53]	Distance Minimization	✓		✓		✓	Failure of existing infrastructure
Tofighi et al. [54]	Distribution time and total cost minimization	✓	✓			✓	Demand, supply and network availability
Our Study	Cost Minimization	✓	✓	✓		✓	Demand

consists the prepositioning and allocation of critical items. The model also considers the penalty cost in the lack of critical items to satisfy demand (medical and protective).The paper basically contributes to emergency management literature. Additionally, the contributions of the paper on stochastic prepositioning and facility location and allocation literature are significant. Another contribution of the paper is to present a real world case study from the eastern and southeastern Anatolian sides of Turkey for response to any large scale emergency(s). It is a novel case study and unique for this region.

3. Two stage stochastic facility location-allocation model

In this section, we propose a capacitated facility location and allocation problem (CFLAP) formulation as a two-stage SP problem. As explained earlier, the objective is to minimize total cost of prepositioning, procurement, inventory holding, transportation and penalty cost of unsatisfied demand.

Now, CFLAP formulation is given as a two-stage SP problem, starting with the notation presented as follows.

Notation and mathematical formulation:

Sets:

I_E: set of existing facility locations,
I_P: set of possible facility locations,
I: set of all facility sites, $I = I_E \cup I_P$, $for\ \forall G, \forall NG$
J_A: set of affected regions,
J_N: set of non- affected (safe) regions,
J: set of all demand points, $J = J_A \cup J_N$ $for\ \forall G, \forall NG$
S: set of all possible scenarios,
K: set of commodities,
G: set of governmental organizations,
NG: set of non-governmental organizations,

Parameters:

f_i: fixed cost for facility $i \in I, for\ \forall G, \forall NG$
cap_i: capacity of facility $i \in I, for\ \forall G, \forall NG$
s: a possible future scenario and $s \in S$
p_s: occurrence probability of scenario $s \in S$
$r_j^s := 1$ if region $j \in J$ is affected in scenario $s \in S$, 0 otherwise
d_j^{ks}: demand of commodity $k \in K$ in scenario $s \in S$ for region $j \in J$
c^k: procurement cost for each unit of commodity $k \in K$
h^k: holding cost for each unit of commodity $k \in K$
v^k: volume of each unit of commodity $k \in K$
u^k: penalty cost for each unsatisfied unit of commodity $k \in K$
dis_{ij}: distance between facility $i \in I$ and region $j \in J$
$maxdis$: maximum distance allowed to transport any commodity
md_j^k: minimum pre-disaster procurement percentage of demand for commodity $k \in K$ in region $j \in J$
t_{ij}: transportation cost of one unit of commodity $k \in K$ from facility $i \in I$ to region $j \in J$

Decision variables:

$x_i := 1$ if facility $i \in I$ is opened, 0 otherwise
$\beta_{ij} := 1$ if facility $i \in I$ is assigned to region $j \in J$, 0 otherwise
α_j^{ks}: unsatisfied demand from commodity $k \in K$ at region $j \in J$ in scenario $s \in S$
y_{ij}^k: pre-disaster procurement from commodity $k \in K$ at facility $i \in I$ to be transported to region $j \in J$
z_{ij}^{ks}: post-disaster procurement of commodity $k \in K$ at facility $i \in I$ to be transported to region $j \in J$ in scenario $s \in S$

In the scenario based formulation of CFLAP, each scenario denotes a different circumstance, the affected regions and non- affected regions with a different level of severity. Each scenario $s \in S$ occurs with a different probability, p_s, and $\sum_{s \in S} p_s = 1$. In total, in case of independent affecting possibilities, we have $|S| = 2^{|J|}$ possible scenarios. Please note that our model does not necessitate any assumption on independence of each scenario. Furthermore, each unit of demand that is not satisfied by any of facility(s) cause a large penalty, u^k $k \in K$, cost. This penalty can be incurred due to casualties or finding an alternative source to treat disaster victims. There are some assumptions need to be highlighted such as all costs are known in advance i.e., fixed cost of locating facilities, holding cost, procurement cost, transportation cost, penalty cost of unsatisfied demand. Distance between facilities and affected regions are gathered from Google Maps [58]. Population of the affected regions is gathered from TUIK [59]. A maximum distance is assumed so that the maximum traveling distance between affected regions and the allocated facility cannot exceed a specific value. Also some limitations are need to be specified such as, if applicator has uncertainty in supply, time, cost etc. the modeler will need to redesign the mathematical model, and if there are larger number of nodes in the network the mathematical model will need to be solved via heuristics or metaheuristics solution approaches.

Here, the CFLAP is formulated as a two-stage stochastic programming problem. In the first stage, the location decisions are made before random large-scale emergencies occur. In the second stage, following the events, the affected region-facility assignments decisions are made for each affected region given that the particular regions are affected and facilities are located. The objective is to determine the set of facilities to be located while minimizing the total cost of open facilities and the expected cost of satisfying demand for affected regions from new opened facilities.

Using the notation, we present the mathematical model for the scenario based CFLAP as a two-stage stochastic program as below, starting with the objective function.

$$\text{Minimize} \quad \sum_{i\in I} f_i x_i + \sum_{i\in I}\sum_{j\in J}\sum_{k\in K}(c^k + h^k)y_{ij}^k + \sum_{s\in S} p_s \left(\sum_{i\in I}\sum_{j\in J}\sum_{k\in K} c^k z_{ij}^{ks} + \sum_{i\in I}\sum_{j\in J}\sum_{k\in K} t_{ij}(y_{ij}^k + z_{ij}^{ks}) + \sum_{i\in I}\sum_{k\in K} u^k \alpha_j^{ks} \right) \quad (1)$$

Subject to

$$\sum_{j\in J}\sum_{k\in K} v^k(y_{ij}^k + z_{ij}^{ks}) \le cap_i x_i \quad \forall i \in I, s \in S \quad (2)$$

$$\sum_{i\in I}(y_{ij}^k + z_{ij}^{ks}) + \alpha_j^{ks} \ge d_j^{ks} r_j^s \quad \forall j \in J, k \in K, s \in S \quad (3)$$

$$\sum_{i\in I} y_{ij}^k \ge md_j^k d_j^{ks} \quad \forall j \in J, k \in K, s \in S \quad (4)$$

$$v^k\left(y_{ij}^k + z_{ij}^{ks}\right) \le cap_i \beta_{ij} \quad \forall i \in I, j \in J, k \in K, s \in S \quad (5)$$

$$\beta_{ij} \le x_i \quad \forall i \in I, j \in J \quad (6)$$

$$dis_{ij}\beta_{ij} \le \max dis \quad \forall i \in I, j \in J \quad (7)$$

$$y_{ij}^k, z_{ij}^{ks}, \alpha_j^{ks} \in \text{int and} \ge 0 \quad \forall i \in I, j \in J, k \in K, s \in S \quad (8)$$

$$x_i, \beta_{ij} \in \{0,1\} \quad \forall i \in I, j \in J \quad (9)$$

The objective function in formulation (1) minimizes the total fixed cost of locating facilities and the expected second stage cost of satisfying demand through opened facilities. Constraint (2) ensures that the total procured commodities at a facility do not exceed its capacity. Constraint (3) ensures that demand of each demand point is satisfied by either open facilities or alternative sourcing, or penalized. Constraint (4) ensures minimum procurement amounts for each commodity and facility. Constraints (5) and (6) prevent procurement at a facility and assignment of any demand point to a facility if it is not opened. Constraint (7) ensures that demand points are assigned to facilities that are within maximum distance. Finally, the constraints (8) and (9) are integrality constraints.

The proposed model provides a generic scenario based model to handle uncertainty in demand. The model can be applied to any region or case where uncertainty occurs in demand. Additionally, the model is easy adaptable to the cases where capacity of the facilities are not issue. By replacing cap_i in the right hand side of constraints (2) and (5) by a big number (let say M) is enough to develop an uncapacitated version of the model. Furthermore if maximum distance to travel per region is not an issue removing constraint (7) will be good enough to revise the model and apply. Another robustness of the model is that it can be solved by heuristics approaches if number of scenarios or number of nodes or number of regions is very large.

4. The case of Turkey

In this section, we present a case study motivated by a real-world problem from eastern and southeastern parts of Turkey. We describe the case details in Section 4.1 and present the results in Section 4.2.

4.1. Case description and data acquisition

This case study focuses on locating new DCs at the eastern and southeastern Anatolian sides of Turkey in response to possible large-scale emergencies. Turkish Red Crescent (TRC) is responsible for administration of Turkish domestic relief networks with a number of DCs, which preserve inventory for emergency supplies [60]. Balcik and Ak [60] note that the TRC currently works on pre-positioning some emergency supplies for a large scale emergency. One of our motivations is to determine the number of DCs to effectively satisfy all demands that may be caused by large scale emergencies.

Although facility location problems are widely experienced in large-scale emergency field, the detailed data related to this problem and DCs' features are not publicly available. Furthermore, there is no standard data set that contains data for emergency event scenarios and demand estimates for relief supplies. We obtain the most of our data from governmental and non-governmental organizations; for the missing parts we develop sample problem sets to perform numerical analysis. Subsequently, the parameters are set realistically without any limiting assumptions. Therefore, the results from these data set samples can be generalized. Medical and protective materials are the most critical supplies for the victim's survival and health. An emergency event might be very severe and affect thousands of people in a very short time period. Therefore, it is very important to distribute medical and protective materials to demand points immediately after or before (if the event is expected beforehand) the emergency event occurs.

In this case study, we address the problems of pre-positioning DCs at specified regions of Turkey and procurement of multiple items (medical and protective materials) at these DCs for pre and post large scale emergencies. The population of the regions (demand points), the distance between DCs and regions, the locations and capacities of current DCs and the cost of critical items are problem specific and based on real data. Therefore, we propose the demand scenarios and related parameters as explained below.

Demand Scenarios: Each scenario represents the set of regions that might be affected by emergency event and the severity level of the event. Demand of each region for a specific scenario is calculated via logic in Jia et al. [4]. Four levels are used in Jia et al. [4], such as ''low, intermediate, intermediate-high and high''. We practice four levels of severity as well. Let sev (:={0.03,0.05,0.07,0.09}) be the severity set of the

emergency event, and sev_w^s be the scenario s's severity at level w,w∈sev. Let ρ_j denote the population of the affected region j. The population data of demand points are obtained from Turkish Statistical Institute's database from its formal website [59] and provided in Table 2. Note that, the demand for different types of commodities is considered to be the same, which is a non-restrictive assumption and easily can be generalized. Then, demand for a scenario is calculated as below.

$$d_j^{ks} = sev_w^s \rho_j \quad \forall j \in J, k \in K, w \in sev, s \in S \quad (11)$$

Lastly, note that each problem set consists of 1024 ($|S| = 2^{|\#\text{of Demand Points}|}$) scenarios. The deterministic equivalent formulation has variables x_i, β_{ij}, y_{ij}^k, z_{ij}^{ks} and α_j^{ks}, in total |I||+|I|×|J|+|I|×|J|×|K|+|I|×|J|×|K|×|S|+|J|×|K|×|S|= 10+10×10+10×10×2+10×10×2×1024+10×2× 1024 = 225,590 variables. Similarly, it has constraints (2), (3), (4), (5), (6), (7) and (8), in total 461,200 constraints.

Table 2. The populations of the regions (demand points)

Region	Population	Region	Population
1	2,125,635	**6**	762,366
2	1,592,167	**7**	1,063,174
3	778,195	**8**	773,026
4	1,799,558	**9**	1,762,075
5	1,483,674	**10**	1,051,975

Minimum Stocked Demand: Medical and protective materials are vital for victims; therefore, these supplies need to be distributed immediately to the affected regions. Pre-positioning a particular amount of supplies at DCs is one of the best ways to respond emergency events on time. Thus, we add the minimum demand constraints to the formulation. As described earlier, md_j^k represents the minimum percentage of demand in affected region j from commodity k that needs to be procured pre-disaster. We practice one for md_j^k (:= {0.3}). The minimum demand that needs be procured is calculated as the production of demand and percentage levels ($md_j^k d_j^{ks}$). Since pre-positioning is the first stage decision variables in SP, the amount of demand that needs to be stocked has to satisfy the constraints in (4) for all scenarios.

Scenario Probabilities: In generating the scenarios, we assume that the regions are affected independently and identically, as the events have Bernoulli distribution with probability q_j (i.e., the occurrence probability of the event at region j). In our experiments, we use two types of occurrence probabilities; uniform failure probability (i.e., $q_j = 1, \dots, |J| = q$), which considers the cases $q = \{0.3, 0.5, 0.8\}$, and randomly selected values.

Capacity: Based on the information obtained from a non-governmental organization, whose major motivation is to manage the distribution of supplies to victims who are affected by disasters, the capacity of DCs varies between $15Km^3$ and $50Km^3$. Therefore, we test eight capacity levels in this study, such as $15K\,m^3$, $20Km^3$, $25Km^3$, $30Km^3$, $35Km^3$, $40Km^3$, $45Km^3$ and $50Km^3$.

Max Distance: Since responding large-scale emergencies is like racing with time, we consider maximum distance constraints, what ensure that a commodity can only be transported from a distribution center to affected regions that are in a specific range. In other words, the service distance levels are identified. Detailed information on service distance minimization can be found in Jia et al. [4] and Lin et al. [40]. The experimental samples are tested with respect to six different levels of distance ranges, such as $350km$, $400km$, $450km$, $500km$, $550km$ and $600km$.

Table 3. Distances between distribution centers and regions (demand points)

	Distances between DCs and Regions (km)									
DCs	**1**	**2**	**3**	**4**	**5**	**6**	**7**	**8**	**9**	**10**
Adana	0	522	808	209	191	392	189	534	346	899
Diyarbakir	522	0	324	313	509	251	369	95	176	377
Elazig	490	153	318	345	477	98	321	248	329	475
Erzurum	808	324	0	637	795	416	639	419	500	414
Mus	742	258	266	571	729	350	573	353	434	223
Gaziantep	209	313	637	0	196	247	80	325	137	690
Hatay	191	509	795	196	0	379	176	521	333	886
Malatya	392	251	416	247	379	0	223	346	269	573
Sanliurfa	346	176	500	137	333	269	217	188	0	553
Van	899	377	414	690	886	573	746	452	553	0

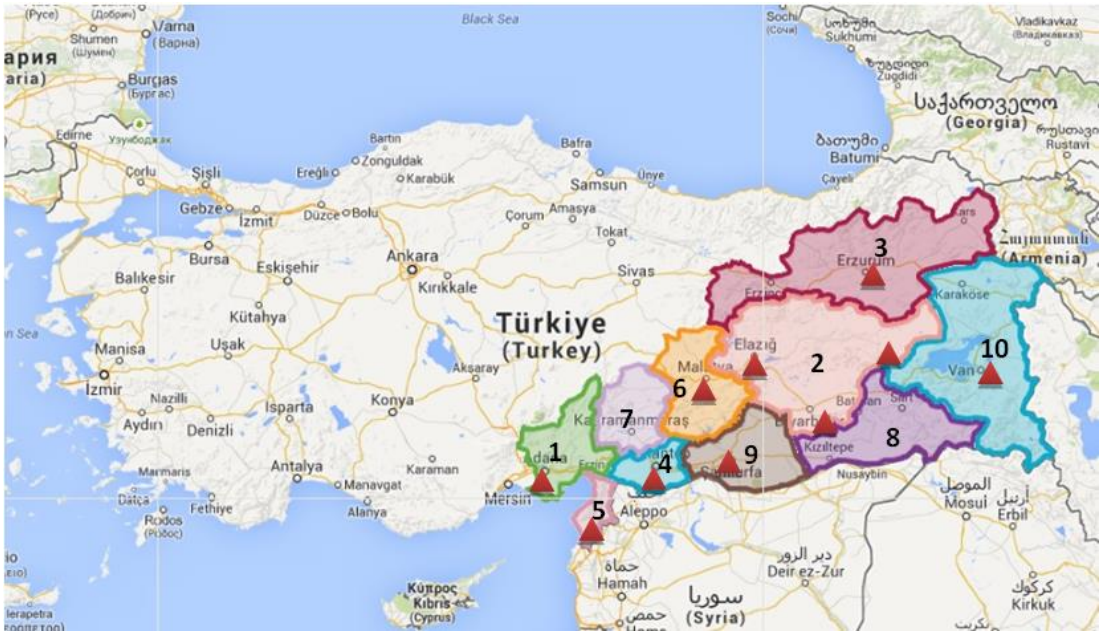

Figure 1. Regions and locations of DCs

Table 4. Effects of capacity on location decisions and total cost

Capacity	Impact	Objective	Open Decisions	Impact	Objective	Open Decisions
15K		50,599,764	1,2,3,4,5,6,7		187,188,418	1,2,3,4,5,6,7,8,9,10
20K		51,984,362	1,3,5,6,7,9		166,402,454	1,2,3,4,5,6,7,8,9,10
25K		52,035,866	5,6,7,8,9		147,390,098	1,2,3,4,5,6,7,8,9,10
30K		52,509,772	5,6,7,8,9		132,785,959	1,2,3,4,5,6,7,8,9,10
35K	**0.03**	51,397,250	5,6,7,9	**0.07**	124,952,934	1,2,3,4,5,6,7,8,9,10
40K		51,828,149	5,6,7,9		122,077,183	1,3,4,5,6,7,8,9,10
45K		52,424,826	5,6,7,9		119,405,632	1,3,5,6,7,8,9,10
50K		50,696,695	5,7,9		116,448,701	1,3,6,7,8,9,10
15K		94,740,147	1,2,3,4,5,6,7,8,9,10		320,907,135	1,2,3,4,5,6,7,8,9,10
20K		87,766,262	1,2,3,4,5,6,7,8,9,10		265,670,113	1,2,3,4,5,6,7,8,9,10
25K		87,536,511	1,3,4,5,6,7,8,9,10		242,583,042	1,2,3,4,5,6,7,8,9,10
30K		86,923,893	1,3,5,6,7,8,9,10		220,700,621	1,2,3,4,5,6,7,8,9,10
35K	**0.05**	85,888,361	1,3,6,7,8,9,10	**0.09**	199,740,250	1,2,3,4,5,6,7,8,9,10
40K		84,395,974	3,6,7,8,9,10		181,120,654	1,2,3,4,5,6,7,8,9,10
45K		84,988,539	4,6,7,8,9,10		166,774,135	1,2,3,4,5,6,7,8,9,10
50K		83,031,958	3,6,7,9,10		157,792,895	1,2,3,4,5,6,7,8,9,10

Distances between DCs and demand points are obtained from the Republic of Turkey General Directorate of Highways' database [61]. The distances between projected to be opened DCs and regions (demand points) are presented in Table 3.

Regions: We group the regions based on their populations (i.e., including overcrowded cities) and strategic importance (i.e., location, population, locating military quarters, etc.). Ten regions are determined at eastern and southeastern Anatolian sides of Turkey. Each region is numbered and differently colored as in Figure 1. The triangles show the possible locations to set up DCs at.*Other Costs:* Set up cost for each DC changes based on its capacity level. Furthermore, this cost does not increase linearly with the incremental in capacity. Set up cost is determined as follows: Incremental cost for one of unit capacity up to $15Km^3$ is $100(TL - Turkish\ Lira)$, between $15K$ and $20K$ is $95(TL)$, and for the ranges between $20K - 25K$, $25K - 30K$, $30K - 35K$, $35K - 40K$, $40K - 45K$ and $45K - 50K$ are $90, 85, 80, 75, 70,$ and $65\ (TL)$, respectively. Then, for instance, cost of

locating a DC with $15Km^3$ is $1.5M$ $(= 15{,}000x100)$ and with $20Km^3$is $1.9M$ $(= 20{,}000x95)$. As mentioned earlier, two types of commodities (medical and protective materials) are considered here. Purchasing cost of each unit is 70 (TL) and 40 (TL) for medical and protective supplies, consecutively. Holding cost for one unit of medical supply is 30 (TL), and for one unit of protective materials is 20 (TL). Penalty cost for each unit of unsatisfied demand is considered as $500(TL)$ for medical, and $300(TL)$ for protective materials.

4.2. Results and discussions

The case samples are solved by using IBM ILOG/CPLEX 12.1.0 on a desktop computer with Intel (R) Core (TM) i5-2400M 3.10GHz CPU.

Effect of capacity decisions: In this subsection, minimum average demand is fixed to 30%, maximum distance to $400(km)$, and scenario probabilities are considered to be random.

Changes in capacities have larger effect on facility decisions when large-scale emergencies have low impact. In other words, results show that the number of opened facilities is more sensitive to capacities in cases of low impact events. On the contrary, the capacity changes have less effect on location decisions, when large-scale emergencies have larger impact. For instance, when capacity is increased from its minimum value $(15K)$ to the maximum value $(50K)$, the number of opened facilities decreases from seven to three, under the impact factor 0.03, and from ten to five, under the impact factor 0.05. Since a large number of facilities are necessary to create extra capacity for responding to large-scale emergencies, more possible facility locations are needed to be determined; because even if all facilities are decided to be opened with the maximum capacity, the demand is still not fully satisfied.

As seen in Table 4, the number of opened facilities reduces along with the increment in capacities. Seven facilities are decided to be located when capacity is $15K$, six when $20K$, five when $25K$ and $30K$, four when $35K, 40K$ and $45K$, and three when $50K$, under the 0.03 impact factor case. The same changes can be observed when impact factor is increased to $0{,}05$. All facilities are opened if selected capacity is less than $25K$. Number of opened facilities continuously reduces from 10 to 5, when capacity is increased up to $50K$. The reason of opening all facilities can be explained with the lack of capacity to satisfy all demand. The lack of capacity causes to open all facilities in almost all cases except when capacity is higher than $35K$ under 0.07 impact factor case. All facilities are opened when impact factor is 0.09. This explanation can be fortified by analyzing the cost elements that constitute the expected total cost. For instance, in the case when impact factor is 0.09 and capacity is $15K$, then 67% of expected total cost is the penalty cost of not being able to satisfy demand, while $5\%, 18\%$, and 10% are fixed, pre-procurement and post-procurement costs, consecutively. The transportation cost constitutes only less than 1% of expected total cost. Moreover, the results indicate that larger number of facilities would be used only for meeting demand requirements if reserve capacities are set sufficiently large.

The results in Figure 2 indicate that the expected total cost generally is sensitive to facility capacities, especially when large-scale emergencies have higher impact. Expected total cost decreases by 62% when capacity is increased to its maximum level from its minimum level under high impact events. In other words, the 67.5% of the expected total cost is caused from expected penalty cost when capacity is at its minimum level $(15K)$, and penalty cost reduces to 4.75% when capacity is at its maximum level $(50K)$. The same conclusion is attained from the case with $0{,}07$ impact events. As a result, larger savings in penalty costs occur in the cases with high impact events via increased facility capacity. Since total available capacity is sufficiently enough to satisfy all demand under low impact events (i.e.0.03), expected total cost may increases, because of redundancy in capacity. We conclude that, any large-scale emergency with a lower impact than 0.03 can be responded with the minimum cost and 100% satisfaction. This satisfaction can be responded either by seven facilities with $15K$ capacity level or three one with $50K$ capacity level. Therefore, it is valuable information for decision makers to locate facilities with higher capacities to response high impact events and lower capacities to response low impact events.

Effect of maximum distance: In this subsection, minimum average demand is fixed to 30%, capacity to $30K\ and\ 50K$, separately, and scenario probabilities are considered to be random.

Facility capacities and maximum distance may highly affect the total costs in settings under high and low impact large-scale emergencies. The samples include a combination of scenarios with high and low impact events, and demand fluctuations across scenarios are large. In this section, we test the sensitivity of costs and location decisions with respect to the changes in capacities and maximum distance. Specially, we perform experiments with maximum distance values that range from $350\ to\ 600$ (km) and facility capacities. Two levels of capacities are performed, such as $30K$ and $50K$. as shown in Table 5, total costs and number of opened facilities are sensitive to maximum distance and capacity, which is consistent with our previous observations.

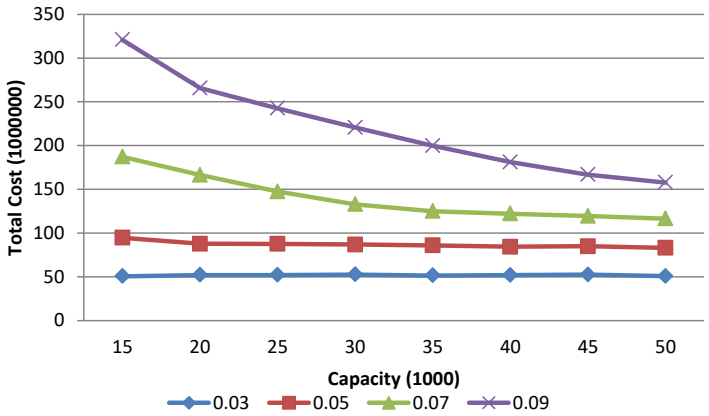

Figure 2. Effects of capacity on total cost

Table 5. Effects of maximum distance on location decisions and total cost

Maximum Distance(km)	Impact	Capacity=30,000 Objective	Capacity=30,000 Open Decisions	Capacity=50,000 Objective	Capacity=50,000 Open Decisions
350	**0.03**	52,510,024	5,6,7,8,9	50,703,287	5,7,9
400		52,509,772	5,6,7,8,9	50,696,695	5,7,9
450		51,464,657	6,7,9,10	49,797,837	7,9,10
500		51,153,242	6,7,9,10	49,694,821	7,9,10
550		51,153,242	6,7,9,10	49,694,821	7,9,10
600		51,062,473	6,7,9,10	49,691,690	7,9,10
350	**0.05**	88,091,898	1,3,4,5,6,7,8,9	85,546,944	4,6,7,8,9,10
400		86,923,893	1,3,5,6,7,8,9,10	83,031,958	3,6,7,9,10
450		86,809,666	1,3,4,6,7,8,9,10	81,774,616	6,7,9,10
500		86,798,057	1,3,4,6,7,8,9,10	81,255,582	6,7,9,10
550		86,798,057	1,3,4,6,7,8,9,10	81,255,582	6,7,9,10
600		86,797,263	1,3,4,6,7,8,9,10	81,104,293	6,7,9,10
350	**0.07**	140,215,849	1,2,3,4,5,6,7,8,9,10	120,816,966	1,3,4,6,7,8,9,10
400		132,785,959	1,2,3,4,5,6,7,8,9,10	116,448,701	1,3,6,7,8,9,10
450		132,226,870	1,2,3,4,5,6,7,8,9,10	116,214,909	1,4,6,7,8,9,10
500		132,144,639	1,2,3,4,5,6,7,8,9,10	116,142,857	1,4,6,7,8,9,10
550		132,144,639	1,2,3,4,5,6,7,8,9,10	116,142,857	1,4,6,7,8,9,10
600		132,080,556	1,2,3,4,5,6,7,8,9,10	116,140,350	1,4,6,7,8,9,10
350	**0.09**	229,490,054	1,2,3,4,5,6,7,8,9,10	168,121,111	1,2,3,4,5,6,7,8,9,10
400		220,700,621	1,2,3,4,5,6,7,8,9,10	157,792,895	1,2,3,4,5,6,7,8,9,10
450		219,702,659	1,2,3,4,5,6,7,8,9,10	157,420,474	1,2,3,4,5,6,7,8,9,10
500		219,585,144	1,2,3,4,5,6,7,8,9,10	157,364,838	1,2,3,4,5,6,7,8,9,10
550		219,584,994	1,2,3,4,5,6,7,8,9,10	157,364,838	1,2,3,4,5,6,7,8,9,10
600		219,438,357	1,2,3,4,5,6,7,8,9,10	157,340,757	1,2,3,4,5,6,7,8,9,10

The samples, in which the maximum distances are increased to $600km$ of their minimum levels, $(350km)$, lead to less expected total cost in all cases and less opened facilities in some cases. For instance, in low impact events (0.05) six facilities $(4, 6, 7, 8, 9, \text{and } 10)$ are opened when maximum distance is restricted to $350km$. However, the number of opened facilities is reduced to five $(3, 6, 7, 9, \text{and } 10)$ when maximum distance is increased to $400km$. The only change is not restricted with the number of opened facilities. Design of the solution is changed; facilities 4 and 8 are not selected to be opened and facility 3 is opened instead.

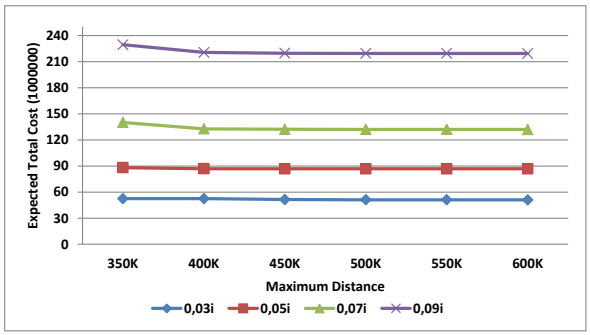

a) Capacity=30.000

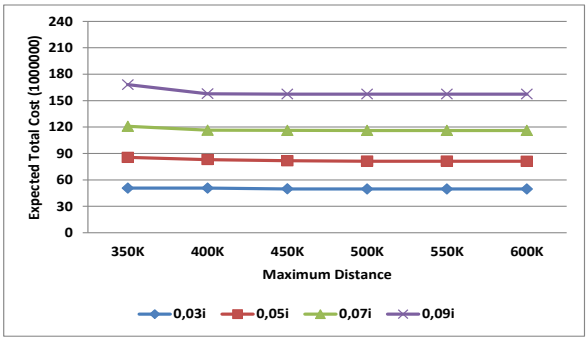

b) Capacity=50.000

Figure 3. Effect of maximum distance on total costs

As realized in Figure 3, expected total costs are more sensitive to maximum distance under high impact events and less sensitive to low impact events. Total expected costs decrease continuously with the increments in maximum distance. In Figure 3 a), expected total cost decreases by 4% under 0.09 impact factor, when maximum distance increases from $350km$ to $600km$. Expected total cost decreases by $6\%, 1\%$ and 3% under $0{,}07, 0{,}05$ and $0{,}03$ impact factor cases, consecutively. The same observation can be gained in Figure 3 b). Expected costs decrease by $2\%, 5\%, 4\%$, and 6% for cases $0.03, 0.05, 0.07$, and 0.09 impact factors, consecutively. Note that capacities are considered 30,000 and 50,000 in Figure 3 a) and b), sequentially. Another observation is that the expected total costs decrease even if the solutions (number of and opened facilities) do not change. We conclude that maximum distance and capacity decisions have relatively high impact on expected total cost and solution.

Effect of scenario probability: In this subsection, minimum average demand is fixed to 30%, capacity to $30K$ *and* $50K$, separately, and maximum distance is considered as $4{,}5\ km$.

In this subsection, we analyze the effects of scenario probabilities on expected total costs and location decisions. We perform experiments with scenario probability values that range from $0.3\ to\ 0.8\ (km)$. Lastly, we make a test with a random scenario probability. In the unique cases, demand points are subjected to be affected with the same probability (i.e., 0.3), while they are subjected to be affected based on their strategic importance and population in the random case.

According to Figure 4 a) and b), we conclude that expected total costs are very sensitive to scenario probabilities. Note that, figure in a) shows the fluctuations of expected total costs respect to scenario probabilities when facilities' capacities are selected as 30K, while figure b) shows the changes when facilities' capacities are selected as 50K. In both cases, expected total costs increase with the increase in scenario probabilities. In figure a), expected total cost is about $24M$ when demand points are subjected to be affected with 0.3 probability with a low impact event (i.e., 0.03). Expected total cost increases to $92M$ if being effected probability is increased to 0.8; this means an 377% increment in expected total cost. Scenario probability has higher effect on higher impact events in terms of expected total cost. For instance, the increment in expected total cost is 449% when scenario probability is increased from 0.3 to 0.8, under high impact events (0.05). Expected total costs are very high under very high impact events (0.07 and 0.09). This is because even if all facilities are opened, demands of affected regions are still not satisfied and penalty cost occurs. The same analyzes are showed for the results shown in Figure4 b).

As expected, fewer facilities are needed to satisfy demand with a minimum cost under low occurrence probability of an event or less impact events and/or higher facility capacities. It is clearly seen from Table 6. We compare the case where impact factor is $0{,}05$ in Table 6; only two facilities (5 and 6) are opened if capacity is $50K$ and three facilities (in regions 6,9 and 10) are opened if capacity is $30K$. The number of opened facilities and solution change and expected total cost decreases.

In summary, given the same data, considering different large-scale emergencies' impact levels in scenario generation may have different cost implications. Therefore, it is important to test the inferences of alternative set of large-scale emergency scenarios in making decisions. In particular, the effects of high impact large-scale emergencies must be wisely analyzed in establishing response strategies.

As can be implied from the analysis, managers face tradeoffs between capacity, number of facilities and cost/distance minimization. To handle these tradeoffs the analyses provided above are good guides to take strategical decisions.

5. Conclusions and future directions

This study addresses a facility location problem for responding large-scale emergencies. We aim to pre-position DCs at the eastern and southeastern Anatolian sides of Turkey to response to any large-scale emergency. Multi supplies, such as medical and protective materials, are considered.

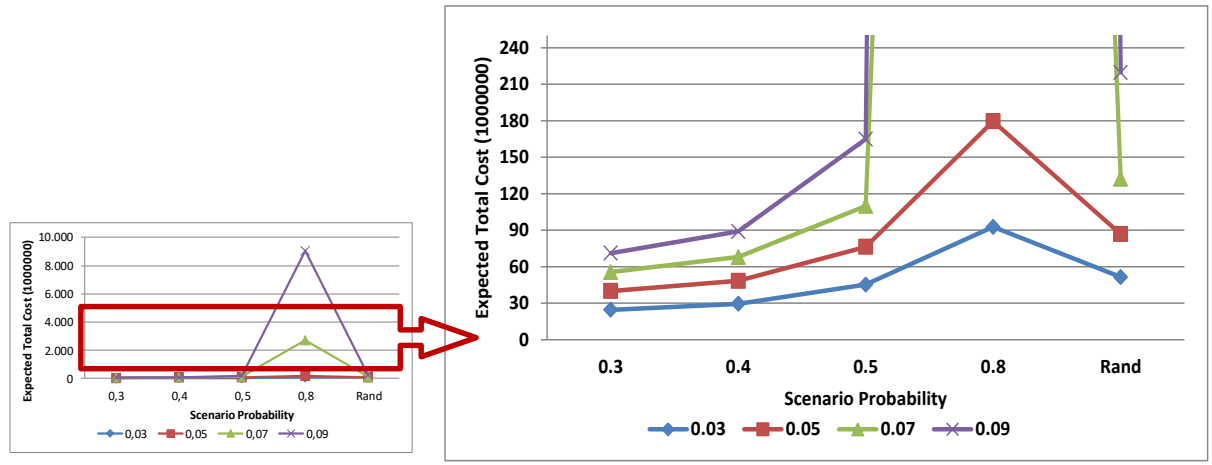

a) Capacity=30,000

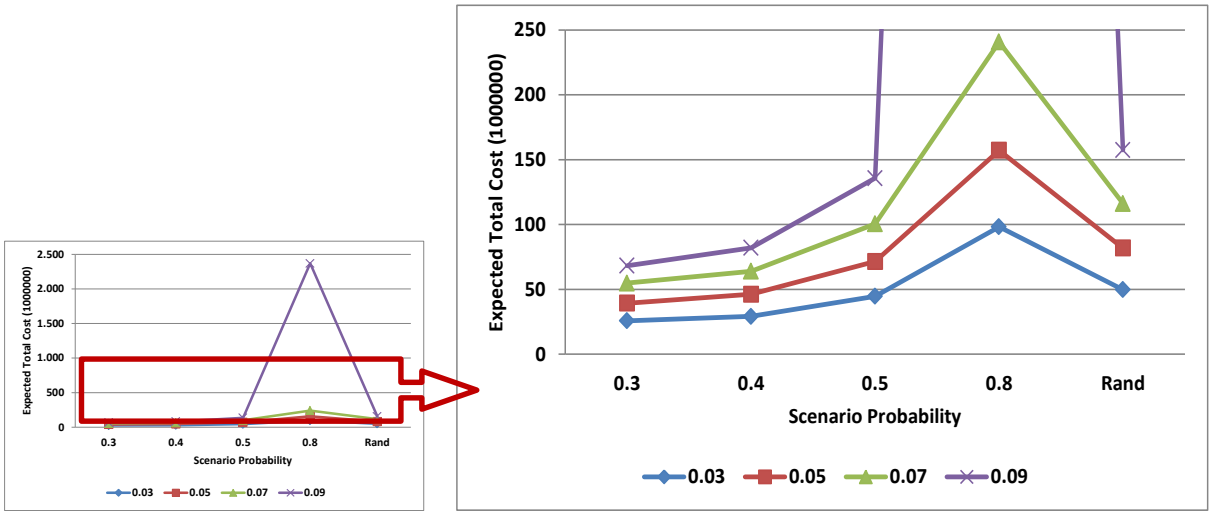

b) Capacity=50,000

Figure 4. Effect of scenario probability

A relief organization must determine the optimal number of opened DCs and locations of DCs pre-disaster under demand uncertainty. We illustrate the uncertainty in demands by defining a set of probabilistic scenarios and developing a scenario based stochastic programming model. Scenarios are created based on impact (severity) of the event and probability of being affected. We perform numerical experiments on a real case study to understand the effects of parameters that may influence the solution. Capacity of facilities, probability of being affected for each demand points, severity of events, maximum distance between a demand point and distribution center are main parameters that are tested. The results provide a framework for relief organizations to determine the location and number of DCs in different settings. The key contribution of this study is to design a response strategy to distribute supplies in a large-scale emergency, that considers distance coverage and demand uncertainty, in addition, multi-type supplies.

The contributions of the paper to the literature are specified as follows: (1) The existing facilities are capacitated; (2) the demand is satisfied which depends on distance to DCs. If distance between any DC and an affected region exceeds a non-desirable distance, then no supply is distributed between them. This is because while planning response to a large-scale emergency scenario, it is rational to assume that the number of people expected to be assigned to a specific DC decreases as their distance to that DC increases; (3) given the unpredictability as to when and where such an emergency scenario could occur and how many people would be affected, there is a significant uncertainty in demand values. Since the amount of demand is uncertain and unknown, a two stage stochastic programming model is developed to express the effects of uncertainty on the strategic decisions; (4) the goal is to determine locations of new DCs while taking into consideration the existing DCs' locations and capacities. Consideration of existing DCs while determining the location of the new DCs is an important contribution to the large-scale emergencies literature; (5) multi type supplies are considered, because in the case of large-scale emergencies not only medical materials but also

protective materials should be considered; (6) a real world case study is presented from the eastern and southeastern Anatolian sides of Turkey to response to any large-scale emergency. It is a novel case study and unique for this region; (7) it is aimed that, the proposed method will be used in different regions of different countries, to evaluate and improve their response strategies to any type of large-scale emergencies.

Table 6. Effect of scenario probability on expected total cost and location decisions

			Capacity=30,000		Capacity=50,000	
		Impact	Objective	Open Decisions	Objective	Open Decisions
Scenario Probability	**0.3**	**0.03**	24,555,936	5.6	25,702,438	6,10
	0.4		29,495,398	7,9,10	29,157,840	6,10
	0.5		45,252,520	6,7,9,10	44,574,995	7,9,10
	0.8		92,658,994	1,2,4,6,7,8,9,10	98,246,602	1,2,4,6,7,8,9,10
	Rand		51,464,657	6,7,9,10	49,797,837	7,9,10
	0.3	**0.05**	40,029,240	6,9,10	39,260,126	5,6
	0.4		48,382,553	7,8,9,10	46,159,088	7,9,10
	0.5		76,311,612	1,3,6,7,8,9,10	71,421,004	6,7,9,10
	0.8		179,579,410	1,2,3,4,5,6,7,8,9,10	157,134,539	1,2,4,6,7,8,9,10
	Rand		86,809,666	1,3,4,6,7,8,9,10	81,774,616	6,7,9,10
	0.3	**0.07**	55,530,956	6,8,9,10	54,751,772	6,9,10
	0.4		67,909,481	6,7,8,9,10	63,880,905	7,8,9,10
	0.5		109,898,741	1,2,3,4,5,6,7,8,9,10	100,492,515	6,7,8,9,10
	0.8		2,721,559,062	1,2,3,4,5,6,7,8,9,10	240,715,621	1,2,3,4,5,6,7,8,9,10
	Rand		132,226,870	1,2,3,4,5,6,7,8,9,10	116,214,909	1,4,6,7,8,9,10
	0.3	**0.09**	71,119,761	6,7,8,9,10	68,257,643	7,9,10
	0.4		89,018,805	1,5,6,7,8,9,10	81,966,059	6,7,8,9,10
	0.5		164,871,554	1,2,3,4,5,6,7,8,9,10	135,735,487	1,3,4,5,6,7,8,9,10
	0.8		9,059,054,031	1,2,3,4,5,6,7,8,9,10	2,368,833,930	1,2,3,4,5,6,7,8,9,10
	Rand		219,702,659	1,2,3,4,5,6,7,8,9,10	157,420,474	1,2,3,4,5,6,7,8,9,10

Since there is lack of studies on these topics, we discuss several future researches. Firstly, some other sources can be used to satisfy demand besides prepositioning, such as framework agreements. More than one option can be considered simultaneously, which may be more effective in response to large-scale emergencies. For example, a future research can consider the decisions related to the amount of supplies to pre-position and reserve from framework agreements in an integrated way. Secondly, since the presented problem is a cost minimization problem, budget constraints can be incorporated into the model. Thus, the problem will be held into a more realistic way. Thirdly, as DCs are located before the large-scale emergencies occur, they may already got affected by the events. Therefore, future research can focus on developing models which incorporate the reliability of the DCs as another uncertainty while designing the network. Lastly, since capacitated facility location problems are very difficult problems, in terms of computational cost, approximation methods such as sample average approximation, genetic algorithms, etc. can be used to solve larger networks.

Acknowledgments

The authors would like to thank the Editors and the three anonymous referees for their helpful comments and suggestions. Also, any opinions, findings, and conclusions are those of the authors and do not necessarily reflect the view of the governmental and non-governmental organizations.

References

[1] Murali, P. Ordóñez, F. & Dessouky, M.M., "Facility location under demand uncertainty: Response to a large-scale bio-terror attack", *Socio-Economic Planning Sciences*, vol. 46 No. 1, pp. 78-87(2012).

[2] Sheu, J. B., "An emergency logistics distribution approach for quick response to urgent relief demand in disasters", *Transportation Research Part E: Logistics and Transportation Review*, Vol. 43 No. 6, pp. 687-709 (2007).

[3] Jia, H. Ordonez, F. & Dessouky, M., "A modeling framework for facility location of medical services

for large-scale emergencies", *IIE Transactions*, Vol. 39 No. 1, pp. 41–55 (2007a).

[4] Jia, H. Ordonez, F. & Dessouky, M., "Solution approaches for facility location of medical supplies for large-scale emergencies", *Computers & Industrial Engineering*, Vol. 52, pp. 257-276 (2007b).

[5] Rawls, C.G. & Turnquist, M.A., "Pre-positioning of emergency supplies for disaster response", *Transportation Research Part B: Methodological*, Vol. 44 No. 4, pp. 521-534 (2010).

[6] Megiddo N. & Supowit K.J., "On the complexity of some common geometric location problems", *SIAM Journal on Computing*, Vol. 13, pp. 182-196 (1984).

[7] Haugen, K.K. Løkketangen, A. & Woodruff, D.L., "Progressive hedging as a meta-heuristic applied to stochastic lot-sizing", *European Journal of Operational Research*, Vol. 132 No. 1, pp. 116-122 (2001).

[8] Birge, J.R. & Louveaux, F., "Introduction to stochastic programming", *Springer-Verlag*, New York (1997).

[9] Aydin, N., and Murat, A.. "A swarm intelligence based sample average approximation algorithm for the capacitated reliable facility location problem", *International Journal of Production Economics*, Vol 145 No. 1, pp. 173-183 (2013).

[10] Ayvaz, B., Bolat, B., & Aydin, N.. "Stochastic reverse logistics network design for waste of electrical and electronic equipment". *Resources, Conservation and Recycling*, Vol 104, pp. 391-404 (2015).

[11] Balcik, B., & Beamon, B. M.. "Facility location in humanitarian relief", International Journal of Logistics, Vol 11 No. 2, pp. 101-121 (2008).

[12] Altay, N. Green, W.G., "OR/MS research in disaster operations management", *European Journal of Operational Research*, Vol. 175 No.1, pp. 475-493 (2006).

[13] Galindo, G. & Batta, R., "Review of Recent Developments in OR/MS Research in Disaster Operations Management", *European Journal of Operational Research*, Vol. 230 No. 2, pp. 201-211 (2013).

[14] Caunhye, A.M. Nie, X. & Pokharel, S., "Optimization models in emergency logistics: A literature review", *Socio-Economic Planning Sciences*, Vol. 46 No. 1, pp.4-13 (2012).

[15] Toregas, C. Swain, R. ReVelle, C. & Bergman, L., "The location of emergency service facilities", *Operations Research*, Vol. 19 No. 6, pp. 1363-1373 (1971).

[16] Psaraftis, H.N. Tharakan, G.G. & Ceder, A., "Optimal response to oil spills: the strategic decision case", *Operations Research*, Vol. 34 No. 2, pp. 203-217 (1986).

[17] Iakovou, E. Ip, C.M. Douligeris, C. & Korde, A., "Optimal location and capacity of emergency cleanup equipment for oil spill response", *European Journal of Operational Research*, Vol. 96 No. 1, pp. 72-80 (1997).

[18] Huang, R. Kim, S. & Menezes, M.B., "Facility location for large-scale emergencies", *Annals of Operations Research*, vol. 181 No. 1, pp. 271-286 (2010).

[19] Shui, W. Ye, H. Zhao, J. & Liu, M., "A Dynamic Multiple Objective Model of Location Problem of Emergency Logistics Distribution Centers", *Logistics*, pp. 929-934 (2009).

[20] Yushimito, W.F. Jaller, M. & Ukkusuri, S., "A Voronoi-based heuristic algorithm for locating distribution centers in disasters", *Networks and Spatial Economics*, Vol. 12 No. 1, pp. 21-39 (2012).

[21] Duran, S. Gutierrez, M.A. & Keskinocak, P., "Pre-positioning of emergency items for care international", *Interfaces*, Vol. 41 No. 3, pp. 223-237 (2011).

[22] Rawls, C.G. & Turnquist, M.A., "Pre-positioning planning for emergency response with service quality constraints", *OR spectrum*, Vol. 33 No. 3, pp. 481-498 (2011).

[23] Verma, A. & Gaukler, G.M., "A stochastic optimization model for positioning disaster response facilities for large-scale emergencies", *Network Optimization*, Springer Berlin Heidelberg, pp. 547-552 (2011).

[24] Döyen, A. Aras, & N. Barbarosoğlu, G., "A two-echelon stochastic facility location model for humanitarian relief logistics", *Optimization Letters*, Vol. 6 No. 6, pp. 1123-1145 (2012).

[25] Hong, X. Lejeune, M.A. & Noyan, N., "Stochastic Network Design for Disaster Preparedness", *Optimization Online*, pp. 1-31 (2012).

[26] Salmerón, J. & Apte, A. (2010), "Stochastic optimization for natural disaster asset prepositioning", *Production and Operations Management*, Vol. 19 No. 5, pp. 561-574.

[27] Lodree Jr, E.J. Ballard, K.N. & Song, C.H., "Pre-positioning hurricane supplies in a commercial supply chain", *Socio-Economic Planning Sciences*, Vol. 46 No.4, pp. 291-305 (2012).

[28] Campbell, A.M. & Jones, P.C., "Prepositioning supplies in preparation for disasters", *European Journal of Operational Research*, Vol. 209 No.2, pp. 156-165 (2011).

[29] Yushimito, W.F. & Ukkusuri, S.V., "A Location-Routing Approach for the Humanitarian Pre-Positioning Problem", *In 87th Annual Meeting of*

the Transportation Research Board, Washington, DC (2007).

[30] Galindo, G. & Batta, R., "Prepositioning of supplies in preparation for a hurricane under potential destruction of prepositioned supplies", *Socio-Economic Planning Sciences*, Vol. 47 No.1, pp. 20-37 (2012).

[31] Mitsakis, E. Stamos I. Salanova Grau J.M. & Aifadopoulou G., "Optimal allocation of emergency response services for managing disasters", *Disaster Prevention and Management*, Vol. 23 No. 4, pp. 329 – 342 (2014).

[32] Chang, M.S. Tseng, Y.L. & Chen, J.W., "A scenario planning approach for the flood emergency logistics preparation problem under uncertainty", *Transportation Research Part E: Logistics and Transportation Review*, Vol. 43 No. 6, pp.737-754 (2007).

[33] Mete, H.O. & Zabinsky, Z.B., "Preparing for disasters: medical supply location and distribution", *In Proceedings of the INFORMS conference*, Seattle, WA, pp. 1-14 (2007).

[34] Mete, H.O. & Zabinsky, Z.B., "Stochastic optimization of medical supply location and distribution in disaster management", *International Journal of Production Economics*, Vol. 126 No. 1, pp. 76-84 (2010).

[35] Gunnec, D. & Salman, F., "A two-stage multi-criteria stochastic programming model for location of emergency response and distribution centers", *In International Network Optimization Conference* (2007).

[36] Yi, W. Özdamar, L., "A dynamic logistics coordination model for evacuation and support in disaster response activities", *European Journal of Operational Research*, Vol. 179 No. 3, pp. 1177-1193 (2007).

[37] Han, Y., Guan, X., & Shi, L., "Optimization based method for supply location selection and routing in large-scale emergency material delivery", *IEEE Transactions on Automation Science and Engineering*, Vol 8 No. 4, pp. 683-693 (2011).

[38] Bozorgi-Amiri, A. Jabalameli, M.S. Alinaghian, M. and Heydari, M., "A modified particle swarm optimization for disaster relief logistics under uncertain environment", *The International Journal of Advanced Manufacturing Technology*, Vol. 60 No. 1-4, pp. 357-371 (2012).

[39] Naji-Azimi, Z., Renaud, J., Ruiz, A., & Salari, M.. "A covering tour approach to the location of satellite distribution centers to supply humanitarian aid", *European Journal of Operational Research*, Vol 222 No. 3, pp. 596-605 (2012).

[40] Lin, Y.H. Batta, R. Rogerson, P.A. Blatt, A. & Flanigan, M., "Location of temporary depots to facilitate relief operations after an earthquake", *Socio-Economic Planning Sciences*, Vol. 46 No. 2, pp. 112-123 (2012).

[41] Paul, J.A. & Hariharan, G., "Location-allocation planning of stockpiles for effective disaster mitigation", *Annals of Operations Research*, Vol. 196 No. 1, pp. 469-490 (2012).

[42] Afshar, A., & Haghani, A., "Modeling integrated supply chain logistics in real-time large-scale disaster relief operations", *Socio-Economic Planning Sciences*, Vol 46 No. 4, pp. 327-338 (2012).

[43] Rawls, C.G. & Turnquist, M.A., "Pre-positioning and dynamic delivery planning for short-term response following a natural disaster", *Socio-Economic Planning Sciences*, Vol. 46 No. 1, pp. 46-54 (2012).

[44] Rath, S., & Gutjahr, W. J., "A math-heuristic for the warehouse location–routing problem in disaster relief", *Computers & Operations Research*, Vol 42, pp. 25-39 (2014).

[45] Abounacer, R. Rekik, M. & Renaud, R., "An exact solution approach for multi-objective location–transportation problem for disaster response", *Computers & Operations Research*, Vol. 41, pp. 83–93 (2014).

[46] Sheu, J. B., & Pan, C., "A method for designing centralized emergency supply network to respond to large-scale natural disasters", *Transportation Research Part B: Methodological*, Vol 67, pp. 284-305 (2014).

[47] Verma, A., & Gaukler, G. M., "Pre-positioning disaster response facilities at safe locations: An evaluation of deterministic and stochastic modeling approaches", *Computers & Operations Research*, Vol 62, pp. 197-209 (2015).

[48] Salman, F. S., & Gül, S., "Deployment of field hospitals in mass casualty incidents", *Computers & Industrial Engineering*, Vol 74, pp. 37-51 (2014).

[49] Caunhye, A. M., Li, M., & Nie, X., "A location-allocation model for casualty response planning during catastrophic radiological incidents", *Socio-Economic Planning Sciences*, Vol 50, pp. 32-44 (2015).

[50] Renkli, Ç., & Duran, S., "Pre-positioning disaster response facilities and relief items", *Human and Ecological Risk Assessment: An International Journal*, Vol 21 No. 5, pp. 1169-1185 (2015).

[51] Rath, S., Gendreau, M., & Gutjahr, W. J., "Bi-objective stochastic programming models for determining depot locations in disaster relief operations", I*nternational Transactions in Operational Research*, DOI: 10.1111/itor.12163 (2015).

[52] Kılcı, F., Kara, B. Y., & Bozkaya, B., "Locating temporary shelter areas after an earthquake: A case

for Turkey", *European Journal of Operational Research*, Vol 243 No. 1, pp. 323-332 (2015).

[53] Aydin, N., "A stochastic mathematical model to locate field hospitals under disruption uncertainty for large-scale disaster preparedness", *An International Journal of Optimization and Control: Theories & Applications (IJOCTA)*, Vol 6 No. 2, pp. 85-102 (2016).

[54] Tofighi, S., Torabi, S. A., & Mansouri, S. A., "Humanitarian logistics network design under mixed uncertainty". *European Journal of Operational Research*, Vol. 250 No.1, pp. 239-250 (2016).

[55] Sheu, J. B., "Dynamic relief-demand management for emergency logistics operations under large-scale disasters", *Transportation Research Part E: Logistics and Transportation Review*, Vol. 46 no. 1, pp. 1-17 (2010).

[56] Chi, T.H. Yang, H. & Hsiao, H.M., "A new hierarchical facility location model and genetic algorithm for humanitarian relief", *5th International Conference on New Trends in Information Science and Service Science (NISS) IEEE*, Vol. 2, pp. 367-374 (2011).

[57] Dantzig, G.B., "Planning under uncertainty", *Annals of Operations Research*, Vol. 85 pp.1-4, (1999).

[58] Google maps [online]. Available from: https://maps.google.com. [accessed 16 September 2013].

[59] TUIK [online]. Available from: http://www.tuik.gov.tr/UstMenu.do?metod=temelist. [accessed 13 September 2013].

[60] Balcik, B. & Ak, D., "Supplier selection for framework agreements in humanitarian relief", *Production and Operations Management*, Vol. 23 No.6, pp.1028-1071 (2013).

[61] KGM [online]. Available from: http://www.kgm.gov.tr/Sayfalar/KGM/SiteEng/Root/MainPageEnglish.aspx. Republic of Turkey General Directorate of Highways (KGM) [accessed 16 September 2013].

Erkan Celik *is an Assistant Professor in the Department of Industrial Engineering at Tunceli University, Tunceli, Turkey. He received BSc. and MSc. degree in Industrial Engineering from Selcuk University, Konya, Turkey in 2008 and 2011, respectively. He received PhD degree in Department of Industrial Engineering at Yildiz Technical University, Istanbul, Turkey in 2015. His research interests are in decision analysis, public transportation, humanitarian logistic and fuzzy sets.*

Nezir Aydin *is currently an Assistant Professor at the Department of Industrial Engineering at Yildiz Technical University/Istanbul/Turkey, which he joined in 2014. He received BSc. and MSc.in Industrial Engineering from Yildiz Technical University in 2005 and 2007, respectively. Later, he received a PhD degree in Industrial and Systems Engineering from Wayne State University/ Detroit/MI/USA. He worked as a researcher (in several projects) and an instructor (taught several graduate and undergraduate level courses) during his PhD studies. He is currently conducting projects related to his research area, which includes optimization, mathematical modeling, humanitarian logistics, decision making, supply chain management, and public transportation.*

Alev Taskin Gumus *is an Associate Professor in the Department of Industrial Engineering, Yildiz Technical University, Istanbul, Turkey. She received BSc and MSc in Industrial Engineering from Yildiz Technical University, MBA from Istanbul Technical University and PhD in Industrial Engineering from Yildiz Technical University. She completed post-doctoral research at Zaragoza Logistics Center, Spain. Her research interests are in supply chain management, public transportation, production and inventory systems, decision analysis, artificial intelligence and fuzzy logic applications in industrial engineering and management sciences.*

An International Journal of Optimization and Control: Theories & Applications
ISSN: 2146-0957 eISSN: 2146-5703
Vol.7, No.1, pp.16-27 (2017)
https://doi.org/10.11121/ijocta.01.2017.00358

RESEARCH ARTICLE

Constructing small WEEE collection system in Istanbul: A decision support system and conceptual design proposal

Vildan Çetinsaya Özkir*

Department of Industrial Engineering, Yildiz Technical University, Turkey
cvildan@yildiz.edu.tr

ARTICLE INFO

Article history:
Received: 16 June 2016
Accepted: 22 September 2016
Available Online: 12 October 2016

Keywords:
Collection network
multiple objectives
conceptual WEEE management system design
bi-objective spanning tree

AMS Classification 2010:
90B10, 90B50

ABSTRACT

The technological advances decrease electrical/electronic product lifecycles and boost consumption of high-tech products. The rapid growth in the electronic market produces electronic waste streams and potential threats arise on sustainability in terms of depleting natural resources and improper disposal. End-of-life electrical/electronic equipment (EEEs) involves complex mixture of materials, has hazardous content, and if not properly disposed, they can cause major environmental and health problems. To prevent the consequences of improper disposal, authorities and researchers conduct large-scale projects aligned with European union legislations. However, these efforts are still not sufficient to establish effective and organized systems due to the problem complexity and the need for specialized arrangements. This study proposes conceptual decision support framework and a bi-objective mathematical model to construct an effective collection network for end-of-life mobile phones. A real case study is presented for constructing an effective collection system in Istanbul. The main reason that we select Istanbul, is the requirement of urgency to deal with the large quantities of e-wastes. The result of this study will encourage academicians to conduct further research studies and strongly assist the authorities to configure well-structured e-waste collection system.

1. Introduction

The electronics industry is very dynamic and one of the fastest growing sectors of the world economy. This rapid growth of the electronics industry has serious effects on daily life in context of social, economic and environmental concerns. The rapid change in technology reduces product lifecycles and increases consumption of high-tech products. Besides the advantages of having technological products, many managerial problems arise for local authorities to solve, such as, Waste Electrical/Electronic Equipment (WEEE) management, social and economic consequences, etc.

An EEE completes its life cycle by passing through introduction, growth, maturity, decline, phase-out, and obsolescence stages, respectively [21]. Each stage has its own specific characteristics to manage effectively. Managing the opportunities and threats in the last phase requires the multidisciplinary effort, which incorporates legal, environmental, social, economic, and engineering views.

WEEEs are described as loosely discarded, surplus, obsolete, or broken electrical or electronic device in WEEE Directive (2002/96/EC). These useless devices often include both valuable and hazardous materials. Widmer et al. [23] emphasized that the ratio of valuable content in e-wastes is over %60 (gold, iron, copper, aluminum and other metal). Together with these valuable contents, e-wastes can contain many toxic materials such as lead, cadmium, beryllium, mercury, and brominated flame-retardants. The informal processing of these toxic materials can cause serious health problems. Regarding the opportunity of recovering valuable ingredients for reuse and diminishing threats of toxic materials on biological life, it is a mandatory requirement to design efficient e-waste management systems. WEEE Directive (2002/96/EC) and RoHS (the Restriction of Hazardous Substances) Directive (2002/96/EC) encourage systems aimed at improving the environmental performance of EEEs and reducing extravagant use of intact natural resources. WEEE directives encourage consumers, governments and producers to explore novel methods for reducing both the amount and

*Corresponding author

undesirable effects of e-wastes. Directive 2002/96/EC aimed at protecting the environment and human health by adapting environmentally conscious management strategies such as product design, separate collection, selective treatments and recycling, technical requirements of storage and treatment sites. Furthermore, Directive 2012/19/EU emphasizes the necessities for a separate e-waste collection system. Separate collection is a requirement for ensuring specific treatment and recycling of WEEE in order to achieve protection of human health and the environment. WEEEs, especially mobile phones, require specific treatment regarding to their users' behavior, material content, high consumption rates, and small sizes.

Owners generally discard their end-of-use EEEs in two different ways. Primarily, people often seek secondary markets if it is believed to preserve its inherent characteristics to fulfill functions in order to make value. Contrarily, if it is believed to be incapable of producing value, it is called an end-of-life product. The distinction between end-of-use EEE and end-of life EEE can mainly be explained related to this behavior. Goodship and Stevels [11] discussed that encouraging secondary market can offset the societal and environmental disadvantages of EEE industry. Thus, the extension of EEEs lifetime via secondary market generates both environmental benefits, in terms of reducing e-waste quantity and use of resources societal benefits, and societal benefits, in terms of employment and affordability of low-income individuals.

This study proposes a decision support model for constructing a WEEE collection system in Istanbul. This study contributes to an understanding of the literature on the association of user behaviors, legislations and regulations of legal authorities, system design and decision making issues. Additionally, the study assists decision makers in constructing coordinated separate collection system by providing a real case study. The rest of the paper is organized as follows: Section 2 presents a brief explanation of WEEE problem, particularly in Turkey. In Section 3, we explain conceptual decision support model and a bi-objective mathematical model to construct an effective collection network. In Section 4, a real case study is presented for constructing WEEE collection system in Istanbul. Obtained results and corresponding assessments are presented in this section. Finally, we conclude by summarizing the findings and present future research suggestions in Section 5.

2. Problem statement

2.1. WEEE material content

EEEs are mainly composed of valuable materials and toxic substances. Particularly, a mobile phone contains more than 40 elements, including N, O, F, S, B, C, H, K, Co, In, Zn, Al, Pb, Ag, Au, Ti, Pd, Cu, Ni, Fe, Mn, Sn and Sb. The metal content of a mobile phone is about 23% of total weight and the remaining is generally composed of plastics [2]. The plastic parts of mobile phones can also include heavy metal levels (Pb, Cd, Ni, and Ag). Nronom and Osibanjo [15] reported that, if managed appropriately, the levels in waste plastic housing of mobile phones do not constitute significant danger. The metals present in parts of mobile phone include precious metals (gold, silver, and palladium) as well as toxic metals such as iron, arsenic, cadmium, copper, lead, antimony, tin, palladium, gold, silver and bromine [23]. These metals can leach into soil and water when mobile phones are dumped in open landfill sites with municipal solid waste and pollute the natural environment [16]. Additionally, Goodship and Stevels [11] imply that a mobile phone has 15 or more high-tech materials that make separation challenging and volumes are not high enough to make reuse practical from a technical and economic point of view. However, UN Report [19] implies the economic benefits and environmental importance of urban mining for metal recovery, especially gold, silver and platinum. The precious metal content of a phone handset is in the order of milligrams only: 250 mg silver, 24 mg gold, 9 mg platinum while 9 g copper is present on average. Furthermore, the Li-ion battery of a phone contains approximately 3.5 g cobalt.

WEEE streams can be considered as precious metal mines. Approximately 250 mg silver, 24 mg gold, 9 mg palladium and 9 g. of copper can be obtained by parsing a scrap mobile phone without its battery. Hagelüken [13] implies that urban mining deposits can be much richer than primary mining ores. Considering the current available gold grade data varying between 1.04 g/ton and 14.44 g/ton in the gold reserves of Turkey, these streams require attention by means of innovative thinking, policy development and strategic planning. To take the advantage of recovering WEEE streams, considerable amount of multidisciplinary effort is needed. Accumulation of millions of discarded EOL product into urban mines of a reasonable size and recovery of low concentrated technology metals from complex products are challenging issues [13]. Moreover, the support of official policies and legislations plays a major role while settling up reliable collection and recovery systems. Assuring the security of personal data in data storing EEEs; such as laptops, mobile phones, etc., and ensuring people's trust to donate/leave their personal EOL products are further challenging subjects.

2.2. Challenges in WEEE management

WEEE Directive (2002/96/EC) categorizes EEEs in 10 different categories. Table 1 introduces these EEE categories and shows the distribution of tonnage of EEE placed on the market in 2010 by EEE categories. The first four categories - large household appliances, small household appliances, IT and telecommunications equipment and consumer equipment - accounts for almost %95 of the WEEE generated [21]. The main purpose of this classification is to support separate collection in order to facilitate e-

waste management and appropriate disposal of EEEs with similar risks to the environment and human health. Although these four e-waste categories constitute the vast majority of electronic waste, each category should be studied extensively due to their content, disposal options and collection strategy. Obviously, the content of each e-waste category, quantities and existent product recovery processes play a determining role while deciding on its management system design. For reducing the amount of any kind of resource needed for production, consumption, and waste disposal, Özkır and Başlıgil [18] introduced the process of efficient product recovery options.

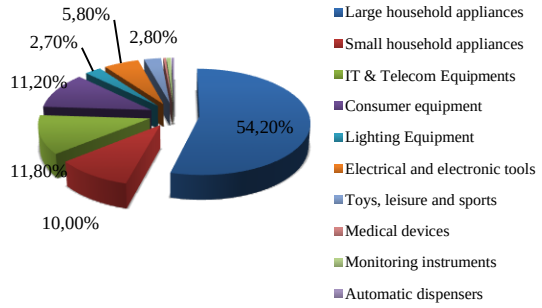

Figure 1. Distribution of tonnage of household and professional EEE placed on the market in 2010 (1,609 kt) by categories of equipment [1].

An extensive analysis on potential threats and opportunities of WEEEs is required before WEEE management system design. These threats and the opportunities can mainly be grouped under economic, societal and healthcare subjects. The main economic opportunity is the recovery of scarce and expensive materials needed for EEE production. The societal opportunities can be summarized as: new businesses on recovery, reuse and disposal operations can be created, new jobs can be described and accordingly unemployment can be decreased. Healthcare related opportunities are the vital ones, which is to prevent diseases emanated from improper disposal of WEEEs. The threats can be summarized as: destruction of scarce resources, compromise to sustainability and incurable diseases.

2.3. Challenges in Turkey and in worldwide

Turkey is officially recognized as a candidate country for full membership to European Union since 1999. Thus, design for WEEE management systems in Turkey is appealing for many researchers. Since the first four of WEEE categories constitutes the vast majority, we will analyze the problems for these categories in Turkey. A WEEE management system, fulfilling the requirements of WEEE Directive, has fundamental importance for Turkey, which is on the edge of European Union. Numerous challenges arise during the implementation phase of WEEE Directive, due to unequal development in operational and legislative progresses in member states [25]. On the other hand, socio-cultural factors play an important role while constructing a service system for a community. For example, people in city X may internalize the throwing-away culture for EEE products, while people in city Y prefer keeping-aside. Thus, the design of WEEE management systems for these cities can substantially be different each other.

Before submitting a system for people to use, the behaviors of people who will use this system need to be understood. Traditionally, Turkish people primarily prefer to give their end-of-use (working) EEEs to their relatives/ acquaintances. Secondarily, people generally follows 'bring the old one and get the new one' campaigns of companies. They leave their products and get new items to meet their requirements. Lastly, secondary market (generally, one of local repairmen) buys these products at low prices and sells them as second hand after minor refurbishments. If the case is for end-of-life EEEs, then secondary market works for component recovery to reuse (working) EEE parts. This process is valid for these four WEEE categories. This spontaneous process flow has several advantages like longer product lifecycles and some disadvantages while implementing regulations. However, this setting is slightly different in size from other WEEEs, ie. mobile phones. People do not assess enough about their end-of-use (working) mobile phones whether to keep it for contingency or to send it to trash. Due to their small size, it is more difficult to create control mechanisms to prevent the thrown away with normal household waste than the large appliances. So, instead of preventing the thrown away to household waste by banning, events should be organized to realize the change this behavior. Mobile phones can be easily stored and forgotten or thrown away with normal household waste due to their relatively small dimensions [4, 7].

Though technological developments increase WEEE amount, these advances, especially in recovery and logistics means, can be employed to reduce it. Ongondo et al. [17] stated that whereas advances in technology can help prevent waste at the production line, effecting change in human behavior is more difficult; therefore, their expectation is more WEEE to be generated rather than prevented at the consumer end of the spectrum. We refer Ongondo et al. [17] for further analysis and reading on the existing and the future perspectives of WEEE management.

World population has reached 7 billion. Considering the global mobile phone sales, the average volume of the last 6 years is around 1.5 billion/year as depicted in Figure 2, with the obsolescence rate about 2 years; the amount of EOL mobile phone is significantly high. The average volume of the last 6 years' mobile phone sales in Turkey is around 14 million/year. Considering the Turkey population is about 70 million, the amount of EOL mobile phone is considerably high.

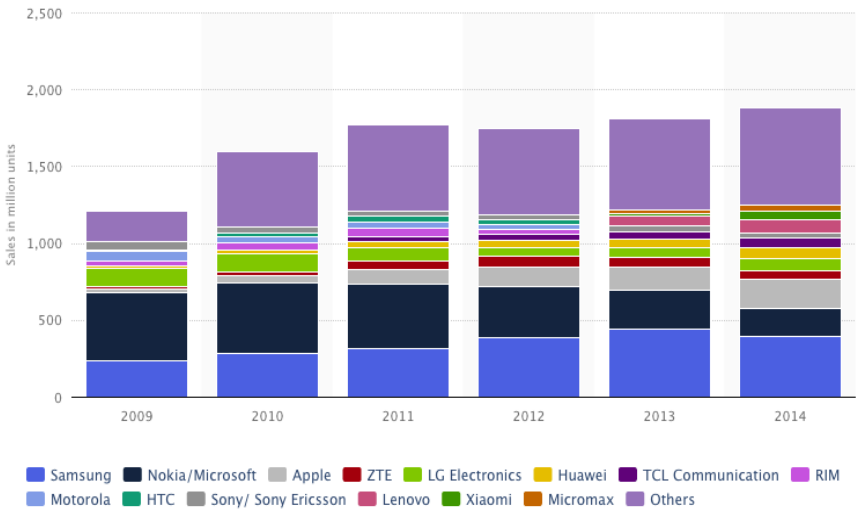

Figure 2. Global mobile phone sales to end-users each year from 2009 to 2014, broken down by vendor [26].

Consequently, the vast number of EOL mobile phones, the striking material content and other mentioned reasons attract the attention of researchers and practitioners in Turkey and Worldwide. Although the number of scientific studies and the founded organizations increase, the efforts are still not sufficient to establish organized systems due to the need for specialized arrangements. By considering the traditional Turkish behaviors, this study aims to support to establish an organized system for WEEE collection in İstanbul, Turkey.

3. Decision support model for WEEE collection system

Owing to fast consumption and obsolescence rates of EEEs, the volume of WEEEs is significantly increasing. Government institutions face compelling problems while constructing integrated systems for different WEEE types. The problem is dramatically critical and urgent for modern crowded cities because of high consumption and turnover rates of electronic products [5]. Therefore, the requirement for constructing an effective decision support system is more critical for metropolitan cities dealing with the large quantities of WEEE.

The relevant literature of WEEE collection network design and corresponding decision support models are investigated in Subsection 3.1. Then, in the proceeding subsections, conceptual framework and proposed decision support model for constructing WEEE collection network are explained, in detail, respectively.

3.1. Literature review

Collection is a critical stage to aggregate and divert the e-waste streams to the desirable treatment facilities. A reliable, safe and efficient collection system will motivate recycling activities and reduce costs [6]. Figueiredo and Mayerle [9] present a conceptual framework, an analytical model, and a three-stage algorithmic solution for the problem of designing minimum-cost recycling networks in in southern states of Brazil. Grunow and Gobbi [12] propose a modeling approach and the corresponding decision support tool aid the government agency in the assignment of collective schemes to municipalities where consumers deliver the waste in Denmark. Ongondo et al. [17] present an extensive research on WEEE management practices around the world. Gomes et al. [10] develop a generic model, which is applied to the design and planning of the Portuguese WEEE recovery network allowing for the definition of the best locations for collection and sorting centers that were chosen simultaneously with the definition of a tactical network planning. Kiddee et al. [14] investigate literature on e-waste management tools; such as, life cycle assessment, material flow analysis, multi-criteria analysis and extended producer responsibility and describes the distinctive features of approaches in different countries. Chi et al. [6] investigate the WEEE collection channels and household recycling behaviors in Taizhou city of China. Çetinsaya Özkır et al. [5] propose a three-stage methodology to initiate the e-waste management activities in Istanbul, Turkey, evaluates the status of current e-waste management efforts and encourages successive studies on creating guidelines and operations management.

3.2. Conceptual design for separate collection in metropolitan cities

WEEE directive (2012/19/EU) includes the provision of national WEEE collection points and processing systems, which allows consumers to put WEEE into a separate waste stream to other waste, resulting in it being processed, accounted for and reported to the national enforcement authority. The directive explains separate collection as a precondition for ensuring specific treatment and recycling of WEEE and is necessary to achieve the chosen level of protection of human health and the environment. Therefore, directive

encourages consumers to actively contribute to the success of such collection to return their end-of-use EEEs. For this purpose, convenient facilities should be set up for the return of WEEE, including public collection points, where private households should be able to return their waste at least free of charge (WEEE Directive - 2012/19/EU).

Setting up effective regulations and provisions concerning the organization of separate WEEE collection is problematic in metropolitan cities due to high population and their consumption behaviors. Daily life routine in a metropolitan city -getting to work, school, and appointments, shopping and socializing- is often exhausting for its residents. For this reason, while establishing an effective collection system for a metropolitan, the frequency and ease of access should also be considered for people living in the metropolis. In particular, the significant paradigm is to make WEEE holders being involved in the collection system without incurring cost and burden. As local authorities realize the importance of this paradigm, the collection system works efficiently by means of diverting material away from landfill and increasing contribution of these holders. Therefore, WEEE collection system should have collection points in public places such as, retail shops, central stations, shopping centers, etc. These points can boost WEEE holders' awareness of the need for separate collection. Figure 3 illustrates the flow of goods in WEEE collection system. If an end-of-use EEE is believed to be an EOL product, then it is accumulated in collection points for further processes, otherwise it is evaluated in the secondary market. Collection points collects the EOL products from users and delivers them to the inspection facilities for further exploration of available product recovery options. In inspection facilities, EOL products are inspected, classified and dispatched for landfill, hazardous waste treatment and recovery operations. In recovery facilities, the appropriate recovery decision is made for each WEEE regarding its current condition, and the result of the decision is concluded by demanufacturing, disassembling or refurbishing processes.

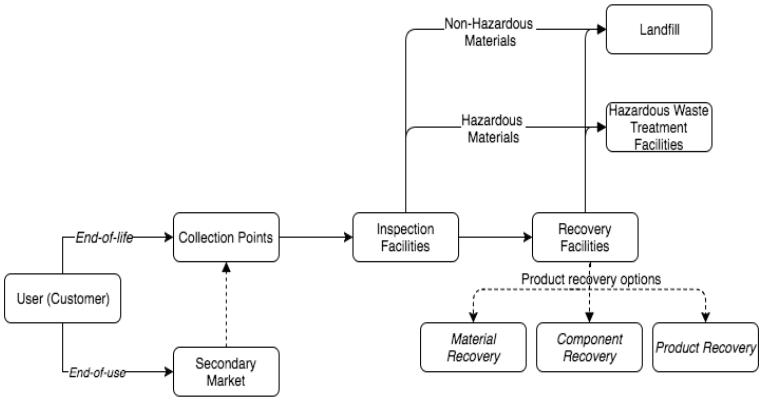

Figure 3. WEEE collection system.

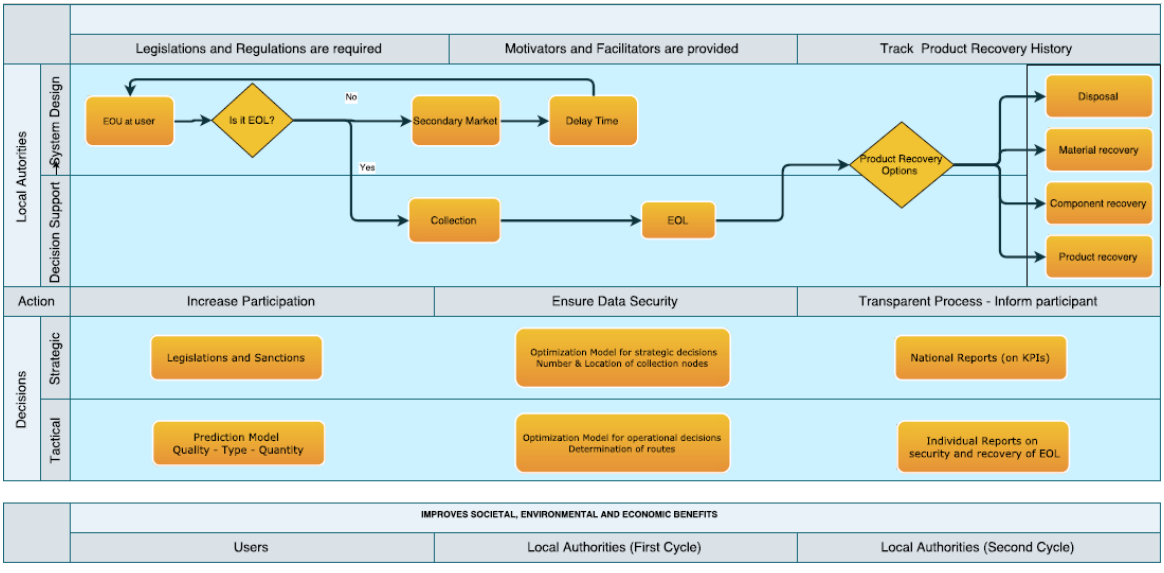

Figure 4. Conceptual design for WEEE collection system..

Moreover, only making legislations is not an adequate effort to prevent small WEEEs going into a landfill. Setting up effective control mechanisms and giving instructions on WEEE collection (leaflets, meetings and panels) are some of the required efforts to be conducted by authorities. Figure 4 summarizes the process, the objectives and related KPIs for a WEEE collection system.

KPIs are defined regarding the concerns of both WEEE holders and authorities. Ensuring data security and the transparent EOL product recovery processes are key expectations for WEEE holders. Furthermore, for authorities, increasing participation is the fundamental element to define the efficiency of the collection system. Additionally, we summarize tactical and strategic issues on modeling and designing the system components. Transparent process phase requires a front-end technology for informing WEEE holders about his individual processes and also for informing second cycle local authorities on system KPIs.

Furthermore, there are many opportunities in a WEEE collection system for authorities. They can support secondary market operations by providing regulations and legislations. Effective and organized secondary market operations can yield benefit to society by means of societal, environmental and economic benefits.

3.3. Multiple objective spanning tree model

The multi-objective minimum spanning tree problem is one of the best-known multi-objective combinatorial optimization problems (Neumann, 2007). In contrast to the single objective spanning tree problem, the objective function $f: \mathcal{T} \to \mathbb{R}^p$ is vector-valued, i.e., composed of component functions $f_k: \mathcal{T} \to \mathbb{R}$. We refer reader the survey of Ruzika and Hamacher [20] for an extensive literature review of algorithms for the MOST problem, and Ehrgott and Gandibleux [8] for further mathematical background of multiple objective combinatorial optimization problems.

Let $G = (V, E)$ be an undirected graph with vertex set $V = \{v_1, \dots, v_n\}$ and the edge set $E = \{e_1, \dots, e_m\}$ where $e_j = (v_{i1}, v_{i2})$ is an unordered pair of vertices. Let $c: E \to \mathbb{R}^p$ be the vector-valued cost function on the edge set. A spanning tree of G is a connected, acyclic subgraph $T \sqsubseteq G$, $T = (V(T), E(T))$, with vertex set $V(T) = V$. Let $\mathcal{T}$ denote the set of spanning trees of a given graph G. The general multi-objective minimum spanning tree (MOST) problem is defined as:

$$\begin{aligned} &Minimize\ f(T) = \left(f_1(T), \dots, f_p(T)\right) \\ &s.t. \qquad T \in \boldsymbol{\mathcal{T}} \end{aligned} \tag{1}$$

Minimum spanning tree models are widely studied in the literature. In this study, we propose a bi-objective spanning tree model for WEEE collection design. Let x_{ij} be 1 if the edge ij is in the tree T. Any subset of k vertices must have at most $(k-1)$ edges contained in that subset S.

$$Min.\ Z_1 = \sum_{ij \in E} d_{ij} x_{ij} \tag{2}$$

$$Min.\ Z_2 = \sum_{ij \in E} p_{ij} x_{ij} \tag{3}$$

$$s.t. \quad \sum_{ij \in E} x_{ij} = n - 1 \tag{4}$$

$$\sum_{ij \in E: i \in S, j \in S} x_{ij} \le |S| - 1 \quad \forall S \subseteq V \tag{5}$$

$$x_{ij} \in \{0,1\} \quad \forall i, j \in E \tag{6}$$

where d_{ij} is the distance between vertex i and vertex j, and p_{ij} is the total population size in vertices i and j. Equation (2) presents the primary objective function aiming to minimize the total distance. In Equation (3), total population covered by the edges is maximized in order to imply the contribution of individuals to the collection system. The district population data encourages constructing a demographically informed spanning Equation (4) ensures $(n-1)$ edges in T and Equation (5) is the sub-tour elimination constraint. Finally, binary variables are introduced in Equation 6.

3.4. Entropy embedded fuzzy AHP

The analytical hierarchy process is a well-known multiple criteria decision making method that is used for complex decision making problems. In the literature, several fuzzy extensions of the AHP method are presented in order to evaluate alternative candidates regarding individual subjective decision criteria under an uncertain decision environment.

The computational procedure of entropy embedded fuzzy AHP is summarized as follows:

Step 1. *Determine the alternatives* by ensuring that all the potential alternatives are listed.

Step 2. *Determine the evaluation criteria* by ensuring that all criteria are distinct and required for assessing alternatives through the goal definition.

Step 3. *Employ data acquisition process* by providing contribution of each decision maker as in the following:
Decision makers are asked to express their assessments in pairwise comparison (PC) using the scale in Table 1.

Corresponding assessment are represented in triangular fuzzy numbers, since these numbers are generally utilized to improve fuzzy decision making methods in order to handle uncertainty. A triangular fuzzy number is generally determined by the triplet $\widetilde{M} = [l, m, u]$ of crisp number with $(l \le m \le u)$ and whose membership function is given by

$$\mu_M(x) = \begin{cases} \dfrac{(x-l)}{(m-l)}, & if\ l \le x \le m \\ \dfrac{(u-x)}{(u-m)}, & if\ m \le x \le u \\ 0, & otherwise \end{cases} \tag{7}$$

Table 1. Fuzzified nine-point scale.

Intensity of Importance		Fuzzy Triangular Form of Importance	
		$\alpha = 0{,}50$	$\alpha = 0{,}75$
$\tilde{1}$	[1,2]	(1,1,1) / (1,1,2)	(1,1,1) / (1,1,3/2)
$\tilde{3}$	[2,4]	(2,3,4)	(5/2,3,7/2)
$\tilde{5}$	[4,6]	(4,5,6)	(9/2,5,11/2)
$\tilde{7}$	[6,8]	(6,7,8)	(13/2,7,15/2)
$\tilde{9}$	[8,9]	(8,9,9)	(17/2,9,9)

Triangular fuzzy numbers in (l, m, u) form can be expressed as an interval of confidence level is α $\forall\alpha \in [0,1]$, as in the following Equation 8.

$$\begin{aligned}\widetilde{M} &= [l^{\alpha}, u^{\alpha}] \\ &= [(m-l)\alpha + l, -(u-m)\alpha + u]\end{aligned} \quad (8)$$

Here, we employ the interval weight normalization procedure proposed by Wang and Elhag [22]. Let $w_i = [w_i^L, w_i^U]$ be interval weights where $0 \le w_i^L \le w_i^U$, $i = 1, \dots, n$ and N be a set of normalized weight vectors, based on the following definition of normalization for interval weights, where $N = \{X = (x_1, \dots, x_n,)\ | w_i^L \le x_i \le w_i^U,\ i = 1, \dots, n,\ \sum_{i=1}^{n} x_i = 1\}$. For more detailed information, we refer the reader to Wang and Elhag [22]. Here, c denotes the number of sub-criteria under the main criterion s. We denote an importance weight vector for each main criterion by $\widetilde{W}_{sc} = [w_1, w_2, \cdots, w_c]$, where S is the total number of main criteria.

Step 4. *Aggregation of decision makers' assessments.* Let $\tilde{x}_{ac}^{d} = (l_{ac}^{d}, m_{ac}^{d}, u_{ac}^{d})$ represents the triangular fuzzy number corresponding assessment of decision maker d on alternative a regarding the criterion c. We associate all assessments of decision makers' by introducing a new fuzzy number, say $\tilde{x}_{as}$, for the assessment of alternative a regarding criterion c.

$$\tilde{x}_{ac} = [\min(l_{ac}^{d}), E(m_{ac}^{d}), \max(u_{ac}^{d})] \quad \forall d \in D \quad (9)$$

Step 5. *Utilize Fuzzy AHP Method to assemble the total fuzzy judgment matrix $\tilde{A}$.* We multiply the importance weight vector w_{sc} by the corresponding column of fuzzy judgment matrix $\tilde{X}$.

$$\tilde{\mathrm{A}} = \left[\tilde{a}_{ij}\right]_{S \times A} \quad (10)$$

$$\tilde{a}_{sa} = \sum_{s} W_{sc} \sim x_{ac} \quad (11)$$

Step 6. *Employ interval arithmetic and optimism index* to perform fuzzy number multiplications and additions using the interval arithmetic and cuts. For any α-cut, we set an optimism index λ to understand the interaction between the decision maker's behavior and the selection process.

$$\hat{a}_{ij}{}^{\alpha} = (1-\lambda)\hat{a}_{ij}{}^{\alpha} + \lambda\hat{a}_{ij}{}^{\alpha} \quad \forall\lambda \in [0,1] \quad (12)$$

Step 7. *Utilize Shannon's entropy to find the aggregated weights.* The matrix $\hat{A}$ is normalized to obtain the matrix $A = [a_{ij}]$ by using Eq.13. Next; the entropies are calculated as in Eq.14.

$$A = [a_{ij}] = \left[\frac{\hat{a}_{ij}{}^{\alpha}}{\sum_{j=1}^{m} \hat{a}_{ij}{}^{\alpha}}\right] \quad (13)$$

$$H_i = -\sum_{j=1}^{n} a_{ij}{}^{\alpha} log_2\left(a_{ij}{}^{\alpha}\right) \quad (14)$$

Step 8. *Rank alternatives.* Alternatives are listed in accord to their entropy values in decreasing order. The higher entropy value means the better alternative; the highest is the best.

The entropy-embedded fuzzy AHP approach is appropriate for selecting the best alternative among a number of candidates.

4. Case Study: Constructing WEEE collection network in Istanbul

Istanbul is the economic, cultural, and historical metropolitan in Turkey, with the population of 14.03 million. The city possesses many qualified historical and modern malls. These shopping centers can be potential collection points considering their annual and daily number of visitors. The daily average number of visitors varies between 30,000 and 150,000. There are also many possible locations to set up collection points, such as central stations, squares, and etc. However, these alternative locations require extra investment in terms of security, controllability, and infrastructure. Considering security and structural investments of shopping centers, they satisfy the major requirements for a collection point, by default.

Çalışkan et al. [3] investigated the spatial diffusion of capital accumulation regime together with its triggering factors with special emphasis to the relations in between and revealed that in terms of spatial proximity, shopping centers set up the greatest relationship with luxury estates, residences and public housing areas, respectively. Considering these findings, the popularity of shopping centers and listed cost criteria, supports the idea of setting up collection points in shopping centers. In Figure 5, red-dots show shopping centers and the general distribution among the city, İstanbul.

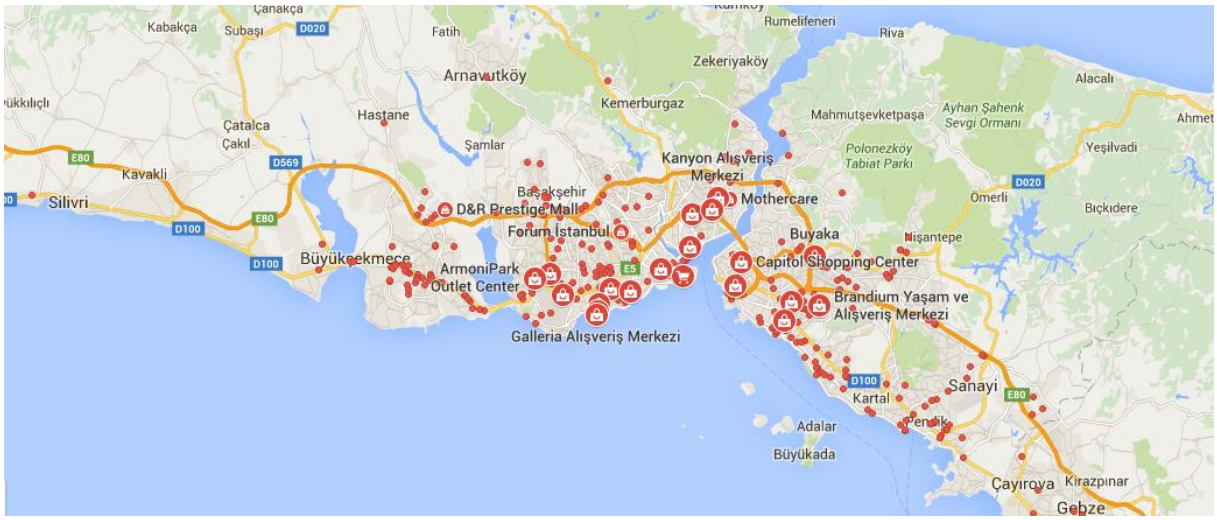

Figure 5. The locations of shopping centers in Istanbul.

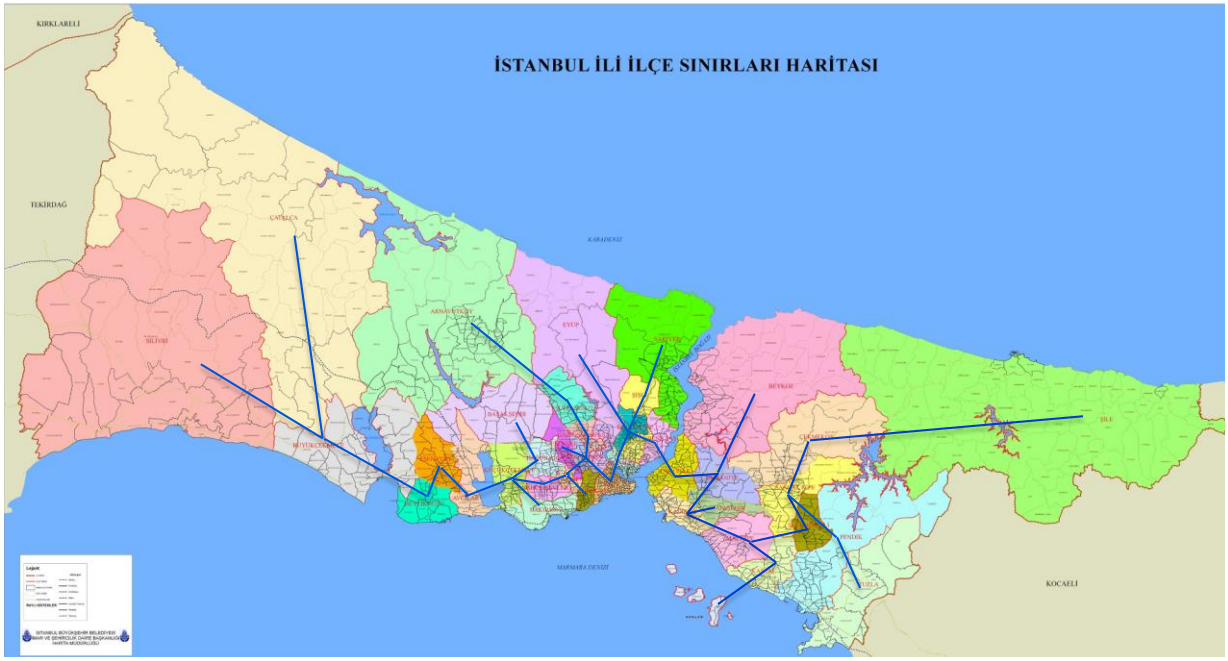

Figure 6. The spanning tree of small WEEE collection network.

In this study, we propose to collect EOL mobile phones due to its vast quantity, small size and remarkable material content. Therefore, the number of scientific studies and the founded organizations increase in the field. However, the efforts are still not sufficient to establish organized systems due to the need for specialized arrangements [5]. District municipalities are performing collection activities independently from each other. They collect nearly all kinds of WEEEs together in a truck by travelling in their district.

Furthermore, these collected items do not follow a systematic and organized route along their reverse flow in the supply chain.

This case study includes two consecutive decision aiding methods to solve the problem. The main objective of this study is to construct a connected network among districts of Istanbul. The network model constructs minimum spanning tree with maximum population weighted arcs.

As a consequence of the problem definition, the results of prior analysis have raised a new problem domain that needs continued investigation. In case of determining any district that have more shopping centers, then a further analysis is required to select among them. Therefore, a multiple criteria decision aid method is utilized introducing new set of criteria except previously considered criteria: distance and population.

4.1. The bi-objective spanning tree model for Istanbul

Primarily, a bi-objective spanning tree model is employed to construct a collection network for these WEEEs. Istanbul has totally 39 districts in its borderlines. The 25 of 39 are in European side and the remaining 14 are located in the Asian side. The distances between districts are obtained from the

Google Maps Directions API. The populations of each district are obtained from Turkish Statistical Institute (http://www.turkstat.gov.tr/). The mathematical model can be given as in the following:

$$Min.\ Z_1 = \sum_{ij \in E} d_{ij} x_{ij} \quad (15)$$

$$Max.Z_2 = \sum_{ij \in E} p_{ij} x_{ij} \quad (16)$$

$$s.t. \quad \sum_{ij \in E} x_{ij} = 39 - 1 \quad (17)$$

$$\sum_{ij \in E: i \in S, j \in S} x_{ij} \leq |S| - 1 \quad \forall S \subseteq V \quad (18)$$

$$x_{ij} \in \{0,1\} \quad \forall ij \in E \quad (19)$$

where x_{ij} be 1 if the district i is connected to district j, 0 otherwise. Here, d_{ij} is the distance between the district i and j, and p_{ij} is the total population size in the district i and district j.

We have utilized ∈-constraint method to solve multiple objective mathematical method. The main reason that we use ∈-constraint method is to eliminate the scaling problem. Additionally, we prefer to present the results of mathematical model with an illustration of connected network on the city map as in Figure 6. Figure 6 implies the shopping centers close to these intersection nodes have high potential in the sense of collecting more small WEEEs. In the European side of the city, the shopping centers in Büyükçekmece, Bayrampaşa, Güngören and Kağıthane districts are superior to the others in terms of population coverage and accessibility cost (defined in kilometers). In the Asian side of the city, the shopping centers in Ümraniye, Kadıköy, Maltepe and Sancaktepe districts has more potential in terms of these criteria. Here, we can list our assumptions as:

1. Shopping centers in the same district have equal population coverage.

2. Population in a district lives in the geographical center of this district.

3. People visit the shopping centers more frequently in the same district that they live.

Regarding these results, we investigated shopping centers in the determined districts. Before, we listed the shopping centers in these districts. Sancaktepe, Maltepe and Kağıthane districts have only one shopping center in its borderlines. Bayrampaşa and Güngören are the districts, which each has two shopping centers in its borderlines. Kadıköy and Ümraniye has respectively four and five shopping centers in their borderlines. According to the quantities of shopping centers in each district, Kadıköy and Ümraniye requires an additional analysis to select the best location. Consequently, we utilized a fuzzy multiple criteria decision aid method to select the appropriate shopping centers for Kadıköy and Ümraniye districts. Rather than utilizing the crisp methods, fuzzy extension is utilized in order to handle uncertainty in the decision environment.

4.2. Entropy embedded fuzzy AHP model for Kadıköy and Ümraniye districts

For further analysis, a group of five decision makers, including 3 experts from metropolitan municipality and 2 experts from a university provide the evaluation criteria and judgments in pairwise comparisons. For ranking alternative shopping centers, they define 4 criteria in regard to previous objectives: distance and population coverage weight. These criteria are rental fee, public transport availability, attractiveness, variety of shops and financial strength. Figure 7 illustrates the AHP decision hierarchy for Ümraniye district. The only difference between two districts' decision hierarchy is that the number of alternatives becomes 4 for Kadıköy.

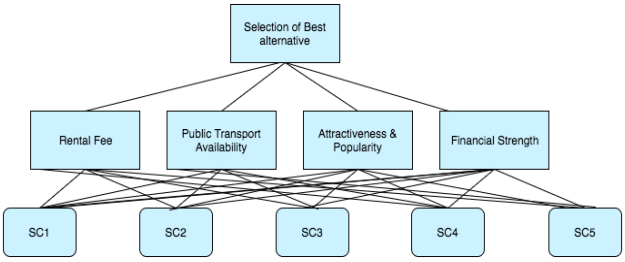

Figure 7. Decision hierarchy for selecting the best location in Ümraniye.

A brief explanation of evaluation criteria can be given as in the following: *Rental fees (RF)* are associated with cost. *Public transport availability (PT)* describes the proximity of shopping center to public transport node. Some shopping centers may also have metro/bus stations in it. A shopping center is said to be *attractive and popular (AP)*, if it has a variety of shopping options and entertainment facilities; such as gourmet concepts, theatres, cinema saloons, play lands for kids, performing arts showplaces etc. *Financial strength (FS)* is a vital concern of business owners, corporate managers and investors. Financial strength can be evaluated as an aggregated performance of a shopping center in terms of profitability, liquidity and investments.

For deciding on the most appropriate shopping centers in both Ümraniye and Kadıköy, we first asked decision makers to provide associated judgments on criteria evaluations. The fuzzy PC matrix is given in Eq. 20.

$$\tilde{X} = \begin{bmatrix} \tilde{1} & \tilde{3} & \tilde{5} & \tilde{3}^{-1} \\ \tilde{3}^{-1} & \tilde{1} & \tilde{1} & \tilde{3}^{-1} \\ \tilde{5}^{-1} & \tilde{1} & \tilde{1} & \tilde{7}^{-1} \\ 3 & \tilde{3} & 7 & \tilde{1} \end{bmatrix} \quad (20)$$

By employing the interval weight normalization procedure [22], we calculate the importance weight vector as: $W_s = [0.2667, 0.1333, 0.0667, 0.5333]$. We collected the decision makers' assessments on each shopping centers regarding four main criteria. They assigned degrees of importance by using a nine-point scale in regard to scale in Table 1and these assessments are consolidated by using Eq. 9. Then; we utilized fuzzy AHP method assemble the total fuzzy judgment matrix.

After that, we investigate the changes in results for varying alpha and lambda levels, which correspond to varying confidence levels and the risk attitudes, respectively. In appendix A, we provide final aggregated entropy weights to rank the alternatives for varying levels of alpha (0.1, 0.25, 0.50, 0.75, 0.9) and for varying levels of lambda (0, 0.25, 0.50, 0.75, 1.00) in Table 2 and Table 3. We illustrate our findings for each lambda level with column charts in Fig.8 and Fig.9 for Ümraniye and Kadıköy districts, respectively.

For Ümraniye, the best alternative is determined as U-SC3 according to the weights derived from entropy based fuzzy AHP. For the most levels of lambda, U-SC3 is superior to remaining alternatives.

The best alternative for Kadıköy is determined as K-SC2 according to the weights derived from entropy based fuzzy AHP. According to the rankings for any lambda level, K-SC2 is superior to remaining alternatives.

5. Conclusion and recommendations

Electronics market is the fastest growing market around the world, as in Turkey. Mobile phones are one of the leading electronic products in replacement with their short life cycles. Constructing separate streams for EOL mobile phones is crucial for preventing them thrown away with normal household waste and ensuring product/data security issues. The vast amount, the precious material content, the ease of portability and storability of EOL mobile phones are some of the striking characteristics of these products to take urgent action. These reasons attract the attention of researchers and practitioners in Turkey and in Worldwide.

However, setting effective regulations to manage separate WEEE streams, especially small sized WEEEs, is very challenging in a metropolis due to high population and complex demographics of residents'. A reliable, safe and efficient collection system will initiate the reverse flow of EOL products and will encourage product recovery activities by reducing costs.

In Istanbul, the reverse flow of EOL products do not follow a systematic and organized route and reverse logistic activities of district municipalities are not coordinated. The main contribution of this study is to support decision makers in constructing coordinated separate collection system in the districts of Istanbul. This study proposes to utilize shopping malls as collection points for EOL mobile phones. In this study, we investigate the challenges in WEEE management both in Turkey and worldwide. Next, we propose a conceptual design framework including key performance indicators, strategic and tactical decisions, system design and decision support concerns for constructing WEEE collection system. Then, we solved a bi-objective spanning tree model and entropy embedded fuzzy AHP method for determining the locations of collection nodes and understanding the possible flow of EOL product. Finally, we conclude by introducing the potential districts.

We encourage future research studies and practical implications since both efforts are still insufficient. Further practical implication of this study is to determine the collection and truck capacities for partial routes. Future research studies, the subjects can be listed as in the following: feasibility studies for separate WEEE collection, WEEE management strategies, data security, WEEE specialized vehicle routing and capacity planning problems.

Acknowledgments

The authors would like to thank the anonymous reviewers for their valuable comments.

Appendices

Table 2. Final aggregated entropies to rank shopping centers in Ümraniye

Lambda	*0*					*0.25*					*0.5*					*0.75*					*1*				
Alpha	*0.1*	*0.25*	*0.5*	*0.75*	*0.9*	*0.1*	*0.25*	*0.5*	*0.75*	*0.9*	*0.1*	*0.25*	*0.5*	*0.75*	*0.9*	*0.1*	*0.25*	*0.5*	*0.75*	*0.9*	*0.1*	*0.25*	*0.5*	*0.75*	*0.9*
U-SC1	1.54	1.55	1.56	1.56	1.56	1.56	1.57	1.57	1.57	1.57	1.58	1.58	1.58	1.58	1.57	0.92	0.91	0.89	0.85	0.83	1.61	1.61	1.60	1.60	1.59
U-SC2	1.47	1.53	1.60	1.66	1.69	1.58	1.60	1.62	1.65	1.68	1.64	1.64	1.64	1.65	1.67	1.38	1.33	1.24	1.16	1.15	1.71	1.70	1.67	1.64	1.61
U-SC3	1.60	1.62	1.65	1.67	1.68	1.66	1.67	1.67	1.68	1.69	1.70	1.70	1.70	1.69	1.69	1.54	1.53	1.50	1.46	1.44	1.75	1.74	1.73	1.71	1.70
U-SC4	1.58	1.59	1.60	1.60	1.61	1.60	1.60	1.61	1.61	1.61	1.61	1.61	1.61	1.61	1.61	1.17	1.18	1.20	1.22	1.23	1.62	1.62	1.62	1.62	1.61
U-SC5	1.64	1.64	1.65	1.65	1.65	1.63	1.64	1.64	1.65	1.65	1.63	1.63	1.64	1.64	1.65	1.27	1.23	1.19	1.22	1.31	1.62	1.62	1.63	1.63	1.65

Table 3. Final aggregated entropies to rank shopping centers in Kadıköy

Lambda	*0*					*0,25*					*0,5*					*0,75*					*1*				
Alpha	*0,1*	*0,25*	*0,5*	*0,75*	*0,9*	*0,1*	*0,25*	*0,5*	*0,75*	*0,9*	*0,1*	*0,25*	*0,5*	*0,75*	*0,9*	*0,1*	*0,25*	*0,5*	*0,75*	*0,9*	*0,1*	*0,25*	*0,5*	*0,75*	*0,9*
K-SC1	1,81	1,79	1,74	1,69	1,66	1,73	1,73	1,71	1,68	1,66	1,67	1,68	1,68	1,67	1,67	0,97	1,04	1,12	1,19	1,22	1,58	1,60	1,63	1,65	1,67
K-SC2	1,71	1,72	1,73	1,74	1,75	1,73	1,73	1,73	1,74	1,75	1,74	1,73	1,73	1,73	1,73	1,58	1,55	1,50	1,45	1,45	1,75	1,74	1,72	1,70	1,68
K-SC3	1,42	1,47	1,53	1,57	1,59	1,53	1,55	1,57	1,59	1,60	1,60	1,60	1,60	1,60	1,60	1,30	1,28	1,24	1,20	1,17	1,67	1,66	1,65	1,63	1,61
K-SC4	1,53	1,53	1,53	1,53	1,52	1,59	1,58	1,56	1,54	1,53	1,62	1,61	1,58	1,55	1,53	1,19	1,13	1,01	0,87	0,77	1,66	1,64	1,61	1,57	1,54

References

[1] ADEME Annual report. Electrical and electronic equipments. Data 2010. [Accessed on 20 June 2015]. http://www2.ademe.fr/servlet/getBin?name=C1D8D3FB0D6D41BC332B8322BD6CDB1F_tomcatlocal1320332164546.pdf (2010).

[2] Arshadi, M. and S.M. Mousavi, Multi-objective optimization of heavy metals bioleaching from discarded mobile phone PCBs: Simultaneous Cu and Ni recovery using Acidithiobacillus ferrooxidans, Separation and Purification Technology, 147, 210-219 (2015).

[3] Çalışkan, Ç.O., Çılgın, K., Dündar, U. and M.C. Yalçıntan, İstanbul Dönüşüm Coğrafyası, Kentsel ve Bölgesel Araştırmalar Sempozyumu, 6-7 December 2012, Ankara, https://istanbuldonusumcografyasi.wordpress.com/bildiri-tam-metni/, [Accessed on December 13, 2015] (2012).

[4] Canning, L., Rethinking market connections: mobile phone recovery, reuse and recycling in the UK, Journal of Business & Industrial Marketing, 21 (5), 320–329, (2006).

[5] Çetinsaya Özkır, V., Efendigil, T., Demirel, T., Çetin Demirel, N., Deveci, M. and B. Topçu, A three-stage methodology for initiating an effective management system for electronic waste in Turkey, Resources, Conservation and Recycling, 96, 61-70, (2015).

[6] Chi, X., Wang M.Y.L., and M.A. Reuter, E-waste collection channels and household recycling behaviors in Taizhou of China, Journal of Cleaner Production, 80, 87-95, (2014).

[7] Darby, L. and L. Obara, Household recycling behaviour and attitudes towards the disposal of small electrical and electronic equipment, Resources Conservation and Recycling, 44 (1), 17–35, (2005).

[8] Ehrgott, M. and X. Gandibleux, Multiple Criteria Optimization: State of the Art Annotated Bibliographic Surveys, Kluwer Academic Publishers, Boston, (2002).

[9] Figueiredo, J.N., and S.F. Mayerle, Designing minimum-cost recycling collection networks with required throughput, Transportation Research Part E: Logistics and Transportation Review, 44 (5), 731-752, (2008).

[10] Gomes, M.I., Barbosa-Povoa, A.P., and A.Q. Novais, Modelling a recovery network for WEEE: A case study in Portugal, Waste Management, 31(7), 1645-1660, (2011).

[11] Goodship, V. and A. Stevels, Waste electrical and electronic equipment (WEEE) handbook", Woodhead publishing, Cambridge, UK, (2012).

[12] Grunow, M. and C. Gobbi, Designing the reverse network for WEEE in Denmark, CIRP Annals - Manufacturing Technology, 58(1), 391-394, (2009).

[13] Hagelüken, C., Towards bridging the materials loop – how producers and recyclers can work together, EU-US Workshop on Mineral Raw Material Flows & Data, 13, 2012, Brussels. (http://ec.europa.eu/enterprise/policies/rawmaterials/files/docs/three_hagelueken_eu_us_2012_09_en.pdf). [Accessed on July 7, 2015] (2012).

[14] Kiddee, P., Naidu, R., and M. H. Wong, Electronic waste management approaches: An overview, Waste Management, 33(5), 1237-1250, (2013).

[15] Nnorom, I.C. and O. Osibanjo, Toxicity characterization of waste mobile phone plastics, Journal of Hazardous Material, 161, 183–188, (2009).

[16] Oguchi, M., Sakanakura, H., Terazono, A., and H. Takigami, Fate of metals contained in waste electrical and electronic equipment in a municipal waste treatment process, Waste Management, 32, 96–103, (2011).

[17] Ongondo, F.O. Williams, I.D. and T.J. Cherrett, How are WEEE doing? A global review of the management of electrical and electronic wastes, Waste Management, 31(4), 714-730, (2011).

[18] Özkır, V. and H. Başlıgil, Modeling Product Recovery Processes in Closed Loop Supply Chain Network Design. International Journal of Production Research, 50(8), 2218-2233, (2012).

[19] Reuter, M. A., Hudson, C., van Schaik, A., Heiskanen, K., Meskers, C., Hagelüken, C., UNEP Metal Recycling: Opportunities, Limits, Infrastructure, A Report of the Working Group on the Global Metal Flows to the International Resource Panel, (2013).

[20] Ruzika, S., and Hamacher, H.W., "A survey on multiple objective minimum spanning tree problems". In J. Lerner, D. Wagner, and K. A. Zweig (Eds.), Algorithmics of Large and Complex Networks, Lecture Notes in Computer Science, 5515, 104–116, Springer, (2009).

[21] Solomon, R., Sandborn, P. and M. Pecht, Electronic Part Life Cycle Concepts and Obsolescence Forecasting, IEEE Transaction on Components and Packaging Technologies, 707-717, (2000).

[22] Wang, Y. and T.M.S. Elhag, "On the normalization of interval and fuzzy weights", Fuzzy Sets and Systems, 157, 2456 – 2471, (2006).

[23] Widmer, R., Oswald-Krapf, H., Sinha-Khetriwal, D., Schnellmann, M. and H. Böni, Global perspectives on e-waste, Environmental Impact Assessment Review, 25, 436-458, (2005).

[24] Yadav, S., Yadav,S. and P. Kumar, Metal toxicity assessment of mobile phone parts using Milli Q water, Waste Management, 34(7), 1274-1278, (2014).

[25] Ylä-Mella, J., Keiski, R.L., and E. Pongrácz, Electronic waste recovery in Finland: Consumers' perceptions towards recycling and re-use of mobile

phones, Waste Management, 45, 374-384, (2015).

[26] http://www.statista.com/statistics/270243/global-mobile-phone-sales-by-vendor-since-2009/ Statistica - Global mobile phone sales data [Accessed, 13 July 2015].

Vildan Çetinsaya Özkır (PhD) *is currently assistant professor in the Department of Industrial Engineering where she is teaching Operations Research 1-2, Numerical Analysis, Economics and Multiple Objective Decision Making courses. She received her BSc degree in industrial engineering, MSc in Systems Engineering and PhD in Industrial Engineering at Yıldız Technical University, Istanbul, Turkey. Her research interests are network models, multiple objective decision analysis, and environmentally conscious manufacturing/logistic systems.*

An International Journal of Optimization and Control: Theories & Applications
ISSN: 2146-0957 eISSN: 2146-5703
Vol.7, No.1, pp.28-34 (2017)
https://doi.org/10.11121/ijocta.01.2017.00334

RESEARCH ARTICLE

Copula approach to select input/output variables for DEA

Olcay Alpay [a *], Elvan Akturk Hayat [b]

[a] *Department of Statistics, Sinop University, Turkey*
[b] *Department of Econometrics, Adnan Menderes University, Turkey*
olcayb@sinop.edu.tr, elvan.hayat@adu.edu.tr

ARTICLE INFO

Article history:
Received: 5 April 2016
Accepted: 15 August 2016
Available Online: 25 October 2016

Keywords:
Data envelopment analysis
Variable selection
Copulas
Local dependence function

AMS Classification 2010:
90C30, 60E99

ABSTRACT

Determination of the input/output variables is an important issue in Data Envelopment Analysis (DEA). Researchers often refer to expert opinions in defining these variables. The purpose of this paper is to propose a new approach to determine the input/output variables, it is important to keep in mind that especially when there is no any priori information about variable selection. This new proposed technique is based on a theoretical method which is called "Copula". Copula functions are used for modeling the dependency structure of the variables with each other. Also we use the local dependence function which analyzes the point dependency of variables of copulas to define the input/output variables. To illustrate the usefulness of the proposed approach, we conduct two applications using simulated and real data and compare the efficiencies in DEA. Our results show that new approach gives values close to perfection.

1. Introduction

Data Envelopment Analysis (DEA) is a data oriented non-parametric method, introduced by Charnes et al. [1] to evaluate the relative efficiency of organizational units called as decision making units (DMUs) according to selected input and output variables [3]. Manufacturing units, departments of schools or hospitals, a set of firms or even practising individuals can be given as examples to DMUs [7].

Nowadays, institutions producing service or product, are obliged to have an effective performance because of intense competitive conditions and limited sources. Although efficiency of the DMU's depends crucially on input/output variables to be selected correctly, there is no any guidelines or systematic procedure to classify the variables. Many researchers often make such determination subjectively or using expert opinions. Some of them use the variables based directly on other's selection results according to calculated efficiency [8].

The issue of variable selection seems to be a subject rarely studied in the literature. Considering the studies over the last 15 years, it can be seen that Pastor et al. [9] defined a measure, namely ECM (efficiency contribution measure), to evaluate the input or output variables. In 2003, Jenkins and Anderson [10] proposed a systematic statistical approach to reduce the number of already defined input and output variables. Ruggiero [11] addressed the subject of input selection using regression analysis. Edirisinghe and Zhang [12] proposed a Generalized DEA approach to determine the type of variable via maximizing the correlation between DEA–based score of financial strength and stock market performance. In 2009, Morita and Avkiran [3] proposed a selection method utilizing diagonal layout design. Finally, Madhanagopal and Chandrasekaran [13] developed a genetic algorithm approach for the selection of input/output variables.

The approach we propose in this study takes into consideration distribution of data and the point dependency between candidate variables, which makes it distinctive amongst the others. Copulas and the local dependence function were used to achieve the correct discrimination of input/output variables. We assume that there is no any information or expert opinion to decide the input/output variables. Performance assessment of our proposed method was made by means of simulation, followed by a real data application. In this way, we were able to make comparison of the efficiencies of the new approach and those of the one based directly on expert opinion selection method for this study. The main goal of this

*Corresponding author

paper is to propose a new theory based approach to determine the input/output variables.

The paper is organized as follows: Section 2 gives a brief summary of the DEA models. In section 3 we define copulas (especially Farlie-Gumbel-Morgenstern "FGM" copula) and local dependence function. In this section an algorithm is also developed to determine the input/output variables. In Section 4, a simulation and a real data applications are conducted and results are evaluated. The last section gives the conclusions.

2. Data envelopment analysis (DEA)

Data envelopment analysis (DEA) is a linear programming based technique to calculate the relative efficiencies of a set of decision making units (DMUs) that have similar inputs and similar outputs. Also it is a non-parametric method as it does not require any assumption about functional form. This technique aims to measure how efficiently a DMU uses the resources available to generate a set of outputs [1]. DMUs can include manufacturing units, departments of big organizations such as universities, schools, bank branches, hospitals, power plants, police stations, tax offices, prisons etc.

The basic frontier model was developed by Charnes et al. [1] known as the CCR model, but now widely called as CRS (constant returns to scale) and was extended by Banker et al. [14] to include variable returns to scale (VRS). So the basic DEA models are known as CCR and BCC referred to as the VRS.

DEA models have two orientations: input-oriented and output-oriented. With input-oriented DEA, the linear programming model is constituted so as to determine how much the input use of a firm could contract if used efficiently in order to achieve the same output level. In contrast, with output-oriented DEA, the linear programme is constituted to determine a firm's potential output given its inputs if it operated efficiently as firms along the best practice frontier [15]. The input oriented model contracts the inputs as far as possible while controlling the outputs. The output oriented model expands the outputs as far as possible while controlling the inputs [16].

The original fractional CRS model Eq.(1) evaluates the relative efficiencies of n DMUs $j=1,\ldots,n$ each with m inputs and s outputs denoted by $x_{1j},x_{2j},..,x_{mj}$ and $y_{1j},y_{2j},..,y_{mj}$ respectively [1]. This is done so by maximizing the ratio of weighted sum of output to the weighted sum of inputs:

$$Max\theta_o = \frac{\sum_{r=1}^{s} u_r y_{ro}}{\sum_{i=1}^{m} v_i x_{io}}$$

s.t.

$$\frac{\sum_{r=1}^{s} u_r y_{rj}}{\sum_{i=1}^{m} v_i x_{ij}} \le 1,\ j=1,\ldots,n,\ r=1,\ldots,s \qquad (1)$$

$$u_r, v_i \ge 0 \text{ for all } r \text{ and } i$$

In model Eq. (1), θ_o is the efficiency of DMU_o and u_r and v_i are the factor weights. For computational convenience the fractional form Eq.(1) is re-expressed in linear program (LP) form as follows which is known asinput oriented CRS model:

$$Max\theta_o = \sum_{r=1}^{s} u_r y_{ro}$$

s.t.

$$\sum_{r=1}^{s} u_r y_{rj} - \sum_{i=1}^{m} v_i x_{ij} \le 0,\ j=1,\ldots,n \qquad (2)$$

$$\sum_{i=1}^{m} v_i x_{io} = 1$$

$$u_r, v_i \ge 0$$

The dual of linear program (LP) model for input oriented CRS model is as follows:

$$Min\theta_o$$

s.t.

$$\theta x_{io} \ge \sum_{j=1}^{n} \lambda_i x_{ij} \quad i=1,\ldots,m \qquad (3)$$

$$y_{ro} \le \sum_{j=1}^{n} \lambda_i y_{rj} \quad r=1,\ldots,s$$

$$\lambda_j \ge 0$$

The output-oriented CRS model is as follows:

$$Max\theta_o$$

s.t.

$$x_{io} \ge \sum_{j=1}^{n} \lambda_i x_{ij} \quad i=1,\ldots,m \qquad (4)$$

$$\theta y_{ro} \le \sum_{j=1}^{n} \lambda_i y_{rj} \quad r=1,\ldots,s$$

$$\lambda_j \ge 0$$

The CRS models (dual and primal) with input orientation are still the most widely known and used DEA models despite the numerous modified models that have appeared [17].

3. Copula, local dependence function and selection procedure

In general, copula is a function which helps re-define the joint distribution function using marginal distribution functions in I^2 when the random variables are dependent. In recent years, copulas have been involved in many studies such as statistics, economics, finance and risk management, dependence measuring, modeling, and serial dependence in time series [18].

Definition 1. *Let $C(u,v)$ is defined as a bivariate function in $I^2=[0,1]\times[0,1]$. If this function has the following properties, it is called as two-dimensional copula function.*

- $C(u,0)=C(0,v)=0$
- $C(u,1)=u$ *and* $C(1,v)=v,\ \forall(u,v)\in I$

For every $0\le u_1\le u_2\le 1$ *and* $0\le v_1\le v_2\le 1$

- $V_c([u,v])=C(u_1,v_1)- C(u_1,v_2)- C(u_2,v_1)+ C(u_2,v_2)\ge 0$

[4].

3.1. Local dependence function (LDF)

Let *X* and *Y* be random variables with marginal distribution functions *F(x), F(y)* and marginal probability density functions *f(x)* and *f(y)* respectively. The following function is obtained from the expression of the Pearson correlation coefficient by replacing mathematical expected values *E(X)* and *E(Y)* conditional expected values *E(X|Y=y)* and *E(Y|X=x)* [6].

$$H(x,y)=\frac{E\{(X-E(X\mid Y=y))(Y-E(Y\mid X=x))\}}{\sqrt{E\{(X-E(X\mid Y=y))^2\}}\sqrt{E\{(Y-E(Y\mid X=x))^2\}}} \quad (5)$$

H(x,y) can be referred as a local dependence function which characterizes the dependence between *X* and *Y* at the point *(x,y).* After simple mathematical transformation $\xi_X=EX-E(X|Y=y)$ and $\xi_Y=EY-E(Y|X=x)$ the equation Eq. (5) can be written as

$$H(x,y)=\frac{\rho+\Phi_X(y)\Phi_Y(x)}{\sqrt{1+\Phi_X^2(y)}\sqrt{1+\Phi_Y^2(x)}}$$

where

$$\rho=\frac{Cov(X,Y)}{\sigma_X\sigma_Y}$$

$$\Phi_X(y)=\frac{\xi_X(y)}{\sigma_X} \qquad \Phi_Y(x)=\frac{\xi_Y(x)}{\sigma_Y}$$

[5].

Local dependence function has the following properties

1. If *X* and *Y* are independent, then $H(x,y)=0$ for all $(x,y)\in N_{X,Y}$.
2. $|H(x,y)|\le 1$, for all $(x,y)\in N_{X,Y}$.
3. If $|H(x,y)|=1$ for some $(x,y)\in N_{X,Y}$, then $\rho\neq 0$.
4. If $\rho=\pm 1$, then $H(x,y)=\pm 1$.
5. If $H(x,y)=0$ for all $(x,y)\in N_{X,Y}$, then either $E(X|Y=y)$ or $E(Y|X=x)$ for all $(x,y)\in N_{X,Y}$ and $\rho=0$.

[6].

3.2. FGM copula

Farlie-Gumbel-Morgenstern (FGM) distribution was introduced by Morgenstern in 1956 with Cauchy marginal. This class was examined by Gumbel for exponential marginal and further generalized by Farlie in 1960 [19].

Let *(X,Y)* be absolutely continuous random variables. The general distribution function is defined as

$$F(x,y)=F(x)G(y)\{1+\alpha A(F(x))B(G(y))\} \quad (6)$$

where $A(x)\to 0$, $B(y)\to 0$ as $x\to 1$, *A(x)* and *B(y)* satisfy certain regularity conditions ensuring that the Eq. (6) is a distribution function with absolutely continuous marginal *F(x)* and *G(y)* [20].

FGM copula is a positive quadrant dependent (PQD) copula and the local dependence function is as follows;

$$H(x,y)=\frac{\alpha/3+\left(\alpha^2/3\right)(1-2x)(1-2y)}{\sqrt{\left[1+\left(\alpha^2/3\right)(1-2x)^2\right]\left[1+\left(\alpha^2/3\right)(1-2y)^2\right]}}$$

where α is the association parameter [5].

3.3. Quadrant dependence

Definition 2. *Let X and Y be random variables. X and Y are positive quadrant dependent (PQD) if all (x,y) variables in* R^2

$$P\{X\le x,Y\le y\}\ge P\{X\le x\}P\{Y\le y\}$$

or equivalently

$$P\{X>x,Y>y\}\ge P\{X>x\}P\{Y>y\}$$

Similarly, X and Y are negative quadrant dependent (NQD) if

$$P\{X\le x,Y\le y\}< P\{X\le x\}P\{Y\le y\}$$

or equivalently

$$P\{X>x,Y>y\}< P\{X>x\}P\{Y>y\}$$

[4].

3.4. Selection procedure

In this part of the study, we present a new algorithm to determine the input/output variables. The following algorithm explained in detail leads to the selection process.

Step-1: Determine the distribution of variables and construct the appropriate copula function (e.g. if the distribution is uniform the FGM is suitable).

Step-2: Construct the LDF of determined copula according to the method as described in Section 3.1.

Step-3: Determine the type of quadrant dependency of the copula mentioned in Section 3.3., to use to decide which group is selected as input/output.

Step-4: Calculate the LDF values for pairwise variables. The variables which have $Max|H(X_i,X_j)|$, selected as reference variables (x_{r1} and x_{r2}) and assign them two separate groups (*Group-1* and *Group-2*). Allocate the rest of variables to the groups according to the following procedure:

If $|H(x_i, x_{r1})|>|H(x_i, x_{r2})|$(where $x_i\neq x_{r1}$ and $x_i\neq x_{r2}$) then x_i is assigned to the Group-1 else it is assigned to the Group-2.

Step-5: Make predetermination about whether the study is input or output oriented.

Step-6: Determine the sign of LDFs which is calculated between the each of the rest of the variables and the reference variables for two separate groups constructed in Step-4.

a. *Suppose that study is input oriented and copula is PQD,*

i. If one of the groups has only positive LDFs and other has only negative, then choose the variables in group which has positive LDFs as input variables.

ii. If all of LDFs are positive in each group, then select the variables in group which has $MaxH(X_i,X_j)$

as input variables. If all of LDFs are negative in each group, then select the variables in group which has $Min|H(X_i,X_j)|$ as input variables.

iii. If groups contain different sign LDFs, then select the variables in group which has $Min|H(X_i,X_j)|$ as input variables.

b. *Suppose that study is input oriented and copula is NQD,*

i. If one of the groups has only positive LDFs and other has only negative, then choose the variables in group which has negative LDFs as input variables.

ii. If all of LDFs are positive in each group, then select the variables in group which has $MinH(X_i,X_j)$ as input variables. If all of LDFs are negative in each group, then select the variables in group which has $Max|H(X_i,X_j)|$ as input variables.

iii. If groups contain different sign LDFs, then select the variables in group which has $Min|H(X_i,X_j)|$ as input variables.

c. *Suppose that study is output oriented and copula is PQD,*

i. If one of the groups has only positive LDFs and other has only negative, then choose the variables in group which has positive LDFs as output variables.

ii. If all of LDFs are positive in each group, then select the variables in group which has $MaxH(X_i,X_j)$ as output variables. If all of LDFs are negative in each group, then select the variables in group which has $Min|H(X_i,X_j)|$ as output variables.

iii. If groups contain different sign LDFs, then select the variables in group which has $Min|H(X_i,X_j)|$ as output variables.

d. *Suppose that study is output oriented and copula is NQD,*

i. If one of the groups has only positive LDFs and other has only negative, then choose the variables in group which has negative LDFs as output variables.

ii. If all of LDFs are positive in each group, then select the variables in group which has $MinH(X_i,X_j)$ as output variables. If all of LDFs are negative in each group, then select the variables in group which has $Max|H(X_i,X_j)|$ as output variables.

iii. If groups contain different sign LDFs, then select the variables in group which has $Min|H(X_i,X_j)|$ as output variables.

Step-7: Run the DEA model and calculate the efficiencies.

4. Application

In this part of the study, a simulation and a real data example have been conducted and DEA have been performed using the package program DEAP 2.1. The data for simulation study were generated from Uniform (0,1) and FGM copula was selected to represent them. We used the Yoluk's [2] data set for the real data example.

4.1. Simulation study

In simulation part of the study, we use five variables and 20 decision making units. Table 1 shows the min, max and absolute values of LDFs.

Table 1. Values of local dependence function.

Pairs of variables	$MinH(X_i,X_j)$	$MaxH(X_i,X_j)$	$\|H(X_i,X_j)\|$
X_1-X_2	0.0613	0.0845	0.0845
X_1-X_3	0.1111	0.2274	0.2274
X_1-X_4	0.0367	0.0431	0.0431
X_1-X_5	-0.0083	-0.0080	0.0083
X_2-X_3	0.0668	0.0956	0.0956
X_2-X_4	0.1348	0.2156	0.2156
X_2-X_5	-0.0851	-0.3029	0.3029
X_3-X_4	0.1482	0.3355	0.3355
X_3-X_5	0.2226	0.0980	0.2226
X_4-X_5	-0.4272	-0.1590	0.4272

Maximum local dependency value is between X_4 and X_5 ($Max|H(X_i, X_j)|$=0.4272). So these variables are selected as reference. Allocated variables according to descending of $Max|H(X_i, X_j)|$ are given below.

Group 1	*Group 2*
X_4	X_5
X_3	X_2
X_1	

$H(X_2,X_5)<0$ and $H(X_1,X_4)$, $H(X_3,X_5)>0$

Suppose that the study is input oriented. So variables in Group 1 are the input variables. DEA results as follows

Table 2. Efficiency scores.

DMU	Efficiency	DMU	Efficiency
1	0.144	11	0.428
2	0.213	12	0.472
3	1.000	13	1.000
4	1.000	14	1.000
5	0.905	15	0.755
6	0.322	16	0.367
7	0.688	17	0.136
8	0.521	18	1.000
9	0.306	19	1.000
10	0.840	20	0.883

4.2. Real data application

In this part of the study we use Yoluk's [2] hospital data given in Table 3. The efficiency analysis was performed as input oriented and the first three variables were taken as input, the last four variables were taken as output variables. We assume that we have no any information about the variables and are not able to get an expert opinion. Firstly, we tested the goodness of fit for all variables to the Uniform distribution and found no departures from the hypothesized distribution. At the second stage the LDF values for FGM copula were computed on these variables standardized to Uniform (0,1) and results

were given in Table 4. Variables have been classified with these values according to the proposed algorithm. The efficiency scores of our approach and Yoluk's results are given in Table 5.

Table 3. Values of real data.

DMU	X_1	X_2	X_3	X_4	X_5	X_6	X_7
1	779	360	599	1691527	33685	52095	199291
2	776	421	807	1510740	40175	52890	266637
3	1090	544	1092	1231625	61132	68642	376193
4	680	431	602	1545480	32376	26424	171229
5	184	193	308	765675	15236	14119	78468
6	142	231	401	414665	11360	10018	65483
7	1105	989	678	555320	28384	42653	214864
8	968	425	1003	779960	63300	36235	314584
9	1039	951	2111	736499	53657	66304	603414

Table 4. Values of local dependence function for real data.

Pairs of variables	$MinH(X_i,X_j)$	$MaxH(X_i,X_j)$	$\|H(X_i,X_j)\|$
X_1-X_2	0.9156	0.1473	0.9156
X_1-X_3	0.8312	-0.0417	0.8312
X_1-X_4	0.2927	0.0969	0.2927
X_1-X_5	0.9337	0.0759	0.9337
X_1-X_6	0.9482	0.4697	0.9482
X_1-X_7	-0.8897	-0.9853	0.9853
X_2-X_3	0.8634	-0.0641	0.8634
X_2-X_4	-0.0743	-0.3236	0.3236
X_2-X_5	0.5622	0.1586	0.5622
X_2-X_6	0.7964	0.2526	0.7964
X_2-X_7	-0.1652	-0.8225	0.8225
X_3-X_4	-0.0660	-0.1027	0.1027
X_3-X_5	0.8775	0.2293	0.8775
X_3-X_6	0.8874	0.1683	0.8874
X_3-X_7	-0.1369	-0.8711	0.8711
X_4-X_5	0.3282	0.1484	0.3282
X_4-X_6	0.5607	0.1477	0.5607
X_4-X_7	-0.1207	-0.6102	0.6102
X_5-X_6	0.9109	0.3518	0.9109
X_5-X_7	-0.2999	-0.9562	0.9562
X_6-X_7	-0.3542	-0.9614	0.9614

X_1 and X_7 are reference variables and the rest of variables are allocated as given below.

Group 1	*Group 2*
X_1	X_7
X_2	X_6
	X_5
	X_4
	X_3

$H(X_1,X_2)>0$ and $H(X_3,X_7)$, $H(X_4,X_7)$, $H(X_5,X_7)$, $H(X_6,X_7)<0$

Variables in Group 1 should be selected as input variables. As seen from the table, the copula approach has almost done exact classifying and has determined input/output variables correctly.

Table 5. The efficiency scores of real data.

DMU	Efficiency§	Efficiency*
1	1.00	1.00
2	1.00	1.00
3	1.00	1.00
4	1.00	1.00
5	1.00	1.00
6	1.00	1.00
7	0.50	0.78
8	1.00	1.00
9	1.00	1.00

§ Copula approach's efficiency scores and

* Yoluk's efficiency scores.

5. Conclusion

Data Envelopment Analysis is the most frequently used method to evaluate the efficiencies of DMUs. Although the determination of input/output variables is one of the most important problem of DEA, there have been limited attempts in the literature to solve this issue. Getting an expert opinion, which is the most preferred method, may actually be a subjective approach and it may also become an expensive way to identify the variables as input/output. The methods to determine the types of variables should be more objective and cost-effective than the current methods. In this study, we proposed a method which has not previously been available in the literature to solve this problem. We took into account of the copula function, which expresses the relation between dependent random variables in statistics, and the local dependence function, which measures the point dependency of variables. Our basic assumption is that the distribution of the variables is known in advance or can be determined.

In the simulation study, we showed how the algorithm of our method seperates a bulk of synthetic variables as input and output variables. In the real data application, we selected a set of variables which was already defined as the input and output in the previous analysis of the same data in the literature. According to the new process, the suggested input/output variables were almost consistent with those of other studies [2]. Also efficiencies were the same for effective DMUs and gave less efficiency score for the ineffective DMU as seen in Table 5.

The results showed that this method has several advantages. If there is no pre-information, input/output variables can be determined objectively. There is no need for expert opinion, so it is a cost-effective method. However, this method depends on the variables which have known distributions and sometimes it becomes a disadvantage. Although there is Archimedean copula family in the copula theory, we prefered a basic copula function (FGM) in this study because Archimedean copulas use a generator function [21] and there is only one study [22] for Local Dependence Function related with Archimedean copulas and its functional structure is not suitable with

our algortihm.

As a conclusion, this is a new kind of approach which has a theoretical structure, to identify the input/output variables and it can be improved for future studies and adapted to data which have different distribution functions.

Acknowledgments

The authors would like to thank the Editors and anonymous reviewers for their valuable comments.

References

[1] Charnes A., Cooper W.W. and Rhodes E., Measuring the Efficiency of Decision Making Units. European Journal of Operational Research, 2(6), 429-444 (1978).

[2] Yoluk, M., Hastane Performasının Veri Zarflama Analizi (VZA) Yöntemi İle Değerlendirilmesi. Thesis (MSc). Atılım University (2010).

[3] Morita, H. and Avkiran, N.K., Selecting Inputs and Outputs in Data Envelopment Analysis by Designing Statistical Experiments. Journal of Operational Research Society of Japan, 52, 163-173 (2009).

[4] Nelsen, R.B., An Introduction to Copulas. Springer, New York (1999).

[5] Bairamov, I. and Kotz, S., On Local Dependence Function for Multivariate Distributions. New Trends in Prob. and Stat., 5, 27-44 (2000).

[6] Bairamov, I., Kotz, S. and Kozubowski, T.J., A New Measure of Linear Local Dependence. Statistics, 37(3), 243-258 (2003).

[7] Ramanathan, R., An Introduction to Data Envelopment Analysis. Sage Publications, New Delhi (2003).

[8] Luo, Y., Bi, G. and Liang, L., Input/Output Indicator Selection for DEA Efficiency Evaluation: An Empirical Study of Chinese Commercial Banks. Expert System with Applications, 39, 1118-1123 (2012).

[9] Pastor, J.T., Ruiz J.L. and Sirvent, I., A Statistical Test for Nested Radial Dea Models. INFORMS, 50(4), 728-735 (2002).

[10] Jenkins, L. and Anderson, M., A multivariate statistical approach to reducing the number of variables in data envelopment analysis. European Journal of Operational Research, 147, 51–61 (2003).

[11] Ruggiero, J., Impact Assessment of Input Omission on DEA. International Journal of Information Technology and Decision Making, 4(3), 359-368, (2005).

[12] Edirisinghe, N.C.P. and Zhang, X., Generalized DEA Model of Fundamental Analysis and Its Application to Portfolio Optimization. Journal of Banking and Finance, 31, 311-335, (2007).

[13] Madhanagopal, R. and Chandrasekaran, R., Selecting Appropriate Variables for DEA Using Genetic Algorithm (GA) Search Procedure. International Journal of Data Envelopment Analysis and Operations Research, 1(2), 28-33 (2014).

[14] Banker, R.D., Charnes, A. and Cooper W.W., Some Models for Estimating Technical and Scale Inefficiencies in Data Envelopment Analysis. Management Science, 30(9), 1078-1092 (1984).

[15] Fare, R. and Grosskopf, S., and Lovell, C.A.K., Production Frontiers. Cambridge University Press (1993).

[16] Martic, M.M., Novakovic, M.S. and Baggia, A., Data Envelopment Analysis - Basic Models and their Utilization, Organizacija. Journal of Management, Informatics and Human Resources, 42(2), 37-43 (2009).

[17] Cooper, W.W., Seiford, L.M. and Zhu, J., Handbook on Data Envelopment Analysis. Springer New York (2011).

[18] Peňa, V.H. and Ibragimov, R., Sharakhmetov, S., Characterizations of Joint Distributions, Copula Information, Dependence and Decoupling, with Applications to Time Series. IMS Lecture Notes-Monograph Series, 2nd Lehmann Symposium-Optimality, 49, 183-209 (2006).

[19] Bairamov, I. and Kotz, S., Dependence Structure and Symmetry of Huang-Kotz FGM Distributions and Their Extensions. Metrica, 56, 55-72 (2002).

[20] Bairamov, I., Kotz, S. and Bekci, M., New Generalized Farlie-Gumbel-Morgenstern Distributions and Concomitants of Order Statistics. Journal of Applied Statistics, 28(5), 521-536 (2001).

[21] Najjari, V., Yeni Arşimedyan Kapula Aileleri ve Finans Alanında Bir Uygulama. Thesis (PhD). Gazi University (2014).

[22] Vandenhende, F., and Lambert, P., Local dependence estimation using semiparametric Archimedean copulas. The Canadian Journal of Statistics, 33(3), 377-388, (2005).

Olcay Alpay *is an Assistant Professor, lecturing at Sinop University in Turkey since 2011. She studied for Msc. and Ph.D in Statistics at Ege University. Her expertise is on Theory of Statistics. Her areas of interest include applied statistics and DEA.*

Elvan Akturk Hayat *is an Assistant Professor in Department of Econometrics, Aydın Faculty of Economics, Adnan Menderes University, Turkey. She received her Ph.D degree from the Department of Statistics, Ege University, Turkey in 2012. Her areas of interest include applied statistics, data envelopment analysis and data mining.*

An International Journal of Optimization and Control: Theories & Applications (http://ijocta.balikesir.edu.tr)

An International Journal of Optimization and Control: Theories & Applications
ISSN: 2146-0957 eISSN: 2146-5703
Vol.7, No.1, pp.35-41 (2017)
https://doi.org/10.11121/ijocta.01.2017.00340

RESEARCH ARTICLE

Pricing in M/M/1 queues when cost of waiting in queue differs from cost of waiting in service

Görkem Sarıyer

Department of Business Administration, Yaşar University, Turkey
gorkem.ataman@yasar.edu.tr

ARTICLE INFO

Article history:
Received: 29 April 2016
Accepted: 24 October 2016
Available Online: 01 November 2016

Keywords:
Equilibrium
Market capture pricing
Monopolistic pricing
M/M/1
Rational customers

AMS Classification 2010:
90B08, 91C08, 91A08

ABSTRACT

Service providers can adjust the entrance price to the state of the demand in real life service systems where the customers' decision to receive the service, is based on this price, state of demand and other system parameters. We analyzed service provider's short and long term pricing problems in unobservable *M/M/1* queues having the rational customers, where, for customers, the unit cost of waiting in the queue is higher than unit cost of waiting in the service. We showed that waiting in the queue has a clear negative effect on customers' utilities, hence the service provider's price values. We also showed that, in the short term, monopolistic pricing is optimal for congested systems with high server utilization levels, whereas in the long term, market capturing pricing is more profitable.

1. Introduction

In real life, most service systems include customer queues. Thus, the potential customers of these systems will inevitably face waiting time before being served. Since time is a very scarce resource in the current environment [1], customers decide rationally upon receiving a service. Based on comparing the value of the received service with the total cost of receiving this service, a decision is made whether or not to join the queue; this decision generates the real state of the demand.

In order to maximize profits, the service provider takes into account the rational decision of the customers while setting the optimal system parameters, such as price or service rate. Until recently, however, pricing studies in the literature assumed that the firm was not able to adjust the price based on the state of the demand. The first model allowing the firm adjust the price to the state of the demand was analyzed by Naor [2]. In this benchmark paper, Naor, analyzed the effect of imposing an entrance fee on socially optimum, when customers will not join the system until after observing the length of the queue. A similar study by Edelson and Hildebrand, had an important difference in that customers were not able to observe the queue length before taking their decision [3]. In very similar settings, Chen and Frank analyzed the pricing problem of the monopoly, or the service provider, when the queue length is observable by customers [4], and when unobservable [5]. In the literature, other studies analyze the pricing problem of the service provider in queueing models. Knudsen allowed more than a single queue in any one firm [6]. Sariyer compared pricing strategies of the service provider in the cases of a single server, and two servers [7]. Some other studies represented socially optimal pricing schemes for different classes of customers [8, 9, 10].

All these cited studies assumed that a queue decreases the utility of the customer from the received service. A more recent view in queueing literature suggest that customer utility will not necessarily decrease due to wait time. Debo et al. showed that expected service time, which, in the literature, was included in total waiting time, is positively correlated with the value of the received service [11]. Anand at al., Alizamir et al., and Wang et al. also considered that service value is correlated with waiting time [12, 13, 14]. Oliveras et al. proposed that customer purchase decisions are not monotonic to queue length [15]. Giebelhausen et al. concluded that longer wait time can signal greater service quality, which positively affects customer decisions [16]. Sariyer combined these two views in the literature and represented the utility function of customers with a different structure, which allowed discrimination between the effect of waiting in the queue and waiting in the service on customer's decision

*Corresponding author

[17].

In this paper, we will analyze the pricing problem of the service provider in which the customer utility function is a modified version of the one represented in [17]. The model assumptions, notations, and utility function of the customer will be presented in Section 2. The pricing problem will be analyzed in both of the market capture and monopolist pricing settings, details of which will be given in Section 3. In the long term, the service provider is capable of adjusting not only the price but also the service rate. The long term analyses will be covered in Section 4. In Section 5 and 6 we respectively present the Numerical Analysis and Conclusions part.

2. Model assumptions

We analyze basic *M/M/1* queues having Poisson arrivals with rate λ, and a unique server having an exponentially distributed service rate of μ. We use monetary values to represent the system parameters, such as value of the service and cost of waiting. The value of the service is denoted by a service reward, *R*, and a customer who receives this service incurs a linear waiting cost with *C* units.

In real life, service systems having queues of customers can be differantiated as observable or unobservable based on the visibility of length of the queue. Cashomat or Automatic Teller Machine (ATM), fast-food or self-service restaurants, banks are examples of service systems including observable queues, since a new arriving customer can observe the number of customers in front of him. On the other hand, some call centers, service systems taking the orders online which share the information of the expected waiting time to be served or receive the order, are examples of systems including unobservable queues, since the customers cannot observe the length of the queue. In this paper, we assume the length of the queue is not observable upon arrival, but, based on the shared information by the service provider or the past experiences of the arriving customers, customers know the expected waiting time in the system. We also assume that the systems are in steady state. The expected waiting time combines two elements: the expected waiting time in the queue, and the expected waiting time during the service. Based on our assumption, the first element has a greater negative effect on customer utility, thus we multiply the unit cost of waiting in the queue with *k*, where *k>1*. A service provider sets a price, *p*, for customers receiving the service. This price clearly decreases the utility of the customer. The customer decides whether or not to join the queue and receive the service. Thus, the customer decision parameter is the probability of joining, denoted by α. All of these are combined to derive utility function of the customer, which is denoted by U(α) as:

$$U(\alpha) = R - kCE[W_1] - CE[W_2] - p$$
$$= R - kC\frac{\lambda\alpha}{\mu(\mu-\lambda\alpha)} - \frac{C}{\mu} - p \qquad (1)$$

In equation (1), $E[W_1]$ and $E[W_2]$ represent expected waiting time in the queue and the expected waiting time during the service respectively. The values of $E[W_1]$ and $E[W_2]$ are found based on the properties of *M/M/1* queues.

While making their decision, customers consider this utility function. If *R-p* is smaller than only the service cost of a unique customer, then joining the system is not optimal, since the customer has negative utility, thus α=0. If *R-p* is greater than total cost of waiting in the system, even if all customers join, then it remains optimal for all potential customers, since they receive positive utility, hence α=1. In between, the customers join with an equilibrium probability, α^{eq}, where $0 < \alpha^{eq} < 1$. This equilibrium probability is found by setting equation (1) to 0, and solving it for α. Hassin and Haviv provides a detailed review of these equilibrium analyses of rational customers [18].

3. Pricing decisions in short term

In the short term, the service provider sets the optimal entrance price to the system for the given model parameters λ and μ. Assuming $\mu > \lambda$, the service rate is sufficiently high to serve all potential customers. The service provider therefore sets either the minimum price, referred to in the literature as *market capturing price*, in order to allow all customers to enter the system, or a higher price, denoted as *monopolistic price*, to push customers to join at an equilibrium rate.

3.1. Market capture pricing

The minimum price which allows all customers to join is found by giving α to 1 in equation (1), setting this utility function to 0, and solving it for *p*. Denoting this market capturing price with symbol p_l, it is derived as:

$$p_l = R - kC\frac{\lambda}{\mu(\mu-\lambda)} - \frac{C}{\mu} \qquad (2)$$

Lemma 1. *p_l is increasing in R and μ, decreasing in λ, k and C.*

Proof.

$$\frac{dp_l}{dR} = 1 > 0, \frac{dp_l}{d\mu} = \frac{kC\lambda(2\mu-\lambda)}{[\mu(\mu-\lambda)]^2} + \frac{C}{\mu^2} > 0$$

$$\frac{dp_l}{dC} = -\frac{k\lambda}{\mu(\mu-\lambda)} - \frac{1}{\mu} < 0, \frac{dp_l}{dk} = -C\frac{\lambda}{\mu(\mu-\lambda)} < 0,$$

$$\frac{dp_l}{d\lambda} = -\frac{kC\mu^2}{[\mu(\mu-\lambda)]^2} < 0$$

Lemma 1 can be clearly interpreted. Since the utility function of the customer increases when *R* increases, the service provider is able to set a higher price. On the other hand, when *k* and *C* increase, the expected cost of waiting increases, thus utility of the customer decreases, which forces the service provider to lower the price. When μ increases, the expected waiting time in the system decreases, which generates an increase in utility function, and pushes the service provider to set a higher price; on the other hand, when λ increases, expected waiting time increases, causing a decrease in the entrance price.

The profit function of the service provider under this market capturing price, $\Pi_{lp}(p_l)$, is derived as:

$$\Pi_{lp}(p_l) = \lambda p_l = \lambda\left(R - kC\frac{\lambda}{\mu(\mu-\lambda)} - \frac{C}{\mu}\right) \quad (3)$$

Lemma 2. *$\Pi_{lp}(p_l)$ is increasing in R and μ, decreasing in k and C, and concave in λ.*

Proof.

$$\frac{d\Pi_{lp}(p_l)}{dR} = \lambda > 0, \frac{d\Pi_{lp}(p_l)}{d\mu} = \frac{kC\lambda^2(2\mu-\lambda)}{[\mu(\mu-\lambda)]^2} + \frac{C\lambda}{\mu^2} > 0$$

$$\frac{d\Pi_{lp}(p_l)}{dC} = -\frac{k\lambda^2}{\mu(\mu-\lambda)} - \frac{1}{\mu} < 0,$$

$$\frac{d\Pi_{lp}(p_l)}{dk} = -C\frac{\lambda^2}{\mu(\mu-\lambda)} < 0,$$

$$\frac{d\Pi_{lp}(p_l)}{d\lambda} = R - \frac{kC\lambda\mu(2\mu-\lambda)}{[\mu(\mu-\lambda)]^2} - \frac{C}{\mu},$$

$$\frac{d^2\Pi_{lp}(p_l)}{d\lambda^2} = -\frac{2kC\mu^4}{[\mu(\mu-\lambda)]^3} < 0$$

In Lemma 2, we showed that profit value is concave in λ. Thus, when the arrival rate increases, the profit value increases up to a certain level, after which value profit decreases, due to congestion in the system. For the other model parameters, *R*, μ, *k* and *C*, the profit function behaves simialrly to price function, $\boldsymbol{p_l}$, as expected.

3.2. Monopolistic pricing

Service provider sets a higher price thus customers join with an equilibrium joining probability which is derived from equation (1) as:

$$U(\alpha) = 0 \rightarrow R - p = \frac{C}{\mu}\left(\frac{k\lambda\alpha}{\mu - \lambda\alpha} + 1\right)$$

$$\rightarrow \alpha^{eq} = \frac{\mu\left(\frac{(R-p)\mu}{C} - 1\right)}{\lambda\left(k + \frac{(R-p)\mu}{C} - 1\right)} \quad (4)$$

Lemma 3. *α^{eq} is increasing in R and μ, and decreasing in λ, p, k and C.*

Proof.

$$\frac{d\alpha^{eq}}{dR} = \frac{\frac{k\mu}{C}}{\lambda\left(k + \frac{(R-p)\mu}{C} - 1\right)^2} > 0,$$

$$\frac{d\alpha^{eq}}{d\mu} = \frac{\left(\frac{(R-p)\mu}{C} - 1\right)\left(k + \frac{(R-p)\mu}{C} - 1\right) + \mu k\frac{(R-p)}{C}}{\lambda\left(k + \frac{(R-p)\mu}{C} - 1\right)^2} > 0,$$

$$\frac{d\alpha^{eq}}{d\lambda} = -\frac{\mu\left(\frac{(R-p)\mu}{C} - 1\right)}{\lambda^2\left(k + \frac{(R-p)\mu}{C} - 1\right)} < 0$$

$$\frac{d\alpha^{eq}}{dp} = -\frac{k\frac{\mu^2}{C}}{\lambda\left(k + \frac{(R-p)\mu}{C} - 1\right)^2} < 0,$$

$$\frac{d\alpha^{eq}}{dk} = -\frac{\mu\left(\frac{(R-p)\mu}{C} - 1\right)}{\lambda\left(\frac{(R-p)\mu}{C} - 1\right)^2} < 0,$$

$$\frac{d\alpha^{eq}}{dC} = -\frac{k\frac{(R-p)\mu^2}{C^2}}{\lambda\left(k + \frac{(R-p)\mu}{C} - 1\right)^2} < 0$$

The interpretation of this result is very similar to Lemma 1.

We will find the expression of the monopolistic price, p_h, by analyzing the profit function of the service provider in this setting. Denoting the profit function with $\pi_{hp}(p)$, we derive it as:

$$\pi_{hp}(p) = \lambda\alpha^{eq}p = \frac{\mu\left(\frac{(R-p)\mu}{C} - 1\right)}{k + \frac{(R-p)\mu}{C} - 1}p \quad (5)$$

Since the derivation of p_h is messy, we will give the analysis numerically in Section 5.

4. Service rate and pricing decisions in long term

In this section, we assume that service provider can adjust both the price and service rate. Thus, the profit functions have two parameters, μ and *p*. As given in Chen and Frank [5], we assume a constant marginal cost of speeding up the service rate, *F*>0.

For the market capturing price setting, the profit function given in equation (3) is rewritten as:

$$\pi_{lp}(\mu) = \lambda p_l - F\mu = \lambda\left(R - kC\frac{\lambda}{\mu(\mu-\lambda)} - \frac{C}{\mu}\right) - F\mu \quad (6)$$

Lemma 5. *$\pi_{lp}(\mu)$ is concave in μ.*

Proof.

$$\frac{d\pi_{lp}(\mu)}{d\mu} = \lambda\left(\frac{kC\lambda(2\mu-\lambda)}{[\mu(\mu-\lambda)]^2} + \frac{C}{\mu^2}\right) - F,$$

$$\frac{d^2\pi_{lp}(\mu)}{d\mu^2} = -C\lambda\left(2k\lambda\frac{3\mu^2 - 3\mu\lambda + \lambda^2}{[\mu(\mu-\lambda)]^3} + \frac{2}{\mu^3}\right)$$

Since $\mu > \lambda$, $3\mu^2 - 3\mu\lambda + \lambda^2 > 0$ for all real λ and μ then the second derivative of the profit function is always negative, which shows that the profit function is concave with respect to μ.

Thus, there is a unique optimal value for the service rate which equates the first derivative function to 0, and maximizes the profit function given in equation (6).

For the monopolistic pricing, the profit function is rewritten as:

Table 1: Price and profit values – short term

R/C	*k*	*λ/μ (ρ)*	p_l	$\Pi_{lp}(p_l)$	α^{eq}	p_h	$\Pi_{hp}(p_h)$
4	1.25	0.95	7.62	76.20	0.87	16.70	144.82
4	1.25	0.67	18.83	188.33	0.97	18.90	183.68
4	2.00	0.95	0.48	4.76	0.82	16.05	132.26
4	2.00	0.67	18.33	183.33	0.98	18.40	180.83
6	1.25	0.95	17.62	176.19	0.91	25.90	233.58
6	1.25	0.67	28.83	288.33	0.97	28.90	280.86
6	2.00	0.95	10.48	104.76	0.87	25.00	216.85
6	2.00	0.67	28.33	283.33	0.98	28.40	279.10

$$\pi_{hp}(\mu, p) = \lambda \alpha^{eq} p - F\mu = \frac{\mu\left(\frac{(R-p)\mu}{C}-1\right)}{k+\frac{(R-p)\mu}{C}-1} p - F\mu \qquad (7)$$

In equation (7), $\pi_{hp}(\mu, p)$ represents the profit function, under monopolistic pricing, as a function of μ and p. In the next section, different numerical experiments are given in order to analyze the optimal model parameters and profit values under different pricing schemes.

5. Numerical results and discussion

Numerical results are first given for the short term. For given levels of *R*, *C*, *k*, λ, and μ, we find the values of the minimum price, p_l, and the profit, $\Pi_{lp}(\boldsymbol{p_l})$, under this price for the market capture pricing setting. Then, for the monopolistic pricing, we will find the equilibrium joining probability, $\boldsymbol{\alpha^{eq}}$, value of the monopolistic price, p_h, and the profit under this price $\Pi_{hp}(p_h)$. Table 1 presents the results.

In our observations presented in Table 1, we fix λ=10, and *C*=5. We take R as 20 and 30 to represent low and high values, and take μ as 10.5 and 15 to represent low and high congestion in the system. We observe that there is a clear difference in the profit values for the high utilization levels, i.e. when the service rate is very close to the arrival rate, in which profit under monopolistic pricing is much higher than under market capture pricing. On the other hand, for low utilization levels, the market capture pricing becomes increasingly more profitable compared to monopolistic pricing, since the rate of the server is sufficiently high to serve all potential arrivals within a limited wait time. As expected from the definition, the price values are always higher under monopolistic pricing setting, i.e. $p_h > p_l$. Since the expected waiting cost in the system increases in *k*, we see that the price and profit values decrease in both of the market capture and monopolistic pricing. On the other hand, in both price settings, the price and profit values increase with increases in the ratio between the reward and unit waiting cost, namely, *R/C*.

In Figure 1, we show how the percentage change in profit value, under market capture and monopolistic pricing settings, is affected by the increase in server utilization, ρ. In this experiment, we fixed *R*=30, *C*=5, λ=10 and increase μ from 10.5 to 20, where ρ changes between [0.5-0.95]. We repeat the analysis for different *k* values, where *k* takes the values of 1, 1.25, 1.5, and 2 respectively for different experiments. In these experiments *k*=1 is taken in order to represent the situation given in literature, where unit cost of waiting in the queue is exactly equal to the unit cost of waiting in service. Then the values of *k* are increased consequetively in order to show how the percentage difference in profit values under market capture and monopolistic pricing, is affected with the increased difference between unit cost of waiting in the queue and in service. Finally, as the highest value of *k*, we take it as 2, and repeat the experiment in order not to differentiate the unit cost of witing in the queue and in service much more (to keep close to literature results). Besides, when *k=2*, as will be seen in Figure1, the sharp difference is obtained to show the related effect. In the vertical column of the figure, we represent $\left(\Pi_{hp}(p_h) - \Pi_{lp}(p_l)\right)/\Pi_{lp}(p_l)$.

In Figure 1, we observe that, for low levels of ρ, i.e higher levels of μ, the market capturing pricing is more profitable, since the percentage difference is negative. This means, for low congested systems, the service provider obtains a higher profit under market capture pricing compared to monopolistic pricing. However, when the system is congested, i.e. λ is very close to μ, the service provider should set a monopolistic price to maximize profits. As seen in this Figure, congested systems are characterized by a sharp difference in profit values. When we analyze the Figure for different *k* values, for low levels of ρ, we cannot observe a clear effect of k values in the percentage difference of profit (i.e. the percentage differences are almost equal for k=1, k=1.25, k=1.5, and k=2 when $\rho \leq 0.85$). The reason behind this observation is, the service provider sets such a monopolistic price that pushes almost all of the customers to join the queue and receive the service when system is not congested, or for high levels of μ.

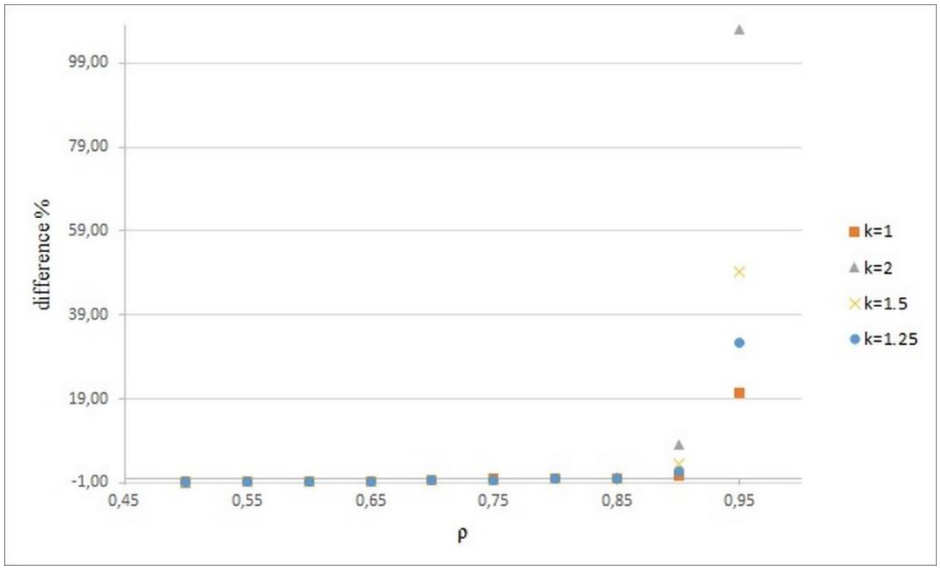

Figure 1. Short term difference % in profit- market capture versus monopolistic pricing

Thus, the profit under monopolistic pricing gets very close to the profit under market capture pricing. However, for congested systems, since the effect of waiting time is sharply increased, under market capturing pricing (i.e. all customers join), the sharp percentage difference in profit values can be observed for different k values. In this case, or for lower levels of μ, the percentage difference in profit values under market capture and monopolistic pricing settings, increases for increasing *k* values. Thus, especially for congested systems, which is generally the case of real life situation, it can be understood that unit cost of waiting in the queue has a direct effect on a service provider's pricing decision, and hence on profit.

We now turn our attention to long term decisions. For this, marginal cost of increasing the service rate was added to the calculations. We give optimal service rate, μ^*, market capturing price given this service rate, $p_l{}^*$, and profit given these parameters, $\pi_{lp}^*(\mu^*, p_l^*)$in Table 2. The values of *R*, *C*, and λ are taken as given in the previous numerical experiments.

Table 2: Service rate, price and profit values of market capture pricing – long term

R/C	*k*	*F*	μ^*	$p_l{}^*$	$\pi_{lp}^*(\mu^*, p_l^*)$
4	1.25	5	13.60	18.36	115.56
4	1.25	10	12.40	17.50	50.97
4	2.00	5	14.40	18.07	108.75
4	2.00	10	13.20	17.25	40.54
6	1.25	5	13.60	28.36	215.56
6	1.25	10	12.40	27.50	150.97
6	2.00	5	14.40	28.07	208.75
6	2.00	10	13.20	27.25	140.54

Table 3: Service rate, price and profit values of monopolistic pricing – long term

R/C	*K*	*F*	α^{eq}	μ^*	$p_h{}^*$	$\Pi_{hp}{}^*(\mu^*, p_h{}^*)$
4	1.25	5.00	0.99	13.25	18.20	114.85
4	1.25	10.00	0.99	12.25	17.35	50.63
4	2.00	5.00	0.99	14.25	18.00	108.68
4	2.00	10.00	0.99	13.00	17.10	40.24
6	1.25	5.00	0.99	13.25	28.20	214.36
6	1.25	10.00	0.99	12.25	27.35	150.42
6	2.00	5.00	0.99	14.25	28.00	208.65
6	2.00	10.00	0.99	13.00	27.10	139.79

Similarly, in Table 3, we give the equilibrium joining probability, α^{eq}, optimal service rate, μ^*, monopolistic price given this service rate, $p_h{}^*$, and profit given these parameters, $\Pi_{hp}{}^*(\mu^*, p_h{}^*)$.

We observe that the optimal strategy for the service provider in the long term, when there is the option to set the service rate, is to set the market capturing price, which has higher profit values compared to monopolistic pricing. So in the long term, the service provider's optimal decision is to set a service rate that can serve all potential customers (until it is profitable, i.e. when Fμ does not exceed the revenue received from the customer). This result is very similar to the findings of Chen and Frank [5]. We also observe that in monopolistic pricing, the optimal action pushes the service provider to set price and service rate values which allow almost all to join the system, i.e. $\boldsymbol{\alpha^{eq}}$ values are almost 1. In both settings, the optimal price and service rate values increase in *R/C*, and decrease in *k* and *F* values.

6. Conclusion

In this paper, we analyzed the pricing decision of the service provider. The system is designed as *M/M/1* queues with rational customers who are unable to observe the length of the queue prior to making decisions. These customers wait in the queue to be served. In contrast to previous studies, we assume that waiting in the queue has a greater negative effect on the utility of the customers, compared to waiting during the service. We have shown an increase in the unit cost of waiting in the queue has a negative effect on the utility of the customer. Since customers are rational, the profit maximizer should be decided by considering customer utility. Thus, service provider's pricing decisions are similarly negatively affected by the customers' unit cost of waiting in the queue.

We have anaylzed the service provider's pricing problem in both the short and long terms. In the short term, when the service provider optimally sets the entrance price for the given service rate, monopolistic pricing was observed as the most efficient setting for high server utilization periods, i.e. when the system is congested. In the long term, however, when the service provider optimally sets the service rate and entrance price, market capture pricing is found to be the most profitable setting. Hence, in the long term, the service provider's optimal action is to set a service rate that allows all customers to join the queue and receive the service at the minimum price.

Acknowledgments

The authors would like to thank the anonymous reviewers for their valuable comments.

References

[1] Leclerc, F., Schmitt, B. H., Dube, L., Waiting time and decision making: Is time like Money? Journal of Consumer Research, 22(1), 110-119 (1995).

[2] Naor, P., The regulation of queue size by levying tolls. Econometrica, 37(1), 15-24 (1969).

[3] Edelson, N. M., Hildebrand, D.K., Congestion tolls for queueing processes. Econometrica, 43, 81-92 (1975).

[4] Chen, H., Frank, M. Z., State dependent pricing with a queue. IIE Transactions, 33, 847-860 (2001).

[5] Chen, H., Frank, M. Z., Monopoly pricing when customers queue. IIE Transactions, 36, 569-581 (2004).

[6] Knudsen, N. C., Individual and social optimization in a multiserver queue with a general cost-benefit structure. Econometrica, 40, 515-528 (1972).

[7] Sariyer, G., Effective service design in strategic customer setting. Journal of Computational and Theoretical Nanoscience, 12(12), 5109-5113 (2015).

[8] Mendelson, H., Whang, S., Optimal incentive-compatible priority pricing for the *M/M/1* queue. Operations Research, 38, 870-883 (1990).

[9] Bradford, R., Pricing, routing, and incentive compatibility in multi-server queues. European Journal of Operational Research, 89(2), 226-236 (1996).

[10] Rao, S., Peterson, E. R., Optimal pricing of priority services. Operations Research, 46, 46-56 (1998).

[11] Debo, L. G., Veeraraghavan, S. K., Equilibrium in queues under unknown service rates and service value. Chicago Booth Research Paper, 2011: 11-45.

[12] Anand, K. S., Pac, M. F., Veereraghavan, S. Quality-speed conundrum: tradeoffs in customer intensive services. Management Science, 57(1), 40-56 (2011).

[13] Alizamir, S., Vericourt, F., Sun, P., Diagnostic accuracy under congestion. Management Science, 59(1), 157-171 (2013).

[14] Wang, S., Debo, L. G., Scheller, W. A., Smith, S. F., Design and analysis of diagnostic service centers. Management Science, 56(11), 1873-1890 (2009).

[15] Oliveras, M., Lu, Y., Musalem, A., Schilkrut, A., Measuring the effect of queues on customer purchases. Management Science, 59(8), 1743-1763 (2013).

[16] Giebelhausen, M. D., Robinson, S. G., Cronin, J. J., Worth waiting for: increasing satisfaction by making consumers wait. Journal of the Academy of Marketing Science, 39(6), 889-905 (2011).

[17] Sariyer, G., Effect of in queue waiting on decision making. International Journal of Basic and Applied Sciences, 14(6), 13-18 (2014).

[18] Hassin, R., Haviv, M., To queue or not to queue. International Series in Operations Research and Management Science, 59, Kluwer Publishing (2002).

Görkem Sarıyer *has been an Assistant Professor in the Faculty of Economics and Administrative Sciences in Yasar University. She has a BA in Software Engineering (Izmir University of Economics/Turkey), M.Sc. in Applied Statistics (Izmir University of Economics/ Turkey), and PhD degree in Industrial Engineering and Operations Management (Koç University/ Turkey). Her research interest includes decision making models of strategic customers, health care services and management, modeling in queues, service operations and management.*

An International Journal of Optimization and Control: Theories & Applications (http://ijocta.balikesir.edu.tr)

An International Journal of Optimization and Control: Theories & Applications
ISSN: 2146-0957 eISSN: 2146-5703
Vol.7, No.1, pp.42-49 (2017)
https://doi.org/10.11121/ijocta.01.2017.00292

RESEARCH ARTICLE

New soliton solutions of the system of equations for the ion sound and Langmuir waves

Seyma Tuluce Demiray* and Hasan Bulut

Department of Mathematics, Firat University, Turkey
seymatuluce@gmail.com, hbulut@firat.edu.tr

ARTICLE INFO

Article history:
Received: 14 January 2016
Accepted: 22 August 2016
Available Online: 29 November 2016

Keywords:
The system of equations
Ion sound wave
Langmuir wave
Generalized Kudryashov method
Dark soliton solutions
Mathematica Release 9

AMS Classification 2010:
35-04, 35C08, 35N05, 68N15

ABSTRACT

This study is based on new soliton solutions of the system of equations for the ion sound wave under the action of the ponderomotive force due to high-frequency field and for the Langmuir wave. The generalized Kudryashov method (GKM), which is one of the analytical methods, has been tackled for finding exact solutions of the system of equations for the ion sound wave and the Langmuir wave. By using this method, dark soliton solutions of this system of equations have been obtained. Also, by using Mathematica Release 9, some graphical simulations were designed to see the behavior of these solutions.

1. Introduction

Nonlinear evolution equations are widely used as models to define large numbers of physical phenomena [1-4]. The system of equations for the ion sound wave under the action of the ponderomotive force due to high-frequency field and for the Langmuir wave, which is one type of nonlinear evolution equations, will be handled in this work. The investigation of new soliton solutions for the ion sound wave and the Langmuir wave has a highly important position among the authors. A number of researchers have focused on the Langmuir solitons. L. M. Degtyarev et al. have tackled some properties of Langmuir solitons [5]. Then, they have considered the Langmuir wave energy dissipation [6]. Some scientists have found the numerical simulations of Langmuir collapse [7-10]. E. S. Benilov has indicated the stability of solitons by using the Zakharov equations which defines the interaction between Langmuir and ion-sound waves [11].

V. E. Zakharov et al. have presented the modelling of Langmuir turbulence [12]. A. I. Dyachenko et al. have done computer simulations of Langmuir collapse [13]. A. M. Rubenchik et al. have handled strong Langmuir turbulence in laser plasma [14]. S. L. Musher et al. have introduced weak Langmuir turbulence [15]. Also, some scholars have focused on Langmuir waves [16-18]. I. Y. Dodin et al. have investigated Langmuir wave evolution in nonstationary plasma [19]. A. Zavlavsky et al. have presented spatial localization of Langmuir waves [20]. Also, Langmuir wave spectral energy densities have been derived from the electric field and compared to the weak turbulence results by H. Ratcliffe et al. [21].

We introduce the system of equations for the ion sound wave under the action of the ponderomotive force due to high-frequency field and for the Langmuir wave [22],

$$i\frac{\partial E}{\partial t}+\frac{1}{2}\frac{\partial^2 E}{\partial x^2}-nE=0,$$
$$\frac{\partial^2 n}{\partial t^2}-\frac{\partial^2 n}{\partial x^2}-2\frac{\partial^2 |E|^2}{\partial x^2}=0, \quad (1)$$

where $Ee^{-iw_p t}$ is the normalized electric field of the Langmuir oscillation and n is the normalized density perturbation. The spatial variable x and the time variable t are also normalized appropriately [22]. The system of equations Eq. (1) for the ion sound and Langmuir waves has been formulated by V. E. Zakharov [23].

*Corresponding author

In this paper, the basic interest is to construct the new soliton solutions of the system of equations for the ion sound and Langmuir waves by performing GKM. In Sec. 2, we discuss general structure of GKM [24-29]. In Sec. 3, we get dark soliton solutions of the system of equations for the ion sound and Langmuir waves by implementing GKM.

2. Basic facts of the GKM

We survey a common nonlinear partial differential equation (NLPDE)

$$P\left(u,u_t,u_x,u_{xx},u_{xxx},\cdots\right)=0. \tag{2}$$

Step 1. Initially, we must perform the travelling wave solution of Eq.(2) as following form;

$$u\left(x,t\right)=e^{i\theta}u\left(\xi\right),\ \theta=kx+mt,\ \xi=px+rt, \tag{3}$$

where k,m,p and r are arbitrary constants. Eq.(2) was reduced to a nonlinear ordinary differential equation:

$$N(u,u',u'',u''',\cdots)=0, \tag{4}$$

where the prime denotes differentiation with regard to ξ.

Step 2. Suggest that the exact solutions of Eq.(4) can be tackled as follows;

$$u\left(\xi\right)=\frac{\sum_{i=0}^{N}a_iQ^i\left(\xi\right)}{\sum_{j=0}^{M}b_jQ^j\left(\xi\right)}=\frac{A\left[Q(\xi)\right]}{B\left[Q(\xi)\right]}, \tag{5}$$

where Q is $\frac{1}{1\pm e^{\xi}}$. We highlight that the function Q is solution Eq. (6)

$$Q_{\xi}=Q^2-Q. \tag{6}$$

Taking account of Eq.(5), we gain

$$\begin{aligned}u'\left(\xi\right)&=\frac{A'Q'B-AB'Q'}{B^2}=Q'\left[\frac{A'B-AB'}{B^2}\right]\\&=\left(Q^2-Q\right)\left[\frac{A'B-AB'}{B^2}\right],\end{aligned} \tag{7}$$

$$\begin{aligned}u''\left(\xi\right)&=\frac{Q^2-Q}{B^2}\left[\left(2Q-1\right)\left(A'B-AB'\right)\right]\\&+\frac{\left(Q^2-Q\right)^2}{B^3}\left[B\left(A''B-AB''\right)-2B'A'B+2A\left(B'\right)^2\right],\end{aligned} \tag{8}$$

$$\begin{aligned}u'''\left(\xi\right)&=\left(Q^2-Q\right)^3\left[\frac{\left(A'''B-AB'''-3A''B'-3B''A'\right)B}{B^3}\right]\\&+\left(Q^2-Q\right)^3\left[\frac{6\left(AB''+B'A'\right)}{B^2}-\frac{6A\left(B'\right)^3}{B^4}\right]\\&+3\left(Q^2-Q\right)^2\left(2Q-1\right)\left[\frac{B\left(A''B-AB''\right)-2B'A'B+2A\left(B'\right)^2}{B^3}\right]\\&+\left(Q^2-Q\right)\left(6Q^2-6Q+1\right)\left[\frac{A'B-AB'}{B^2}\right].\end{aligned} \tag{9}$$

Step 3. The solution of Eq.(4) can be expressed as follows:

$$u\left(\xi\right)=\frac{a_0+a_1Q+a_2Q^2+\cdots+a_NQ^N+\cdots}{b_0+b_1Q+b_2Q^2+\cdots+b_MQ^M+\cdots}. \tag{10}$$

To compute the values M and N in Eq.(10) that is the pole order for the general solution of Eq.(4), we develop comparably as in the classical Kudryashov method on balancing the highest order nonlinear terms in Eq.(4) and we can establish a relation of M and N. We can find values of M and N.

Step 4. Substituting Eq.(5) into Eq.(4) ensures a polynomial $R\left(Q\right)$ of Q. Extracting the coefficients of $R\left(Q\right)$ to zero, we get a system of algebraic equations. Solving this system, we can identify c and the variable coefficients of $a_0,a_1,a_2,\cdots,a_N,b_0,b_1,b_2,\cdots,b_M$. Thus, we gain the exact solutions to Eq.(4).

3. GKM for the system of equations for the ion sound and the Langmuir waves

In this section, we seek the exact solutions of the system of equations for the ion sound and Langmuir waves by using GKM.

In an effort to find travelling wave solutions of the Eq. (1), we get the transformation by use of the wave variables

$$\begin{aligned}&E\left(x,t\right)=e^{i\theta}u\left(\xi\right),\ n\left(x,t\right)=v\left(\xi\right),\\&\theta=kx+mt,\ \xi=px+rt,\end{aligned} \tag{11}$$

where k,m,p and r are arbitrary constants.

Inserting Eqs. (12-14) into Eq. (1),

$$iE_t=-me^{i\theta}u+ire^{i\theta}u', \tag{12}$$

$$E_{xx}=-k^2e^{i\theta}u+2ipke^{i\theta}u'+p^2e^{i\theta}u'', \tag{13}$$

$$n_{tt}=r^2v'',\ n_{xx}=p^2v'',\ \left(\left|E\right|^2\right)_{xx}=p^2\left(u^2\right)'', \tag{14}$$

we obtain the following system

$$i\left(r+pk\right)u'\left(\xi\right)=0, \tag{15}$$

$$p^2u''-\left(2m+k^2\right)u-2uv=0, \tag{16}$$

$$\left(r^2-p^2\right)v''-2p^2\left(u^2\right)''=0. \tag{17}$$

By setting the integration constant to zero, we integrate function v with respect to ξ, we find

$$v\left(\xi\right)=\frac{2p^2}{r^2-p^2}u^2\left(\xi\right). \tag{18}$$

Putting Eq.(18) into Eq.(16) and by using Eq. (15), we gain

$$p^2\left(k^2-1\right)u''-\left(k^2-1\right)\left(2m+k^2\right)u-4u^3=0, \tag{19}$$

where the prime remarks the derivative with respect to ξ.

Substituting Eqs. (5) and (8) into Eq. (19) and balancing the highest order nonlinear terms of u'' and u^3 in Eq. (19), then the following formula is found

$$N-M+2=3N-3M\Rightarrow N=M+1. \tag{20}$$

If we take $M=1$ so $N=2$,then

$$u\left(\xi\right)=\frac{a_0+a_1Q+a_2Q^2}{b_0+b_1Q}, \tag{21}$$

$$u'\left(\xi\right)=\left(Q^2-Q\right)\left[\frac{\left(a_1+2a_2Q\right)}{\left(b_0+b_1Q\right)}\right]-\left(Q^2-Q\right)\left[\frac{b_1\left(a_0+a_1Q+a_2Q^2\right)}{\left(b_0+b_1Q\right)^2}\right], \tag{22}$$

$$\begin{aligned}u''\left(\xi\right)=&\frac{Q^2-Q}{\left(b_0+b_1Q\right)}\left(2Q-1\right)\left(a_1+2a_2Q\right)\\&-\frac{Q^2-Q}{\left(b_0+b_1Q\right)^2}\left(2Q-1\right)\left[b_1\left(a_0+a_1Q+a_2Q^2\right)\right]\\&+\frac{\left(Q^2-Q\right)^2}{\left(b_0+b_1Q\right)^2}\left[2a_2\left(b_0+b_1Q\right)-2b_1\left(a_1+2a_2Q\right)\right]\\&+\frac{\left(Q^2-Q\right)^2}{\left(b_0+b_1Q\right)^3}\left[2b_1^2\left(a_0+a_1Q+a_2Q^2\right)\right],\end{aligned} \tag{23}$$

$$\begin{aligned}u'''\left(\xi\right)=&\left(Q^2-Q\right)\left(6Q^2-6Q+1\right)\left[\frac{\left(a_1+2a_2Q\right)}{\left(b_0+b_1Q\right)}\right]\\&-\left(Q^2-Q\right)\left(6Q^2-6Q+1\right)\left[\frac{b_1\left(a_0+a_1Q+a_2Q^2\right)}{\left(b_0+b_1Q\right)^2}\right]\\&+3\left(Q^2-Q\right)^2\left(2Q+1\right)\left[\frac{2a_2\left(b_0+b_1Q\right)-2b_1\left(a_1+2a_2Q\right)}{\left(b_0+b_1Q\right)^2}\right]\\&+3\left(Q^2-Q\right)^2\left(2Q+1\right)\left[\frac{2b_1^2\left(a_0+a_1Q+a_2Q^2\right)}{\left(b_0+b_1Q\right)^3}\right]\\&+\left(Q^2-Q\right)^3\left[\frac{-6a_2b_1\left(b_0+b_1Q\right)+6b_1^2\left(a_1+2a_2Q\right)}{\left(b_0+b_1Q\right)^3}\right]\\&-\left(Q^2-Q\right)^3\left[\frac{6b_1^3\left(a_0+a_1Q+a_2Q^2\right)}{\left(b_0+b_1Q\right)^4}\right].\end{aligned} \tag{24}$$

The exact solutions of Eq.(1) is obtained as the following;

Case 1

$$\begin{aligned}a_0&=-\frac{\sqrt{\left(-1+k^2\right)p^2}\,b_0}{2\sqrt{2}},\\a_2&=-2a_1+\frac{\sqrt{2}\sqrt{\left(-1+k^2\right)p^2a_1^2}\;b_0}{a_1},\\b_1&=\frac{-2\left(\sqrt{2}\sqrt{\left(-1+k^2\right)p^2a_1^2}-\left(-1+k^2\right)p^2b_0\right)}{\left(-1+k^2\right)p^2},\\m&=\frac{1}{4}\left(-2k^2-p^2\right),\end{aligned} \tag{25}$$

When we substitute Eq.(25) into Eq.(21), we get dark soliton solutions of Eq.(1)

$$\begin{aligned}E_1\left(x,t\right)&=e^{i(kx+mt)}\left[A\tanh\left(p_1x+r_1t\right)\right],\\n_1\left(x,t\right)&=\left(\frac{2p^2}{r^2-p^2}\right)\left[A\tanh\left(p_1x+r_1t\right)\right]^2,\end{aligned} \tag{26}$$

where $A=-\frac{\sqrt{\left(-1+k^2\right)p^2}}{2\sqrt{2}}$, $p_1=\frac{p}{2}$, and $r_1=\frac{r}{2}$.

Case 2

$$a_0=\frac{-a_1}{2},\ a_2=-a_1,\ b_0=\frac{-ia_1}{\sqrt{2p^2-2k^2p^2}},\quad b_1=\frac{2ia_1}{\sqrt{2p^2-2k^2p^2}},\ m=-\frac{k^2}{2}-p^2, \tag{27}$$

If we substitute Eq.(27) into Eq.(21), we gain dark soliton solutions of Eq.(1)

$$E_2(x,t)=e^{i(kx+mt)}\left[B\left(\coth\left(p_1x+r_1t\right)+\tanh\left(p_1x+r_1t\right)\right)\right],$$
$$n_2(x,t)=\left(\frac{2p^2}{r^2-p^2}\right)\left[B\left(\coth\left(p_1x+r_1t\right)+\tanh\left(p_1x+r_1t\right)\right)\right]^2, \tag{28}$$

where $B=-\frac{1}{4}i\sqrt{2p^2-2k^2p^2}$.

Case 3

$$a_0=0,\ a_2=-a_1,\ b_0=\frac{a_1}{\sqrt{2}\sqrt{\left(-1+k^2\right)p^2}},\quad b_1=\frac{-\sqrt{2}a_1}{\sqrt{\left(-1+k^2\right)p^2}},\ m=\frac{1}{2}\left(-k^2+p^2\right), \tag{29}$$

When we substitute Eq.(30) into Eq.(21), we have dark soliton solutions of Eq.(1)

$$E_3(x,t)=e^{i(kx+mt)}\left[C\left(\tanh\left(p_1x+r_1t\right)-\coth\left(p_1x+r_1t\right)\right)\right],$$
$$n_3(x,t)=\left(\frac{2p^2}{r^2-p^2}\right)\left[C\left(\tanh\left(p_1x+r_1t\right)-\coth\left(p_1x+r_1t\right)\right)\right]^2, \tag{30}$$

where $C=-\frac{1}{4\sqrt{2}\sqrt{\left(-1+k^2\right)p^2}}$.

In Figures 1-2, we plot two and three dimensional graphics of $E_1(x,t)$ in Eq. (26), which explain the vitality of solutions with suitable parameters. In Figure 3, we draw two and three dimensional graphics of $n_1(x,t)$ in Eq. (26), which indicate the dynamics of solutions with proper parameters. Also, in Figures 4-5, we plot two and three dimensional graphics of $E_3(x,t)$ in Eq. (30), which express the vitality of solutions with appropriate parameters. Finally, in Figure 6, we draw two and three dimensional graphics of $n_3(x,t)$ in Eq. (30), which show the dynamics of solutions with proper parameters.

Remark 1. The exact solutions of Eq. (1) were found via GKM, have been calculated by using Mathematica 9. As far as we know, the solutions of Eq. (1) obtained in this study, are new and are not observable in former literature.

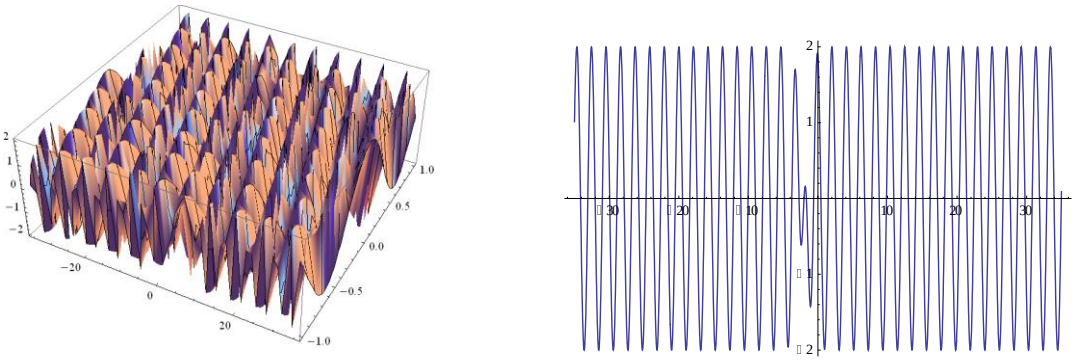

Figure 1. Graph of imaginary values of $E_1(x,t)$ in Eq. (26) is shown at $k=3, m=5, p=2, r=4, -35<x<35, -1<t<1$ and the second graph represents imaginary values of $E_1(x,t)$ in Eq. (26) for $-35<x<35,\ t=1$.

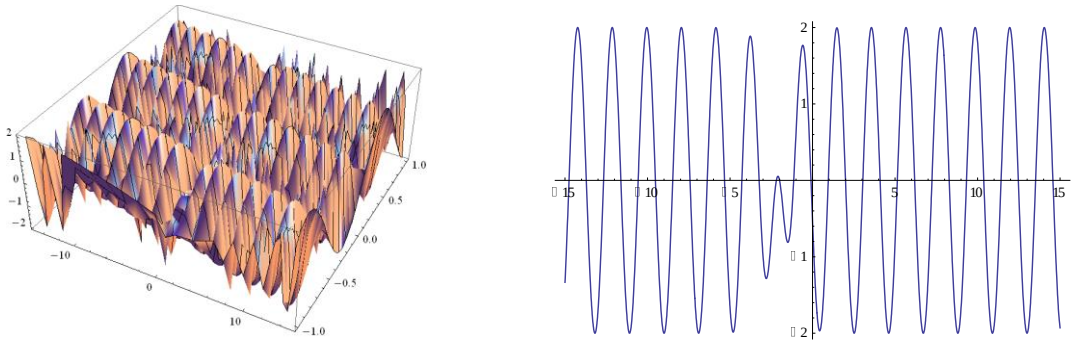

Figure 2. Graph of real values of $E_1\left(x,t\right)$ in Eq. (26) is indicated at $k=3, m=5, p=2, r=4, -15<x<15, -1<t<1$ and the second graph introduces real values of $E_1\left(x,t\right)$ in Eq. (26) for $-15<x<15, t=1.$

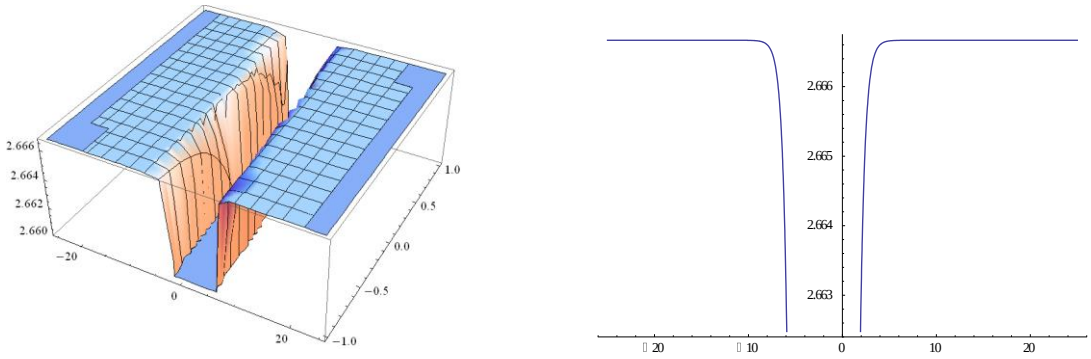

Figure 3. Graph of $n_1\left(x,t\right)$ in Eq. (26) is shown at $k=3, p=2, r=4, -25<x<25, -1<t<1$ and the second graph represents $n_1\left(x,t\right)$ in Eq. (26) for $-25<x<25, t=1.$

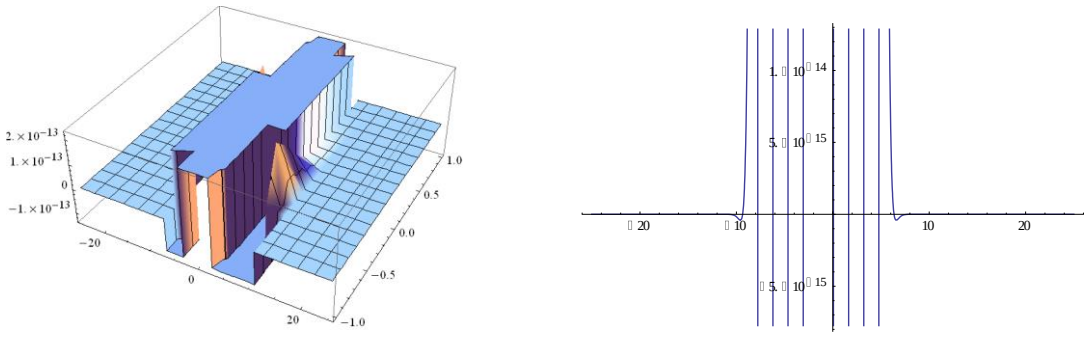

Figure 4. Graph of imaginary values of $E_3\left(x,t\right)$ in Eq. (30) is indicated at $k=2, m=3, p=4, r=6,$ $-25<x<25, -1<t<1$ and the second graph denotes imaginary values of $E_3\left(x,t\right)$ in Eq. (30) for $-25<x<25, t=1.$

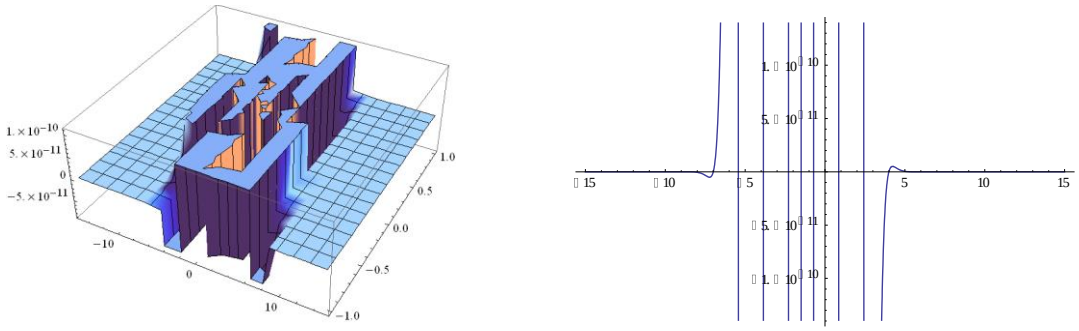

Figure 5. Graph of real values of $E_3\left(x,t\right)$ in Eq. (30) is shown at $k=2, m=3, p=4, r=6, -15<x<15, -1<t<1$ and the second graph remarks real values of $E_3\left(x,t\right)$ in Eq. (30) for $-15<x<15, t=1$.

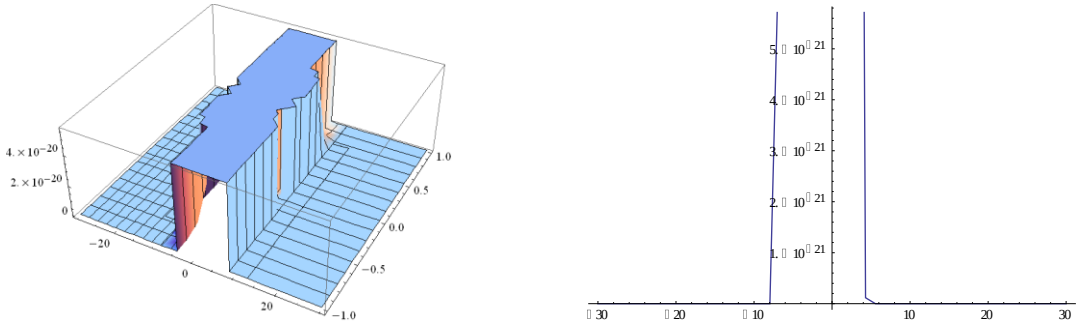

Figure 6. Graph of $n_3\left(x,t\right)$ in Eq. (30) is shown at $k=2, p=4, r=6, -30<x<30, -1<t<1$ and the second graph represents $n_3\left(x,t\right)$ in Eq. (26) for $-30<x<30, t=1$.

4. Physical explanation

In this section, we will present physical interpretation of the system of equations for the ion sound wave under the action of the ponderomotive force due to high-frequency field and for Langmuir wave.

Solitons are very special types of solitary waves. Soliton solutions occur in two kinds such as dark soliton and bright soliton. If the solution is in terms of sech function, the soliton is called bright soliton. But if the solution is in terms of tanh function, the soliton is called dark soliton. In the view of such information, the solutions Eqs. (26), (28) and (30) of Eq. (1) are dark soliton solutions.

5. Conclusion

In this paper, we obtain dark soliton solutions of the system of equations for the ion sound and Langmuir waves by using GKM. Then, for suitable parametric choices, we plot two and three dimensional graphics of some dark soliton solutions of this system of equations by using Mathematica Release 9. This method provides us to do complicated and tedious algebraic calculations. That is to say the availability of computer programmes such as Mathematica facilitates the tedious algebraic calculations.

The above results show that GKM has been efficient for the analytical solutions of the system of equations for the ion sound and Langmuir waves. Also, this method is a powerful mathematical tool in finding new dark and bright soliton solutions. Thus, we can point out that GKM has a key role to obtain analytical solutions of NLPDEs. The graphical demonstrations clearly indicate the effectiveness of the recommended method. We suggest that this method can also be applied to other NLPDEs.

References

[1] Cher, Y., Czubak, M., and Sulem, C., Blowing Up Solutions to the Zakharov System for Langmuir

Waves, Laser Filamentation, Springer International Publishing, 77-95 (2016).

[2] Eslami, M., Trial solution technique to chiral nonlinear Schrodinger's equation in (1+2)-dimensions, Nonlinear Dynamics, 85, 813-816 (2016).

[3] Hammouch, Z., and Mekkaoui, T., Traveling-wave solutionsof the generalized Zakharov equation with time-space fractional derivatives, Mathematics in Engineering, Science and Aerospace, 5(4), 489-498 (2014).

[4] Hammouch, Z., and Mekkaoui, T., Travelling-wavesolutions for some fractional partial differential equation by means ofgeneralized trigonometry functions, International Journal of Applied Mathematical Research, 1(2), 206-212 (2012).

[5] Degtyarev, L.M., Nakhan'kov, V.G., and Rudakov, L.I., Dynamics of the formation and interaction of Langmuir solitons and strong turbulence, Zh. Eksp. Teor. Fiz., 67, 533-542 (1974).

[6] Degtyarev, L.M., Zakharov, V.E., Sagdeev, R.Z., Solov'ev, G.I., Shapiro, V.D., Shevchenko, V.I., Langmuir collapse under pumping and wave energy dissipation, Zh. Eksp. Teor. Fiz., 85, 1221-1231 (1983).

[7] Anisimov, S.I., Berezovskii, M.A., Ivanov, M.F., Petrov, I.V., Rubenchick, A.M., Zakharov, V.E., Computer simulation of the Langmuir collapse, Phys. Lett. A, 92(1), 32-34 (1982).

[8] Anisimov, S.I., Berezovskii, M.A., Zakharov, V.E., Petrov, I.V., Rubenchik, A.M., Numerical simulation of a Langmuir collapse, Zh. Eksp. Teor. Fiz., 84, 2046-2054 (1983).

[9] D'yachenko, A.I., Zakharov, V.E., Rubenchik, A.M., Sagdeev, R.Z., Shvets, V.F., Numerical simulation of two-dimensional Langmuir collapse, Zh. Eksp. Teor. Fiz., 94, 144-155 (1988).

[10] Zakharov, V.E., Pushkarev, A.N., Rubenchik, A.M., Sagdeev, R.Z., Shvets, V.F., Numerical simulation of three-dimensional Langmuir collapse in plasma, Pis'ma v Zh. Eksp. Teor. Fiz., 47, 287-290 (1988).

[11] Benilov, E. S., Stability of plasma solitons, Zh. Eksp. Theor. Fiz., 88, 120-128 (1985).

[12] Zakharov, V.E., Pushkarev, A.N., Sagdeev, R.Z., Soloviev, S.I., Shapiro, V.D., Shvets, V.F., Shevchenko, V.I., "Throughout" modelling of the one-dimensional Langmuir turbulence, Sov. Phys. Dokl. 34, 248-251 (1989).

[13] Dyachenko, A.I., Pushkarev, A.N., Rubenchik, A.M., Sagdeev, R.Z., Shvets, V.F., Zakharov, V.E., Computer simulation of Langmuir collapse, Physica D, 52(1), 78-102 (1991).

[14] Rubenchik, A.M., Zakharov, V.E., Strong Langmuir turbulence in laser plasma, Handbook of Plasma Physics, Elsevier Science Publishers, 3, 335-360 (1991).

[15] Musher, S.L., Rubenchik, A.M., Zakharov, V.E., Weak Langmuir turbulence, Phys. Rep. 252(4), 178-274 (1995).

[16] Robinson, P.A., Willes, A.J., and Cairns, I.H., Dynamics of Langmuir and ion-sound waves in type III solar radio sources, The Astrophysical Journal, 408, 720-734 (1993).

[17] Chen, Y-H, Lu, W., and Wang, W-H, The Nonlinear Langmuir Waves in a Multi-ion-Component Plasma, Commun. Theor. Phys., 35, 223-228 (2001).

[18] Soucek, J., Krasnoselskikh, V., Dudok de Wit, T., Pickett, J., and Kletzing, C., Nonlinear decay of foreshock Langmuir waves in the presence of plasma inhomogeneities: Theory and Cluster observations, Journal of Geophysical Research, 110, A08102:1-10 (2005).

[19] Dodin, I.Y., Geyko V.I., and Fisch, N.J., Langmuir wave linear evolution in inhomogeneous nonstationary anisotropic plasma, Physics of Plasmas, 16, 112101:1-9 (2009).

[20] Zaslavsky, A., Volokitin, A.S., Krasnoselskikh, V.V., Maksimovic M., and Bale, S.D., Spatial localization of Langmuir waves generated from an electron beam propagating in an inhomogeneous plasma: Applications to the solar wind, Journal of Geophysical Research, 115, A08103:1-11 (2010).

[21] Ratcliffe, H., Brady, C.S., Che Rozenan, M.B., and Nakariakov, V.M., A comparison of weak-turbulence and particle-in-cell simulations of weak electron-beam plasma interaction, AIP-Physics of Plasmas, 21, 122104:1-9 (2014).

[22] Ajima, N.Y., and Wa, M.O., Formation and Interaction of Sonic-Langmuir Solitons, Progress of Theoretical Physics, 56(6), 1719-1739 (1976).

[23] Zakharov, V.E., Collapse of Langmuir Waves, Zh. Eksp. Teor. Fiz., 62, 1745-1759 (1972).

[24] Tuluce Demiray, S., Pandir, Y., and Bulut, H., New Soliton Solutions for Sasa-Satsuma Equation, Waves in Random and Complex Media, 25(3) , 417-428 (2015).

[25] Tuluce Demiray, S., Pandir, Y., and Bulut, H., New Solitary Wave Solutions of Maccari System, Ocean Engineering, 103, 153-159 (2015).

[26] Tuluce Demiray, S., and Bulut, H., New Exact Solutions of the New Hamiltonian Amplitude Equation and Fokas Lenells Equation, Entropy, 17, 6025-6043 (2015).

[27] Tuluce Demiray, S., Pandir, Y., and Bulut, H., All Exact Travelling Wave Solutions of Hirota Equation and Hirota-Maccari System, Optik, 127, 1848-1859 (2016).

[28] Tuluce Demiray, S., and Bulut, H., Generalized Kudryashov method for nonlinear fractional double

sinh-Poisson equation, J. Nonlinear Sci. Appl., 9, 1349-1355 (2016).

[29] Tuluce Demiray, S., Pandir, Y., and Bulut, H., The Analysis of The Exact Solutions of The Space Fractional Coupled KD Equations, AIP Conference Proceedings, 1648, 370013-(1-5) (2015).

Seyma Tuluce Demiray is a Research Assist. Dr. in Department of Mathematics at Firat University; Elazig (Turkey). She has published more than 20 articles in journals. Her research interests include analytical methods for nonlinear differential equations, numerical solutions of the partial differential equations and computer programming.

Hasan Bulut is currently an Assoc. Prof. Dr. in Department of Mathematics at Firat University. He has published more than 100 articles in journals. His research interests include stochastic differential equations, fluid and heat mechanics, finite element method, analytical methods for nonlinear differential equations, mathematical physics, and numerical solutions of the partial differential equations, computer programming.

An International Journal of Optimization and Control: Theories & Applications (http://ijocta.balikesir.edu.tr)

An International Journal of Optimization and Control: Theories & Applications
ISSN: 2146-0957 eISSN: 2146-5703
Vol.7, No.1, pp.50-58 (2017)
https://doi.org/10.11121/ijocta.01.2017.00408

RESEARCH ARTICLE

The effects of LT-SN on energy dissipation and lifetime in wireless sensor networks

Zeydin Pala [*]

[*] *Department of Computer Engineering, Muş Alparslan University, Turkey*
z.pala@alparslan.edu.tr

ARTICLE INFO

Article history:
Received: 22 October 2016
Accepted: 26 November 2016
Available Online: 29 November 2016

Keywords:
Long-term sleep nodes
Energy dissipation
Linear programming
Modelling
Optimization

AMS Classification 2010:
90C05, 65K05

ABSTRACT

Wireless sensor networks (WSNs) still attract the attention of researchers, users and the private sector despite their low power and low range tendency for malfunction. This attraction towards WSNs results from their low cost structure and the solutions they offer for many prevalent problems. Many conditions, which remain unforeseen or unexpected during the design of the system, may arise after the initialization of the system. Similarly, many situations where security vulnerabilities take place may emerge in time in WSNs operating normally. In this study, we called nodes which enter sleeping mode without any further waking up and causing a sparser number of nodes in the network without any function in data transmission as Long-Term Sleep Nodes (LT-SN); and considered energy spaces caused by such nodes as a problem; and established two Linear Programming (LP) models based on the efficiency of the present nodes. We offered two different models which present the effect of sensor nodes, which were initially operating in wireless sensor network environment and did not wake up following sleep mode, on network lifetime. The results of the present study report that as the number of LT-SN increases, the lifetime of the network decreases.

1. Introduction

Technological developments in Wireless sensor networks (WSNs) field are indicating that WSNs will be much more prevalently utilized in the future. Important advancements were made regarding the solution of many bottlenecks thanks to studies carried out on WSNs until now [1]. However, many more studies have to be carried out in order to provide solutions for the energy efficiency and high lifetime bottlenecks [2]. There are more challenges (i.e., computation/communication, save energy, balance energy, maximize network lifetime, minimize energy consumption, minimizing processing time, communication and message complexity, optimized and select the best transmission routes, query huge amount of data) to be overcome in WSNs.

When a node's energy is a critical level, it cannot provide sensor data to the network, and it cannot forward data from other nodes. This situation leads to the formation of energy gaps in the network and higher energy consumption. Due to these holes, both security vulnerability occurs and more load is put on the rest of the nodes [3]. Hence, this affects the network lifetime adversely [4]. Problems like this have their negative effects on network robustness and stability [5]. Energy is one of the main sources that has to be used effectively in WSNs. In the present case, since studies related to the wireless charging of the sensor nodes have not reached a sufficient level yet [6], our primary objective is the best utilization of the battery energy in the nodes of the sensor network. By using the energies of the nodes in the network more effectively, the lifetime of the networks is extended and more long term operation can be maintained. Therefore, it can be inferred that a linear relationship is present between the lifetime of the network and effective use of the energy. Spaces are forming in a sensor network with full initial coverage area due to nodes entering sleeping mode and losing connection with the network over time. These spaces both cause security issues and more workload on the remaining nodes which are required to protect and observed the same related area. This naturally causes high level energy consumption due to the forming spaces and as a result of excessive energy

[*]Corresponding author

consumption, the lifetime of the network is negatively affected due to this fact.

In this paper, we accepted the effects on the lifetime of the network and the consumed energy due to the energy spaces caused by LT-SN nodes, which are not participating in data transmission, as a problem. Our purpose was the most efficient lifetime extension of the network and minimization of the consumed energy by using program codes written in a mathematical programming and optimization environment and compatible with the configured mathematical model despite the presence of LT-SN nodes with known locations in the network environment which are not performing sensing duties.

We can define the contribution of this paper to the literature as follows: (1) introducing the LT-SN concept to wireless sensor networks and developing a model compatible with this concept, (2) configuration of the same area in the most optimal way with the remaining nodes for observation by using two different algorithms and (3) analysing the performance of the suggested LP mathematical model related to the researched problem via the performed simulations.

The remain of this paper is organized as follows: The Section 2 gives a brief review of the literature review efforts on minimizing energy and maximizing the lifetime WSN. Section 3 gives system model, and LP formulations. Analysis based on LP models are given in Section 4. Section 5 gives the conclusion of the paper.

2. Literature review

In this section, we shortly summarize related research efforts on minimizing dissipation energy, and maximizing the lifetime of WSN, which involves looking at the mathematical LP formulation of the impact LT-SN on dissipation energy, and maximum lifetime. Recently, significant efforts have been made on reducing the energy consumed by node or to extend the lifetime of the network [7,8]. Bulut and Korpeoglu [7] proposed a novel model named dynamic sleep scheduling protocol (DSSP), for extending the lifetime by keeping only a necessary set of sensor nodes active. Singh and Bharti [8] proposed a sleep management protocol which support sleep or awake mode to conserve energy consumption. Jurdak and Ruzelli [9] proposed a node energy model which includes energy components for radio transmission, reception, listening, and sleeping mode. Despite the fact that some previous studies have investigated the impact of short-term sleeping node on network lifetime in wireless sensor network [10,11], the impact of LT-SN on the network lifetime has not been fully investigated. Wang et al [10] proposed a scheduling algorithm, namely, energy-consumption-based CKN, to prolong the network lifetime. Chachra and Marefat [11] proposed several distributed algorithms to perform sensor and radio sleep scheduling in WSNs. Saraswat et al. [12] proposed a scheme and the lifetime of the nodes based on overall energy consumption is estimated and studied the effect of duty cycle on expected energy consumption was studied. Pagar et al. [13] proposed radio power modes which dynamically change according to current traffic situation in the network. They addressed deep sleep mode pulled low current, but it caused more energy costs due to delays. Mahani et al. [14] studied the multi-mode structures from credibility viewpoint of the sleep modes. They showed sleep modes lead to long path length from source to sink and so decreased the message credibility. In this study, we tried to draw the attention of researchers especially to the observation and sensing requirement of the emptied areas caused by LT-SN nodes as well as the required extra energy. This study carries similarities with Cardei et al. [15] if considered regarding the coverage or protection, however differs completely with the LT-SN concept. This is because they aim to increase the energy efficiency by holding one part of the nodes in sleeping mode while sustaining the other part in a waked state. In our study however, the nodes entering sleeping modes do not wake up again, therefore they have no role in data production or data transmission. As time passes, the remaining nodes which have the objective of protecting the area are facing an increased data transmission load and are consuming more energy caused by the disappearance of the LT-SN nodes in some sense. Yuksel et al. [16] researched the most critical node in network environment by resolving the LP problem which maximizes lifetime parameter. Our present study is in parallel with the study of [16] both in terms of investigating the effects of network on general life when certain nodes are out-of-service and with regard to LP model. Pala et al. [17] investigated the excess energy due to nodes in partial sleeping mode, which are only able to transmit the sensed data to the center or which have no source or in-between node role at all. Our present study differs from in [17] study in three regards: (i) two different LP models which are more advanced, maximizing the lifetime and minimizing the power consumptions were used. (ii) the LT-SN in this present model are not used as a source or node in-between in any way. (iii) the present model is able to transmit data, produced by single as well as multiple sources, to the target.

3. Concept and model

Throughout this research paper, our main aim is to investigate the effects of LT-SN that are not served during the data transfer [18] on energy dissipation characteristics of sensor nodes. In this section, we clarify the assumptions, define our system model, and formulate the optimization problem. By using the developed model, we formulate minimizing consumed energy and maximizing lifetime in the network as an LP framework.

3.1. System model

Network topology is a G (W, A) diagram which is complete and directional. W is the set of all sensors including the base station. V is indicating the set of sensor nodes excluding base station (BS) V=W \ {1}.

A = {(x, y): x ∈ V, y ∈ W-x} is the cluster of all border points.

All messages that will be sent from node N_x to node N_y during network lifetime are referred as β_{xy}.

All system notations used in this study are presented in Table 1.

Table 1. Summary of notation

Variable	Description
A	Set of arcs
W	The set of nodes including the base station (BS)
V	The set of nodes excluding the BS
S_x	The data generated by node N_x
N	The number of nodes in a network environment
N_S	Number of source nodes
$N_{LT\text{-}SN}$	Number of long-term sleep nodes
V_A	Deployment area
N_{SRC}	Source node
U	Set of source nodes
ε	Transmitters efficiency
ρ	The energy consumed in the electronic circuit
α	Transmission path loss exponent
e_x	The battery power of each node in a network environment
β_{xy}^{z}	Data flow from node N_x to node N_y (z-source data stream)
E_{rx}	The amount of consumed energy for receiving data
E_{tx}	The amount of consumed energy whereas transmitting one bit of data form node N_x to node N_y
d_{xy}	The distance between two nodes
L	Network lifetime (s)

Throughout this study, we use the first order radio parameters given in [19].

$$E_{Tx,xy} = \rho + \varepsilon(d_{xy})^{\alpha} \quad (1)$$

$$E_{Rx} = \rho \quad (2)$$

$$d_{xy} = \sqrt{(x_2 - x_1)^2 + (y_2 - x_1)^2} \quad (3)$$

Eq. (1) and Eq. (2) illustrate the amount of energy for transmission (from node N_x to N_y) and reception of a bit, respectively.

Where ρ models the energy dissipation on electronic circuitry (ρ = 50 nJ), ε indicate the transmitter's efficiency (ε = 100 pJ), α represents the path loss exponent, and d_{xy} is the distance between N_x and N_y, based on Euclidean distance as shown in Eq. (3).

The Euclidean distance is calculated between each sensor node and BS.

In this study, the life of the network is considered as the duration between the time network starts operation and the time when the first node in the network consumes entire its energy and dies [20].

On the same network area 100 nodes, 50 nodes and 25 nodes network topologies were used.

The placement of the nodes in the network environment was different for each topology.

In each simulation, which carried out the node placement is kept constant.

The only thing that varies in each simulation was randomly selected source nodes.

3.2. LP framework

Equations of the LP optimization problem which are minimizing the battery energy of the sensor nodes are given in the Eq. (4)-Eq. (11) interval, while the equations of the LP optimization problem which are extending the lifetime are given in the Eq. (12)-Eq. (19) interval [21].

If the given model equations are solved with the optimization program, the data produced by the sources is sent to the collecting node via the most ideal way and lowest energy utilization possible, dependent on the obtained data transmission model. The multiple to single (convergecast) transmission mode was used during data transmission.

All nodes except the source node, collection node and LT-SN nodes are able to operate as a relay (in-between node).

In scenarios multiple sources are used (double, triple, quintet), each source is programmed in such a way that they can operate as a potential relay node for the other source nodes.

For example, three of 100 randomly distributed nodes with the purpose of observing a disc shaped area with a radius of R=100 m shall act as source nodes (N_{15}, N_{21} and N_{95}) and 5% (N_2, N_{13}, N_{33}, N_{59} and N_{66}) shall be LT-SN. The LP model accepts all nodes as in-between nodes except the LT-SN and the target and sends data produced in three separate to the target node in an energy minimizing fashion.

Each node that is producing data is able to act as a potential relay node for the other data producing nodes.

The objective function of optimization problem is to minimize the $\mathbf{e}_x$ parameters as given below:

Minimize e_x

Subject to the following constraints:

$$\beta_{xy} \geq 0 \ \forall (x, y) \in W \quad (4)$$

$$\beta_{xy} = 0, if\ N_x = N_y \text{ and } N_x = N_1 \ \forall (x, y, z) \in W \quad (5)$$

$$\beta_{xy} = 0, if\ N_y = N_{LT-SN} \ \forall y \in U_{LT-SN} \quad (6)$$

$$\beta_{xy} = 0, if\ N_x = N_{LT-SN} \ \forall x \in U_{LT-SN} \quad (7)$$

$$\sum_{y \in V} \beta_{xy} = \sum_{y \in V} \beta_{yx} + S_x \ \forall x \in U_{SRC} \quad (8)$$

$$S_x + \sum_{y \in V} \beta_{xy} = \sum_{y \in V} \beta_{yx} \ \forall x \in U_{DST} \quad (9)$$

$$\sum_{y \in V} \beta_{xy} = \sum_{y \in V} \beta_{yx} \ \forall x \in V,\ N_x \neq N_{SRC} \quad (10)$$

$$E_{Rx} \sum_{z \in U} \sum_{y \in V} \beta_{xy} + \sum_{z \in U} \sum_{y \in V} E_{Tx} * \beta_{yx} \leq e_x \ \forall x \in V \quad (11)$$

Seeing that the objective is to minimize the energy dissipation of nodes for this model, our first problem is the minimization of the maximum energy consumption in the network by finding the βxy that satisfier the constraints. The equations belonging to the recommended first LP framework may be explained briefly as follows:

Eq. (4) shows that all currents flowing in the network are positive.

Eq. (5) shows currents that should and should not be present within the network. For example, a node cannot send data to itself. Similarly, a base station cannot send data to a node.

Eq. (6) shows that none of the nodes within the network can send data to the LT-SN nodes.

Eq. (7) shows that none of the LT-SN nodes can send data to the nodes within the network.

Eq. (8) shows that the data sent by nodes to other nodes is equal to the data produced by that node and the data obtained by other nodes.

Eq. (9) shows that the sum of data produced by one node and the data obtained by other nodes is equal to the data sent to other nodes by that node.

Eq. (10) shows that each node can act as a node in-between, except the base station, LT-SN and node operating as a source. Eq. (11) shows that the sum of total energy consumed for receiving the total energy by each node and the sum of the total energy consumed for the sent data is not greater than its battery energy, except for base station and LT-SN. Our purpose with the second LP model is the maximization of the network lifetime (Eq. (12). Equations of this model are given in the Eq. (13)-Eq. (19) interval. While single, double, triple and quintet data sources were used simultaneously in the first LP model which is minimizing the consumed energy, single and triple sources were used in the second LP model which maximizes the lifetimes.

The objective function of optimization problem is to maximize the L parameters as given below:

Maximize L (12)

Subject to the following constraints:

$$\beta_{xy} \geq 0 \ \forall (x, y) \in W \quad (13)$$

$$\beta_{xy} = 0, if\ \ N_x = N_y \forall (x, y) \in W \quad (14)$$

$$\beta_{xy} = 0, if\ \ N_y = N_{LT-SN} \forall y \in U_{LT-SN} \quad (15)$$

$$\beta_{xy} = 0, if\ \ N_x = N_{LT-SN} \text{ and } N_x = N_1 \quad (16)$$

$$\sum_{y \in V} \beta_{xy} + S_x L = \sum_{y \in V} \beta_{yx} \ \forall x \in U_{SRC} \quad (17)$$

$$\sum_{y \in V} \beta_{xy} = \sum_{y \in V} \beta_{yx} \ \forall x \in V, N_x \neq N_{SRC} \quad (18)$$

$$E_{Rx} \sum_{y \in V} \beta_{xy} + \sum_{y \in V} E_{Tx} * \beta_{yx} \leq e_x \ \forall x \in V \quad (19)$$

4. Analysis

In the first scenario where the effects of the LT-SN on the general lifetime of the network are investigated by using two different LP models, the utilized energy is minimized in the best way possible by a linear program coded in a General Algebraic Modeling System (GAMS) optimization and modeling software environment [22] while in the second scenario, the lifetime of the nodes was tried to be maximized [23,24].

While single, double, triple and quintet sources were used in the first LP model, single and triple sources were used in the second LP model. Initially, a R=100 radius, disc shaped area was observed by 100 sensor nodes. In this scenario, the data was initially produced by a single source as 1024 bit. The data producing source changes on each operation. In this regard, the produced data are sent to the exact center of the disc area and the N_1 collecting node present at the coordinates (0,0) via the most ideal algorithm together with energy minimization through linear programming. In this scenario, the nodes are operating normally and no LT-SN node is present. The average of the lowest energy consumption values of 1000 operations were obtained in this scenario and are kept for the later obtainment of single source normalized reference values. This is because the scenario in which all nodes are operating is a normal scenario. As time progresses, the number of LT-SN increases and the results obtained in each run are divided with normal values in order to obtain the normalized values. The state of the consumed energy or obtained network lifetime durations will be evaluated in accordance to the values obtained under normal conditions.

The initial scenario of 100 nodes protecting and observing the disc area with one source is afterwards repeated with double sources, triple sources and quintet sources. In the quintet operation, the data produced by any five sources distributed randomly within the disc area, with the exception of the collecting node, is transmitted to the collecting node via the remaining nodes.

In the following scenarios, single source, double source, triple source and quintet source operations are carried out with 50 nodes in the R=100 m radius disc shaped area. The same procedure is carried out for 25 nodes in single source, double source, triple source and quintet source as well. Each run is repeated 1000 times and the obtained mean values are saved for normalization. Initially, the locations of the sensor nodes scattered in the area did not change at all. As the LT-SN decrease after some time, the distance between the remaining nodes increases naturally.

New analysis was carried out under the assumption that the LT-SN nodes within the wireless sensor network are emerging as time progresses and that their numbers increase by 1%, 4%, 6%, 8%, 10%, 20%, 30%, 40%, 50%, 60%, 70%, 80% and 90%. In the case of increase; the number of the nodes (25, 50 and 100) as well as the number of sources was considered. Analysis that had been carried out as single source initially were performed with multiple sources afterwards in respective order. During these studies, the LT-SN nodes were not allowed to operate in source, target or in-between node mode in any way. Nodes other than these were allowed to produce data as single, double, triple or quintet source nodes and the data produced by the sources was transmitted to the central node via the remaining nodes, except the LT-SN nodes.

The first LP model used in the study was mathematically minimizing the energy consumption. After the solution of the first model with a program coded in the GAMS environment, Figure 1, Figure 2, Figure 3, Figure 4 and Figure 5 were obtained following the analysis.

The second LP model on the other hand was maximizing the lifetime. Figure 6 and Figure 7 was obtained via the solution of the second model.

In Figure 1, the consumed normalized energy values, in the case where single, double, triple and quintet sources are used for N=100, are given as a function of the percentage increase of the LT-SN nodes. The LT-SN nodes increase in 1%, 4%, 6%, 8%, 10%, 20%, 30%, 40%, 50%, 60%, 70%, 80% and 90% steps. As it can be observed in the graph, as the number of sources that are simultaneously producing data increases, the consumed energy increases as well. As the number of LT-SN nodes increases for each scenario shown in the graph, the remaining nodes receive a higher data transmission load and therefore the consumed energy increases as well. While the lowest energy consumption was observed in the single source scenario, the highest energy consumption was observed in the quintet scenario. As shown in Table 2, in an area with 100 nodes present, a LT-SN node increase of 10% corresponds to 0.9%, 1.0%, 9.0% and 11.1% utilized and normalized energy values for single, double, triple and quintet sources, respectively. In the scenario where N=100 nodes were used, the utilized and normalized energy values for single, double, triple and quintet sources in the case where the LT-SN nodes reached 20% was 5.6%, 7.7%, 18.4% and 19.4%, respectively.

Table 2. Percentage consumed power in case of using single and dual source node

Increase of the percentage consumed energy (for N = 25)				
$N_{LT\text{-}SN}$ (%)	N_S=1	N_S=2	N_S=3	N_S=5
10	9.1%	11.0%	14.1%	25.2%
20	18.4%	21.8%	23.0%	29.3%
30	19.7%	24.8%	25.8%	56.0%
Increase of the percentage consumed energy (for N = 50)				
$N_{LT\text{-}SN}$ (%)	N_S=1	N_S=2	N_S=3	N_S=5
10	5.8%	12.0%	13.9%	15.3%
20	9.5%	13.0%	15.5%	21.4%
30	12.9%	14.7%	16.3%	29.9%
Increase of the percentage consumed energy (for N = 100)				
$N_{LT\text{-}SN}$ (%)	N_S=1	N_S=2	N_S=3	N_S=5
10	0.9%	1.0%	9.0%	11.1%
20	5.6%	7.7%	18.4%	19.4%
30	11.7%	12.2%	19.8%	19.9%

In Figure 2, the consumed normalized energy values, in the case where single, double, triple and quintet sources are used for N=50, are given as a function of the percentage increase of the LT-SN nodes. As the number of LT-SN nodes increases for each scenario shown in the graph, the remaining nodes receive a higher data transmission load and therefore the consumed energy increases as well. While the lowest energy consumption was observed in the single source scenario, the highest energy consumption was observed in the quintet scenario. As shown in Table 2, in an area with 50 nodes present, a LT-SN node increase of 10% corresponds to 5.8%, 12.0%, 13.9% and 15.3% utilized and normalized energy values for single, double, triple and quintet sources, respectively. If the N=100 and N=50 node scenarios are evaluated for a LT-SN node increase of 10%, it can be inferred that the latter consumes more energy. This is because it is more advantageous to protect the present area with 100 nodes instead of 50 nodes.

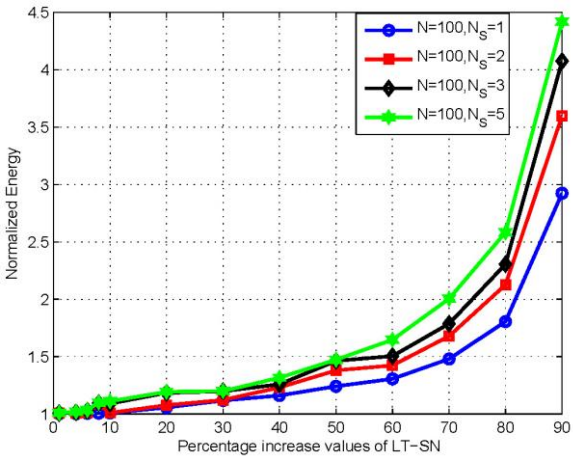

Figure 1. In the case where single, double, triple and quintet sources are used for N=100, the consumed normalized

energy value as a function of LT-SN nodes is.

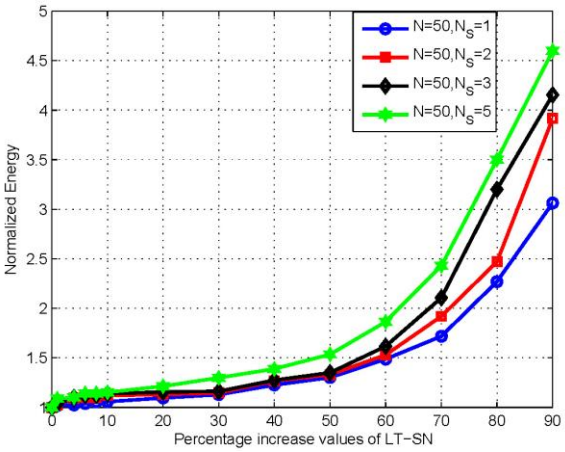

Figure 2. In the case where single, double, triple and quintet sources are used for N=50, the consumed normalized energy value as a function of LT-SN nodes is.

In Figure 3, the consumed normalized energy values, in the case where single, double, triple and quintet sources are used for N=25, are given as a function of the percentage increase of the LT-SN nodes. As the number of LT-SN nodes increases for each scenario shown in the graph, the remaining nodes receive a higher data transmission load and therefore the consumed energy increases as well. While the lowest energy consumption was observed in the single source scenario, the highest energy consumption was observed in the quintet scenario. As shown in Table 2, in an area with 25 nodes present, a LT-SN node increase of 10% corresponds to 9.1%, 11.0%, 14.1% and 25.2% utilized and normalized energy values for single, double, triple and quintet sources, respectively. If the N=50 and N=25 node scenarios are evaluated for a LT-SN node increase of 10%, it can be inferred that the latter consumes more energy. This is because it is more advantageous to protect the present area with 50 nodes instead of 25 nodes. The results obtained for the case where a single source was used for N=25, N=50 and N=100 nodes is graphically and collectively shown, in Figure 4. We can infer that all three curves are displaying a tendency for increase due to the increased number of LT-SN nodes. The energy consumption changes in relation with the number of nodes used in the network, as the number of nodes increases, the consumed energy decreases. While the highest energy consumption was observed in the N=25 node condition, the most ideal energy consumption was observed at N=100. The results obtained for the case where quintet sources were used for N=25, N=50 and N=100 nodes is graphically and collectively shown, in Figure 5. In the graph, we can observe that all three curves are displaying a tendency for increase due to the increased number of LT-SN nodes and that they display a higher increase than the single source. The energy consumption changes in relation with the number of nodes used in the network, as the number of nodes increases, the consumed energy decreases. While the highest energy consumption for quintet sources was observed in the N=25 node condition, the most ideal energy consumption for quintet sources was observed at N=100.

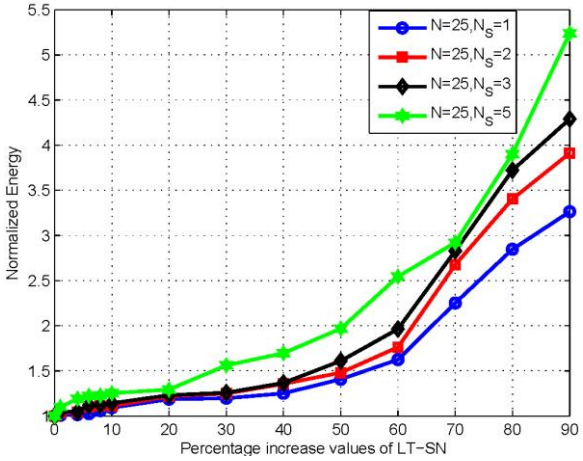

Figure 3. In the case where single, double, triple and quintet sources are used for N=25, the consumed normalized energy value as a function of LT-SN nodes is.

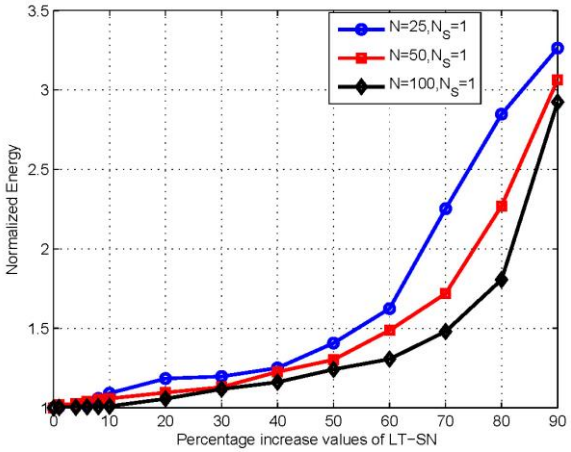

Figure 4. In the case where single sources are used for N=25, N=50 and N=100 the consumed normalized energy value as a function of LT-SN nodes is.

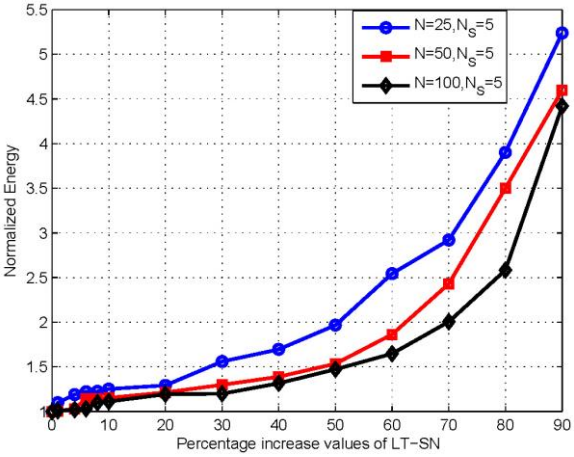

Figure 5. In the case where quintet sources are used for N=25, N=50 and N=100 the consumed normalized energy value as a function of LT-SN nodes is.

As it is shown in Figure 6, which was obtained via the solution of the second model, the normalized lifetime durations obtained for N=25, N=50 and N=100 nodes where a single source was used, are given as a function of the LT-SN nodes. While the highest lifetime durations are given with the curve where N=100 nodes were used, the lowest lifetime durations are given with the curve where N=25 nodes were used. The lifetime durations decreased due to the increased LT-SN nodes in all three curves. The lifetime durations decreased 13.0%, 4.0% and 1.9% for N=25, N=50 and N=100 nodes, respectively. As it is shown in Figure 7, which was obtained via the solution of the second model, the normalized lifetime durations obtained for N=25, N=50 and N=100 nodes where a triple source was used, are given as a function of the LT-SN nodes.

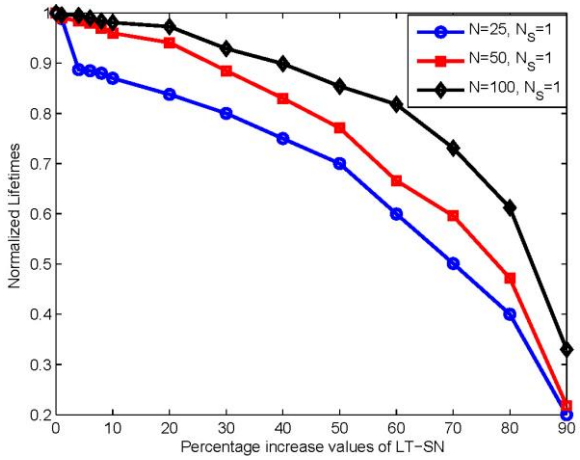

Figure 6. In the case where single sources are used for N=25, N=50 and N=100 the obtained normalized lifetime as a function of LT-SN nodes is.

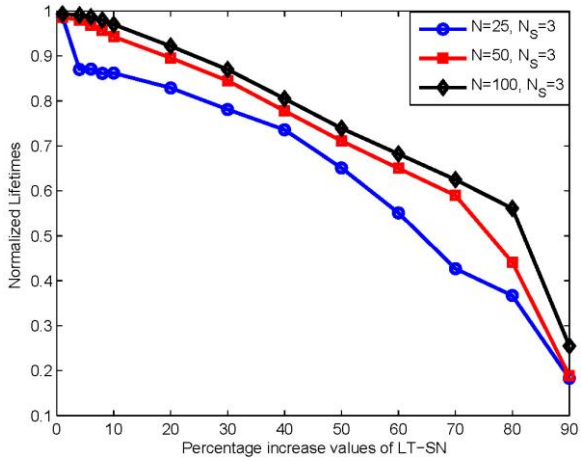

Figure 7. In the case where triple sources are used for N=25, N=50 and N=100 the obtained normalized lifetime as a function of LT-SN nodes is.

While the highest lifetime durations are given with the curve where N=100 nodes were used, the lowest lifetime durations are given with the curve where N=25 nodes were used. The lifetime in all three curves decreased due to the increased LT-SN nodes as well as the increasing number of sources. The lifetime durations for triple sources are 13.8%, 5.7% and 3.0% for N=25, N=50 and N=100 nodes, respectively.

5. Conclusion

In this study, we accepted the effects on the lifetime of the network and the consumed energy due to the energy spaces caused by LT-SN nodes, which are entering long term sleeping mode and are not waking up, thus are not participating in data transmission and are causing security issues, as a problem. We widely studied the effect of the LT-SN nodes on the network lifetime as well as the energy consumption. For this reason, we established two different linear programming models which minimize the energy consumption, extend the lifetime and carry out the most ideal data guidance.

The decreased number of the nodes placed randomly on the area was defined as LT-SN nodes in order to cover the present area in a complete manner with the remaining nodes after each run. Particularly the analysis results of our second LP model are similar with the results reported in [16]. Authors [16] found the effect of the most critical node as 2.0% in the topology where 100-sensor node was preferred by using discrete energy consumption model. In the present study, it was found that the network lifetime would fall down 1.9% when 10% nodes were out of service in case that same number of nodes, same topology and continuous energy model were used through LP.

References

[1] Yildiz, H.U., Bicakci, K., Tavli, B., Gultekin, H., İncebacak. D., "Maximizing wireless sensor network lifetime by communication/computation energy optimization of non-repudiation security service: Node level versus network level strategies", *Ad Hoc Networks*, Vol 37 No. 2, pp. 301-323 (2016).

[2] Weijie, L., Donglin, B., "Energy-efficient distributed lifetime optimizing scheme for wireless sensor networks", *Transactions of Tianjin University*, Vol 22 No.1, pp.11-18 (2016).

[3] Kashi, S.S., Sharifi, M., "Connectivity weakness impacts on coordination in wireless sensor and actor networks", Comm. *Surveys & Tutorials*, Vol 15 No.1, pp. 145-166 (2013).

[4] Jaquez, J., Valencia, D., Balakrishnan, M., Johnson E.E., Huang, H., "Implementation of TEAN-sleep for wireless sensor networks", *MILCOM'09 Proceedings of the 28th IEEE conference on Military communications*, NJ, pp. 824-830 (2009).

[5] Abdelsalam, H.S., Olariu, S., "On prolonging network lifetime by adjusting sleep/awake cycles in wireless sensor networks", *In Networked Sensing Systems (INSS) Sixth International Conference*, Pittsburgh, PA, pp. 1-6 (2009).

[6] Basha, E., Eiskamp, M., Johnson, J., Detweiler, C., "UAV Recharging opportunities and policies for sensor networks",. *Int. J. of Distributed Sensor Networks*, Vol 11 No. 8, pp. 1-10 (2015).

[7] Bulut, E., Korpeoglu, İ., "DSSP: A dynamic sleep scheduling protocol for prolonging the lifetime of wireless sensor networks". *In Advanced Information Networking and Applications Workshops*, Niagara Falls, Ont., pp. 725-730 (2007).

[8] Singh, H.K., Bharti, J., "A novel solution for sleep scheduler in wireless sensor networks", *International Journal of Advanced Smart Sensor Network Systems*,Vol 2 No 1, pp.13:19 (2012).

[9] Jurdak, R., Ruzelli, A.G., O'Hare, M.P., "Radio sleep mode optimization in wireless sensor networks", *Mobile Computing*, Vol 9, pp. 955-968 (2010).

[10] Wang, L., Yuan, Z., Shi, L., Qin. Z., "An energy-efficient CKN algorithm for duty-cycled wireless sensor networks", *International Journal of Distributed Sensor Networks*, Vol 2012, pp. 1-15 (2012).

[11] Chachra, S., Marefat, M., "Distributed algorithms for sleep scheduling in wireless sensor networks", *In Proc. Rob. and Aut.*, Orlando, FL; pp. 3101-3107 (2006).

[12] Saraswat, J., Bhattacharya, P.P., "Effect of duty cycle on energy consumption in wireless sensor networks", *International Journal of Computer Networks & Communications*, Vol 5, pp. 125-140 (2013).

[13] Pagar, A.R., Mehetre, D.C., "A Survey on energy efficient sleep scheduling in wireless sensor network",. *International Journal of Advanced Research in Computer Science and Software Engineering*, Vol 5, pp.557-562 (2015).

[14] Mahani, A., Ansari, M.S., Kavian, Y.S., "Yeliability or performance: A tradeoff in wireless sensor networks", "*In Proc. Communication Systems, Networks & Digital Signal Processing, 8th International Symposium*, Poznan, pp. 5-6 (2012).

[15] Cardei, M., Jie, W., Mingming, L., Pervaiz, M.O., "Maximum network lifetime in wireless sensor networks with adjustable sensing ranges", *IEEE International Conference on Wireless and Mobile Computing, Networking and Communications*, pp. 438-445 (2005).

[16] Yuksel, A., Uzun, E., Tavli, B., "The impact of elimination of the most critical node on Wireless Sensor Network lifetime", *In Sensors Applications Symposium (SAS)*, pp.1-5 (2015).

[17] Pala, Z., "Impact of sleep mode on energy dissipation in wireless sensor ad hoc networks", *Global Journal on Technology*, Vol 3, pp. 955-963 (2013).

[18] Veeravalli, V., Fuemmeler, J., "Efficient tracking in a network of sleepy sensors" *In Proc. Acoustics, Speech and Signal Processing*, Vol 5, pp. V (2006).

[19] Cheng, Z., Perillo, M., Heinzelman, W., "General network lifetime and cost models for evaluating sensor network deployment strategies", *IEEE Transactions on Mobile Computing*, Vol 7, pp. 484-497 (2008).

[20] Chang, J.H., Tassiulas, L., "Maximum lifetime routing in wireless sensor networks", *IEEE/ACM Transactions on Networking*, Vol l, pp. 609-619 (2004).

[21] Ergen, S., Varaiya, P., "On multi-hop routing for energy efficiency", *IEEE Communications Letters*, Vol 9, pp. 880-881 (2005).

[22] Rosenthal, R.E., GAMS-A user guide, Washington, DC, USA, GAMS Development Corporation (2015).

[23] Xue, Y., Cui, Y., Nahrstedt, K., "Maximizing Lifetime for Data Aggregation in Wireless Sensor Networks", *Mobile Networks and Applications*, Vol 10, pp. 853-864 (2005).

[24] Dietrich, I., Dressler, F., "On the lifetime of wireless sensor networks", *ACM Transactions on Sensor Networks*, Vol 5, 1-38 (2009).

Zeydin Pala *is currently an assistant professor at the Department of Computer Engineering. He received his BS degree in Electrical and Electronics Engineering in 1993 from Istanbul University, Turkey. He received his MS and PhD degrees in Electrical and Electronics Engineering in 2007 from Yuzuncu Yil University, Van, Turkey and in 2012 from Firat University, Elazig, Turkey, respectively. His research interests lie in areas of wireless communication, WSN, ad hoc networks, and RFID technology.*

An International Journal of Optimization and Control: Theories & Applications
ISSN:2146-0957 eISSN:2146-5703
Vol.7, No.1, pp.59-65 (2017)
http://doi.org/10.11121/ijocta.01.2017.00299

RESEARCH ARTICLE

Compactness of the set of trajectories of the control system described by a Urysohn type integral equation

Nesir Huseyin*

Faculty of Education, Cumhuriyet University, Sivas, Turkey
nhuseyin@cumhuriyet.edu.tr

ARTICLE INFO

Article History:
Received 28 January 2016
Accepted 29 June 2016
Available 12 December 2016

Keywords:
Nonlinear integral equation
Control system
Integral constraint
Set of trajectories

AMS Classification 2010:
45G15, 93B03, 93C23

ABSTRACT

The control system with integral constraint on the controls is studied, where the behavior of the system by a Urysohn type integral equation is described. It is assumed that the system is nonlinear with respect to the state vector, affine with respect to the control vector. The closed ball of the space $L_p(E;\mathbb{R}^m)$ $(p > 1)$ with radius r and centered at the origin, is chosen as the set of admissible control functions, where $E \subset \mathbb{R}^k$ is a compact set. It is proved that the set of trajectories generated by all admissible control functions is a compact subset of the space of continuous functions.

1. Introduction

Nonlinear integral equations appear in many problems of contemporary physics and mechanics (see., e.g. [1] - [7]). Integral constraint on the control functions is inevitable if the control effort is exhausted by consumption. Such controls arise in various problems of economics, medicine, biology, mechanics and physics (see, [8] - [11]). Note that control system with integral constraint on the control functions, where the behavior of the system is given by a nonlinear differential equation is investigated in [8, 9].

In this paper the control system described by a Urysohn type integral equation is considered. It is assumed that integral equation is nonlinear with respect to the state vector and is affine with respect to the control vector. The closed ball of the space $L_p(E;\mathbb{R}^m)$ $(p > 1)$ with radius r and centered at the origin is chosen as the set of admissible control functions. The compactness of the set of trajectories of the system generated by all admissible control functions is studied. Note that compactness of the set of trajectories guaranties the existence of the optimal trajectories in the optimal control problem with continuous payoff functional. Compactness of the set of trajectories of control systems described by the Volterra type integral equations is studied in [12, 13].

The paper is organized as follows: In Section 2 the conditions which satisfy the system are formulated (Conditions A, B and C). In Section 3 it is proved that every admissible control function generates a unique trajectory of the system (Theorem 1). In Section 4 it is shown that the set of trajectories is bounded (Theorem 2). Precompactness of the set of trajectories is specified in Section 5 (Theorem 3). In Section 6 the closedness of the set of trajectories is shown (Theorem 4), and hence compactness of the set of trajectories is obtained (Theorem 5).

2. Preliminaries

The control system described by an integral equation

*Corresponding Author

$$x(\xi) = f(\xi, x(\xi)) + \lambda \int_E \big[K_1(\xi, s, x(s)) + K_2(\xi, s, x(s))\, u(s)\big] ds \quad (1)$$

is considered, where $x \in \mathbb{R}^n$ is the state vector, $u \in \mathbb{R}^m$ is the control vector, $\xi \in E$, $E \subset \mathbb{R}^k$ is a compact set.

Let $p > 1$ and $r > 0$ be given numbers. The function $u(\cdot) \in L_p\big(E; \mathbb{R}^m\big)$ such that $\|u(\cdot)\|_p \le r$ is said to be an admissible control function, where $\|u(\cdot)\|_p = \left(\int_E \|u(s)\|^p ds \right)^{\frac{1}{p}}$, $\|\cdot\|$ denotes the Euclidean norm.

The set of all admissible control functions is denoted by symbol $U_{p,r}$, i.e.

$$U_{p,r} = \big\{u(\cdot) \in L_p\big(E; \mathbb{R}^m\big) : \|u(\cdot)\|_p \le r\big\}.$$

If $u(\cdot) \in U_{p,r}$, then Hölder's inequality yields that

$$\int_E \|u(s)\|\, ds \le [\mu(E)]^{\frac{p-1}{p}}\, r\ , \quad (2)$$

where $\mu(E)$ denotes the Lebesgue measure of the set E.

It is assumed that the functions and a number $\lambda \in \mathbb{R}^1$ given in system (1) satisfy the following conditions:

A. The functions $f(\cdot) : E \times \mathbb{R}^n \to \mathbb{R}^n$, $K_1(\cdot) : E \times E \times \mathbb{R}^n \to \mathbb{R}^n$ and $K_2(\cdot) : E \times E \times \mathbb{R}^n \to \mathbb{R}^{n \times m}$ are continuous;

B. There exist $l_0 \in [0, 1)$, $l_1 \ge 0$ and $l_2 \ge 0$ such that

$$\|f(\xi, x_1) - f(\xi, x_2)\| \le l_0 \|x_1 - x_2\|$$

for every $(\xi, x_1) \in E \times \mathbb{R}^n$, $(\xi, x_2) \in E \times \mathbb{R}^n$ and

$$\|K_1(\xi, s, x_1) - K_1(\xi, s, x_2)\| \le l_1 \|x_1 - x_2\|,$$

$$\|K_2(\xi, s, x_1) - K_2(\xi, s, x_2)\| \le l_2 \|x_1 - x_2\|$$

for every $(\xi, s, x_1) \in E \times E \times \mathbb{R}^n$, $(\xi, s, x_2) \in E \times E \times \mathbb{R}^n$;

C. The inequality

$$0 \le \lambda \left[l_1 \mu(E) + l_2 [\mu(E)]^{\frac{p-1}{p}}\, r \right] < 1 - l_0$$

is satisfied.

We set

$$l(\lambda) = l_0 + \lambda \left[l_1 \mu(E) + l_2 [\mu(E)]^{\frac{p-1}{p}}\, r \right]. \quad (3)$$

If $u(\cdot) \in U_{p,r}$, then (2) and condition C yield

$$\frac{\lambda}{1 - l_0} \int_E (l_1 + l_2 \|u(s)\|)\, ds \le \frac{\lambda}{1 - l_0} \left(l_1 \mu(E) + l_2 [\mu(E)]^{\frac{p-1}{p}}\, r \right) < 1. \quad (4)$$

Let us define a trajectory of the system (1) generated by an admissible control function $u(\cdot) \in U_{p,r}$. A continuous function $x(\cdot) : E \to \mathbb{R}^n$ satisfying the integral equation (1) for every $\xi \in E$ is said to be a trajectory of the system (1) generated by the admissible control function $u(\cdot) \in U_{p,r}$. The set of trajectories of the system (1) generated by all control functions $u(\cdot) \in U_{p,r}$ is denoted by $\mathbf{X}_{p,r}$.

For $\xi \in E$ we denote

$$\mathbf{X}_{p,r}(\xi) = \{x(\xi) \in \mathbb{R}^n : x(\cdot) \in \mathbf{X}_{p,r}\}. \quad (5)$$

The set $\mathbf{X}_{p,r}(\xi)$ is useful for visualization of the set of trajectories.

Now, let us give an auxiliary proposition, which will be used in following arguments.

Proposition 1. *Let $E \subset \mathbb{R}^k$ be a compact set, $v(\cdot) : E \to \mathbb{R}$ and $h(\cdot) : E \to \mathbb{R}$ be continuous functions, $\psi(\cdot) : E \to [0, +\infty)$ be a Lebesgue integrable function, $\int_E \psi(s) ds < 1$ and*

$$v(\xi) \le h(\xi) + \int_E \psi(s) v(s) ds \quad (6)$$

for every $\xi \in E$. Then the inequality

$$v(\xi) \le h(\xi) + \frac{\int_E h(s)\psi(s) ds}{1 - \int_E \psi(s) ds} \quad (7)$$

holds for every $\xi \in E$.

Moreover, if $h(\xi) = h_*$ for every $\xi \in E$, then it follows from (7) that

$$v(\xi) \le \frac{h_*}{1 - \int_E \psi(s) ds} \quad (8)$$

for every $\xi \in E$.

Proof. Since $\psi(\cdot)$ is nonnegative function, we have from (6)

$$v(\xi)\psi(\xi) \le h(\xi)\psi(\xi) + \psi(\xi) \int_E \psi(s) v(s) ds$$

for every $\xi \in E$, and hence

$$\int_E v(s)\psi(s) ds \le \int_E h(s)\psi(s) ds + \int_E \psi(s) ds \cdot \int_E \psi(s) v(s) ds.$$

Since $\int_E \psi(s)ds < 1$, then the last inequality implies

$$\int_E v(s)\psi(s)ds \leq \frac{\int_E h(s)\psi(s)ds}{1-\int_E \psi(s)ds}\,. \tag{9}$$

(6) and (9) yield the validity of (7). □

3. Existence and Uniqueness of Trajectories

Conditions A - C guarantee that every admissible control function generates a unique trajectory.

Theorem 1. *Let the conditions A - C be satisfied and $u_*(\cdot) \in U_{p,r}$. Then the system (1) has unique trajectory $x_*(\cdot)$ generated by the admissible control function $u_*(\cdot)$.*

Proof. Define a map $x(\cdot) \to A(x(\cdot))$, $x(\cdot) \in C(E;\mathbb{R}^n)$, setting

$$A(x(\cdot))|(\xi) = f(\xi, x(\xi)) + \lambda \int_E \big[K_1(\xi, s, x(s)) + K_2(\xi, s, x(s))\, u_*(s)\big]ds,\ \xi \in E, \tag{10}$$

where $C(E;\mathbb{R}^n)$ is the space of continuous functions $x(\cdot) : E \to \mathbb{R}^n$ with norm $\|x(\cdot)\|_C = \max\{\|x(\xi)\| : \xi \in E\}$. Since $u_*(\cdot) \in U_{p,r}$, $x(\cdot) \in C(E;\mathbb{R}^n)$ then by virtue of condition A we have that the map $\xi \to A(x(\cdot))|(\xi)$, $\xi \in E$, is continuous, and hence $A(x(\cdot)) \in C(E;\mathbb{R}^n)$.

Let $x_1(\cdot) \in C(E;\mathbb{R}^n)$ and $x_2(\cdot) \in C(E;\mathbb{R}^n)$ be arbitrarily chosen functions. From condition B, (2) and (3) it follows that the inequality

$$\begin{aligned}
&\big\|A(x_2(\cdot))|(\xi) - A(x_1(\cdot))|(\xi)\big\| \\
&\leq l_0 \|x_2(\xi) - x_1(\xi)\| \\
&\quad + \lambda l_1 \int_E \|x_2(s) - x_1(s)\|\, ds \\
&\quad + \lambda l_2 \int_E \|x_2(s) - x_1(s)\|\, \|u_*(s)\|\, ds \\
&\leq \left[l_0 + \lambda l_1 \mu(E) + \lambda l_2 \int_E \|u_*(s)\|\, ds\right] \\
&\quad \cdot \|x_2(\cdot) - x_1(\cdot)\|_C \\
&\leq \left[l_0 + \lambda l_1 \mu(E) + \lambda l_2 [\mu(E)]^{\frac{p-1}{p}} r\right] \\
&\quad \cdot \|x_2(\cdot) - x_1(\cdot)\|_C \\
&= l(\lambda)\, \|x_2(\cdot) - x_1(\cdot)\|_C
\end{aligned}$$

holds for every $\xi \in E$, and consequently

$$\begin{aligned}
&\big\|A(x_2(\cdot))|(\cdot) - A(x_1(\cdot))|(\cdot)\big\|_C \\
&\quad \leq l(\lambda)\, \|x_2(\cdot) - x_1(\cdot)\|_C\,.
\end{aligned} \tag{11}$$

According to the condition C and (3) we have $l(\lambda) < 1$. (11) implies that the map $A(\cdot) : C(E;\mathbb{R}^n) \to C(E;\mathbb{R}^n)$ defined by (10) is contractive, and hence it has a unique fixed point $x_*(\cdot) \in C(E;\mathbb{R}^n)$ which is unique solution of the equation

$$\begin{aligned}
x_*(\xi) &= f(\xi, x_*(\xi)) + \lambda \int_E \big[K_1(\xi, s, x_*(s)) \\
&+ K_2(\xi, s, x_*(s))\, u_*(s)\big]ds,\ \xi \in E.
\end{aligned}$$

□

4. Boundedness

In this section the boundedness of the set of trajectories $\mathbf{X}_{p,r}$ is proved. Denote

$$\gamma_0 = \max\{\|f(\xi, 0)\| : \xi \in E\}\,, \tag{12}$$

$$\gamma_1 = \max\{\|K_1(\xi, s, 0)\| : (\xi, s) \in E \times E\}\,, \tag{13}$$

$$\gamma_2 = \max\{\|K_2(\xi, s, 0)\| : (\xi, s) \in E \times E\}\,. \tag{14}$$

Proposition 2. *Let the functions $f(\cdot) : E \times \mathbb{R}^n \to \mathbb{R}^n$, $K_1(\cdot) : E \times E \times \mathbb{R}^n \to \mathbb{R}^n$ and $K_2(\cdot) : E \times E \times \mathbb{R}^n \to \mathbb{R}^{n\times m}$ satisfy the conditions A and B. Then*

$$\begin{aligned}
\|f(\xi, x)\| &\leq \gamma_0 + l_0 \|x\|\,, \\
\|K_1(\xi, s, x)\| &\leq \gamma_1 + l_1 \|x\|\,, \\
\|K_2(\xi, s, x)\| &\leq \gamma_2 + l_2 \|x\|
\end{aligned}$$

for every $(\xi, s, x) \in E \times E \times \mathbb{R}^n$, where the constants l_0, l_1 and l_2 are given in condition B.

Proof. Let us prove the validity of 3rd inequality. The proofs of 1st and 2nd inequalities are similar. According to the conditions A and B we have

$$\|K_2(\xi, s, x) - K_2(\xi, s, 0)\| \leq l_2 \|x\|$$

for every $(\xi, s, x) \in E \times E \times \mathbb{R}^n$, and hence

$$\begin{aligned}
\|K_2(\xi, s, x)\| &\leq l_2 \|x\| \\
&+ \max\{\|K_2(\xi, s, 0)\| : (\xi, s) \in E \times E\}
\end{aligned}$$

The last inequality and (14) complete the proof. □

Denote

$$\gamma_* = \frac{\gamma_0 + \lambda\gamma_1 \mu(E) + \lambda\gamma_2 [\mu(E)]^{\frac{p-1}{p}} r}{1 - l(\lambda)}\,, \tag{15}$$

where $l(\lambda)$ is defined by (3), $\gamma_0 \geq 0$, $\gamma_1 \geq 0$ and $\gamma_2 \geq 0$ are defined by (12), (13) and (14) respectively.

Theorem 2. *Let the conditions A - C be satisfied. Then for every $x(\cdot) \in \mathbf{X}_{p,r}$ the inequality*

$$\|x(\cdot)\|_C \leq \gamma_*$$

holds.

Proof. Let $x(\cdot) \in \mathbf{X}_{p,r}$ be an arbitrary trajectory, generated by the admissible control function

$u(\cdot) \in U_{p,r}$. Proposition 2 and (2) imply

$$\begin{aligned}\|x(\xi)\| &\le \gamma_0 + l_0 \|x(\xi)\| \\ &+\lambda \int_E (\gamma_1 + l_1 \|x(s)\|)\, ds \\ &+\lambda \int_E (\gamma_2 + l_2 \|x(s)\|)\, \|u(s)\|\, ds \\ &\le l_0 \|x(\xi)\| + \gamma_0 + \lambda\gamma_1\mu(E) \\ &+\lambda\gamma_2 [\mu(E)]^{\frac{p-1}{p}} r \\ &+\lambda \int_E (l_1 + l_2 \|u(s)\|)\, \|x(s)\|\, ds\end{aligned}$$

for every $\xi \in E$. Since $l_0 \in [0,1)$, then we obtain from the last inequality

$$\|x(\xi)\| \le \frac{\gamma_0 + \lambda\gamma_1\mu(E) + \lambda\gamma_2 [\mu(E)]^{\frac{p-1}{p}} r}{1-l_0} + \frac{\lambda}{1-l_0} \int_E (l_1 + l_2 \|u(s)\|)\, \|x(s)\|\, ds \quad (16)$$

for every $\xi \in E$. Since $u(\cdot) \in U_{p,r}$, then from (3), (4), (15), (16) and Proposition 1 it follows

$$\begin{aligned}\|x(\xi)\| &\le \frac{\gamma_0 + \lambda\gamma_1\mu(E) + \lambda\gamma_2 [\mu(E)]^{\frac{p-1}{p}} r}{1-l_0} \\ &\cdot \frac{1}{1 - \frac{\lambda}{1-l_0} \int_E (l_1 + l_2 \|u(s)\|)\, ds} \\ &\le \frac{\gamma_0 + \lambda\gamma_1\mu(E) + \lambda\gamma_2 [\mu(E)]^{\frac{p-1}{p}} r}{1-l_0} \\ &\cdot \frac{1}{1 - \frac{\lambda}{1-l_0} \left[l_1\mu(E) + l_2 [\mu(E)]^{\frac{p-1}{p}} r\right]} \\ &= \frac{\gamma_0 + \lambda\gamma_1\mu(E) + \lambda\gamma_2 [\mu(E)]^{\frac{p-1}{p}} r}{1-l(\lambda)} = \gamma_*\end{aligned}$$

for every $\xi \in E$, and hence $\|x(\cdot)\|_C \le \gamma_*$. □

5. Precompactness

Let $\Delta > 0$ be a given number, $\gamma_* > 0$ be defined by (15), $B_n(\gamma_*) = \{x \in \mathbb{R}^n : \|x\| \le \gamma_*\}$. Denote

$$G_1 = E \times B_n(\gamma_*), \quad G_2 = E \times E \times B_n(\gamma_*), \quad (17)$$

$$\begin{aligned}\omega_0(\Delta) = \max\big\{ &\|f(\xi_2, x) - f(\xi_1, x)\| : \\ &\|\xi_2 - \xi_1\| \le \Delta, \\ &(\xi_1, x) \in G_1,\ (\xi_2, x) \in G_1\big\}, \end{aligned} \quad (18)$$

$$\begin{aligned}\omega_1(\Delta) = \max\big\{ &\big\|K_1(\xi_2, s, x) - K_1(\xi_1, s, x)\big\| : \\ &\|\xi_2 - \xi_1\| \le \Delta,\ \ (\xi_1, s, x) \in G_2, \\ &(\xi_2, s, x) \in G_2\big\}, \end{aligned} \quad (19)$$

$$\begin{aligned}\omega_2(\Delta) = \max\big\{ &\|K_2(\xi_2, s, x) - K_2(\xi_1, s, x)\| : \\ &\|\xi_2 - \xi_1\| \le \Delta,\ \ (\xi_1, s, x) \in G_2, \\ &(\xi_2, s, x) \in G_2\big\}, \end{aligned} \quad (20)$$

$$\begin{aligned}\varphi(\Delta) &= \frac{1}{1-l_0}\Big\{\omega_0(\Delta) + \lambda\mu(E)\omega_1(\Delta) \\ &+ \lambda\omega_2(\Delta) [\mu(E)]^{\frac{p-1}{p}} r\Big\}. \end{aligned} \quad (21)$$

The function $\varphi(\cdot) : (0, +\infty) \to [0, +\infty)$ is not decreasing and $\varphi(\Delta) \to 0^+$ as $\Delta \to 0^+$.

Proposition 3. *Let the conditions A - C be satisfied. Then for every $x(\cdot) \in \mathbf{X}_{p,r}$, $\xi_1 \in E$, $\xi_2 \in E$ the inequality*

$$\|x(\xi_2) - x(\xi_1)\| \le \varphi(\|\xi_2 - \xi_1\|)$$

holds, where $\varphi(\cdot)$ is defined by (21).

Proof. Let us choose an arbitrary $x(\cdot) \in \mathbf{X}_{p,r}$ and $\xi_1 \in E$, $\xi_2 \in E$. Then there exists $u(\cdot) \in U_{p,r}$ such that

$$\begin{aligned}x(\xi) &= f(\xi, x(\xi)) + \lambda \int_E \big[K_1(\xi, s, x(s)) \\ &+ K_2(\xi, s, x(s))\, u(s)\big] ds\end{aligned}$$

for every $\xi \in E$, and hence

$$\begin{aligned}&\|x(\xi_2) - x(\xi_1)\| \\ &\le \|f(\xi_2, x(\xi_2)) - f(\xi_1, x(\xi_2))\| \\ &\quad + \|f(\xi_1, x(\xi_2)) - f(\xi_1, x(\xi_1))\| \\ &\quad +\lambda \int_E \big\|K_1(\xi_2, s, x(s)) \\ &\quad -K_1(\xi_1, s, x(s))\big\| ds \\ &\quad +\lambda \int_E \big\|K_2(\xi_2, s, x(s)) \\ &\quad -K_2(\xi_1, s, x(s))\big\|\, \|u(s)\|\, ds\,. \end{aligned} \quad (22)$$

By virtue of condition B we have

$$\begin{aligned}&\|f(\xi_1, x(\xi_2)) - f(\xi_1, x(\xi_1))\| \\ &\le l_0 \|x(\xi_2) - x(\xi_1)\|, \end{aligned} \quad (23)$$

where $l_0 \in [0,1)$. Since $x(\cdot) \in \mathbf{X}_{p,r}$, then it follows from Theorem 2 that

$$x(s) \in B_n(\gamma_*) \quad (24)$$

for every $s \in E$. (17), (18), (19), (20) and (24) imply

$$\begin{aligned}&\|f(\xi_2, x(\xi_2)) - f(\xi_1, x(\xi_2))\| \\ &\le \omega_0(\|\xi_2 - \xi_1\|), \end{aligned} \quad (25)$$

$$\begin{aligned}&\|K_1(\xi_2, s, x(s)) - K_1(\xi_1, s, x(s))\| \\ &\le \omega_1(\|\xi_2 - \xi_1\|), \end{aligned} \quad (26)$$

$$\begin{aligned}&\|K_2(\xi_2, s, x(s)) - K_2(\xi_1, s, x(s))\| \\ &\le \omega_2(\|\xi_2 - \xi_1\|) \end{aligned} \quad (27)$$

for every $s \in E$.

From (2), (21), (22), (23), (25), (26) and (27) we obtain that

$$\begin{aligned}\left\|x(\xi_2)-x(\xi_1)\right\| &\le \frac{1}{1-l_0}\Big\{\omega_0\left(\|\xi_2-\xi_1\|\right)\\ &+\lambda\mu(E)\omega_1\left(\|\xi_2-\xi_1\|\right)\\ &+\lambda\omega_2\left(\|\xi_2-\xi_1\|\right)\int_E\|u(s)\|\,ds\Big\}\\ &\le \frac{1}{1-l_0}\Big\{\omega_0\left(\|\xi_2-\xi_1\|\right)\\ &+\lambda\mu(E)\omega_1\left(\|\xi_2-\xi_1\|\right)\\ &+\lambda\omega_2\left(\|\xi_2-\xi_1\|\right)[\mu(E)]^{\frac{p-1}{p}}\,r\Big\}\\ &=\varphi\left(\|\xi_2-\xi_1\|\right).\end{aligned}$$

□

Proposition 4. *Let the conditions A - C be satisfied. Then the set of trajectories $\mathbf{X}_{p,r}\subset C\left(E;\mathbb{R}^n\right)$ is a set of equicontinuous functions.*

Proof. Since $\varphi(\Delta)\to 0^+$ as $\Delta\to 0^+$, then for given $\varepsilon>0$ there exists $\Delta_*(\varepsilon)>0$ such that for every $\Delta\in(0,\Delta_*(\varepsilon)]$ the inequality

$$\varphi(\Delta)\le\varepsilon \tag{28}$$

is satisfied, where $\varphi(\cdot)$ is defined by (21).
Now let $x(\cdot)\in\mathbf{X}_{p,r}$ be an arbitrarily chosen trajectory, $\xi_1\in E$, $\xi_2\in E$ be such that $\|\xi_2-\xi_1\|\le\Delta_*(\varepsilon)$. Since the function $\varphi(\cdot):(0,+\infty)\to[0,+\infty)$ is not decreasing, then from (28) and Proposition 3 it follows

$$\|x(\xi_2)-x(\xi_1)\|\le\varphi\left(\|\xi_2-\xi_1\|\right)\le\varphi\left(\Delta_*(\varepsilon)\right)\le\varepsilon,$$

and hence the set of trajectories $\mathbf{X}_{p,r}\subset C\left(E;\mathbb{R}^n\right)$ is a set of equicontinuous functions. □

Theorem 2 and Proposition 4 yield the validity of the following theorem.

Theorem 3. *Let the conditions A - C be satisfied. Then the set of trajectories $\mathbf{X}_{p,r}$ is a precompact subset of the space $C\left(E;\mathbb{R}^n\right)$.*

The Hausdorff distance between the sets $P\subset\mathbb{R}^n$ and $S\subset\mathbb{R}^n$ is denoted by $H(P,S)$ and defined as

$$H(P,S)=\max\{\sup_{p\in P}d(p,S),\sup_{s\in S}d(s,P)\},$$

where $d(p,S)=\inf\{\|p-s\|:s\in S\}$.
Proposition 3 implies the validity of the following proposition.

Proposition 5. *Let the conditions A - C be satisfied. Then for every $\xi_1\in E$ and $\xi_2\in E$ the inequality*

$$H\left(\mathbf{X}_{p,r}(\xi_2),\mathbf{X}_{p,r}(\xi_1)\right)\le\varphi\left(\|\xi_2-\xi_1\|\right)$$

is satisfied, where the function $\varphi(\cdot):(0,\infty)\to[0,\infty)$ is defined by (21), the sets $\mathbf{X}_{p,r}(\xi_1)$ and $\mathbf{X}_{p,r}(\xi_2)$ are defined by (5).

Since $\varphi(\Delta)\to 0^+$ as $\Delta\to 0^+$ then we conclude the validity of the following corollary.

Corollary 1. *Let the conditions A - C be satisfied. Then the set valued map $\xi\to\mathbf{X}_{p,r}(\xi)$, $\xi\in E$, is continuous.*

6. Closedness

Theorem 4. *Let the conditions A - C be satisfied. Then the set of trajectories $\mathbf{X}_{p,r}$ is a closed subset of the space $C\left(E;\mathbb{R}^n\right)$.*

Proof. Let us choose a sequence of trajectories $\{x_i(\cdot)\}_{i=1}^{\infty}$, where $\|x_i(\cdot)-x_*(\cdot)\|_C\to 0$ as $i\to\infty$ and $x_*(\cdot)\in C\left(E;\mathbb{R}^n\right)$. We have to prove that $x_*(\cdot)\in\mathbf{X}_{p,r}$.
Since $x_i(\cdot)\in\mathbf{X}_{p,r}$, then there exists $u_i(\cdot)\in U_{p,r}$ such that

$$\begin{aligned}x_i(\xi) &= f\left(\xi,x_i\left(\xi\right)\right)+\lambda\int_E\big[K_1\left(\xi,s,x_i\left(s\right)\right)\\ &+ K_2\left(\xi,s,x_i\left(s\right)\right)u_i\left(s\right)\big]ds\end{aligned}\tag{29}$$

for every $\xi\in E$. Since the set of admissible control functions $U_{p,r}\subset L_p\left(E;\mathbb{R}^n\right)$ is weakly compact, then without loss of generality, one can assume that the sequence $\{u_i(\cdot)\}_{i=1}^{\infty}$ weakly converges to a $u_*(\cdot)\in U_{p,r}$. Let $y_*(\cdot):E\to\mathbb{R}^n$ be a trajectory of the system (1) generated by the admissible control function $u_*(\cdot)\in U_{p,r}$. Then

$$\begin{aligned}y_*(\xi) &= f\left(\xi,y_*\left(\xi\right)\right)+\lambda\int_E\big[K_1\left(\xi,s,y_*\left(s\right)\right)\\ &+ K_2\left(\xi,s,y_*\left(s\right)\right)u_*\left(s\right)\big]ds\end{aligned}\tag{30}$$

for every $\xi\in E$. (29), (30) and condition B yield that

$$\begin{aligned}&\|x_i\left(\xi\right)-y_*\left(\xi\right)\|\\ &\le\frac{\lambda}{1-l_0}\int_E\left(l_1+l_2\|u_i(s)\|\right)\\ &\quad\cdot\|x_i\left(s\right)-y_*\left(s\right)\|\,ds\\ &\quad+\frac{\lambda}{1-l_0}\Big\|\int_E K_2\left(\xi,s,y_*\left(s\right)\right)\\ &\quad\cdot\left(u_i(s)-u_*(s)\right)ds\Big\|\end{aligned}\tag{31}$$

for every $\xi\in E$. Denote $w(\xi,s)=K_2\left(\xi,s,y_*\left(s\right)\right)$. Since the function $w(\cdot):E\times E\to\mathbb{R}^{n\times m}$ is continuous and the sequence $\{u_i(\cdot)\}_{i=1}^{\infty}$ weakly converges to $u_*(\cdot)\in U_{p,r}$ in the space $L_p\left(E;\mathbb{R}^n\right)$, then we have that for each fixed $\xi\in E$

$$\Big\|\int_E w(\xi,s)\left[u_i(s)-u_*(s)\right]ds\Big\|\to 0\tag{32}$$

as $i\to\infty$. From (32) we obtain that for $\varepsilon>0$ and fixed $\xi\in E$ there exists $N(\varepsilon,\xi)>0$ such that for

every $i > N(\varepsilon, \xi)$ the inequality

$$\left\| \int_E w(\xi, s) [u_i(s) - u_*(s)] ds \right\| < \varepsilon \qquad (33)$$

is satisfied.

Now let us prove that for each $\varepsilon > 0$ there exists $N(\varepsilon) > 0$ (which does not depend on ξ) such that for every $i > N(\varepsilon)$ and $\xi \in E$ the inequality

$$\left\| \int_E w(\xi, s) (u_i(s) - u_*(s)) ds \right\| < \varepsilon \qquad (34)$$

holds.

Let us assume the contrary, i.e. let there exist $\varepsilon_* > 0$, $i_j > 0$ and $\xi_j \in E$ $(j = 1, 2, \ldots)$ such that $i_j \to \infty$ as $j \to \infty$ and

$$\left\| \int_E w(\xi_j, s) \left[u_{i_j}(s) - u_*(s)\right] ds \right\| \geq \varepsilon_* \,. \qquad (35)$$

Since $\xi_j \in E$ for every $j = 1, 2, \ldots$ and $E \subset \mathbb{R}^k$ is a compact set, then without loss of generality one can assume that $\xi_j \to \xi_*$ as $j \to \infty$ and $\xi_* \in E$.

(33) implies that for $\varepsilon_* > 0$ and $\xi_* \in E$ there exists $N_1 > 0$ such that for every $j > N_1$ the inequality

$$\left\| \int_E w(\xi_*, s) \left[u_{i_j}(s) - u_*(s)\right] ds \right\| < \frac{\varepsilon_*}{4} \qquad (36)$$

is verified.

Continuity of the function $w(\cdot) : E \times E \to \mathbb{R}^{n \times m}$ and compactness of the set E yield that for given $\dfrac{\varepsilon_*}{8 [\mu(E)]^{\frac{p-1}{p}} r}$ there exists $N_2 > 0$ such that for every $j > N_2$ and $s \in E$ the inequality

$$\|w(\xi_j, s) - w(\xi_*, s)\| < \frac{\varepsilon_*}{8 [\mu(E)]^{\frac{p-1}{p}} r} \qquad (37)$$

holds. Since $u_*(\cdot) \in U_{p,r}$, $u_{i_j}(\cdot) \in U_{p,r}$ for every $j = 1, 2, \ldots$, then from (2) and (37) it follows

$$\begin{aligned} &\left\| \int_E [w(\xi_j, s) - w(\xi_*, s)] \left[u_{i_j}(s) - u_*(s)\right] ds \right\| \\ &\leq \frac{\varepsilon_*}{8 [\mu(E)]^{\frac{p-1}{p}} r} \int_E \left[\left\|u_{i_j}(s)\right\| + \|u_*(s)\| \right] ds \\ &\leq 2 \frac{\varepsilon_*}{8 [\mu(E)]^{\frac{p-1}{p}} r} [\mu(E)]^{\frac{p-1}{p}} r = \frac{\varepsilon_*}{4} \end{aligned} \qquad (38)$$

for every $j > N_2$.

Denote $N_* = \max\{N_1, N_2\}$. Then (36) and (38) imply that

$$\begin{aligned} &\left\| \int_E w(\xi_j, s) \left[u_{i_j}(s) - u_*(s)\right] ds \right\| \\ &\leq \left\| \int_E [w(\xi_j, s) - w(\xi_*, s)] \cdot \left[u_{i_j}(s) - u_*(s)\right] ds \right\| \\ &\quad + \left\| \int_E w(\xi_*, s) \left[u_{i_j}(s) - u_*(s)\right] ds \right\| \\ &< \frac{\varepsilon_*}{4} + \frac{\varepsilon_*}{4} = \frac{\varepsilon_*}{2} < \varepsilon_* \end{aligned} \qquad (39)$$

for every $j > N_*$. The inequalities (35) and (39) contradict, and hence the inequality (34) is held. Thus, from (31) and (34) we have that for every $\xi \in E$ and $i > N(\varepsilon)$ the inequality

$$\begin{aligned} \|x_i(\xi) - y_*(\xi)\| \leq{}& \frac{\lambda\varepsilon}{1 - l_0} \\ &+ \frac{\lambda}{1 - l_0} \int_E (l_1 + l_2 \|u_i(s)\|) \\ &\cdot \|x_i(s) - y_*(s)\| ds \end{aligned} \qquad (40)$$

is satisfied.

Since $u_i(\cdot) \in U_{p,r}$ for every $i = 1, 2, \ldots$, then from (4), (40) and Proposition 1 we have that for every $i > N(\varepsilon)$ and $\xi \in E$ the inequality

$$\begin{aligned} &\|x_i(\xi) - y_*(\xi)\| \\ \leq{}& \frac{\lambda\varepsilon}{1 - l_0} \cdot \frac{1}{1 - \dfrac{\lambda}{1 - l_0} \displaystyle\int_E (l_1 + l_2 \|u_i(s)\|) ds} \\ \leq{}& \frac{\lambda\varepsilon}{1 - l_0} \cdot \frac{1}{1 - \dfrac{\lambda}{1 - l_0} \left[l_1 \mu(E) + l_2 [\mu(E)]^{\frac{p-1}{p}} r\right]} \\ ={}& \frac{\lambda}{1 - l(\lambda)} \cdot \varepsilon \end{aligned}$$

holds, where $l(\lambda)$ is defined by (3). This means that $x_i(\cdot) \to y_*(\cdot)$ as $i \to +\infty$. From uniqueness of the limit we have $x_*(\cdot) = y_*(\cdot)$ and hence $x_*(\cdot) \in \mathbf{X}_{p,r}$. □

Theorem 3 and Theorem 4 imply compactness of the set of trajectories.

Theorem 5. *Let the conditions A - C be satisfied. Then the set of trajectories $\mathbf{X}_{p,r}$ is a compact subset of the space $C(E; \mathbb{R}^n)$.*

References

[1] Brauer, F., On a nonlinear integral equation for population growth problems. *SIAM J. Math. Anal.*, 6(2), 312-317 (1975).

[2] Browder, F.E., Nonlinear functional analysis and nonlinear integral equations of Hammerstein and Urysohn type. Contributions to nonlinear functional analysis. Academic Press, New York 425-500 (1971).

[3] Joshi, M., Existence theorems for Urysohn's integral equation. *Proc. Amer. Math. Soc.*, 49(2), 387-392 (1975).

[4] Kolomy, J., The solvability of nonlinear integral equations. *Comment. Math. Univ. Carolinae*, 8, 273-289 (1967).

[5] Krasnoselskii, M.A. and Krein, S.G., On the principle of averaging in nonlinear mechanics. *Uspekhi Mat. Nauk*, 10(3), 147-153 (1955). (In Russian)

[6] Polyanin, A.D. and Manzhirov, A.V., Handbook of integral equation. CRC Press, Boca Raton (1998).

[7] Urysohn, P.S., On a type of nonlinear integral equation. *Mat. Sb.*, 31, 236-255 (1924). (In Russian)

[8] Guseinov, Kh.G., Ozer, O., Akyar, E. and Ushakov, V.N., The approximation of reachable sets of control systems with integral constraint on controls. *Nonlinear Different. Equat. Appl. (NoDEA)*, 14(1-2), 57-73 (2007).

[9] Guseinov, Kh.G., Approximation of the attainable sets of the nonlinear control systems with integral constraint on controls. *Nonlinear Anal., TMA*, 71(1-2), 622-645 (2009).

[10] Krasovskii, N.N., Theory of control of motion: Linear systems. Nauka, Moscow (1968). (In Russian)

[11] Subbotin, A.I. and Ushakov, V.N., Alternative for an encounter-evasion differential game with integral constraints on the players controls. *J. Appl. Math. Mech.*, 39(3), 367-375 (1975).

[12] Huseyin, A. and Huseyin, N., Precompactness of the set of trajectories of the controllable system described by a nonlinear Volterra integral equation. *Math. Model. Anal.*, 17(5), 686-695 (2012).

[13] Huseyin, N. and Huseyin, A., Compactness of the set of trajectories of the controllable system described by an affine integral equation. *Appl. Math. Comput.*, 219(16), 8416-8424 (2013).

Nesir Huseyin *is an Assistant Professor in Department of Elementary Mathematics Teaching, Faculty of Education, Cumhuriyet University, Turkey. He received the Ph.D. in Mathematics from Anadolu University, Turkey, in 2014. His research interests include mathematical theory of control systems, set valued analysis and applications, mathematics education.*

An International Journal of Optimization and Control: Theories & Applications
ISSN:2146-0957 eISSN:2146-5703
Vol.7, No.1, pp.66-74 (2017)
http://doi.org/10.11121/ijocta.01.2017.00308

RESEARCH ARTICLE

Approximate solution of generalized pantograph equations with variable coefficients by operational method

Yalçın Öztürk[a*] and Mustafa Gülsu[b]

[a] *Ula Ali Koçman Vocational School, Muğla Sıtkı Koçman University, Muğla, Turkey*
[b] *Department of Mathematics, Faculty of Science, Muğla Sıtkı Koçman University, Muğla, Turkey*
yozturk@mu.edu.tr, mgulsu@mu.edu.tr

ARTICLE INFO

Article History:
Received 15 February 2016
Accepted 09 October 2016
Available 12 December 2016

Keywords:
Pantograph equations
Chebyshev polynomials
Approximation method
Operational matrix method

AMS Classification 2010:
65D15, 65L03, 65L60

ABSTRACT

In this paper, we present an efficient direct solver for solving the generalized pantograph equations with variable coefficients. An approach is based on the second kind Chebyshev polynomials together with operational method. The main characteristic behind this approach is that it reduces such problem to ones of solving systems of algebraic equations. Only a small number of Chebyshev polynomials are needed to obtain a satisfactory result. Numerical results with comparisons are given to confirm the reliability of the proposed method for solving generalized pantograph equations with variable coefficients.

1. Introduction

Functional-differential equations with proportional delays are usually referred to as pantograph equations or generalized pantograph equations. Pantograph equations have gained more interest in many application fields such a biology, physics, engineering, economy, electrodynamics [1–7]. In recent years, there has been a growing interest in the numerical treatment of pantograph equations of the retarded and advanced type. A special feature of this type of equation is the existence of compactly supported solutions [6]. Pantograph equations are characterized by the presence of a linear functional argument and play an important role in explaining many different phenomena. In particular they turn out to be fundamental when ODEs-based model fail. In the literature, special attention has been given to applications of Taylor polynomials method, variation iteration method, Adomian decomposition method etc. [8–21,25–28]

Consider the generalized linear pantograph equations of the form

$$\sum_{k=0}^{m} P_k(x)y^{(k)}(x) + \sum_{j=0}^{J}\sum_{s=0}^{n} H_{js}(x)y^{(s)}(\alpha_j x - \beta_j) = g(x) \quad (1)$$

for $x \in [-1,1]$, under the mixed condition, for $1 \le c_j \le 1,\ i = 0,1,2,...,m-1$

$$\sum_{k=0}^{m-1}\sum_{j=0}^{r} c_{ij}^{k} y^{(k)}(c_j) = \lambda_i \quad (2)$$

which is the $y(x)$ an unknown function, the known function $P_k(x),\ H_{js}(x),\ g(x)$ are defined on an interval and also c_{ij}^{k} are appropriate constant.

Our aim is to find an approximate solution expressed in terms of polynomial of degree N in the form

$$y_N(x) = \sum_{r=0}^{N} a_r U_r(x) \quad (3)$$

*Corresponding Author

where a_r unknown coefficients and N is chosen any positive integer such that $N \geq m$.

2. Chebyshev polynomial

Orthogonal functions, often used to represent an arbitrary time function, have received considerable attention in dealing with various problems of dynamical system. The main characteristic of this technique is that it reduces these problems to those of solving a system of algebraic equations, thus greatly simplifying the problem.

Definition 1. *The Chebyshev polynomial of the second kind $U_n(x)$ is a polynomial in x of degree n, defined by the relation*

$$U_n(x) = \frac{sin(n+1)\theta}{sin\theta}, \quad when \quad x = cos(\theta).$$

If the range of the variable x is the interval $[-1, 1]$, the range the corresponding variable θ can be taken $[0, \pi]$. We suppose without lose of generality that the interval of Eq.(1) is $[-1, 1]$ which domain of the Chebyshev polynomial of the second kind, since any finite $[a, b]$ can be transformed to interval $[-1, 1]$ by linear maps [23, 24]. Using Moivre's Theorem we obtained the fundamental recurrence relation [22, 23]

$$U_n(x) = 2xU_{n-1}(x) - U_{n-2}(x), \quad n = 2, 3, ...$$

which together with the initial conditions

$$U_0(x) = 1, \quad U_2(x) = 2x$$

These polynomials have the following properties:
i) $U_{n+1}(x)$ has exactly $n + 1$ real zeroes on the interval $[-1, 1]$. The m-th zero $x_{n,m}$ of $U_n(x)$ is located at

$$x_{n,m} = cos(\frac{m\pi}{n+2})$$

ii) These polynomials are orthogonal on $[-1, 1]$ with respect to the weight function $\omega(x) = (1 - x^2)^{1/2}$

$$\int_{-1}^{1} U_r(x)U_s(x)\omega(x)dx = \begin{cases} \pi, & \text{r=s=0;} \\ \frac{\pi}{2}, & r = s \neq 0; \\ 0, & r \neq s. \end{cases}$$

iii) It is well known that [23] the relation between the powers x^n and the Chebyshev polynomials $U_n(x)$ is

$$x^n = 2^{-n} \sum_{j=0}^{||\frac{n}{2}||} \left(\binom{n}{j} - \binom{n}{j-1} \right) U_{n-2j}(x) \quad (4)$$

iv) Any function $y(x) \in L^2[-1, 1]$ can be approximated as a sum of the second kind Chebyshev polynomials as:

$$y(x) = \sum_{n=0}^{\infty} c_n U_n(x) \quad (5)$$

where, for $n = 0, 1, ...$

$$c_n = \Big\langle y(x), U_n(x) \Big\rangle = \int_{-1}^{1} y(x)U_n(x)dx. \quad (6)$$

3. Fundamental matrix relations

Let us write Eq. (1) in the form

$$D(x) + H(x) = g(x) \quad (7)$$

where

$$D(x) = \sum_{k=0}^{m} P_k(x)y^{(k)}(x),$$

and

$$H(x) = \sum_{j=0}^{J} \sum_{s=0}^{n} H_{js}(x)y^{(s)}(\alpha_j x - \beta_j).$$

We convert these parts and the mixed conditions in to the matrix form. Let us consider the Eq. (1) and find the matrix forms of each term of the equation. We first consider the solution $y_N(x)$ and its derivative $y_N^{(k)}(x)$ defined by a truncated Chebyshev series. Then we can put series in the matrix form

$$y_N(x) = U(x)A, \; y_N^{(k)}(x) = U^{(k)}(x)A \quad (8)$$

where

$$\begin{aligned} U(x) &= \begin{bmatrix} U_0(x) & U_1(x) & \cdots & U_N(x) \end{bmatrix} \\ U^{(k)}(x) &= \begin{bmatrix} U_0^{(k)}(x) & U_1^{(k)}(x) & \cdots & U_N^{(k)}(x) \end{bmatrix} \\ A &= \begin{bmatrix} a_0 & a_1 & \cdots & a_N \end{bmatrix}^T \end{aligned}$$

By using (4), we obtained the corresponding matrix relation as follows:

$$\begin{aligned} &X^T(x) = DU^T(x) \text{ and } X(x) = U(x)D^T \\ &\text{and so } U(x) = X(x)(D^T)^{-1} \end{aligned} \quad (9)$$

where

$$X(x) = \begin{bmatrix} 1 & x & ... & x^N \end{bmatrix}.$$

for odd N,

$$D=\begin{bmatrix} \frac{1}{2^0}\binom{0}{0} & 0 & 0 & \dots & 0 \\ 0 & \frac{1}{2^1}\binom{1}{0} & 0 & \dots & 0 \\ \frac{1}{2^2}(\binom{2}{1}-\binom{2}{0}) & 0 & \frac{1}{2^2}\binom{2}{0} & \dots & 0 \\ \vdots & \vdots & \vdots & \ddots & \vdots \\ 0 & \frac{1}{2^N}(\binom{N}{\frac{N-1}{2}}-\binom{N}{\frac{N-3}{2}}) & 0 & \dots & \frac{1}{2^N}\binom{N}{0} \end{bmatrix}$$

for even N,

$$D=\begin{bmatrix} \frac{1}{2^0}\binom{0}{0} & 0 & 0 & \dots & 0 \\ 0 & \frac{1}{2^1}\binom{1}{0} & 0 & \dots & 0 \\ \frac{1}{2^2}(\binom{2}{1}-\binom{2}{0}) & 0 & \frac{1}{2^2}\binom{2}{0} & \dots & 0 \\ \vdots & \vdots & \vdots & \ddots & \vdots \\ \frac{1}{2^N}(\binom{N}{\frac{N}{2}}-\binom{N}{\frac{N-2}{2}}) & 0 & \frac{1}{2^N}(\binom{N}{\frac{N-2}{2}}-\binom{N}{\frac{N-4}{2}}) & \dots & \frac{1}{2^N}\binom{N}{0} \end{bmatrix}$$

Moreover it is clearly seen that the relation between the matrix $X(x)$ and its derivative $X^{(k)}(x)$,

$$X^{(k)}(x)=X(x)B^k \tag{10}$$

where

$$B=\begin{bmatrix} 0 & 1 & 0 & \cdots & 0 \\ 0 & 0 & 2 & \cdots & 0 \\ \vdots & \vdots & \vdots & \ddots & \vdots \\ 0 & 0 & 0 & \cdots & N \\ 0 & 0 & 0 & \cdots & 0 \end{bmatrix}$$

and

$$B^k=\underbrace{BB...B}_{k-times}.$$

The derivative of the matrix $U(x)$ defined in (8), by using the relation (9), can expressed as

$$\begin{aligned} U^{(k)}(x) &= X^{(k)}(x)(D^T)^{-1} \\ &= X(x)B^k(D^T)^{-1}. \end{aligned} \tag{11}$$

By substituting (10) into (8), we obtain, for $k=0,1,...,N$

$$y_N^{(k)}(x)=X(x)B^k(D^T)^{-1}A. \tag{12}$$

Now, the matrix representation of differential part can be given by

$$D(x)=\sum_{k=0}^{m}P_k(x)X(x)B^k(D^T)^{-1}A. \tag{13}$$

We know that;

$$X(\alpha_j x-\beta_j)=X(x)B_j \tag{14}$$

where

$$B_j=\begin{bmatrix} \binom{0}{0}\alpha_j^0(-\beta_j)^0 & \binom{1}{1}\alpha_j^0(-\beta_j)^1 & \binom{2}{2}\alpha_j^0(-\beta_j)^2 & \dots & \binom{N}{N}\alpha_j^0(-\beta_j)^N \\ 0 & \binom{1}{0}\alpha_j^1(-\beta_j^0) & \binom{2}{1}\alpha_j^1(-\beta_j)^1 & \dots & \binom{N}{N-1}\alpha_j^1(-\beta_j)^{N-1} \\ 0 & 0 & \binom{2}{0}\alpha_j^2(-\beta_j)^0 & \dots & \binom{N}{N-2}\alpha_j^2(-\beta_j)^{N-2} \\ \vdots & \vdots & \vdots & \ddots & \vdots \\ 0 & 0 & 0 & \dots & \binom{N}{0}\alpha_j^N(-\beta_j)^0 \end{bmatrix}$$

Using relation (10), we can write

$$X^{(s)}(\alpha_j x-\beta_j)=X(x)B^sB_j \tag{15}$$

In a similarly way as (12) , we obtain

$$\begin{aligned} y^{(s)}(\alpha_j x-\beta_j) &= U^{(s)}(\alpha_j x-\beta_j)A \\ &= X(x)B^sB_j(D^T)^{-1}A. \end{aligned} \tag{16}$$

So that, the matrix representation of $H(x)$ part can be given by

$$H(x)=\sum_{j=0}^{J}\sum_{s=0}^{n}H_s(x)X(x)B^sB_j(D^T)^{-1}A. \tag{17}$$

4. Method of solution

In this section, we presents the method for solving Eq.(1) with conditions Eq.(2). Firstly, we can write the Eq.(1) follow as:

$$\Big(\sum_{k=0}^{m}P_k(x)X(x)B^k(D^T)^{-1}+ \sum_{j=0}^{J}\sum_{s=0}^{n}H_{js}(x)X(x)B^sB_j(D^T)^{-1}\Big)A=g(x). \tag{18}$$

Then, residual $R_N(x)$ can be written as

$$\begin{aligned} R_N(x)\approx &\Big(\sum_{k=0}^{m}P_k(x)X(x)B^k(D^T)^{-1} \\ &+\sum_{j=0}^{J}\sum_{s=0}^{n}H_{js}(x)X(x)B^sB_j(D^T)^{-1}\Big)A \\ &-G^TX(x)(D^T)^{-1}. \end{aligned} \tag{19}$$

Applying typical tau method [29–33], Eq.(19) can be converted in $(N-m)$ linear or nonlinear equations by applying

$$\begin{aligned}\Big\langle R_N(x), U_n(x)\Big\rangle &= \int_{-1}^{1} R_N(x)U_n(x)dx \\ &= 0 \end{aligned} \tag{20}$$

for $n = 0, 1, ..., N-m$. The initial conditions are given by

$$\sum_{k=0}^{m-1}\sum_{j=0}^{r} c_{ij}^{k} X(c_j)B^k(D^T)^{-1}A = \lambda_i \tag{21}$$

where $-1 \le c_j \le 1$, $i = 0, 1, 2, ..., m-1$

$$X(c_j) = \left[\begin{array}{cccc} c_j^0 & c_j^1 & \cdots & c_j^N \end{array}\right].$$

Hence, we obtain the $(N+1)$ sets of linear or nonlinear algebraic equation with $(N+1)$ unknowns by Eq.(20) and Eq.(21). Using the Maple program, we solve the $(N+1)$ sets of linear or nonlinear algebraic equations with $(N+1)$ unknowns and so approximate solution $y_N(x)$ can be calculated.

4.1. Checking of Solution

Likewise we can easily check the accuracy of the obtained solutions as follows: Since the obtained the Chebyshev polynomial of the second kind expansion is an approximate solution of Eq.(1), when the function $y_N(x)$ and its derivatives are substituted in Eq.(1), the resulting equation must be satisfied approximately; that is for [24]

$$E_N(x) = \Big|\sum_{k=0}^{m} P_k(x)y_N^{(k)}(x) + \sum_{j=0}^{J}\sum_{s=0}^{n} H_{js}(x)y_N^{(s)}(\alpha_j x - \beta_j) - g(x)\Big| \cong 0$$

5. Illustrative example

In this section, several numerical examples are given to illustrate the accuracy and effectiveness of the properties of the method and all of them were performed on the computer using a program written in Maple 13. The absolute errors in tables are the values of $N_e = |y(x) - y_N(x)|$ at selected points.

Example 1. *Let us consider the first order pantograph equation [11, 20, 21]*

$$y'(x) - \frac{1}{2}y(x) - \frac{1}{2}e^{\frac{x}{2}}y(\frac{x}{2}) = 0 \tag{22}$$

with $y(0) = 1$ *and the exact solution* $y = e^x$. *Then* $P_0(x) = -\frac{1}{2}$, $P_1(x) = 1$, $H_{00}(x) = -\frac{1}{2}e^{\frac{x}{2}}$, $g(x) = 0$, $\alpha_0 = \frac{1}{2}$, $\beta_0 = 0$. *We seek the approximate solution for* $N = 4$. *Then, we have residual*

$$\begin{aligned} R_4(x) \approx &\Big(P_1(x)X(x)B(D^T)^{-1} \\ &+P_0(x)X(x)(D^T)^{-1} + H_{00}(x)X(x)B_0(D^T)^{-1}\Big)A \end{aligned}$$

where

$$B = \left[\begin{array}{ccccc} 0 & 1 & 0 & 0 & 0 \\ 0 & 0 & 2 & 0 & 0 \\ 0 & 0 & 0 & 3 & 0 \\ 0 & 0 & 0 & 0 & 4 \\ 0 & 0 & 0 & 0 & 0 \end{array}\right] B_0 = \left[\begin{array}{ccccc} 1 & 0 & 0 & 0 & 0 \\ 0 & \frac{1}{2} & 0 & 0 & 0 \\ 0 & 0 & \frac{1}{4} & 0 & 0 \\ 0 & 0 & 0 & \frac{1}{8} & 0 \\ 0 & 0 & 0 & 0 & \frac{1}{16} \end{array}\right]$$

If the residual $R_4(x)$ *are substituted (19) for* $n = 0, 1, 2, 3$ *and with initial condition, we obtain a linear algebraic equations system. Solving this linear equations system, we obtain the Chebyshev coefficients follows as:*

$$\begin{aligned} &a_0 = 1.130077, a_1 = 0.542776 \\ &a_2 = 0.132856, a_3 = 0.223357E-1 \\ &a_4 = 0.277975E-2 \end{aligned}$$

then so, we get the approximate solution for $N = 4$

$$\begin{aligned} y_4(x) = &0.999999 + 0.996210x + 0.498070x^2 \\ &+0.178686x^3 + 0.044476x^4 \end{aligned}$$

Table 1 shows approximate solutions of the Eq.(22) for $N = 4, 6, 8$ *by the above mentioned method. Figure 1 display the exact solution and numerical solutions for* $N = 6, 8$. *Figure 2 displays error function* $N = 6$ *and Figure 3 displays error function* $N = 8$ *Figure 3 compare the error functions and* $E_N(x)$ *for* $N = 6, 8$.

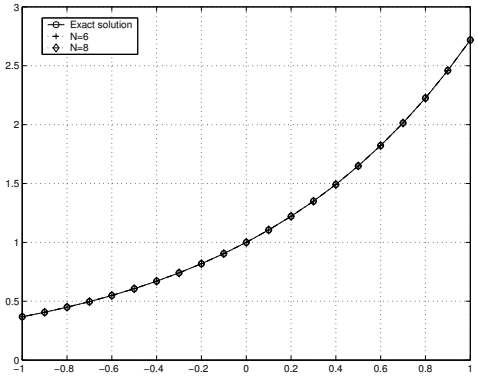

Figure 1. Comparison of exact solution and approximate solutions of Example 1 for various N.

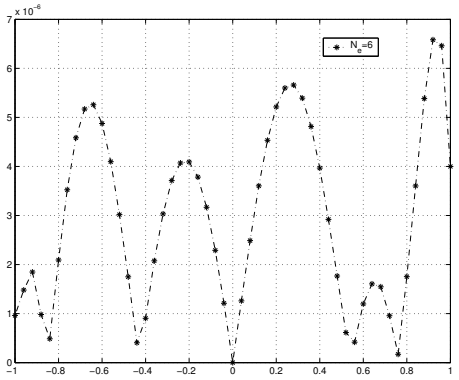

Figure 2. Error functions of Example 1 for various N.

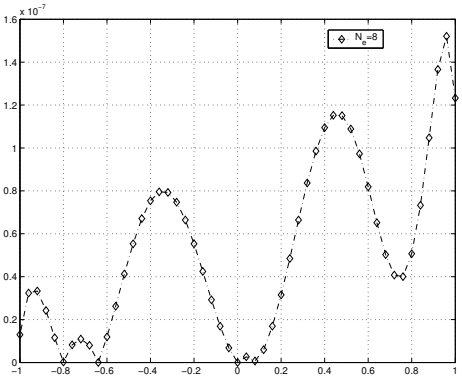

Figure 3. Error functions of Example 1 for various N.

Example 2. *Let us consider the following pantograph equation of first-order [21]*

$$y'(x) + 2y^2(\frac{x}{2}) = 1 \qquad (23)$$

with $y(0) = 0$ *and exact solution is* $y(x) = sin(x)$. *Table 2 shows numerical solutions Eq.(23) with* $N = 5, 7$ *and* 9 *by present method. We see that the approximation solutions obtained by present method has good agreement with exact solution. In Table 2 compare the absolute errors and* $E_N(x)$ *some selected points. Figure 4 display values of the absolute error and* $E_N(x)$.

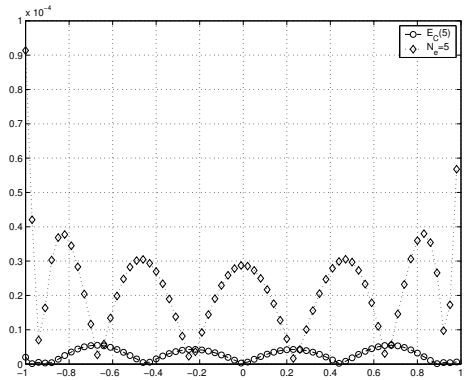

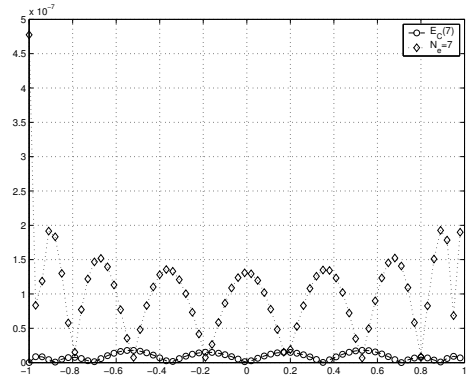

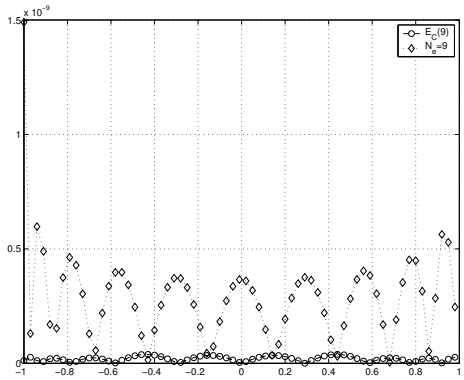

Figure 4. Comparison of error functions and $E_N(x)$of Example 2 for various N.

Example 3. *Let us consider the linear delay differential equation with constant coefficients and proportional delay* qx

$$y'(x) = ay(x) + by(qx),\ 0 < q < 1 \qquad (24)$$

with initial condition

$$y(0) = \gamma$$

arose in the mathematical modeling of the wave motion in the supply line to an overhead current collector (pantograph) of an electric locomotive [1-2]. For values of $a = -1$,$b = -1$, $q = 0.8$ *and* $\gamma = 1$ *[8], Table 3 shows solutions of Eq.(24) with* $N = 8$ *by present method. Moreover, the previous results of Walsh series approach (WSA) [34], delayed unit step function series approach (DUSFA) [35], Laguerre series approach (LSA) [36], Taylor series method (TSM) [8] and present method (PM) are also given in Table 3 for comparison. The present method seems more rapidly convergent than Laguerre series and Taylor series and with errors more under control than Walsh or DUSFA series. The truncated errors for Eq.(24) are* $O(9)$ *and* $O(15)$ *for* $N = 8$ *and* $N = 15$ *respectively are also indicated.*

Example 4. *Consider the nonlinear pantograph equation of third order [11, 20],*

$$y'''(x) = -1 + 2y^2(\frac{x}{2}),$$
$$y(0) = 0,\ y'(0) = 1,''(0) = 0 \qquad (25)$$

which has the exact solution $y(x) = sin(x)$. *If we take* $N = 9$, *we get the difference between the exact and numerical solutions given in Table 4. Table 4 shows previous results of HPM [20], Adomian decomposition method (ADM) [11] and Present method (PM) for comparison. This shows that the errors are very small. Then, Figure 5 displays the comparison of error function and* $E_N(x)$ *for* $N = 15$.

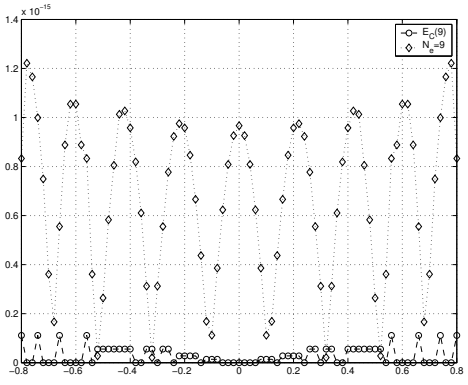

Figure 5. Comparison of error function and $E_{15}(x)$of Example 4.

Example 5. *We consider the equation with* $y(0) = 1$

$$y'(x) = -y(x) + \mu_1(x)y(0.5x)$$
$$+\mu_2(x)y(0.25x) \qquad (26)$$

Here $\mu_1(x) = -exp^{-0.5x}sin(0.5x)$, $\mu_2(x) = -2exp^{-0.75x}cos(0.5x)sin(0.25x)$. *It can be seen that the exact solution of Eq.(26) is* $y(x) = e^{-x}cos(x)$. *Using present method, we obtain the numerical solution for* $N = 10$. *In Figure 6 we give the exact solution and numerical solutions corresponding.*

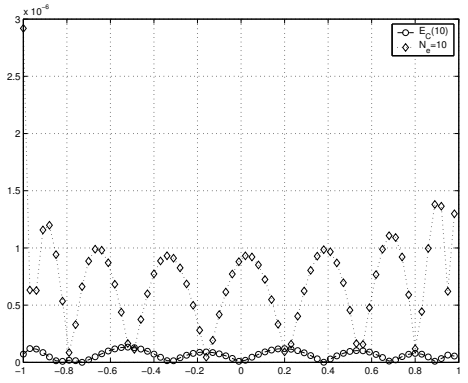

Figure 6. Comparison of error function and $E_{10}(x)$of Example 5.

6. Conclusion

A new method based on the truncated Chebyshev series of the second kind is developed to numerical solve generalized pantograph equations with mixed conditions. Pantograph equations are usually difficult to solve analytically. In many cases, it is required to obtain the approximate solution. For this propose, the present method can be proposed. In this paper, the second kind Chebyshev polynomial approach has been used for the approximate solution of generalized pantograph equations. Thus the proposed method is suggested as an efficient method for generalized pantograph equations. Examples with the satisfactory results are used to demonstrate the application of this method. Suggested approximations make this method rather attractive and contributed to the good agreement between approximate and exact values in the numerical examples for only a few terms. Then examples shows truncated errors, absolute errors and $E_N(x)$ are coherent, and performed on the computer using a program written in Maple 13. Moreover, suggested method is applicable for the approximate solution of the pantograph-type integro-differential equations with variable delays.

Acknowledgments

The authors would like to thank the Editors and referees for their helpful comments and suggestions.

References

[1] Ockendon, J.R. and Tayler, A.B., The dynamics of a current collection system for an electric locomotive. Proc. Roy. Soc. London, Ser. A, 322, 447-468 (1971).

[2] Tayler, A.B., Mathematical Models in Applied Mathematics. Clarendon Press, Oxford, (1986).

[3] Ajello, W.G., Freedman, H.I. and Wu, J., Analysis of a model representing stage-structured population growth with state-dependent time delay. SIAM J. Appl. Math., 52, 855-869 (1992).

[4] Buhmann, M.D. and Iserles, A., Stability of the discretized pantograph differential equation. Math. Comput., 60, 575-589 (1993).

[5] Derfel, G., On compactly supported solutions of a class of functional-differential equations, in Modern Problems of Function Theory and Functional Analysis. Karaganda University Press, Kazakhstan, (1980).

[6] Feldstein, A. and Liu, Y., On neutral functional-differential equations with variable time delays. Math. Proc. Camb. Phil. Soc., 124, 371-384 (1998).

[7] Derfeland, G. and Levin, D., Generalized refinement equation and subdivision process. J. Approx. Theory, 80, 272-297 (1995).
[8] Sezer, M. and Akyuz, A., A Taylor method for numerical solution of generalized pantograph equation with linear functional argument. J. Comp. Appl. Math., 200, 217-225 (2007).
[9] Sezer, M., Yalnbas, S. and Sahin, N., Approximate solution of multi-pantograph equation with variable coefficients. J. Comp. Appl. Math., 214, 406-416 (2008).
[10] Saadatmandi, A. and Dehghan, M., Variational iteration method for solving a generalized pantgoraph equation. Comp. Math. Appl., 58, 2190-2196 (2009).
[11] Evans, D.J. and Raslan, K.R., The Adomian decomposition method for solving delay differential equation. Int. J. Comp. Math., 82(1), 49-54 (2005).
[12] Buhmann, M. and Iserles, A., Stability of the discretized pantograph differential equation. J. Math. Comp., 60, 575-589 (2005).
[13] Li, D. and Liu, M.Z., Runge-Kutta methods for the multi-pantograph delay equation. Appl. Math. Comp., 163, 383-395 (2005).
[14] Shakeri, F. and Dehghan, M., Solution of the delay differential equations via homotopy perturbation method. Math. Comp. Modelling, 48, 486-498 (2008).
[15] Muroya, Y., Ishiwata, E. and Brunner, E., On the attainable order of collocation methods for pantograph integro-differential equations. J. Comp. Appl. Math., 152, 347-366 (2003).
[16] Huan-Yu, Z., Variational iteration method for solving the multi-pantograph delay equation. Physics Letter A, 372 (43), 6475-6479 (2008).
[17] Sezer, M. and Gulsu, M., A new polynomial approach for solving difference and Fredholm integro-difference equations with mixed argument. Appl. Math. Comp., 171, 332-344 (2005).
[18] Ping Yang, S. and Xiao, A.G., Convergence of the variational iteration method for solving multidelay differential equaitons. Comp. Math. Appl., 61(8), 2148-2151 (2011).
[19] Liu, M.Z. and Li, D., Properties of analitic solution and numerical solution of multi-pantograph equation. Appl. Math. Comp., 155, 853-871 (2004).
[20] Yusufoglu, E., An efficint algorithm for solving generalized pantograph equation with linear functional argument. Appl. Math. Comp., 217, 3591-3595 (2010).
[21] El-Safty, Salim, M.S. and El-Khatib, M.A., Convergence of the spline function for delay dynamic system. Int. J. Comp. Math., 80(4),509-518 (2004).
[22] Fox, L. and Parker, I.B., Chebyshev Polynomials in Numerical Analysis. Oxford University Press, London, (1968).
[23] Mason, J.C. and Handscomb, D.C., Chebyshev polynomials. Chapman and Hall/CRC, New York, (2003).
[24] Body, J.P., Chebyshev and fourier spectral methods, University of Michigan, New York, (2000).
[25] Saadatmandi, A. and Dehghan, M., Numerical solotion of hyperbolic telegraph equation using the Chebshev tau method. Numer. Meth. Partial Diff. Equations, 26, 239-252 (2010).
[26] Lakestani, M. and Dehghan, M., Numerical solution of Riccati equation using the cubic B spline scaling functions and Chebyshev cardinal functions. Comp. Physics Communications, 181, 957-966 (2010).
[27] Lakestani M. and Dehghan, M., Numerical solution of fourth order integro differential equations using Chebyshev cardinal functions. Inter. J. Com. Math., 87, 1389-1394 (2010).
[28] Saadatmandi, A. and Dehghan, M., The numerical solution of problems in calculus of variation using Chebyshev finite difference method. Physi. Letter A, 22, 4037-4040 (2008).
[29] Pandey, R.K. and Kumar, N., Solution of Lane-Emden type equations using Berstein operational matrix of differentiation. New Astronomy, 17, 303-308 (2012).
[30] Saadatmandi, A. and Dehghan, M., A new aperational matrix for solving fractional-order differential equations. Comp. Math. Appl., 59, 1326-1336 (2010).
[31] Parand, K. and Razzaghi, M., Rational Chebyshev tau method for solving higher-order ordinary differential equations. Int. J. Comput. Math., 81, 73-80 (2004).
[32] Razzaghi, M. and Yousefi, S., Legendre wavelets operational matrix of integration. Int. J. Syst. Sci., 32(4), 495-502 (2001).
[33] Babolian E. and F. Fattahzadeh, Numerical solution of differential equations by using Chebyshev wavelet operational matrix of integration. Appl. Math. Comp., 188, 417-425 (2007).
[34] Rao G.P. and Palanisamy, K.R., Walsh stretch matrices and functional differential equations. IEEE Trans. Autom. Control, 27, 272-276 (1982).
[35] Hwang, C., Solution of a functional differential equation via delayed unit step functions. Int. J. Syst. Sci., 14(9), 1065-1073 (1983).4
[36] Hwang, C. and Shih, Y.P., Laguerre series solution of a functional differential equation. Int. J. Syst. Sci., 13(7), 783-788 (1982).

Yalçın Öztürk *was born on November 01th 1983 in Manavgat-Antalya, Turkey. He finished Ph.D. degree under the supervision of Prof. Dr. Mustafa GÜLSU in Applied Mathematics at the Muğla Sıtkı Koçman University in 2015. His main research interests include differential and integral equations and their numerical solutions.*

Mustafa Gülsu *was born in Istanbul, Turkey. He received the B.Sc. degrees in Mathematics from Marmara University,Turkey, M.Sc.degrees in Mathematics in Northeastern University,USA, and the Ph.D. degree in mathematics from Ege University, Turkey in 2002. Currently, he is a full professor at Mathematics department of Muğla Sıtkı Koçman University, Turkey. His main research interests are ordinary and partial differential equations, integral and difference equations, and their numerical solutions.*

Table 1. Numerical results of Example 1 for different N.

		Present Method					
x	Exact Solution	$N=4$	$N_e=4$	$N=6$	$N_e=6$	$N=8$	$N_e=8$
-1.0	0.367879	0.367649	0.229E-3	0.367878	0.592E-6	0.367879	0.129E-7
-0.8	0.449328	0.448526	0.802E-3	0.449331	0.245E-5	0.449328	0.253E-9
-0.6	0.548811	0.548746	0.646E-4	0.548816	0.481E-5	0.548811	0.119E-7
-0.4	0.670320	0.670909	0.589E-3	0.670318	0.113E-5	0.670320	0.753E-7
-0.2	0.818730	0.818730	0.591E-3	0.818726	0.405E-5	0.818730	0.553E-7
0.0	0.999999	1.000000	0.000E-0	1.000000	0.221E-6	0.999999	0.700E-14
0.2	1.221402	1.221402	0.737E-3	1.221408	0.525E-5	1.221402	0.314E-7
0.4	1.491824	1.491824	0.107E-2	1.491824	0.373E-5	1.491824	0.109E-6
0.6	1.822118	1.822118	0.726E-3	1.822117	0.125E-5	1.822118	0.818E-7
0.8	2.225540	2.225540	0.102E-3	2.228543	0.211E-6	2.225540	0.506E-7
1.0	2.718281	2.718281	0.838E-3	2.718284	0.244E-5	2.718281	0.123E-6

Table 2. Numerical results of Example 2 for different N.

		Present Method					
x	Exact Solution	E_5	$N_e=5$	E_7	$N_e=7$	E_9	$N_e=9$
-1.0	-0.841470	0.913568E-4	0.200902E-5	0.477454E-6	0.224832E-9	0.149014E-8	0.115905E-10
-0.8	-0.717356	0.359449E-4	0.319621E-5	0.840162E-8	0.773644E-8	0.448240E-9	0.833401E-11
-0.6	-0.564642	0.157055E-4	0.469280E-5	0.102028E-6	0.147040E-7	0.363683E-9	0.626964E-11
-0.4	-0.389418	0.269612E-4	0.149996E-5	0.127995E-6	0.697329E-8	0.144294E-9	0.357318E-10
-0.2	-0.198669	0.737766E-5	0.418202E-5	0.191299E-7	0.149003E-7	0.193295E-9	0.290406E-10
0.0	0.000000	0.287867E-4	0.000000E-0	0.131290E-6	0.000000E-0	0.368155E-9	0.000000E-0
0.2	0.198669	0.737766E-5	0.418202E-5	0.191299E-7	0.149003E-7	0.193295E-9	0.290406E-10
0.4	0.389418	0.269612E-4	0.149996E-5	0.127995E-6	0.697329E-8	0.144294E-9	0.357318E-10
0.6	0.564642	0.157055E-4	0.469280E-5	0.102028E-6	0.147040E-7	0.363683E-9	0.626964E-11
0.8	0.717356	0.359449E-4	0.319621E-5	0.840162E-8	0.773644E-8	0.448240E-9	0.833401E-11
1.0	0.814470	0.913568E-4	0.200902E-5	0.477454E-6	0.224832E-9	0.149014E-8	0.115905E-10

Table 3. Comparison of the solution of Eq.(24)

x	WSA	DUSFA $m=100$	LSA $n=20$	TSM $N=8$	TSM E_{19}	PM $N=8$	PM $N=15$	PM E_{15}
0.0	1.000000	1.000000	0.999971	1.000000	0.844E-14	1.000000	1.00000000000	0.200E-18
0.2	0.665621	0.664677	0.664703	0.664691	0.138E-13	0.664691	0.66469100082	0.318E-16
0.4	0.432426	0.433540	0.433555	0.433561	0.322E-3	0.433560	0.43356077877	0.170E-15
0.6	0.275140	0.276460	0.276471	0.276483	0.125E-13	0.276481	0.27648233022	0.972E-15
0.8	0.170320	0.171464	0.171482	0.171494	0.738E-14	0.171484	0.17148411197	0.206E-14
1.0	0.100856	0.102652	0.102679	0.102744	0.155E-13	0.102670	0.10267012657	0.814E-14

Table 4. Comparison of the solution of Eq.(25)

x	Exact solution	ADM	HPM	PM
0.0	0.0	0.0	0.0	0.0
0.2	0.19866933079506122	0.19866933079506122	0.19866933079506122	0.19866933079506121
0.4	0.38941834230865050	0.38941834230865050	0.38941834230865050	0.38941834230865049
0.6	0.56464224733950355	0.56464224733950355	0.56464224733950355	0.56464247339503535
0.8	0.71735609089952280	0.71735609089952270	0.71735609089952280	0.71735609089952276
1.0	0.84147109848078965	0.84147109848078966	0.84147109848078965	0.84141098480789650

An International Journal of Optimization and Control: Theories & Applications (http://ijocta.balikesir.edu.tr)

An International Journal of Optimization and Control: Theories & Applications
ISSN:2146-0957 eISSN:2146-5703
Vol.7, No.1, pp.75-82 (2017)
http://doi.org/10.11121/ijocta.01.2017.00312

RESEARCH ARTICLE

Brezzi-Pitkaranta stabilization and a priori error analysis for the Stokes control

Aytekin Cıbık*, Fikriye Yılmaz

Department of Mathematics, Gazi University, Turkey
aytechin@gmail.com, yfikriye@gmail.com

ARTICLE INFO

Article History:
Received 5 March 2016
Accepted 22 August 2016
Available 12 December 2016

Keywords:
Finite element
Brezzi-Pitkaranta stabilization
Optimal control
Stokes equations

AMS Classification 2010:
65K10, 65K15, 76D07

ABSTRACT

In this study, we consider a Brezzi-Pitkaranta stabilization scheme for the optimal control problem governed by stationary Stokes equation, using a P1-P1 interpolation for velocity and pressure. We express the stabilization as extra terms added to the discrete variational form of the problem. We first prove the stability of the finite element discretization of the problem. Then, we derive a priori error bounds for each variable and present a numerical example to show the effectiveness of the stabilization clearly.

1. Introduction

This study deals with the optimal control problem of the stationary Stokes equation. Numerical solution of the Stokes equation needs some extra caution due to the coupling of velocity and pressure. Finite element methods are mostly used for the solution of Stokes equation but inaccurate pressure singularities are encountered unless some stable finite element pairs are used for the standard Galerkin finite element approach. Stable finite element pairs are chosen as they satisfy the so called inf-sup condition to overcome such problems. This condition, in particular, does not allow the use of simple interpolations like equal order ones, which are desirable from a computational view point [6]. Thus, if one uses such simple finite element pairs, a pressure stabilization mechanism must be cast to the system in order to avoid pressure singularities.

In most of these stabilized methods, one adds some extra terms to the discrete variational form of the problems to ensure stability. The first and most well-known stabilization technique applied on a Stokes system is the Brezzi-Pitkaranta method [8], which is considered in this study to stabilize the optimal control problem. This method adds a weighted Laplace operator on the pressure space, which results in an optimally convergent scheme for equal order finite element approximations [5]. Some other popular methods are GLS method [13], SUPG method along with PSPG method [9], the Douglas-Wang method [12], bubble function method [4], Pressure Gradient Projection methods [11] and VMS methods [20]. Some of these stabilization methods are transferred to the Navier-Stokes systems as tested in Stokes flows and demonstrate a good success. Thus, Stokes flow problems bears a great importance as it plays a role as a test bed for more complicated and convective problems such as uncoupled and coupled Navier-Stokes systems. Making use of the Brezzi-Pitkaranta stabilization for the control of the Stokes equation is advantageous

*Corresponding Author

since it doesn't require numerical residual explicitly as in GLS methods and thus, strong differential formulation of the problem is not needed. The Brezzi-Pitkaranta stabilization technique also will not require extra regularity conditions as in some well-known stabilization procedures [19].

There are various studies in the literature concerning the optimal control of flow problems. In [25], a discontinuous galerkin finite element method (DG) with interior penalties for the optimal control problem of the convection-diffusion equation was studied and in [18], an edge stabilized galerkin finite element method for the same optimal control system was considered. Moreover, local error estimates for SUPG solutions of advection-dominated elliptic linear-quadratic optimal control problems was studied in [17]. Similarly, the local (DG) for optimal control problem governed by convection-diffusion equations was analyzed in [27]. In [14], authors presented an analysis concerning the optimal control of fully discretized Stokes equations and a priori error analysis of the same optimal control system are presented in [23]. In most similar studies, researchers choose inf-sup stable finite element pairs for velocity and presuure approximations. The originality of this study comes from the idea of combining the pressure stabilization technique and optimal control problem of Stokes problem with unstable and lower order finite element pairs. To the best of the authors knowledge, this is the first study on optimal control problem of Stokes equations including the Brezzi-Pitkaranta stabilization applied on an equal order finite element interpolations.

In this work, we use Lagrange approach to get the first order optimality conditions. Then, we formulate the discrete optimal control problem. Stabilization terms are added to both weak formulations of the discrete state and adjoint variables. In order to solve the optimal control problem, we use a gradient descent type algorithm. In the numerical example, one can easily see the efficiency of the stabilization for both the state and the adjoint variables.

The organization of the paper is as follows: We first give some notational notes and mathematical preliminaries in order to define the problem and its variational form. Then, we give the finite element discretization of the optimal control problem and prove the stability properties. A priori error analysis of the control problem is proceeded in the following section. We conclude our study with a numerical example.

2. Problem Formulation and Optimal Control Problem

In this work, we consider the optimal control problems governed by the Stokes equations. Let Ω be a bounded polygonal domain in $\mathbb{R}^d$, with $d = 2$ or 3, and its Lipschitz boundary be $\Sigma = \partial\Omega$. Then, we state the distributed control problem as:

$$\min \; J(y,u) = \frac{1}{2}\|y - y_d\|_\Omega^2 + \frac{\beta}{2}\|u\|_\Omega^2 \qquad (1)$$

$$\begin{aligned} \text{subject to} \quad -\nu\Delta y + \nabla p &= u \;\text{ in } \Omega, \\ \nabla . y &= 0 \;\text{ in } \Omega, \\ y &= 0 \;\text{ on } \Sigma, \end{aligned} \qquad (2)$$

where $y : \Omega \mapsto \mathbb{R}^d$ is the fluid velocity, $p : \Omega \mapsto \mathbb{R}$ denotes the pressure and u is the control variable. The kinematic viscosity is denoted by $\nu > 0$. Here, $\beta > 0$ stands for the regularization parameter and y_d is the desired state.

We follow the well-known Lagrange approach [21] to get the first order optimality conditions. We let λ denote the adjoint variable that satisfies

$$\begin{aligned} \text{subject to} \quad -\nu\Delta\lambda + \nabla\xi &= y - y_d \;\text{ in } \Omega, \\ \nabla . \lambda &= 0 \;\text{ in } \Omega, \\ \lambda &= 0 \;\text{ on } \Sigma, \end{aligned} \qquad (3)$$

and

$$\beta u + \lambda = 0 \text{ in } \Omega, \qquad (4)$$

where $\xi : \Omega \mapsto \mathbb{R}$.

We use the standard notations for Sobolev and Lebesgue spaces as in Adams [3] throughout the paper. We denote the velocity space by $Y = H_0^1(\Omega)$, the pressure space by $Q = L_0^2(\Omega)$ and the control space $U = L^2(\Omega)$. The usual norm in $L^2(\Omega)$ is denoted with $\|.\|$ and the norm of $H^1(\Omega)$ space is shown with $\|.\|_1$. We would like to recall here the dual space of $Y = H_0^1(\Omega)$, namely the space $H^{-1}(\Omega)$ equipped with the -1-norm

$$\|z\|_{-1} = \sup_{y \in Y} \frac{| < z, y > |}{\|y\|_1}. \qquad (5)$$

Here, $< ., . >$ denotes the duality pairing. We introduce the following bilinear forms in order to define the variational form of the problem, for $y, v \in Y$ and $q \in Q$:

$$a(y,v) = \nu\int_\Omega \nabla y : \nabla v dx,$$
$$d(v,q) = \int_\Omega q\nabla\cdot v dx.$$

Now, the weak forms of the equations (2) and (3) read as: Find $y \in Y$, $u \in U$ and $q \in Q$ satisfying

$$a(y,v) - d(v,p) + d(y,q) = (u,v),\ \forall (v,q) \in Y\times Q, \quad (6)$$

for the state part. For the adjoint equation, the problem is: Find $\lambda \in Y$ and $\varphi \in Q$ satisfying

$$a(\lambda,w) - d(w,\xi) + d(\lambda,\varphi) = (y-y_d,w)\ \forall (w,\varphi)\in Y\times Q. \quad (7)$$

Assuming the solution operator $S : U \mapsto H_0^1(\Omega)\cap H^2(\Omega)$, we define the reduced cost function:

$$J(y,u) = J(S(u),u) := j(u),$$

where $S(u)$ solves the auxiliary problem

$$a(y(u),v) - d(v,p) + d(y(u),q) = (u,v)\ \ \forall (v,q)\in Y\times Q. \quad (8)$$

Optimality conditions give the gradient equation as

$$j'(u)(\tilde u - u) = (\lambda(u) + \beta u, \tilde u - u),\ \ \forall \tilde u \in U, \quad (9)$$

with $\lambda(u)$ solves the following system:

$$a(\lambda(u),w) - d(w,\xi) + d(\lambda(u),\varphi) = (y(u)-y_d,w)\ \ \forall (w,\varphi)\in Y\times Q. \quad (10)$$

We can use the second order sufficient optimality condition to get the positive definiteness of the reduced hessian [21, 26]:

$$j''(u)(\delta u,\delta u) \geq \alpha \left\|\delta u\right\|^2_{L^2(\Omega)} \quad \forall \delta u \in U. \quad (11)$$

We would like to note here that, unless stated otherwise, the letter C will stand for a generic constant, which is independent from the mesh size h throughout the entire paper.

3. Discretization

In this section, we will discretize our continuous problems using a finite element approach and the Brezzi-Pitkaranta stabilization term will appear in discrete variational problem. We let $Y^h \subset Y$,$Q^h \subset Q$ and $U^h \subset U$ be the finite element spaces with a quasiuniform triangulation τ^h of Ω. The corresponding triangles of the domain are denoted by $K_1, K_2, ..., K_n$. We let $h_i = diam(K_i)$ and $h = max\{h_1, h_2, ..., h_n\}$. We consider Y^h and Q^h to be the spaces of continuous piecewise linears (P1-P1 pair), which is an unstable pair known not to satisfy discrete inf-sup condition. We also make the standard assumptions that the finite element spaces satisfy the following approximation properties:

$$\inf_{y^h\in Y^h, q^h\in Q^h}\Big\{\|(y-y^h)\| + h\|\nabla(y-y^h)\| + h\|p-q^h\|\Big\} \leq Ch^2(\|y\|_2 + \|p\|_1), \quad (12)$$

for $(y, p \in (Y\cap H^2(\Omega), Q\cap H^1(\Omega))$. We also assume that the control variable u satisfies

$$\|u-\tilde u\| \leq Ch^2\|u\|_2 \quad \text{for } u \in U\cap H^2(\Omega), \quad (13)$$

where $\tilde u$ is the L^2 projection from U to U^h. Now, the finite element scheme considered for the optimal control problem here reads as follows: Find $y^h, \lambda^h \in Y^h$, $u^h \in U^h$ and $q^h, \xi^h \in Q^h$ such that

$$\min J(y^h,u^h) = \frac{1}{2}\left\|y^h - y_d\right\|^2 + \frac{\alpha}{2}\left\|u^h\right\|^2 \quad (14)$$

subject to

$$a(y^h,v^h) - d(v^h,p^h) + d(y^h,q^h) + c(p^h,q^h) = (u^h,v^h),\ \forall (v^h,q^h)\in Y^h\times Q^h, \quad (15)$$

$$a(\lambda^h,w^h) - d(w^h,\xi^h) + d(\lambda^h,\varphi^h) + c(\xi^h,\varphi^h) = (y^h-y_d,w^h)\ \forall (w^h,\varphi^h)\in Y^h\times Q^h. \quad (16)$$

Here, the terms $c(p^h,q^h)$ and $c(\xi^h,\varphi^h)$ stand for the Brezzi-Pitkaranta stabilization. α is a positive parameter and $c(.,.)$ is a mesh dependent bilinear form, which is defined by

$$c(p^h,q^h) = \alpha\sum_{i=1}^n h_i^2\int_{K_i}\nabla p^h.\nabla q^h dx\ \ \forall p^h,q^h\in Q^h,$$

and assumed to satisfy following properties [19]:

i. $c(p^h,q^h)$ is defined for all $p^h,q^h\in Q^h$.
ii. $c(q^h,q^h) = \alpha[q^h]^2,\ \forall q^h\in Q^h$ is a mesh dependent norm.
iii. $c(p^h,q^h)$ is continuous in the sense that, $c(p^h,q^h)\leq [p^h][q^h]$.
iv. For $\forall y^h\in Y^h, q^h\in Q^h$; $\exists$ a positive constant γ, which is independent from h and satisfies
$$d(y^h,q^h) \leq \gamma\frac{1}{h^k}\left\|y^h\right\|[q^h],\ \ k = 1, 1/2.$$
v. $\exists c_0$, a positive constant independent from h, such that
$$\forall q^h\in Q^h\ [q^h] \leq c_0h^k\left\|q^h\right\|_1,\ \ k = 1, 1/2.$$

Similar to continuous case, we can define the discrete solution operator S_h such that $S_h(u) = y_h(u)$. Then, there hold

$$j_h'(u)(\tilde u - u) = (\lambda^h(u) + \alpha u, \tilde u - u),\ \ \forall \tilde u\in U, \quad (17)$$

and

$$j_h''(u)(\delta u, \delta u) \geq \alpha \left\|\delta u\right\|^2_{L^2(\Omega)}, \quad \forall \delta u \in U. \quad (18)$$

The discrete auxiliary problem in variational formulation follows as:

$$\begin{aligned} &a(y^h(u), v^h) - d(v^h, p^h) + d(y^h(u), q^h) \quad (19)\\ &+c(p^h, q^h) = (u, v^h) \ \ \forall (v^h, q^h) \in Y^h \times Q^h, \end{aligned}$$

$$\begin{aligned} &a(\lambda^h(u), w^h) - d(w^h, \xi^h) + d(\lambda^h(u), \psi^h)\\ &+c(\xi^h, \psi^h) = (y^h(u) - y_d, w^h)\\ &\forall (w^h, \psi^h) \in Y^h \times Q^h. \quad (20) \end{aligned}$$

Now, we will obtain the stability results for both state and adjoint state variables in the following lemma.

Lemma 1. *The discrete state and adjoint state variables (15)-(16) are stable and there hold*

$$\nu \left\|\nabla y^h\right\|^2 \leq C\nu^{-1} \left\|u^h\right\|^2, \quad (21)$$

and

$$\nu \left\|\nabla \lambda^h\right\|^2 \leq C\nu^{-1} \left\|y^h - y_d\right\|^2. \quad (22)$$

Proof. We let $v^h = y^h$ in (15) to get

$$a(y^h, y^h) - d(y^h, p) + d(y^h, q) = (u^h, y^h).$$

We choose $q = p$ and applying the Cauchy-Schwartz and Young's inequalities we get the desired result for the state part. We proceed the similar argument for the stability of the adjoint state variable.

□

4. Finite element error analysis

In this section, we derive the error estimates for the control, state and adjoint state variables.

Lemma 2. *Let $(y(u), p)$ and $(y^h(u), p^h)$ be solutions of (6) and (19), respectively. Then, we have*

$$\begin{aligned} &\nu\|\nabla(y(u) - y^h(u))\|^2 + [p - p^h]^2\\ &\leq \inf_{\tilde{y}\in Y^h, \tilde{p}\in Q^h} C\\ &\left\{\nu^{-1}\left\|\nabla(y(u) - \tilde{y})\right\|^2 + \nu^{-1}\left\|(p - \tilde{p})\right\|^2\right.\\ &\left. + h^{-1}\left\|\nabla(y(u) - \tilde{y})\right\|^2 + [p - \tilde{p}]^2 + [p]^2\right\}. \end{aligned}$$

Proof. We subtract (19) from (6) via the same test functions v^h, q^h. Thus, we get the error equation

$$\begin{aligned} &a(y(u) - y^h(u), v^h) - d(v^h, p - p^h) +\\ &d(y(u) - y^h(u), q^h) - c(p^h, q^h)\\ &= 0, \ \forall (v^h, q^h) \in Y^h \times Q^h. \end{aligned}$$

Now we split the error term $y - y^h(u)$ as $y - y^h(u) = y - \tilde{y} - (y^h(u) - \tilde{y}) = \eta - \phi^h$, where $\tilde{y}$ is the best approximation of y in Y^h. So the error equation becomes:

$$\begin{aligned} &a(\eta - \phi^h, v^h) - d(v^h, p - p^h)\\ &+d(\eta - \phi^h, q^h) - c(p^h, q^h) = 0. \end{aligned}$$

Rearranging the new error equation and adding and subtracting $c(p, q^h)$ with the test function choice $v^h = \phi^h$ yield:

$$\begin{aligned} a(\phi^h, \phi^h) = a(\eta, \phi^h) - d(\phi^h, p - p^h) - d(\phi^h, q^h)\\ +d(\eta, q^h) + c(p - p^h, q^h) - c(p, q^h). \end{aligned}$$

Splitting the error in the pressure in a similar manner gives $p - p^h = p - \tilde{p} - (p^h - \tilde{p}) = \zeta - \psi^h$, where $\tilde{p}$ is the best approximation of p in Q^h. Then, we have

$$\begin{aligned} a(\phi^h, \phi^h) = a(\eta, \phi^h) - d(\phi^h, \zeta - \psi^h) - d(\phi^h, q^h)\\ +d(\eta, q^h) + c(\zeta - \psi^h, q^h) - c(p, q^h). \end{aligned}$$

Picking $q^h = \psi^h$ gives:

$$\begin{aligned} &a(\phi^h, \phi^h) + c(\psi^h, \psi^h) = a(\eta, \phi^h) - d(\phi^h, \zeta)\\ &+d(\phi^h, \psi^h) - d(\phi^h, \psi^h) + d(\eta, \psi^h)\\ &+c(\zeta, \psi^h) - c(p, \psi^h) = a(\eta, \phi^h) - d(\phi^h, \zeta)\\ &+d(\eta, \psi^h) + c(\zeta, \psi^h) - c(p, \psi^h). \quad (23) \end{aligned}$$

We now estimate absolute value of each term at right-hand side of (23) separately. By using Cauchy-Schwartz and Young's inequalities we have:

$$\begin{aligned} \left|a(\eta, \phi^h)\right| &\leq \nu \left\|\nabla\eta\right\| \left\|\nabla\phi^h\right\|\\ &\leq \frac{\nu}{4}\left\|\nabla\phi^h\right\|^2 + C\nu^{-1}\left\|\nabla\eta\right\|^2, \end{aligned}$$

$$\begin{aligned} \left|-d(\phi^h, \zeta)\right| &\leq C\left\|\zeta\right\| \left\|\nabla\phi^h\right\|\\ &\leq \frac{\nu}{4}\left\|\nabla\phi^h\right\|^2 + C\nu^{-1}\left\|\zeta\right\|^2. \end{aligned}$$

Making use of Poincare-Friedrich's inequality and property (iv) of the bilinear form $c(.,.)$, we have

$$\begin{aligned} \left|-d(\eta, \psi^h)\right| &\leq Ch^{-1/2}\left\|\nabla\eta\right\|[\psi^h]\\ &\leq \frac{1}{6}[\psi^h]^2 + Ch^{-1}\left\|\nabla\eta\right\|^2. \end{aligned}$$

For stabilization terms, we use the properties along with the usual inequalities to get:

$$\left|c(\zeta,\psi^h)\right| \leq [\zeta][\psi^h] \leq \frac{1}{6}[\psi^h]^2 + C[\zeta]^2,$$

and

$$\left|c(p,\psi^h)\right| \leq [p][\psi^h] \leq \frac{1}{6}[\psi^h]^2 + C[p]^2.$$

Rearranging the error equation with obtained bounds will result:

$$\frac{\nu}{2}\left\|\nabla\phi^h\right\|^2 + \frac{1}{2}[\psi^h]^2 \leq C\left\{\nu^{-1}\left\|\nabla\eta\right\|^2 + \nu^{-1}\left\|\zeta\right\|^2 + h^{-1}\left\|\nabla\eta\right\|^2 + [\zeta]^2 + [p]^2\right\}.$$

Making a final use of triangle inequality gives the desired result now.

□

Lemma 3. *Let (λ,ξ) and $(\lambda^h(u),\xi^h)$ be solutions of (10) and (20), respectively. Then, we have*

$$\begin{aligned}\nu\|\nabla(\lambda(u)-\lambda^h(u))\|^2 + [\xi-\xi^h]^2 \leq \inf_{\tilde{\lambda}\in Y^h,\tilde{\xi}\in Q^h}\\ C\left\{\nu^{-1}\left\|\nabla(\lambda(u)-\tilde{\lambda})\right\|^2 + \nu^{-1}\left\|(\xi-\tilde{\xi})\right\|^2\right.\\ + h^{-1}\left\|\nabla(\lambda(u)-\tilde{\lambda})\right\|^2 + [\xi-\tilde{\xi}]^2\\ \left.+[\xi]^2 + \nu^{-1}\left\|\nabla(y(u)-y^h(u))\right\|^2\right\}.\end{aligned}$$

Proof. We omit the proof since it is very similar to the previous case. □

In order to get an estimate for the control variable, we need a relation between the discrete continuous and auxiliary solutions for both state and adjoint state equations.

Lemma 4. *If (y^h,p^h) and $(y^h(u),p^h)$ be solutions of (15) and (19), respectively. Then, there holds*

$$\nu\left\|\nabla(y^h-y^h(u))\right\|^2 \leq \frac{C}{\nu}\left\|u-u^h\right\|^2. \quad (24)$$

Similarly, if (λ^h,ξ^h) and $(\lambda^h(u),\xi^h)$ be solutions of (16) and (20), respectively. Then, there holds

$$\nu\left\|\nabla(\lambda^h-\lambda^h(u))\right\|^2 \leq \frac{C}{\nu}\left\|y^h-y^h(u)\right\|^2. \quad (25)$$

Proof. For the state part, we subtract (19) from (15). Since the pressure terms are independent of the control, the proof is trivial. □

Lemma 5. *The first derivative of the reduced cost function for the continuous and the discrete cases satisfy*

$$\|j'(u)(\delta) - j_h'(u)(\delta)\| \leq \left\|\lambda(u)-\lambda^h(u)\right\|\|\delta\| \quad \forall u,\delta\in U. \quad (26)$$

Proof. The result is obtained by using Eqns. (9) and (17) directly. □

The following lemma gives the error estimate for the control variable u [5].

Lemma 6. *Let (u,y) and (u^h,y^h) be solutions to (6) and (15), respectively. Then, we have*

$$\left\|u-u^h\right\| \leq \|u-\tilde{u}\| + \frac{1}{\alpha}\left\|\lambda(u)-\lambda^h(u)\right\|, \quad \tilde{u}\in U, \quad (27)$$

where $\lambda(u)$ and $\lambda^h(u)$ are solutions to (7) and (20), respectively.

Corollary 1. *The error in state variable y satisfies:*

$$\begin{aligned}\nu\|\nabla(y-y^h)\|^2 + [p-p^h]^2 \leq \inf_{\tilde{y}\in Y^h,\tilde{p}\in Q^h}\\ C\left\{\nu^{-1}\left\|\nabla(y(u)-\tilde{y})\right\|^2 + \nu^{-1}\left\|(p-\tilde{p})\right\|^2\right.\\ +h^{-1}\left\|\nabla(y(u)-\tilde{y})\right\|^2 + [p-\tilde{p}]^2 + [p]^2\\ \left.+\nu^{-1}\left\|u-u^h\right\|^2\right\}.\end{aligned} \quad (28)$$

Proof. The corollary is the combination of Lemma (2) and Lemma (4). □

Corollary 2. *The error in adjoint state variable λ satisfies:*

$$\begin{aligned}\nu\|\nabla(\lambda-\lambda^h)\|^2 + [\xi-\xi^h]^2 \leq \inf_{\tilde{\lambda},\tilde{y}\in Y^h,\tilde{\xi},\tilde{p}\in Q^h}\\ C\left\{\nu^{-1}\left\|\nabla(y(u)-\tilde{y})\right\|^2 + \nu^{-1}\left\|(p-\tilde{p})\right\|^2 + [p]^2\right.\\ +[p-\tilde{p}]^2 + h^{-1}\left\|\nabla(y(u)-\tilde{y})\right\|^2 + \nu^{-1}\left\|u-u^h\right\|^2\\ +\nu^{-1}\left\|\nabla(\lambda(u)-\tilde{\lambda})\right\|^2 + \nu^{-1}\left\|(\xi-\tilde{\xi})\right\|^2 +\\ \left.h^{-1}\left\|\nabla(\lambda(u)-\tilde{\lambda})\right\|^2 + [\xi-\tilde{\xi}]^2 + [\xi]^2\right\}.\end{aligned} \quad (29)$$

Proof. The proof is just a combination of the results of Lemma (3) and Lemma(4). □

We are now in a position to state approximation results. We give corollaries for each variable. We first assume that y,u,p,λ,ξ are sufficiently smooth, before stating the approximation results.

Corollary 3. *The control variable u satisfies*

$$\|u-u^h\| \cong \mathcal{O}(h^{1/2}).$$

Proof. Making use of approximation assumptions (12), (13) and property (v.) of the bilinear form $c(.,.)$ in Lemma 6, we get

$$\|u-u^h\| \leq C(u)h^2 + C(\nu^{-1},\alpha^{-1},y,\lambda,p,\xi)h^{1/2},$$

which completes the proof. □

Corollary 4. *The adjoint state variable λ satisfies*

$$\nu\|\nabla(\lambda-\lambda^h)\|^2+[\xi-\xi^h]^2\cong\mathcal{O}(h).$$

Proof. The proof is similar to the previous case, which is stated for u. □

Corollary 5. *The state variable y satisfies*

$$\nu\|\nabla(y-y^h)\|^2+[p-p^h]^2\cong\mathcal{O}(h).$$

Proof. The proof is similar to the previous cases, which are stated for u and λ. □

Remark 1. *By the property (v.) of the bilinear form $c(.,.)$, the norm $[.]$ is approximated as $h^{1/2}\|.\|_1$. Thus, the pressure error terms at left-hand side of all error relations does not give any convergence for pressure. Since pressure is not guaranteed to be unique, this situation is expected. However, the discrete pressure remains bounded in any case* [19].

5. Numerical Application

In this section, we perform a numerical experiment to verify the effectiveness of the proposed method. We use the finite element software package Freefem++ [16] to carry out all computations. In considered test case, we study in the domain $(0,1)^2$ with a mesh resolution of 32×32. We choose the parameters as $\nu=1$ and $\beta=0.1$. The stabilization parameter α is calculated as:

$$\alpha=\frac{|K|^2}{5(c_1^2+c_2^2+c_3^2)}.$$

Here K denotes any triangle in τ^h and $|K|^2$ is its area. c_1,c_2,c_3 stands for the lengths of sides of the triangle K.

Example As a numerical test, we consider the driven cavity problem. In this problem, the horizontal velocity on the upper boundary is 1 and the vertical component is 0. We consider a numerical experiment from [14]. We do not have any constraint on the control or the state variable. Let the desired state be

$$y_d=\begin{pmatrix}\sin(\pi x)^2\sin(\pi y)\cos(\pi y)\\ -\sin(\pi y)^2\sin(\pi x)\cos(\pi x)\end{pmatrix}.$$

In Figure 1, we compare the pressure terms of the state equation for both stabilized and unstabilized solutions. We observe that unstabilized pressure diverges. Similarly, for the adjoint state, unstabilized pressure blows up in Figure 2. Finally, we compare the first component of the stabilized and unstabilized solutions. One can easily see the efficiency of the stabilization through comparison of these figures.

6. Conclusion and Outlook

In this work, we have studied Brezzi-Pitkaranta stabilization scheme for the optimal control problems governed by Stokes equations. We have obtained the stability results for both the state and adjoint state variables. We derived a priori error bounds for each variable and proved that the error is of order 1/2. In the numerical example, we have shown the efficiency of the stabilization in both solutions of the state and adjoint state. As future works, we will consider the optimal control of time dependent and nonlinear flow problems.

References

[1] Abergel, F., Temam, R., On some optimal control problems in fluid mechanics, Theoret. Comput. Fluid Mech., 1 (6), 303-325, 1990.

[2] Arnold, D., Brezzi, F., Fortin, M., A stable finite element for the Stokes equations, Calcolo 21, 337-344, 1984.

[3] Adams, R.A., Sobolev Spaces, Academic Press, New York, 1975.

[4] Baiocchi, C., Brezzi, F. and Franca, L., Virtual bubbles and Galerkin-least-squares type methods (Ga. L. S.), Comput. Methods Appl. Mech. Engrg., 105, 125-141, 1993.

[5] Becker, R. and Hansbo, P., A simple pressure stabilization method for the Stokes equation, Commun. Numer. Meth. Engng, 24, 2008.

[6] Barrenechea, G.R. and Blasco, J., Pressure stabilization of finite element approximations of time-dependent incompressible flow problems, Computer Methods in Applied Mechanics and Engineering, 197:1-4, 219-231, 2007.

[7] Bochev, P. and Gunzburger, M., Least-squares finite-element methods for optimization and control for the Stokes equations, Comput. Math. Appl., 48, 1035-1057, 2004.

[8] Brezzi, F. and Pitkaranta, J., On the stabilization of finite element approximations of the Stokes problem, in Efficient Solution of Elliptic Systems, W. Hackbush, ed., vol. 10 of Notes on Numerical Fluid Mechanics, Vieweg, 11-19, 1984.

[9] Brooks, A. and Hughes, T., Streamline upwind/Petrov-Galerkin formulations for convection dominated flows with particular emphasis on the incompressible Navier-Stokes equations, Computer Methods in Applied Mechanics and Engineering, 32, 199-259, 1982.

[10] Casas, E., Optimality conditions for some control problems of turbulent flows, in: Flow Control, Minneapolis, MN, 1992, in: IMA Vol. Math. Appl., vol. 68, Springer, New York, 127-147, 1995.

[11] Codina, R. and Blasco, J., Analysis of a pressure-stabilized finite element approximation of the stationary Navier-Stokes equations, Numer. Math., 87, 59-81, 2000.

Figure 1. Comparison of pressure solution of the state equation: stabilized(left) and unstabilized(right)

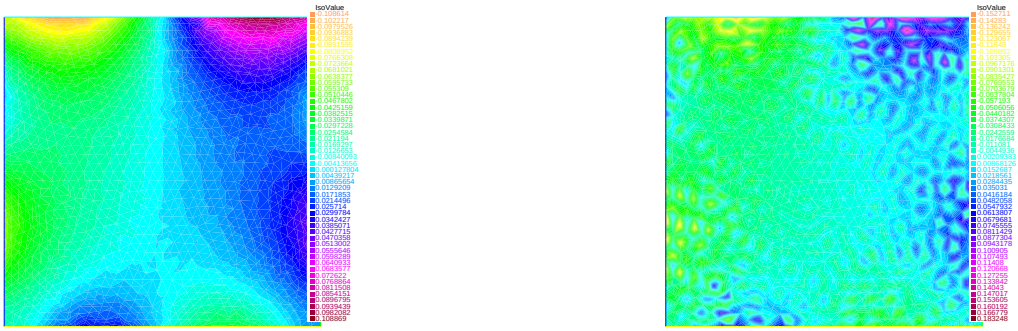

Figure 2. Comparison of pressure of the adjoint the state equation: stabilized(left) and unstabilized(right)

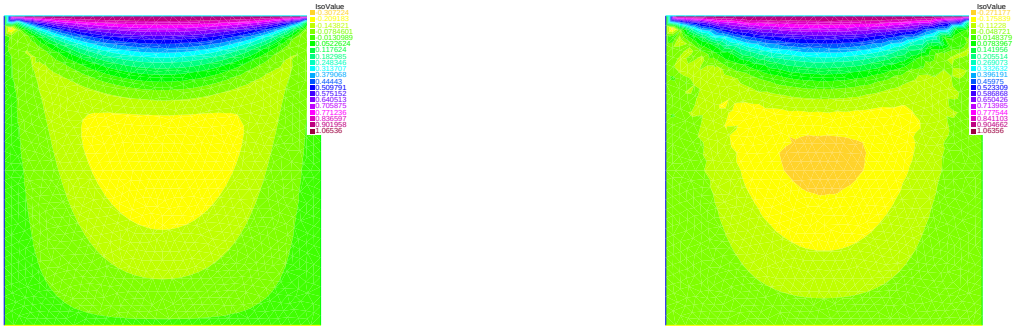

Figure 3. Comparison of first component of the solutions of the state variable: stabilized(left) and unstabilized(right)

[12] Douglas, J. and Wang, J., An absolutely stabilized finite element method for the Stokes problem, Math. Comp., 52,495-508, 1989.

[13] Franca, L. and Hughes, T., Convergence analyses of Galerkin-Least-Squares methods for symmetric advective-diffusive forms of the Stokes and incompressible Navier-Stokes equations, Comput. Methods. Appl. Mech. Engrg., 105 ,285-298.,1993.

[14] De los Reyes, J.C., Meyer, C. and Vexler, B., Finite element error analysis for state-constrained optimal control of the Stokes equations, WIAS Preprint No. 1292, 2008.

[15] Gunzburger, M., Finite Element Methods for Viscous Incompressible Flows: A Guide to Theory, Practice and Algorithms, Academic Press, Boston, 1989.

[16] Hecht, N., New development in FreeFem++, J. Numer. Math. 20, no. 3-4, 251-265, 2012.

[17] Heinkenschloss, M. and Leykekhman, D., Local Error Estimates for SUPG Solutions of Advection-Dominated Elliptic Linear-Quadratic Optimal Control Problems, Rice University, Houston, CAAM Technical Report TR08-30, 2008.

[18] Hinze, M., Yan, N. and Zhou, Z., Variational discretization for optimal control governed by convection dominated diffusion equations, J. Comput. Math., 27, 237-253, 2009.

[19] Latche, J.-C. and Vola, D., Analysis of the Brezzi-Pitkaranta Stabilized Galerkin Scheme for Creeping Flows of Bingham Fluids, Siam J. Numer. Anal., 42:3, 1208-1225, 2004.

[20] Layton, W.J., A connection between subgrid scale eddy viscosity and mixed methods, Appl. Math. Comput., 133, 147-157, 2002.
[21] Lions, J.L., Optimal control of systems governed by partial differential equations, Springer Verlag, New York, 1971.
[22] Rees, T. and Wathen, A.J., Preconditioning Iterative Methods for the Optimal Control of the Stokes Equations, SIAM J. Sci. Comput., 33(5), 2903-2926, 2011.
[23] Rösch, A. and Vexler, B., Optimal Control of the Stokes Equations: A Priori Error Analysis for Finite Element Discretization with Postprocessing, SIAM J. Numer. Anal., 44, 1903-1920, 2006.
[24] Stoll, M. and Wathen, A., All-at-once solution of time-dependent Stokes control, Journal of Computational Physics, 231(1), 498-515, 2013.
[25] Sun, T., Discontinuous Galerkin finite element method with interior penalties for convection diffusion optimal control problem. Int. J. Numer. Anal. Model. 7, 87-107, 2010.
[26] Tröltzsch, F., Optimal Control of Partial Differential Equations: Theory, Methods and Applications, Amer Mathematical Society, 2010.
[27] Zhou, Z. and Yan, N., The local discontinuous Galerkin method for optimal control problem governed by convection-diffusion equations, International Journal of Numerical Analysis & Modeling 7, 681-699, 2010.

Aytekin Cıbık *was born in Şanlıurfa. He received his Ph.D. degree from the department of mathematics, Middle East Technical University (METU) in 2011. He works as an assistant professor at the department of mathematics, Gazi University. His research interests are numerical analysis and computational fluid dynamics.*

Fikriye Yılmaz *was born in Ankara. She received his B.D and Ph.D. degrees from the department of mathematics, Middle East Technical University (METU) in 2004 and 2011, respectively. She works as an assistant professor at the department of mathematics, Gazi University. Her research interests are numerical analysis and optimal control problems.*

An International Journal of Optimization and Control: Theories & Applications
ISSN:2146-0957 eISSN:2146-5703
Vol.7, No.1, pp.83-89 (2017)
http://doi.org/10.11121/ijocta.01.2017.00338

RESEARCH ARTICLE

Canal surfaces in 4-dimensional Euclidean space

Betül Bulca[a], Kadri Arslan[a], Bengü Bayram[b] and Günay Öztürk[c*],

[a] *Department of Mathematics, Uludağ University, 16059 Bursa, Turkey*
[b] *Department of Mathematics, Balikesir University, 10145 Balikesir, Turkey*
[c] *Department of Mathematics, Kocaeli University, 41380 Kocaeli, Turkey*
bbulca@uludag.edu.tr,arslan@uludag.edu.tr, benguk@balikesir.edu.tr, ogunay@kocaeli.edu.tr

ARTICLE INFO

Article History:
Received 26 April 2016
Accepted 22 November 2016
Available 13 December 2016

Keywords:
Canal surface
Curvature ellipse
Superconformal surface

AMS Classification 2010:
53C40, 53C42

ABSTRACT

In this paper, we study canal surfaces imbedded in 4-dimensional Euclidean space $\mathbb{E}^4$. We investigate these surface curvature properties with respect to the variation of the normal vectors and ellipse of curvature. Some special canal surface examples are constructed in $\mathbb{E}^4$. Furthermore, we obtain necessary and sufficient condition for canal surfaces to become superconformal in $\mathbb{E}^4$. At the end, we present the graphs of projections of canal surfaces in $\mathbb{E}^3$.

Given a space curve $\gamma(u)$ called spine curve, a canal surface associated to this curve is defined as a surface swept by a family of spheres of varying radius $r(u)$. If $r(u)$ is constant, the canal surface is called a tube or a pipe surface. Apart from being used in pure mathematics, canal surfaces are widely used in many areas especially in CAGD, e.g. construction of blending surfaces, i.e. canal surface with a rational radius, shape reconstruction or robotic path planning (see, [5], [11], [12]). Greater part of the studies on canal surfaces within the CAGD context is related to the search of canal surfaces with rational spine curve and rational radius function. Canal surfaces are also useful in visualising long thin objects such as poles, 3D fonts, brass instruments or internal organs of the body in solid/surface modeling and CG/CAD. A national question is when the canal surface is developable. It is well known that, at regular points, the Gaussian curvature of a developable surface is identically zero. In [14] it has been proved that developable canal surface is either a cylinder or a cone.

This study consists of 5 sections: In section 2, we explain some well-known properties of the surfaces in $\mathbb{E}^4$. In section 3, we give the canal surfaces in $\mathbb{E}^4$ and some examples are presented. Section 4 investigates the ellipse of curvature of canal surfaces in $\mathbb{E}^4$. Additionally we prove necessary and sufficient condition of canal surfaces to become superconformal in $\mathbb{E}^4$. In Section 5, the visualization of canal surfaces are given with using Maple programme.

1. Basic concepts

Let M be a regular surface in $\mathbb{E}^4$ given with the parametrization $X(u,v) : (u,v) \in D \subset \mathbb{E}^2$. The tangent space of M at an arbitrary point $p = X(u,v)$ is spanned by the vectors X_u and X_v. The first fundamental form coefficients of M are computed by

$$E = \langle X_u, X_u \rangle, F = \langle X_u, X_v \rangle, G = \langle X_v, X_v \rangle, \quad (1)$$

where $\langle , \rangle$ is the scalar product of the Euclidean space. We consider the surface patch $X(u,v)$ is regular, which implies that $W^2 = EG - F^2 \neq 0$. For the point $p \in M$, we can take the decomposition $T_p\mathbb{E}^4 = T_pM \oplus T_p^{\perp}M$, where $T_p^{\perp}M$ is the

*Corresponding Author

orthogonal component of T_pM in $\mathbb{E}^4$ with the Riemannian connection $\widetilde{\nabla}$.

The induced Riemannian connection ∇ on M for any given local vector fields X_1, X_2 tangent to M, is given by

$$\nabla_{X_1} X_2 = (\widetilde{\nabla}_{X_1} X_2)^T, \tag{2}$$

where T expresses the tangential part.

Let us consider the spaces of the smooth vector fields $\chi(M)$ and $\chi^{\perp}(M)$ which are tangent and normal to M, respectively. The second fundamental map is defined as follows:

$$\begin{aligned} h &: \chi(M)\times\chi(M)\to\chi^{\perp}(M) \\ h(X_i,X_j) &= \widetilde{\nabla}_{X_i}X_j - \nabla_{X_i}X_j \quad 1\le i,j\le 2. \end{aligned} \tag{3}$$

This map is well-defined, symmetric and bilinear.

If we take the orthonormal frame field $\{N_1, N_2\}$ of M, then the shape operator which is self-adjoint and bilinear can be given by

$$\begin{aligned} A &: \chi^{\perp}(M)\times\chi(M)\to\chi(M) \\ A_{N_i}X_i &= -(\widetilde{\nabla}_{X_i}N_i)^T, \quad X_i\in\chi(M) \end{aligned} \tag{4}$$

which satisfies the equation:

$$\langle A_{N_k}X_j, X_i\rangle = \langle h(X_i,X_j), N_k\rangle = c_{ij}^k,\ 1\le i,j,k\le 2 \tag{5}$$

for any X_1, $X_2\in T_pM$.

The equality (3) is known as the Gaussian equation, where

$$\nabla_{X_i}X_j = \sum_{k=1}^{2}\Gamma_{ij}^k X_k\ ,\quad 1\le i,j\le 2 \tag{6}$$

and

$$h(X_i,X_j) = \sum_{k=1}^{2} c_{ij}^k N_k \qquad 1\le i,j\le 2. \tag{7}$$

Here Γ_{ij}^k are Christoffel symbols and c_{ij}^k are the coefficients of the second fundamental form.

The Gaussian curvature are given by

$$K = \frac{\langle h(X_1,X_1), h(X_2,X_2)\rangle - \|h(X_1,X_2)\|^2}{g} \tag{8}$$

and the mean curvature are given by

$$\|H\| = \frac{1}{4g^2}\langle h(X_1,X_1)+h(X_2,X_2), h(X_1,X_1)+h(X_2,X_2)\rangle \tag{9}$$

where

$$g = \|X_1\|^2\|X_2\|^2 - \langle X_1,X_2\rangle^2 .$$

If the mean curvature of M vanishes identically in $\mathbb{E}^n$, then M is said to be minimal [3]. See also [1].

2. Canal surfaces in $\mathbb{E}^4$

Let $\gamma(u) = (f_1(u), f_2(u), f_3(u), 0)$ be a curve given with arclength parameter. Then the Frenet formulae have the following form:

$$\begin{aligned} \gamma'(u) &= e_1(u), \\ {e_1}'(u) &= \kappa(u)e_2(u), \\ {e_2}'(u) &= -\kappa(u)e_1(u) + \tau(u)e_3(u), \\ {e_3}'(u) &= -\tau(u)e_2(u), \\ {e_4}'(u) &= 0, \end{aligned} \tag{10}$$

where $\{e_1(u), e_2(u), e_3(u), e_4(u)\}$ is the Frenet orthonormal basis of γ. The canal surface in $\mathbb{E}^4$ has the following parametrization (see [6]):

$$M: X(u,v) = \gamma(u) + r(u)\left(e_3(u)\cos v + e_4(u)\sin v\right). \tag{11}$$

Example 1. *Consider the helix* $\gamma(u) = (a\cos\frac{u}{c}, a\sin\frac{u}{c}, \frac{bu}{c})$ *in* $\mathbb{E}^3$. *Then the canal surface of* γ *in* $\mathbb{E}^4$ *has the following parametrization*

$$\begin{aligned} X(u,v) &= (a\cos\frac{u}{c} + \frac{b}{c}r(u)\sin\frac{u}{c}\cos v, \\ &\quad a\sin\frac{u}{c} - \frac{b}{c}r(u)\cos\frac{u}{c}\cos v, \\ &\quad \frac{bu}{c} + \frac{a}{c}r(u)\cos v, r(u)\sin v). \end{aligned} \tag{12}$$

Example 2. *Consider the generalized helix* $\gamma(u) = (\frac{(1+u)^{\frac{3}{2}}}{3}, \frac{(1-u)^{\frac{3}{2}}}{3}, \frac{u}{\sqrt{2}})$ *in* $\mathbb{E}^3$. *Then the canal surface of* γ *in* $\mathbb{E}^4$ *has the following parametrization*

$$\begin{aligned} X(u,v) &= (\frac{(1+u)^{\frac{3}{2}}}{3} - r(u)\frac{(1+u)^{\frac{1}{2}}}{2}\cos v, \\ &\quad \frac{(1-u)^{\frac{3}{2}}}{3} + r(u)\frac{(1-u)^{\frac{1}{2}}}{2}\cos v, \\ &\quad \frac{u}{\sqrt{2}} + \frac{1}{\sqrt{2}}r(u)\cos v, r(u)\sin v). \end{aligned} \tag{13}$$

The space which is tangent to M is spanned by

$$\begin{aligned} X_u &= e_1(u) - r\tau\cos v e_2 \\ &\quad + r'\cos v e_3 + r'\sin v e_4, \\ X_v &= -r\sin v e_3 + r\cos v e_4. \end{aligned} \tag{14}$$

The first fundamental form coefficients become

$$\begin{aligned} E &= 1 + (r')^2 + r^2\tau^2\cos^2 v, \\ F &= 0, \\ G &= r^2. \end{aligned} \tag{15}$$

The Christoffel symbols Γ_{ij}^k are given by

$$\begin{aligned} \Gamma_{11}^1 &= \frac{1}{2E}\partial_u(E) = \frac{1}{E}\langle X_{uu}, X_u\rangle, \\ \Gamma_{11}^2 &= -\frac{1}{2G}\partial_v(E) = -\frac{1}{G}\langle X_{vu}, X_u\rangle, \\ \Gamma_{12}^1 &= \frac{1}{2E}\partial_v(E) = \frac{1}{E}\langle X_{vu}, X_u\rangle, \\ \Gamma_{12}^2 &= \frac{1}{2G}\partial_u(G) = \frac{1}{G}\langle X_{vu}, X_v\rangle, \\ \Gamma_{22}^1 &= -\frac{1}{2E}\partial_u(G) = -\frac{1}{E}\langle X_{vu}, X_v\rangle, \\ \Gamma_{22}^2 &= \frac{1}{2G}\partial_v(G) = \frac{1}{G}\langle X_{vv}, X_v\rangle = 0. \end{aligned} \tag{16}$$

and they are symmetric according to the covariant indices ([7], p.398).

If we take the second partial derivatives of $X(u,v)$, we find:

$$\begin{aligned} X_{uu} &= \kappa r\tau\cos v e_1 + (\kappa - (r\tau)'\cos v - r'\tau\cos v)e_2 \\ &\quad + \cos v(r'' - r\tau^2)e_3 + r''\sin v e_4, \\ X_{uv} &= r\tau\sin v e_2 - r'\sin v e_3 + r'\cos v e_4, \\ X_{vv} &= -r\cos v e_3 - r\sin v e_4, \end{aligned} \tag{17}$$

Hence, by using (3), we find the Gaussian equations;

$$\begin{aligned} \widetilde{\nabla}_{X_u}X_u &= X_{uu} = \nabla_{X_u}X_u + h(X_u, X_u), \\ \widetilde{\nabla}_{X_u}X_v &= X_{uv} = \nabla_{X_u}X_v + h(X_u, X_v), \\ \widetilde{\nabla}_{X_v}X_v &= X_{vv} = \nabla_{X_v}X_v + h(X_v, X_v), \end{aligned} \tag{18}$$

where

$$\begin{aligned} \nabla_{X_u}X_u &= \Gamma_{11}^1 X_u + \Gamma_{11}^2 X_v, \\ \nabla_{X_u}X_v &= \Gamma_{12}^1 X_u + \Gamma_{12}^2 X_v, \\ \nabla_{X_v}X_v &= \Gamma_{22}^1 X_u + \Gamma_{22}^2 X_v. \end{aligned} \tag{19}$$

Substituting (16) and (18) in (19), we obtain

$$\begin{aligned} h(X_u, X_u) &= X_{uu} - \frac{1}{E}\langle X_{uu}, X_u\rangle X_u \\ &\quad + \frac{1}{G}\langle X_{uv}, X_u\rangle X_v, \\ h(X_u, X_v) &= X_{uv} - \frac{1}{E}\langle X_{uv}, X_u\rangle X_u \\ &\quad - \frac{1}{G}\langle X_{uv}, X_v\rangle X_v, \\ h(X_v, X_v) &= X_{vv} + \frac{1}{E}\langle X_{uv}, X_v\rangle X_u. \end{aligned} \tag{20}$$

Further using (20)

$$\begin{aligned} \langle h(X_u, X_u), h(X_v, X_v)\rangle &= \langle X_{uu}, X_{vv}\rangle \\ &\quad - \frac{1}{E}\langle X_{uu}, X_u\rangle\langle X_{vv}, X_u\rangle, \\ \langle h(X_u, X_v), h(X_u, X_v)\rangle &= \langle X_{uv}, X_{uv}\rangle \\ &\quad - \frac{1}{E}\langle X_{uv}, X_u\rangle^2 \\ &\quad - \frac{1}{G}\langle X_{vu}, X_v\rangle^2, \\ \langle h(X_u, X_v), h(X_v, X_v)\rangle &= \langle X_{uv}, X_{vv}\rangle \\ &\quad - \frac{1}{E}\langle X_{uv}, X_u\rangle\langle X_{vv}, X_u\rangle, \\ \langle h(X_u, X_u), h(X_u, X_u)\rangle &= \langle X_{uu}, X_{uu}\rangle \\ &\quad - \frac{1}{E}\langle X_{uu}, X_u\rangle^2 \\ &\quad + \frac{\langle X_{uv}, X_u\rangle}{G}(2\langle X_{uu}, X_v\rangle \\ &\quad + \langle X_{uv}, X_u\rangle), \\ \langle h(X_v, X_v), h(X_v, X_v)\rangle &= \langle X_{vv}, X_{vv}\rangle \\ &\quad + \frac{1}{E}\langle X_{uv}, X_v\rangle(1 + 2\langle X_{vv}, X_u\rangle), \\ \langle h(X_u, X_u), h(X_u, X_v)\rangle &= \langle X_{uu}, X_{uv}\rangle - \frac{1}{E}\langle X_{uv}, X_u\rangle \\ &\quad - \frac{1}{G}\langle X_{uu}, X_v\rangle\langle X_{uv}, X_v\rangle \end{aligned} \tag{21}$$

Thus, using (14) with (17) we get

$$\begin{aligned} \langle X_{uu}, X_{vv}\rangle &= r^2\tau^2\cos^2 v - rr'', \\ \langle X_{uv}, X_{uv}\rangle &= r^2\tau^2\sin^2 v + (r')^2, \\ \langle X_{uu}, X_{uu}\rangle &= (\kappa r\tau\cos v)^2 \\ &\quad + (\kappa - (r\tau)'\cos v - r'\tau\cos v)^2 + \\ &\quad + \cos^2 v(r'' - r\tau^2)^2 + (r'')^2\sin^2 v, \\ \langle X_{vv}, X_{vv}\rangle &= r^2, \\ \langle X_{uu}, X_u\rangle &= r\tau(r\tau)'\cos^2 v + r'r'', \\ \langle X_{uu}, X_v\rangle &= r^2\tau^2\cos v\sin v, \\ \langle X_{vv}, X_u\rangle &= -rr', \\ \langle X_{uv}, X_u\rangle &= -r^2\tau^2\cos v\sin v, \\ \langle X_{uv}, X_v\rangle &= rr', \\ \langle X_{uv}, X_{vv}\rangle &= 0 \\ \langle X_{uu}, X_{uv}\rangle &= r\tau\sin v(\kappa - (r\tau)'\cos v) \end{aligned} \tag{22}$$

Proposition 1. *The Gaussian curvature of the canal surface M with the parametrization (11) in $\mathbb{E}^4$ is given by*

$$\begin{aligned} K &= \frac{1}{g}(\langle X_{uu}, X_{vv}\rangle - \frac{1}{E}\langle X_{uu}, X_u\rangle\langle X_{vv}, X_u\rangle \\ &\quad - \langle X_{uv}, X_{uv}\rangle + \frac{1}{E}\langle X_{uv}, X_u\rangle^2 + \frac{1}{G}\langle X_{uv}, X_v\rangle^2) \end{aligned} \tag{23}$$

where $g = EG - F^2$.

Proof. By using the equation (8), we find

$$K = \frac{1}{g}\left(\langle h(X_u, X_u), h(X_v, X_v)\rangle - \langle h(X_u, X_v), h(X_u, X_v)\rangle\right), \tag{24}$$

which is the Gaussian curvature of the canal surface M. Taking into account (21) and (24) we obtain (23). □

From the equations (22) with (23) we obtain;

Corollary 1. *The Gaussian curvature of the canal surface M with the parametrization (11) in $\mathbb{E}^4$ is given by*

$$\begin{aligned} K &= \frac{r}{gE}\{r\cos^2 v(2\tau^2+2(r')^2\tau^2-rr''\tau^2+r'\tau(r\tau)') \\ &\quad +r^3\tau^4\cos^4 v - r'' - r\tau^2(1+(r')^2)\}, \end{aligned} \tag{25}$$

where

$$\begin{aligned} E &= 1+(r')^2+r^2\tau^2\cos^2 v, \\ g &= r^2(1+(r')^2+r^2\tau^2\cos^2 v). \end{aligned}$$

Proposition 2. *The mean curvature of the canal surface M with the parametrization (11) in $\mathbb{E}^4$ is given by*

$$\begin{aligned} 4\|H\|^2 &= \frac{\langle X_{uu},X_{uu}\rangle}{E^2}+2\frac{\langle X_{uu},X_{vv}\rangle}{EG}+\frac{\langle X_{vv},X_{vv}\rangle}{G^2} \\ &\quad +\frac{\langle X_{uv},X_v\rangle}{EG^2}(2\langle X_{vv},X_u\rangle+\langle X_{uv},X_v\rangle) \\ &\quad +\frac{\langle X_{uv},X_u\rangle}{E^2G}(2\langle X_{uu},X_v\rangle+\langle X_{uv},X_u\rangle) \\ &\quad -\frac{2}{E^2G}\langle X_{uu},X_u\rangle\langle X_{vv},X_u\rangle-\frac{\langle X_{uu},X_u\rangle^2}{E^3}. \end{aligned} \tag{26}$$

Proof. By considering (9) the mean curvature of the canal surface M becomes

$$\|H\| = \frac{1}{4g^2}\left(\langle h(X_u,X_u)+h(X_v,X_v), h(X_u,X_u)+h(X_v,X_v)\rangle\right), \tag{27}$$

Taking into account (21) and (27) we get the result. □

By the use of (22) and Proposition 2, we have the following results:

Corollary 2. *The mean curvature of the canal surface M with the parametrization (11) in $\mathbb{E}^4$ is given by*

$$\begin{aligned} \|H\|^2 &= \frac{1}{4E^2r^2}[-\frac{r^2}{E}(r\tau(r\tau)'\cos^2 v+r'r'')^2 \\ &\quad +r^2\cos^2 v((\tau kr)^2+ \\ &\quad ((r\tau)'+r'\tau)^2-r^2\tau^4+4\tau^2+ \\ &\quad +3(r')^2\tau^2-2r\tau^2r''+2r'\tau(r\tau)') \\ &\quad +4r^4\tau^4\cos^4 v-2kr^2\cos v((r\tau)'+r'\tau)+ \\ &\quad +k^2r^2-2rr''+1+(r')^2]. \end{aligned}$$

Corollary 3. *If the base curve γ of the canal surface M is a straight line, then the Gaussian and mean curvatures of M are*

$$K = \frac{-r''}{r(1+(r')^2)^2},$$

and

$$\begin{aligned} \|H\|^2 &= \frac{-1}{4r^2(1+(r')^2)^3}\left\{(rr'r'')^2\right. \\ &\quad \left.+(2rr''-1)(1+(r')^2)\right\}, \end{aligned}$$

respectively.

3. Ellipse of curvature of the canal surfaces in $\mathbb{E}^4$

Let M be a regular surface given with the parametrization $X(u,v):(u,v)\in\mathbb{D}\subseteq\mathbb{E}^2$. Consider a circle given with the angle $\theta\in[0,2\pi]$ in the tangent space T_pM. The intersection of the direct sum of the tangent direction of $X=\cos\theta X_1+\sin\theta X_2$ and the normal space $T_p^{\perp}M$ with the surface M forms a curve. Such a curve is called as a normal section curve in the direction θ. Denote this curve by γ_θ. Normal curvature vector η_θ of γ_θ lies in $T_p^{\perp}M$. When θ changes from 0 to 2π, the normal curvature vector constitutes an ellipse called as a ellipse of curvature of M at p in $T_p^{\perp}M$. Thus, the curvature ellipse of M at point p is given as follows with the second fundamental form h:

$$E(p)=\{h(X,X)\mid X\in T_pM,\ \|X\|=1\}.$$

To see that this shows an ellipse, it is enough to have a look at the formulas

$$X=\cos\theta X_1+\sin\theta X_2$$

and

$$h(X,X)=\overrightarrow{H}+\cos 2\theta\overrightarrow{B}+\sin 2\theta\overrightarrow{C}. \tag{28}$$

Here,

$$\overrightarrow{B}=\frac{1}{2}(h(X_1,X_1)-h(X_2,X_2)),\overrightarrow{C}=h(X_1,X_2), \tag{29}$$

are normal vectors and $\overrightarrow{H}=\frac{1}{2}(h(X_1,X_1)+h(X_2,X_2))$ is the mean curvature vector. This implies that, the vector $h(X,X)$ goes twice around the ellipse of curvature centered at $\overrightarrow{H}$, while X goes once around the unit tangent circle [9].

From the equation (28), one can get that $E(p)$ is a circle if and only if for some orthonormal basis of $T_p(M)$ it holds that

$$\langle h(X_1,X_2),h(X_1,X_1)-h(X_2,X_2)\rangle=0, \tag{30}$$

and

$$\|h(X_1,X_1)-h(X_2,X_2)\|=2\|h(X_1,X_2)\|. \tag{31}$$

General aspects of the ellipse of curvature for surfaces in $\mathbb{E}^4$ studied by Wong [13]. (See also [2], [8], [9] and [10])

Definition 1. *The surface M with the parametrization $X(u,v)$ in $\mathbb{E}^4$ is superconformal if and only if its ellipse of curvature is a circle, i.e. $\left\langle\overrightarrow{B},\overrightarrow{C}\right\rangle=0$ and $\left\|\overrightarrow{B}\right\|=\left\|\overrightarrow{C}\right\|$ holds* [4]. *If the equality $\left\langle\overrightarrow{B},\overrightarrow{C}\right\rangle=0$, the surface M is called weak superconformal.*

Theorem 1. *The canal surface M with the parametrization (11) in $\mathbb{E}^4$ is superconformal if and only if the equalities*

$$\langle\frac{1}{E}h(X_u,X_u)-\frac{1}{G}h(X_v,X_v),\frac{1}{\sqrt{EG}}h(X_u,X_v)\rangle=0 \tag{32}$$

and

$$2\left\|\frac{1}{\sqrt{EG}}h(X_u,X_v)\right\| = \left\|\frac{1}{E}h(X_u,X_u)-\frac{1}{G}h(X_v,X_v)\right\| \tag{33}$$

hold.

Proof. If we use the orthonormal frame

$$X_1=\frac{X_u}{\|X_u\|}=\frac{X_u}{\sqrt{E}}, X_2=\frac{X_v}{\|X_v\|}=\frac{X_v}{\sqrt{G}}, \tag{34}$$

we get

$$\begin{aligned} h(X_1,X_1) &= \frac{1}{E}h(X_u,X_u), \\ h(X_1,X_2) &= \frac{1}{\sqrt{EG}}h(X_u,X_v), \\ h(X_2,X_2) &= \frac{1}{G}h(X_v,X_v)\ . \end{aligned} \tag{35}$$

Therefore, from (29) the normal vectors $\overrightarrow{B}$ and $\overrightarrow{C}$ become

$$\overrightarrow{B}=\frac{1}{2}(\frac{1}{E}h(X_u,X_u)-\frac{1}{G}h(X_v,X_v)) \tag{36}$$

and

$$\overrightarrow{C}=\frac{1}{\sqrt{EG}}h(X_u,X_v). \tag{37}$$

Suppose M is superconformal then by Definition 1 $\langle\overrightarrow{B},\overrightarrow{C}\rangle=0$ and $\left\|\overrightarrow{B}\right\|=\left\|\overrightarrow{C}\right\|$ hold. Thus by the use of the equalities (36) and (37) we get the result.

Conversely, if the equations (32) and (33) hold then by the use of the equalities (36) and (37) we obtain $\langle\overrightarrow{B},\overrightarrow{C}\rangle=0$ and $\left\|\overrightarrow{B}\right\|=\left\|\overrightarrow{C}\right\|$, which shows that M is superconformal. □

Substituting (21) and (22) into (32) we obtain the following results.

Corollary 4. *Let M be a canal surface in $\mathbb{E}^4$ given with the parametrization (11). Then M is weak superconformal if and only if the equality*

$$\begin{aligned} 0 &= r^3\tau\sin v((k-(r\tau)'\cos v)(1+(r')^2) \\ &\quad +r\tau\cos v(r'r''+kr\tau\cos v)) \end{aligned}$$

holds.

Corollary 5. *Every canal surface whose spine curve is a straight line of the form $\gamma(u)=(a_1u+b_1,a_2u+b_2,a_3u+b_3,0)$ is weak superconformal, where a_1, a_2, a_3, b_1, b_2, b_3 are real constants.*

4. Visualization

The 3D-surfaces geometric modeling are very important in the surface modeling systems such as; CAD/CAM systems and NC-processing. We give the visualization of the surfaces with the parametrization

$$X(u,v)=(x(u,v),y(u,v),z(u,v),w(u,v))$$

in $\mathbb{E}^4$ by use of Maple Software Program. We plot the graph of the surface with plotting command

$$plot3d([x,y,z+w],u=a..b,v=c..d). \tag{38}$$

We construct the geometric model of the canal surfaces defined in Example 1 for the following values (see, Figure 1);

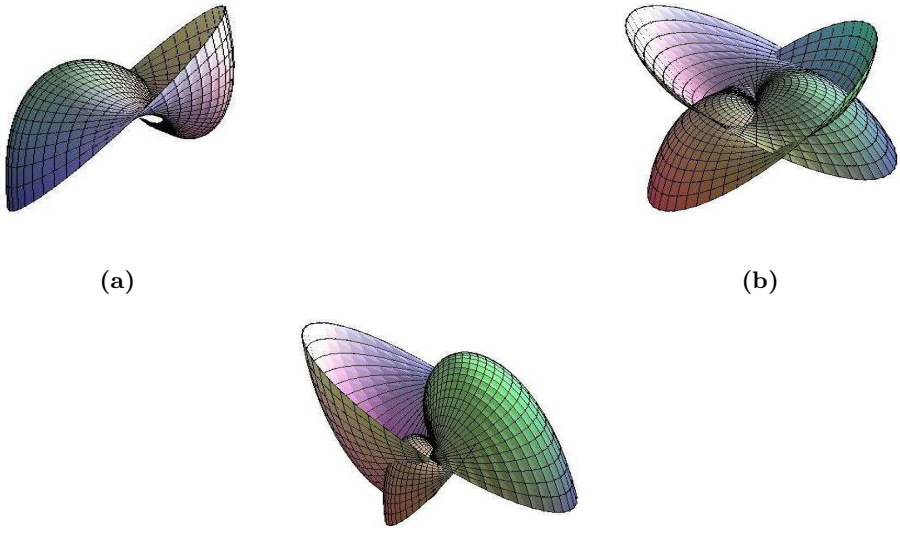

(a) **(b)**

(c)

Figure 1. The projections of canal surfaces of helix in $\mathbb{E}^3$

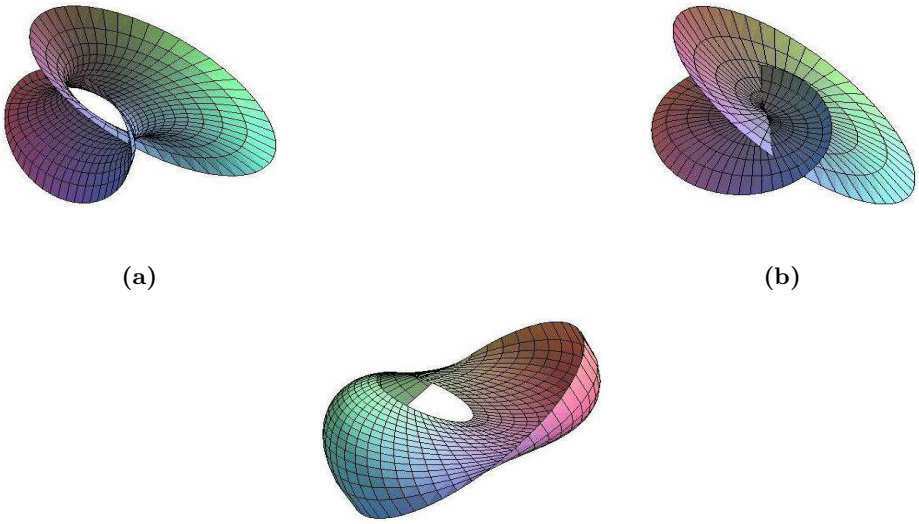

(a) **(b)**

(c)

Figure 2. The projections of canal surfaces of general helix in $\mathbb{E}^3$

(a) **(b)**

Figure 3. The projections of canal surfaces of straight line in $\mathbb{E}^3$

$$\begin{aligned} a)\ r(u) &= e^{u/3}, \\ b)\ r(u) &= u^2, \\ c)\ r(u) &= 3u+5. \end{aligned}$$

Further, we construct the geometric model of the canal surfaces defined in Example 2 for the following values (see, Figure 2);

$$\begin{aligned} a)\ r(u) &= e^{u^2}, \\ b)\ r(u) &= 5u^2, \\ c)\ r(u) &= 3u+5. \end{aligned}$$

Additionally, we construct the geometric model of the canal surfaces defined in Corollary 3 for the following values (see, Figure 3);

$$\begin{aligned} a)\ r(u) &= e^{u}, \\ b)\ r(u) &= \sinh u. \end{aligned}$$

5. Conclusion

In this manuscript, we considered canal surfaces in the 4-dimensional Euclidean space $\mathbb{E}^4$. Most of the literature on canal surfaces within the CAGD context has been motivated by the observation that canal surfaces with rational spine curve. We have proved this property mathematically and also illustrated with some nice examples.

References

[1] Arslan, K., Bayram, K. B., Bulca, B. and Öztürk, G., Generalized rotation surfaces in $\mathbb{E}^4$. Results in Mathematics, 61, 315-327 (2012).

[2] Bayram, K. B., Bulca, B., Arslan, K. and Öztürk, G., Superconformal ruled surfaces in $\mathbb{E}^4$. Mathematical Communications, 14(2), 235-244 (2009).

[3] Chen, B. Y., Geometry of submanifolds. Dekker, New York, (1973).

[4] Dajczer, M. and Tojeiro, R., All superconformal surfaces in $\mathbb{R}^4$ in terms of minimal surfaces. Mathematische Zeitschrift, 261, 869-890 (2009).

[5] Farouki, R.T. and Sverrissor, R., Approximation of rolling-ball blends for free-form parametric surfaces. Computer-Aided Design, 28, 871-878 (1996).

[6] Gal, R.O. and Pal, L., Some notes on drawing twofolds in 4-dimensional Euclidean space. Acta Univ. Sapientiae, Informatica, 1-2, 125-134 (2009).

[7] Gray, A., Modern differential geometry of curves and surfaces. CRC Press, Boca Raton Ann Arbor London Tokyo, (1993).

[8] Mello, L. F., Orthogonal asymptotic lines on surfaces immersed in $\mathbb{R}^4$. Rocky Mountain J. Math., 39(5), 1597-1612 (2009).

[9] Mochida, D. K. H., Fuster, M.D.C.R and Ruas, M.A.S., The geometry of surfaces in 4-Space from a

contact viewpoint. Geometriae Dedicata., 54, 323-332 (1995).
[10] Rouxel, B., Ruled A-submanifolds in Euclidean space $\mathbb{E}^4$. Soochow J. Math., 6, 117-121 (1980).
[11] Shani, U. and Ballard, D.H., Splines as embeddings for generalized cylinders. Computer Vision,Graphics and Image Processing, 27, 129-156 (1984).
[12] Wang, L., Ming, C.L., and Blackmore, D., Generating sweep solids for NC verification using the SEDE method. Proceedings of the Fourth Symposium on Solid Modeling and Applications, Atlanta, Georgian, May 14-16, 364-375 (1995).
[13] Wong, Y.C., Contributions to the theory of surfaces in 4-space of constant curvature. Trans. Amer. Math. Soc., 59, 467-507 (1946).
[14] Xu, Z., Feng, R. and Sun, JG., Analytic and algebraic properties of canal surfaces. Journal of Computational and Applied Mathematics, 195(1-2), 220-228 (2006).

Betül Bulca *is currently an asistant professor at Uludag University in Turkey. Her research interests include curves and surfaces.*

Kadri Arslan *is currently a professor at Uludag University in Turkey. His research interests include curves and surfaces.*

Bengü Bayram *is currently an associate professor at Balikesir University in Turkey. Her research interests include curves and surfaces.*

Günay Öztürk *is currently an associate professor at Kocaeli University in Turkey. His research interests include curves and surfaces.*

An International Journal of Optimization and Control: Theories & Applications (http://ijocta.balikesir.edu.tr)

An International Journal of Optimization and Control: Theories & Applications
ISSN: 2146-0957eISSN: 2146-5703
Vol.7, No.1, pp.90-97 (2017)
https://doi.org/10.11121/ijocta.01.2017.00345

RESEARCH ARTICLE

Assessment and optimization of thermal and fluidity properties of high strength concrete via genetic algorithm

Barış Şimşek[a *], Emir H. Şimşek[b]

[a]*Department of Chemical Engineering, Çankırı Karatekin University, Turkey*
[b]*Department of Chemical Engineering, Ankara University, Turkey*
barissimsek@karatekin.edu.tr, simsek@ankara.edu.tr

ARTICLE INFO

Article history:
Received: 15 May 2016
Accepted: 26 November 2016
Available Online: 22 December 2016

Keywords:
Genetic algorithm
High strength concrete
Optimization
Thermal properties

AMS Classification 2010:
80M50, 78M32, 62K20

ABSTRACT

This paper proposes a Response Surface Methodology (RSM) based Genetic Algorithm (GA) using MATLAB® to assess and optimize the thermal and fluidity of high strength concrete (HSC). The overall heat transfer coefficient, slump-spread flow and T_{50} time was defined as thermal and fluidity properties of high strength concrete. In addition to above mentioned properties, a 28-day compressive strength of HSC was also determined. Water to binder ratio, fine aggregate to total aggregate ratio and the percentage of super-plasticizer content was determined as effective factors on thermal and fluidity properties of HSC. GA based multi-objective optimization method was carried out by obtaining quadratic models using RSM. Having excessive or low ratio of water to binder provides lower overall heat transfer coefficient. Moreover, T_{50} time of high strength concrete decreased with the increasing of water to binder ratio and the percentage of superplasticizer content. Results show that RSM based GA is effective in determining optimal mixture ratios of HSC.

1. Introduction

Optimizing the mixture parameters of high performance concrete is important to save raw materials used [1-3]. Although many studies on finding the optimal mixture proportions for various concrete types [3] such as steel fiber reinforced concrete composition [4], recycled aggregate concretes [5], paper mill residuals mixed concrete [6], geopolymer concrete [7], and high strength self-compacting concrete [8], there is still a need for hybrid optimization techniques. In optimization phase; experimental design such as response surface methodology (RSM) is not widely practiced with Genetic algorithm (GA). However, there are some studies to optimize wire electric discharge machining process [9], cutting parameters [10], biodiesel production process [11], and optimal cultivation [12]. In recent years, genetic algorithm was generally preferred to optimize parameters due to the success in solving complex optimization problems.

RSM comprise of a group of mathematical and statistical techniques that can be used to identify the relationships between the response and the factors[13], [14]. RSM describes the effect of the factors, alone or in combination, in the processes [15]. Moreover in analyzing the effects of the factors, this experimental method also creates a mathematical model [16-18]. GAs show a classic strong optimization method in solving involution optimal problems that could be nonlinear or linear [15, 19]. GA consults the information from the achieved probable solution in the former stages to form the new set of points where improved results are anticipated [15, 20]. In the initial generation, GA is an evolutionary algorithm which can be used for the solution of more complicated optimization problems [15, 20]. GA can be described through three stages briefly: initial generation; operations such as reproduction, mutation, crossover etc.; determination of fitness value [15, 20].

This paper proposes a systematic methodology including experimental design based GA to assess and optimize thermal and fluidity properties of high strength concrete (HSC). Certainly, the overall heat transfer coefficient should be evaluated with the other essential properties such as T_{50} time, slump-flow spread and comprehensive strength for the HSC. For this purpose, the RSM must be applied with multi-objective optimization methods such as genetic

*Corresponding author

algorithm. The main contribution of this article, the overall heat transfer coefficient of HSC was modeled empirically as a function of mixture parameters. The overall heat transfer coefficient was also optimized with other parameters using RSM-based GA. Furthermore, the overall heat transfer coefficient and T_{50} time were also analyzed in accordance with the mixed ingredients.

2. Materials and method

2.1. Materials

CEM I 42.5R type cement with 425 kg/m^3 dosage was used in this study. The cement has a specific gravity of 3.11 and Blaine fineness of 3696 cm^2/g.120 kg/m^3 of fly ash with a specific gravity of 2.38 is used. A polycarboxylic ether based superplasticizer was used in all concrete mixtures. Super-plasticizer content is identified as the ratio of SP amount of 100 kg cement. Crushed sands (with a size of smaller than 4 mm as fine aggregate and with a size between 4 mm to 11mm as the coarse aggregate are used in concrete mixtures. The fine and coarse aggregates has specific gravities of 2.61 and 2.72 and mean water absorptions of 1.4% and 1.1 %, respectively.

2.2. Proposed methodology

Low heat loss provides benefits in energy savings. The overall heat transfer coefficient was evaluated with other important criteria for HSC such as slump-spread diameter, T_{50} time and 28th day compressive strength to meet HSC qualifications. The flow chart which consists of 10 steps and which is aimed at optimizing the HSC performance was given in Figure 1.In this research, GA was used for the optimization of useful models obtained with RSM for the overall heat transfer coefficient, slump-spread diameter, T_{50} time and 28th day compressive strength.

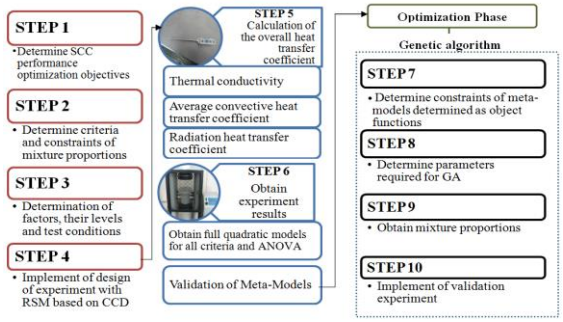

Figure 1. Proposed performance optimization and modeling framework

2.3. Thermal and fluidity properties of high strength concrete

In Turkey, 80% of the energy consumption in households is used for heating aims [21]. New methods have to be designed in order to contribute building professionals in their effort to optimize designs and to improve energy performance [22]. In our study, radiation heat-transfer coefficient was calculated to predict and model the overall heat transfer coefficient taking into account relationship radiation heat-transfer coefficient between convective heat transfer coefficients. Lakatos and Kalmar examines the change of the overall heat transfer coefficient of building structures in function of water content [23]. The first criterion is identified as the overall heat transfer coefficient that should be low. Quality characteristics for modeling phase are presented in Table 1.

Table 1. Quality criteria and their target values for optimization phase

Quality feature	Sign	Definition	Kind of concrete test	Objective
1	U	The overall heat transfer coefficient (W/m^{2}K)	Freshly mixed concrete	Minimize
2	S	Slump-spread diameter (mm)	Freshly mixed concrete	Maximize
3	T_{50}	T_{50} time (s)	Freshly mixed concrete	Minimize
4	f_{cs28}	Compressive strength (N/mm^2) 28 days	Hardened concrete test	Maximize

2.4. Determination of factors and their levels

The ranges of factors and their levels were determined taking into account the findings obtained by TOPSIS-based Taguchi Optimization [8]. Three factors (variables) are characterized as A, B, C and their five levels are given in Table 2. The factors in our experiment are percentage of water to binder materials (A), fine aggregate (I) amount to total aggregate amount ratio (B) and the percentage of PCE (C).

Table 2. Factor levels for response surface methodology

Factors Description		Levels				
		-2	-1	0	1	2
		First level	Second level	Third level	Fourth level	Fifth level
A	Water to binder materials ratio	0.36	0.365	0.37	0.375	0.38
B	Fine aggregate (I) amount to total aggregate amount ratio	0.58	0.59	0.60	0.61	0.62
C	The percentage of PCE (%)	1.15	1.20	1.25	1.30	1.35

3. The calculation of heat transfer coefficients

Δx is the specimen length (150 mm), λ_c is thermal conductivity of concrete, h_c is convective heat transfer coefficient [8, 24] and h_f is radiation heat transfer coefficient; The heat transfer process may be represented by the resistance network and the overall heat transfer can be calculated as the ratio of the

Table 3. The overall heat transfer coefficient

Exp.No.	T_c, ^{0}C	T_∞, ^{0}C	T_f, K	Re	Nu	λc(W/mK)*	hc(W/ m^{2}K)‡	hf(W/ m^{2}K)#	U(W/ m^{2}K)
1	21.8	14.2	291.15	20169.02	84.11580	1.639177	14.40864	3.527020	2.250035
2	21.4	14.2	290.95	20191.28	84.16466	1.639919	14.40781	3.519696	2.247241
3	20.8	14.2	290.65	20224.76	84.23810	1.641032	14.40657	3.508735	2.243049
4	20.6	14.2	290.55	20235.95	84.26262	1.641404	14.40616	3.505088	2.241652
5	20.9	14.2	290.70	20219.18	84.22585	1.640847	14.40678	3.510560	2.243748
6	21.0	14.2	290.75	20213.59	84.21360	1.640661	14.40698	3.512385	2.244446
7	21.4	13.8	290.75	20213.59	84.21360	1.639919	14.40698	3.512505	2.244287
8	21.3	13.8	290.70	20219.18	84.22585	1.640104	14.40678	3.510678	2.243588
9	20.7	13.8	290.40	20252.75	84.29944	1.641218	14.40554	3.499732	2.239393
10	20.1	13.8	290.10	20286.44	84.37321	1.642332	14.40431	3.488815	2.235199
11	20.6	13.8	290.35	20258.36	84.31172	1.641404	14.40533	3.497910	2.238694
12	20.5	13.8	290.30	20263.97	84.32401	1.641589	14.40513	3.496089	2.237995
13	20.8	13.8	290.45	20247.15	84.28716	1.641032	14.40574	3.501554	2.240093
14	21.0	13.8	290.55	20235.95	84.26262	1.640661	14.40616	3.505201	2.241491
15	21.1	14.3	290.85	20202.43	84.18912	1.640476	14.40740	3.516010	2.245884
16	20.8	14.3	290.70	20219.18	84.22585	1.641032	14.40678	3.510532	2.243789
17	21.9	14.3	291.25	20157.90	84.09140	1.638991	14.40906	3.530655	2.251471
18	20.2	14.3	290.40	20252.75	84.29944	1.642146	14.40554	3.499599	2.239598
19	20.6	14.3	290.60	20230.36	84.25036	1.641404	14.40636	3.506884	2.242392
20	20.7	14.3	290.65	20224.76	84.23810	1.641218	14.40657	3.508708	2.243090

* The average of the lower thermal conductivity and upper thermal conductivity of the concrete
‡ The average of the coefficients of the convection heat transfer of three 150 mm specimens [8]
# The average of the coefficients of the radiation heat transfer of three 150 mm specimens

overall temperature difference to the sum of the thermal resistance (U) [25]:

$$U = \frac{1}{\left(\frac{1}{h_c} + \frac{\Delta x}{\lambda_c} + \frac{1}{h_f}\right)} \tag{1}$$

The thermal conductivity of concrete λ_c (in W/m*K), 20^0C < T_w< 1200^0C, can be calculated between the lower(LL) and upper limit (UL)values as follows [25]:

$$\lambda_c = \begin{cases} 2 - 0.245(T_w/100) + 0.011(T_w/100)^2, \text{UL} \\ 1.36 - 0.136(T_w/100) + 0.006(T_w/100)^2, \text{LL} \end{cases} \tag{2}$$

In this study, the average thermal conductivity ($\bar{\lambda}_c$), which is the average of the lower thermal conductivity and upper thermal conductivity of the concrete, was calculated by using Eq. (2) for all experiments given in Table 3.

The details of calculation of the convective heat transfer coefficient can be found in [8]. T_w, T_∞ and T_f are the temperature of the concrete surface, the temperature of the air and film temperature, respectively.

The coefficient of the average convection heat transfer (h_c) which is the average of the coefficients of the convection heat transfer of three 150 mm cubes given in Table 3 [8].

The radiation heat transfer coefficient ($\bar{h}_f$) which is the average of the coefficients of the radiation heat transfer of three 150 mm cubes given in Table 3, are calculated by using Eq. (3) for all experiments[8].

$$h_f = \frac{\sigma^* \varepsilon^* F_{1,2}}{T_w - T_\infty}[T_w^4 - T_\infty^4] \tag{3}$$

ε is emissivity 0.63 for concrete; σ is Stephan-Boltzmann constant 5,67*10^{-8} W/m^{2}K^4 and $F_{1,2}$ = 1 radiation shape factor [8, 26].

4. Modeling and optimization

4.1. Modeling

Experimental matrix of RSM based Central Composite Design (CCD) were given in third, fourth and fifth columns of Table 4. In our study, rotatable experimental design is carried out as central composite design (CCD) which consists of 20 experiments. As shown in Table 4, three independent variables was symbolized as A (water to binder materials ratio), B (fine aggregate (II) amount to total aggregate amount ratio) and C (super plasticizer amount ratio to one hundred kilogram binder materials) [16].

The regression equations given in Table 5 were achieved from the analysis of variances (ANOVA). From the "p" values ($p < 0.05$) presented in also Table 5, regression equations were found significant for all thermal and fluidity properties [16]. The results demonstrate that the experimental results approximate to the estimated results (see R^2 values in Table 5). The estimated and theoretical values for the all thermal and fluidity properties were given in Table 5.

Table 4. Experimental results

Exp. No.	*CCD*						Responses			
	Factors have been fixed, 1 m3			Factors used in experimental design, 1 m3 (%)			U (W/m^{2}K)	S mm	T_{50} s	f_{cs28} N/m^3
	Cement, kg	Fly ash, kg	Total aggregate, kg	A	B	C				
MD1	425	120	1668	36.5	59	1.15	2.250035	680	5.1	71.0
MD2	425	120	1668	37.5	61	1.15	2.247241	710	4.7	68.1
MD 3	425	120	1668	37.5	59	1.30	2.243049	780	3.8	68.6
MD 4	425	120	1668	36.5	61	1.30	2.241652	750	4.1	69.0
MD 5	425	120	1668	37.0	60	1.25	2.243748	750	4.5	68.7
MD 6	425	120	1668	37.0	60	1.25	2.244446	750	4.6	68.1
MD 7	425	120	1668	37.5	59	1.20	2.244287	760	4.2	67.3
MD 8	425	120	1668	36.5	61	1.20	2.243588	720	5.0	68.4
MD 9	425	120	1668	36.5	59	1.30	2.239393	750	4.8	71.3
MD 10	425	120	1668	37.5	61	1.30	2.235199	790	4.2	66.9
MD 11	425	120	1668	37.0	60	1.25	2.238694	740	4.4	68.3
MD 12	425	120	1668	37.0	60	1.25	2.237995	750	4.5	67.8
MD 13	425	120	1668	36.0	60	1.25	2.240093	670	5.2	71.5
MD 14	425	120	1668	38.0	60	1.25	2.241491	750	4.3	67.3
MD 15	425	120	1668	37.0	58	1.25	2.245884	740	4.4	68.5
MD 16	425	120	1668	37.0	62	1.25	2.243789	740	4.5	68.2
MD 17	425	120	1668	37.0	60	1.15	2.251471	700	5.1	69.9
MD 18	425	120	1668	37.0	60	1.35	2.239598	770	3.8	70.4
MD 19	425	120	1668	37.0	60	1.25	2.242392	750	4.5	68.7
MD 20	425	120	1668	37.0	60	1.25	2.243090	750	4.5	69.0

Table 5. Regression equations and analysis of variances of all responses

Regression equations (obtained by uncoded variables)	R^2, %	P value
$U = -2.36 + 23.91X1+1.98X2-0.74X3-13.30X1^2+5.88\ X2^2+0.30\ X3^2-23.94X1X2+0.21X1X3-0.208X2X3$	77.29‡	0.024*
$S = -65018 + 296687X1+33056X2+45X3-327126X1^2-6782X2^2-720X3^2-81954X1X2-1316X1X3+4342X2X3$	91.75‡	0.000*
$T_{50} = 971.54 – 3970.44X1-873.44X2+66.41X3+1929.89X1^2-267.53X2^2-21.56X3^2+3743.68X1X2+197.37X1X3-151.32X2X3$	93.88‡	0.000*
$f_{cs28} = 2271.0 – 9524.57X1-991.79X2-148.74X3+7661.11X1^2-709.72X2^2+139.11X3^2+6011.11X1X2+23.68X1X3-338.16X2X3$	87.03‡	0.002*

*significant at 5% (p-value)
‡regression coefficient values plotted predicted values against observed values for validation meta-models

Table 6. The results of genetic algorithm

No.	Variables			Responses							
				U, W/m^{2}K		S, mm		T_{50}, sec		f_{cs28}, N/mm^2	
	A	B	C	GA*	PV‡	GA	PV	GA	PV	GA	PV
1	0.3800	0.5800	1.1500	2.2537	2.2537	734.9912	734.9912	3.1423	3.1423	66.5157	66.5157
2	0.3800	0.5800	1.2038	2.2492	2.2492	754.8319	754.8189	3.2983	3.2982	66.0818	66.0618
3	0.3800	0.6130	1.3139	2.2334	2.2334	766.9671	766.8106	4.2555	4.2569	67.6885	67.6903
4	0.3600	0.5805	1.3327	2.2362	2.2362	680.0251	679.5703	5.2985	5.3040	74.9295	74.9462
5	0.3607	0.5825	1.3210	2.2365	2.2365	688.6627	688.2686	5.2184	5.2226	74.0219	74.0352
6	0.3601	0.5809	1.1512	2.2449	2.2449	625.4983	625.9799	6.0024	5.9954	73.2638	73.2440
7	0.3672	0.5815	1.2033	2.2445	2.2445	714.7011	714.9063	4.8445	4.8408	69.7007	69.6999
8	0.3648	0.5960	1.2466	2.2396	2.2396	718.0428	718.3367	4.9185	4.9155	70.0038	69.9997
9	0.3616	0.5836	1.1845	2.2426	2.2427	658.3094	658.6406	5.6925	5.6874	72.0325	72.0178
10	0.3617	0.5820	1.2611	2.2383	2.2383	683.9930	684.3451	5.4638	5.4590	72.3077	72.2926
R^2, %				100.0		100.0		100.0		100.0	

*Predicted results for response using GA; ‡Predicted values for response using meta-models obtained RSM

The regression meta-models obtained from RSM experiments were determined as the objective functions for genetic algorithm were given in Table 5. Bounds were defined as $0.36 \leq A \leq 0.38$, $0.58 \leq B \leq 0.62$ ve $1.15 \leq C \leq 1.35$ used in RSM. The trial and error method was used to determine the parameters in GAs using MATLAB® optimization toolbox [15]. In all combinations of parameters used the trial and error method was achieved over 99% fitness value. Genetic algorithm parameters which have the highest fitness value and selected by trial and error method; the number of initial population, crossover rate, and number of generations are 40, 0.8 and 150 respectively. Ten runs have been executed with these parameters to determine genetic algorithm method efficiency (Table 6).

In order to confirm the optimum mix-design proportion achieved using genetic algorithm, one empirical study was implemented to check whether the genetic algorithm could really predict of quality criteria by the proposed optimum mixture proportions. Optimal mixture parameters were determined as A = 0.38, B = 0.58 and C = 1.15 for genetic algorithm. The results prove that the experimental results are very close to the estimated results (Table 7).

5. Discussion

Having excessive or low ratio of water to cement materials provides less heat transfer due to low overall heat transfer coefficient as shown in contour plot (Figure 2 and 3) [17]. Fine aggregate to total aggregate ratio should be fixed at 0.60-0.61 also decreases heat transfer. The percentage of super plasticizer content, factor C, causing the highest variation in the overall heat transfer coefficient is the most important factor. The relationship between the overall heat transfer coefficient (U) and factors (A, B, C) can be analyzed using this contour plots. As shown in Figure 2, the stationary point of the response surface shows the saddle point for that property (the third factor was kept constant at 1.25). Moreover, T_{50} time of high strength concrete decreased with the increasing of water to binder ratio and the percentage of super plasticizer content. Also, T_{50} time did not change the fluctuation of fine aggregate ratio (Figure 3). T_{50} time of fresh concrete has been negatively affected by the interaction between water to binder materials and fine aggregate ratio (Figure 3).

Table 7. The results of genetic algorithm

Number	Responses	Estimated values	Confirmation experiment	Difference (d)	Mean, $\bar{d}$	Standard deviation	Test Statistics‡	$t_{3;0.025}$ ($t_{n-1,\alpha/2}$)
1	U	2.1537	2.1539	-0.0002	1.26	2.49	*1.012	3.18
2	S	734.9912	730	4.9912				
3	T_{50}	3.1423	3.1	0.0423				
4	f_{cs28}	66.5157	66.5	0.0157				
Total	n=4							

*Null hypothesis H_0= The X_i's are interdependent and identically distributed random variables with distribution function F. Since 1.012<3.18, null hypothesis would not reject. ‡$t = \bar{d}\sqrt{n/s_d}$[17]

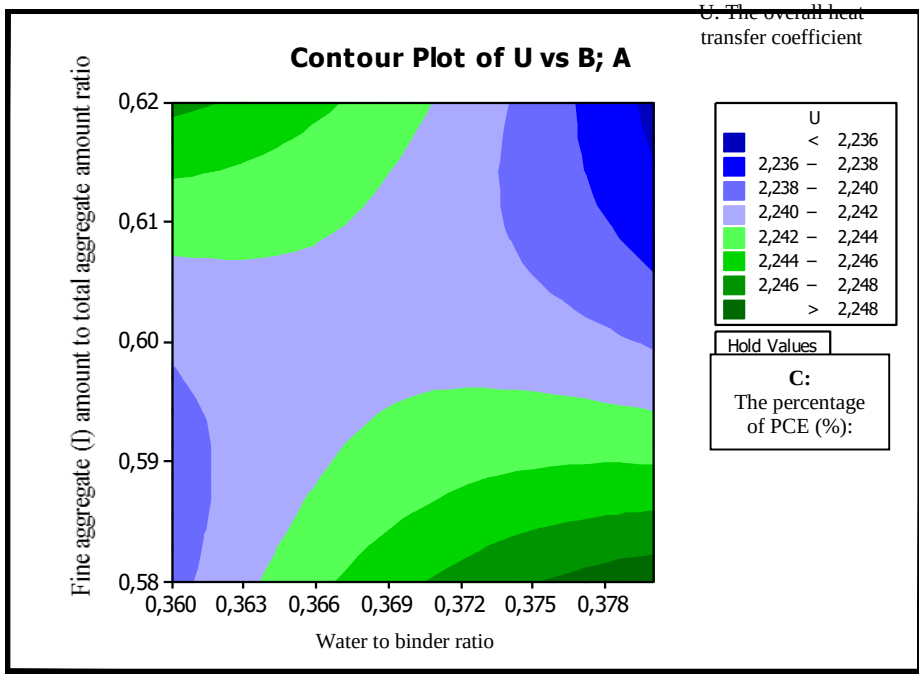

Figure 2. Contour plots of the overall heat transfer coefficient in uncoded values

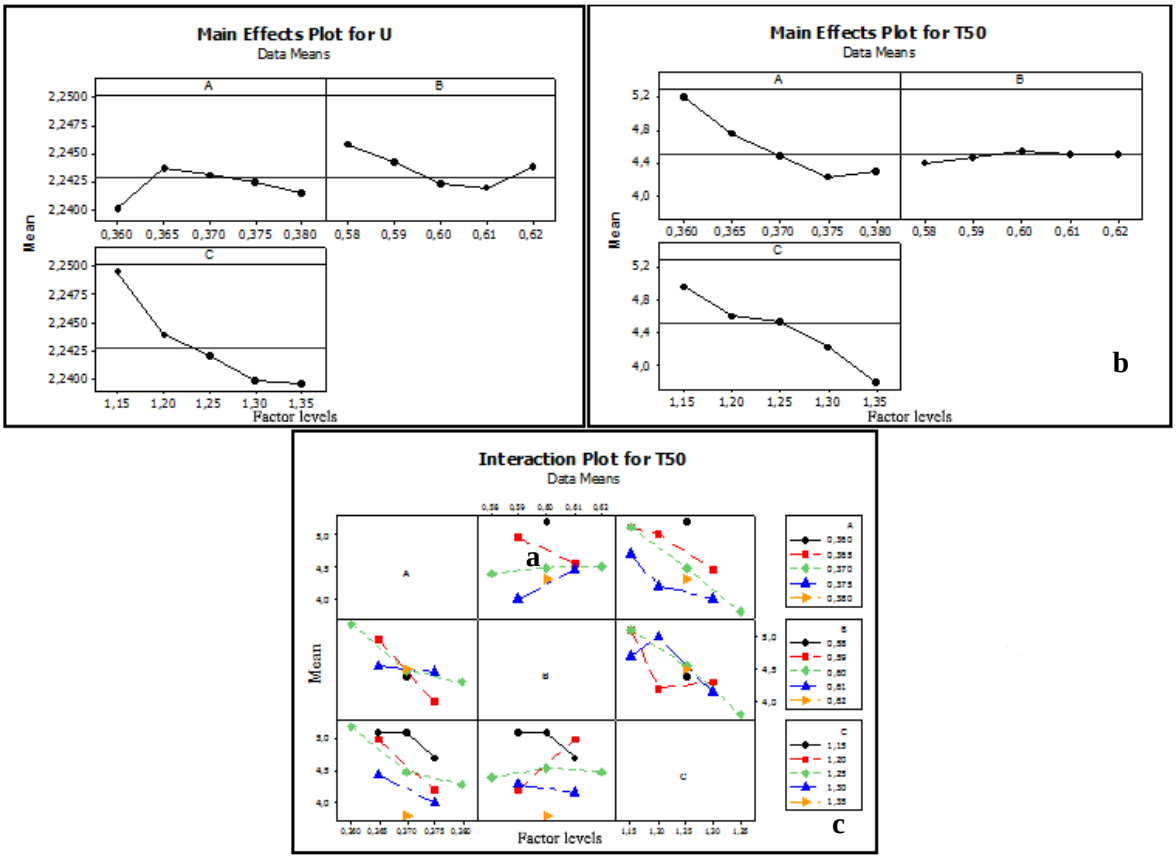

Figure 3. a) Main effect plot for overall heat transfer coefficient b) Main effect plot for T_{50} time c) Interaction effects plot for T_{50} time

6. Conclusion

In this study, the modeling of mixture proportions including overall heat transfer coefficient of high strength concrete was performed by using a RSM. The quadratic models based on RSM were useful and significant at % 5 statistically for prediction of overall heat transfer coefficient (with a p-value of 0.024), slump-spread diameter (with a p-value of 0.000), T_{50} time (with a p-value of 0.000) and 28^{th} day compressive strength (with a p-value of 0.002).

Response surface methodology is such a design of experiment technique; it can be used to optimize only one response. If there is more than one response, response surface methodology should be used with other optimization techniques such as the desirability function approach, the nonlinear programming methodologies, and the metaheuristic algorithms. Non-linear programming or desirability function approach contains complex mathematical operations and requires algorithm knowledge. However, genetic algorithm application is easy to perform compared to non-linear programming or desirability function approach. Moreover, genetic algorithm has been preferred to solve the multi-response optimization more quickly.

According to these findings; RSM can be used the modeling of the thermal and fluidity properties of high strength concrete. Following the RSM stage; genetic algorithm using MATLAB® optimization toolbox based experiments was applied to determine optimal mixture parameters of HSC. The results show that response surface methodology based on genetic algorithm is quite an effective tool in solving the mixture proportions optimization problem.

The RSM-based GA can be used effectively in the other possible application areas such as product design and improvement in material engineering, parameter design in control engineering, mix design in chemical engineering.

References

[1] Yan, S., Lin, H.-C. and Y.-C. Liu, Optimal schedule adjustments for supplying ready mixed concrete following incidents. *Automation in Construction*, 20 (8), 1041-1050 (2011).

[2] Chang, C.Y., Huang, R., Lee, P. C. and Weng, T.L., Application of a weighted Grey-Taguchi method for optimizing recycled aggregate concrete mixtures. *Cement and Concrete Composites*, 33(10), 1038-1049 (2011).

[3] Şimşek, B., İç, Y.T. and Şimşek, E.H., A Full Factorial Design Based Desirability Function Approach for Optimization of Properties of C 40/50 Concrete Class. *Mathematical and Computational Applications*, 18(3), 330 (2013).

[4] Dvorkin, L., Dvorkin, O., Zhitkovsky, V. and Ribakov, Y., A method for optimal design of steel fiber reinforced concrete composition. *Materials & Design*, 32(6), 3254-3262 (2011).

[5] Lovato, P.S., Possan, E., Molin, D.C.C.D., Masuero, A.B. and Ribeiro, J.l.D., Modeling of mechanical properties and durability of recycled aggregate concretes. *Construction and Building Materials*, **26**(1), 437-447 (2012).

[6] Mohammed, B.S., Fang, O.C., Anwar Hossain, K.M. and Lachemi, M., Mix proportioning of concrete containing paper mill residuals using response surface methodology. *Construction and Building Materials*, 35, 63-68 (2012).

[7] Olivia, M. and Nikraz, H., Properties of fly ash geopolymer concrete designed by Taguchi method. *Materials & Design*, 36, 191-198 (2012).

[8] Şimşek, B., İç,Y.T. and Şimşek, E.H., A TOPSIS-based Taguchi optimization to determine optimal mixture proportions of the high strength self-compacting concrete. *Chemometrics and Intelligent Laboratory Systems*, 125, 18-32 (2013).

[9] Sharma, N., Khanna, R. and Gupta, R.D., WEDM process variables investigation for HSLA by response surface methodology and genetic algorithm. *Engineering Science and Technology, an International Journal*, 18(2), 171-177 (2015).

[10] Subramanian, M., Sakthivel, M., Sooryaprakash, K., Sudhakaran, R., Optimization of Cutting Parameters for Cutting Force in Shoulder Milling of Al7075-T6 Using Response Surface Methodology and Genetic Algorithm. *Procedia Engineering*, 64, 690-700, 2013.

[11] Fayyazi, E., Ghobadian, B., Najafi, G., Hosseinzadeh, B., Mamat, R. and Hosseinzadeh, J., An ultrasound-assisted system for the optimization of biodiesel production from chicken fat oil using a genetic algorithm and response surface methodology. *Ultrasonics Sonochemistry*, 26, 312-320 (2015).

[12] Kumar, A., Pathak, A.K. and Guria, C., NPK-10:26:26 complex fertilizer assisted optimal cultivation of Dunaliella tertiolecta using response surface methodology and genetic algorithm. *Bioresource Technology*, 194, 117-129 (2015).

[13] Baş, D. and Boyacı, İ.H., Modeling and optimization II: Comparison of estimation capabilities of response surface methodology with artificial neural networks in a biochemical reaction. *Journal of Food Engineering*, 78(3), 846-854 (2007).

[14] Baş, D. and Boyacı, İ.H., Modeling and optimization I: Usability of response surface methodology. *Journal of Food Engineering*, 78(3), 836-845 (2007).

[15] Lin, H.C., Su, C.T., Wang, C.C., Chang, B. H. and Juang, R.C., Parameter optimization of continuous sputtering process based on Taguchi methods, neural networks, desirability function, and genetic algorithms. *Expert Systems with Applications*, 39 (17), 12918-12925 (2012).

[16] Şimşek, B., İç, Y.T., Şimşek, E.H., Güvenç, A.B., Development of a graphical user interface for determining the optimal mixture parameters of normal weight concretes: A response surface methodology based quadratic programming approach. *Chemometrics and Intelligent Laboratory Systems*, 136, 1-9 (2014).

[17] Şimşek, B., İç, Y.T. and Şimşek, E.H. A RSM-Based Multi-Response Optimization Application for Determining Optimal Mix Proportions of Standard Ready-Mixed Concrete. *Arabian Journal for Science and Engineering*, 41(4), 1435-1450 (2016).

[18] Basri, M., Rahman, R.N.Z.R.A., Ebrahimpour, A., Salleh, A.B., Gunawan, E.R. and Rahman, M.B.A., Comparison of estimation capabilities of response surface methodology (RSM) with artificial neural network (ANN) in lipase-catalyzed synthesis of palm-based wax ester. *BMC Biotechnology*, 7(1), 1-14 (2007).

[19] Ortiz Jr, F., Simpson, J. R., Pignatiello, Jr, J.J., Heredia-Langner, A., A genetic algorithm approach to multiple-response optimization. *Journal of Quality Technology*, 36(4), 432 (2004).

[20] Chandwani, V., Agrawal, V. and Nagar, R., Modeling slump of ready mix concrete using genetic algorithms assisted training of Artificial Neural Networks. *Expert Systems with Applications*, 42(2), 885-893 (2015).

[21] Dombaycı, Ö.A., The prediction of heating energy consumption in a model house by using artificial neural networks in Denizli–Turkey. *Advances in Engineering Software*, 41(2), 141-147 (2010).

[22] Foucquier, A., Robert, S., Suard, F., Stephan, L. and Jay, A., State of the art in building modelling and energy performances prediction: A review. *Renewable and Sustainable Energy Reviews*, 23, 272-288 (2013).

[23] Lakatos, Á., Investigation Of The Effect Of Moisture In The Time Lag Of Building Walls With Different Insulating Materials. *Environmental Engineering And Management Journal*, 13(11), 2853-2858 (2014).

[24] Lee, Y., Choi, M.S., Yi, S.T. and Kim, J.K., Experimental study on the convective heat transfer coefficient of early-age concrete. *Cement and Concrete Composites*, 31(1), 60-71 (2009).

[25] Lennon, T., Designers' Guide to EN 1991-1-2, EN 1993-1-2 and EN 1994-1-2: Handbook for the Fire Design of Steel, Composite and Concrete Structures to the Eurocodes. Thomas Telford (2007).

[26] Simsek, B., Simsek, E.H. and Altunok, T. Empirical and Statistical Modeling of Heat Loss from Surface of a Cement Rotary Kiln System. *Journal of the Faculty of Engineering and Architecture of Gazi University*, 28(1), 59-66 (2013).

Barış Şimşek *is an Assistant Professor of Department of Chemical Engineering at the Çankırı Karatekin University. He received a PhD degree in Chemical Engineering from Ankara University Institute of Science and Technology, Turkey. His research interests include application of expert systems to manufacturing systems, modeling and optimization of production systems, multi-criteria decision making, and design of* experiment.

Emir Hüseyin Şimşek *is an Assistant Professor of Department of Chemical Engineering at the Ankara University. He received a PhD degree in Chemical Engineering from Ankara University Institute of Science and Technology, Turkey. His research interests include application of coal liquefaction, supercritical fluid extraction, liquefaction mechanisms of coal, photo degradation of polystyrene plastics wastes.*

An International Journal of Optimization and Control: Theories & Applications
ISSN:2146-0957 eISSN:2146-5703
Vol.7, No.1, pp.98-111 (2017)
http://doi.org/10.11121/ijocta.01.2017.00342

RESEARCH ARTICLE

Artificial bee colony algorithm variants on constrained optimization

Bahriye Akay*, Dervis Karaboga

Department of Computer Engineering, Erciyes University, Kayseri, Turkey
bahriye@erciyes.edu.tr, karaboga@erciyes.edu.tr

ARTICLE INFO

Article History:
Received 29 September 2016
Accepted 15 November 2016
Available 12 January 2017

Keywords:
Artificial bee colony algorithm
Constrained optimization
Deb's rules

AMS Classification 2010:
65K10

ABSTRACT

Optimization problems are generally classified into two main groups: unconstrained and constrained. In the case of constrained optimization, special techniques are required to handle with constraints and to produce solutions in the feasible space. Intelligent optimization techniques that do not make assumptions on the problem characteristics are preferred to produce acceptable solutions to the constrained optimization problems. In this study, the performance analysis of artificial bee colony algorithm (ABC), one of the intelligent optimization techniques, is examined on constrained problems and the effect of some modifications on the performance of the algorithm is examined. Different variants of the algorithm were proposed and compared in terms of efficiency and stability. Depending on the results, when DE operators were integrated into ABC algorithm, an enhancement in the performance was gained in addition to preserving the stability of the basic ABC. The ABC algorithm is a simple optimization algorithm that can be efficiently used for constrained optimization without requiring a priori knowledge.

1. Introduction

Design problems are optimization problems in which the parameters of the system are decided in order to obtain the best performance. Formulating design problems as optimization problems and solving them by using an appropriate optimization tool minimizes the experimental costs and errors. In most of the design problems, problems have some constraints that the solutions must satisfy.

Traditional optimization algorithms are not successful when the problems are nonlinear and have many constraints and discrete variables. Evolutionary algorithms (EAs) [1] that mimic the genetic inheritance and natural selection do not make assumptions on the problem characteristics and can be used for constrained, nonlinear design problems successfully [2]. In EAs, a population of solutions are assigned fitness values and new child solutions are produced after reproduction, mutation, crossover operators. Better solutions are retained in the population applying a selection operator and the population quality is increased which means convergence to better solutions.

Swarm intelligence (SI) based algorithms employ similar operators to those of evolutionary algorithms while SI algorithms are also capable of using collective intelligence coming due to the interactions of individuals in the swarm. Genetic algorithm [3], Differential Evolution [4] are typical examples of EAs; Ant Colony Optimization [5], Particle Swarm Optimization [6] and Artificial Bee Colony [7] algorithms are examples of SI based algorithms.

All these algorithms were initially proposed for unconstrained optimization and their basic versions did not have any mechanism to produce solutions in feasible space or to prefer feasible solution to infeasible one. Some operators are integrated to the algorithms in order to search the feasible space and solve constrained problems such as

*Corresponding Author

transforming operator that preserve feasibility of solutions, penalty functions to penalize constraint violations in the cost function, distinction operator that separate feasible and infeasible, hybrid methods that incorporates evolutionary methods and deterministic procedures [8]. Artificial Bee Colony Algorithm proposed for constrained optimization [9, 10] prefers feasible solutions to infeasible solutions applying Deb's rules [11] in the selection phase. Another modification in basic ABC concerns fitness assignment scheme which considers both feasible solutions and infeasible solutions because the population can include both types of solutions to maintain diversity in the population.

Although there are some studies related to ABC on the constrained optimization, effect of the neighbor production mechanism has not been studied to analyze how they cover feasible space or whether they are capable of making distinction between feasible and infeasible space or which one is more efficient for constrained optimization. In this study, various ABC algorithm variants, which employ different neighbor productions mechanisms and neighborhood topologies, are analyzed in terms of success rates. Effect of the neighbor solution production in the search behavior of the algorithms and in the convergence are investigated. Basic ABC algorithm for unconstrained optimization and proposed ABC algorithm variants for constrained optimization are summarized in the second and the third sections, respectively. In the forth section, the experimental studies are presented and the results are discussed. The last section is dedicated to the conclusion.

2. Artificial bee colony algorithm

Honey bees perform many intelligent tasks and foraging is one of the most important tasks in the colony. The foraging is performed using the collective intelligence based on the communication and interaction of the bees. Bees are specialized depending on the task they are assigned to. In a real colony, there are three types of bees assigned to the foraging task: employed bees, onlooker bees and scout bees. The scout bees search for new food sources of which the nectar will be loaded to the hive. Discovered sources are exploited by the employed bees and the employed bees share information with the onlooker bees who wait in the hive. Onlooker bees select a food source to fly based on the information taken from the employed bees. When a source is exhausted, it is abandoned and its bee switches her role to a scout bee. In the foraging task, bees try to maximize the nectar amount loaded to hive by finding the most profitable sources in the environment.

ABC algorithm [7] simulates the foraging behavior of honey bees in nature. Locations of the food sources correspond to the parameters of the problem and finding the location of the most profitable source is an optimization problem. Nectar amount of the solution is measured by the fitness of a parameter vector. Main steps of the algorithm are given in Alg. 1:

Algorithm 1. *Pseudo-code of ABC algorithm*

1: *Initialization*
2: *Evaluation*
3: *cycle=1*
4: ***repeat***
5: *Employed Bees Phase*
6: *Calculate Probabilities for Onlookers*
7: *Onlooker Bees Phase*
8: *Scout Bees Phase*
9: *Memorize the best solution so far*
10: *cycle=cycle+1*
11: ***until*** *cycle=Maximum Cycle Number*

In the initialization phase of the algorithm, values are passed to the control parameters: the number of food sources (CS), maximum cycle number (MCN) and the limit that controls whether a source is exhausted or not. If the problem has D parameters to be optimized, a population of CS number of D dimensional solutions are generated randomly using Eq. 1.

$$x_i^j = x_{min}^j + rand(0,1)(x_{max}^j - x_{\min}^j) \qquad (1)$$

where x_{min}^j and x_{max}^j are lower and upper bound of the parameter j, respectively.

In the evaluation phase, each solution is substituted in the cost function and assigned a fitness value using the cost function associated with the problem. Subsequently, the employed bee, onlooker bee and scout bee phases are repeated until the cycle number reaches to MCN.

In the employed bee phase, a local search is carried out in the vicinity of each solution by Eq. 2:

$$x'_{ij} = x_{ij} + \phi_{ij}(x_{ij} - x_{kj}) \qquad (2)$$

where $k \neq i$ is a neighbor solution drawn randomly from the population, ϕ_{ij} is random real number within the range [-1,1] drawn from uniform distribution. After new solution is assigned a fitness value, ABC algorithm performs greedy

selection by which if the fitness of $\vec{x}'$ is better than the fitness of $\vec{x}$, $\vec{x}$ is discarded and $\vec{x}'$ is included in the population. Otherwise, $\vec{x}$ is retained in the population. To be used in the scout bee phase, a counter associated with each solution holds the number of times that the solution is retained in the population. In the onlooker bee phase, onlooker bees use the information obtained from employed bees and select high quality sources to fly. Each solution is assigned a probability value (Eq. 3) proportional to its fitness value obtained from the employed bee phase. In basic ABC algorithm, a roulette wheel selection scheme is applied to select potentially high quality solutions but also to give chance to low quality solutions to be selected.

$$p_i = \frac{fitness_i}{\sum_{i=1}^{CS} fitness_i} \tag{3}$$

Once a solution is determined using roulette wheel selection, a local search is performed using Eq. 2. As in the employed bee phase, a greedy selection is applied and counters are updated. The onlooker bee phase promotes more local searches around the better solutions which is a positive feedback feature.

In the scout bee phase, counters associated with each solution are checked and if a counter is higher than the control parameter limit, that source is assumed to be exhausted. The exhausted source is replaced with a new solution produced by Eq. 1 and its counter is set to 0. This phenomena arises a negative feedback effect and fluctuation in the algorithm which avoids to trap local minima.

The algorithm performs a balanced exploration and exploitation and has the advantage of employing less control parameters. ABC algorithm has been applied to many problems in wide range of fields [12, 13, 14] and has shown superior performance on high dimensional multimodal problems [15, 9]

3. Artificial bee colony algorithm for constrained optimization

In most of the design problems, problems have some constraints that the solutions must satisfy. A constrained design problem is defined as in Eq. 4.

$$\begin{array}{ll} \text{minimize } f(\vec{x}), & \vec{x} = (x_1, \ldots, x_n) \in \mathbb{R}^n \\ & l_i \leq x_i \leq u_i, \\ & i = 1, \ldots, n \\ \text{subject to :} & g_j(\vec{x}) \leq 0, \\ & \text{for } j = 1, \ldots, q \\ & h_j(\vec{x}) = 0, \\ & \text{for } j = q+1, \ldots, m \end{array} \tag{4}$$

where f is defined in n-dimensional search space, (S), and each $\vec{x_i}$ parameter is bounded by the range $[l_i, u_i]$. Constrained optimization finds a parameter vector $\vec{x}$ which minimizes the cost function,$(f(\vec{x}))$ and does not violate inequality $(g_j(\vec{x}))$ and equality $(h_j(\vec{x}))$ constraints. A feasible solution satisfies all constraints and in feasible space $F \subseteq S$, which is defined by $m \geq 0$ constraints [16]. Like the other EAs, ABC algorithm was initially proposed for unconstrained optimization and some modifications have to be made in the algorithm in order to cope with the constraints and provide solutions in the feasible space (F). In the subsequent sections, proposed ABC algorithm variants for constraint optimization are explained.

3.1. ABCV1: ABC algorithm for constrained optimization

ABC algorithm for constrained optimization [9, 10] uses the same framework with the basic ABC algorithm. ABCV1 includes employed bees, onlooker bees and scout bees phases as well while there have been some modifications inside the phases. ABCV1 does not need initial solutions to be in feasible space and initial solutions are produced using Eq. 1 as in basic ABC algorithm.

In the employed bee phase of ABCV1, a local search is conducted in the neighborhood of the solution in bee's memory using Eq. 5 instead of Eq. 2. Eq. 2 makes modification on one dimension of the current solution while Eq. 5 makes modification on dimensions if a uniformly distributed random number R_j is lower than perturbation rate, MR. MR is a control parameter introduced in ABCV1. High values of MR speeds up the convergence but has negative effect on fine tuning.

$$\upsilon_{ij} = \begin{cases} x_{ij} + \phi_{ij}(x_{ij} - x_{kj}) & , \quad if \quad R_j < MR \\ x_{ij} & , \quad \text{otherwise} \end{cases} \tag{5}$$

After generating a mutant solution υ_{ij} for each solution, instead of greedy selection, ABCV1 applies Deb's rules [11] that are listed below:

- A feasible solution ($violation_i \leq 0$) is chosen against an infeasible solution ($violation_j > 0$) (solution i is dominant),
- If both of the solutions are feasible($violation_i \leq 0$, $violation_j \leq 0$), the one with better objective function value is chosen ($f_i < f_j$, solution i is dominant),
- If both of the solutions are infeasible ($violation_i > 0$, $violation_j > 0$), the one with smaller constraint violation is chosen ($violation_i < violation_j$, solution i is dominant).

In the constrained optimization, the cost function value obtained evaluating an infeasible solution might be lower than the one obtained with a feasible solution. In the probability assignment scheme, the feasible solutions should have higher fitness values than infeasible solutions to promote feasible regions. Therefore, the probability of the feasible solutions starts from 0.5 (within the range [0.5,1])and the probability of the infeasible solutions are assigned within the range [0,0.5] based the violation of the solutions. Eq. 6 can be used for this purpose:

$$p_i = \begin{cases} 0.5 + \left(\frac{fitness_i}{\sum_{j=1}^{CS} fitness_j} \right) * 0.5 & if\ feasible \\ \left(1 - \frac{violation_i}{\sum_{j=1}^{CS} violation_j} \right) * 0.5 & if\ infeasible \end{cases} \tag{6}$$

Eq. 6 assigns higher values to the feasible solutions but the solutions with lower probability value have also chance to be chosen by the roulette wheel selection. This property provides population diversity and search ability near the boundary lines. In order to avoid feasible solutions to be discarded quickly in the scout phase, the limit checking is performed in each SPP cycles instead of each cycle. SPP is also another control parameter introduced in ABCV1.

3.2. ABCV2: Each parameter from different solution

In ABCV2, Eq. 5 is replaced with a different search operator defined by Eq 7. Eq. 5 exploits kth solution for all dimensions while Eq 7 uses a different neighbor (k_j) for each dimension so that information of more individuals are spread and more interaction can be obtained from the population. For each parameter, a random number is drawn and a random neighbor is selected. If the random number is less than MR, Eq. 7 changes this parameter using the information of the neighbor selected.

$$x'_{ij} = \begin{cases} x_{ij} + \phi_{ij}(x_{k_j j} - x_{ij}), & R_j < MR \\ x_{ij} & otherwise \end{cases} \tag{7}$$

The other parts of the algorithm are retained as in ABCV1.

3.3. ABCV3: ABC algorithm utilizing individuals in a neighborhood topology

In ABCV1 and ABCV2, selected neighbors are drawn from the population in a global manner without considering any criterion between the solutions. In ABCV3, it is proposed to select the neighbors from a neighborhood topology which comprises the solutions within a predefined radius. Neighborhood of i the solution, N_i, is defined by the expression given by Eq. 8:

$$N_i = \left\{ \bigcup_{k \neq i} x_k \,|d_{ik} \leq d_{avg} \right\} \tag{8}$$

As seen from the expression, a solution x_k, is assumed to be a neighbor of the current solution, x_i, if the distance between them (d_{ik}) is less than the average Euclidian distance (d_{avg}). In ABCV3, Eq. 9 is used to produce a new solution:

$$x'_{ij} = \begin{cases} x_{ij} + \phi_{ij}(x_{k_j j} - x_{ij}), & R_j < MR, \quad \text{and } \mathrm{x_{k_j}} \in \mathrm{N_i} \\ x_{ij}, & otherwise \end{cases} \tag{9}$$

3.4. ABCV4:ABC algorithm using a neighborhood topology in the Onlooker bee phase

The quick ABC algorithm [13] is proposed to enhance the local search capability of the basic ABC algorithm. In the basic ABC algorithm, an onlooker bee performs perturbation the solution selected based on the roulette wheel selection while in quick ABC algorithm, an onlooker bee performs on the best solution of a neighborhood defined by a radius, NR.

3.5. ABCV5,ABCV6,ABCV7:ABC algorithms using the mutation and crossover operators of differential evolution algorithm

Differential Evolution algorithm [4], proposed by Storn and Price, is an iterative and population-based optimization algorithm for optimizing the

continuous functions. It is a fast, simple and easy applicable algorithm. As in the other evolutionary algorithms, it has evaluation, mutation, crossover and selection phases. In mutation phase, for each solution, a mutant solution is produced by weighing the difference of the solutions chosen randomly (Eq. 10):

$$\hat{x}_i = x_{r_1} + F(x_i - x_{r_2}) \tag{10}$$

where $r1 \neq r2 \neq i$ and F is real valued scaling factor within the range [0,2]. The mutant solution is subjected to the crossover operation with the original solution (Eq. 11):

$$y_i = \begin{cases} \hat{x}_i, & R_j \leq C_R \\ x_i, & R_j > C_R \end{cases} \tag{11}$$

where C_R is crossover rate, R_j is a random real value drawn within the range [0,1]. New solution is evaluated using the cost function and greedy selection operator is applied to decide whether the original solution or new solution will be retained in the population. These steps are repeated until the termination criteria is satisfied. Although DE algorithm produces efficient results on some functions, the statistics related to its stability such as mean value and standard deviation are not satisfactory [9]. For this reason, DE's operators are integrated with ABC algorithm in order to combine DE's success on unimodal functions and to preserve stability of the ABC algorithm. To achieve this, Eq. 5 in ABC is replaced with Equations 10 and 11. This modification is carried out only in employed bee phase in ABCV5, only is onlooker bee phase in ABCV6 and both in employed bee phase and in onlooker bee phase in ABCV7 variant.

3.6. ABCV8:ABC algorithm using the global best

In order to include the information due to the best solution into the neighborhood, Eq. 12 is introduced which also uses the weighted difference of the current solution and global best solution, *gbest*.

$$x'_{ij} = \begin{cases} x_{ij} + \phi_{ij}(x_{kj} - x_{ij}) + \theta_{ij}(gbest_j - x_{ij}), & R_j < MR \\ x_{ij} & otherwise \end{cases} \tag{12}$$

where θ_{ij} is a random real number within the range [-1,1] drawn from uniform distribution.

3.7. ABCV9:ABC algorithm with adaptive Scout behavior

In the basic ABC algorithm, the limit value to abandon a food source is fixed for all solutions during the population evolution. In this proposed version, each food source is assigned a counter value which is proportional to its fitness value if the solution is feasible and disproportional to its constraint violation amount if the solution is infeasible. This gives more search opportunity in the locality of the high quality solutions. For this purpose, the counter of each solution is divided by the probability value defined by Eq. 6 (Eq. 13)

$$counter_i = \frac{counter_i}{p_i} \tag{13}$$

Vicinity of the better solutions have higher chance to be explored compared to the others.

4. Experimental study and results

In this study, different variants of the ABC algorithm are analyzed on constrained optimization test problems. The details of the thirteen test problems used are given at the end of the paper and characteristics of the problems are given in Table 1.

The common control parameters of the ABC algorithm variants are the number food sources (CS) that are exploited during search, the maximum number of cycles (MCN) that the phases are repeated for, modification rate (MR) that control the number of parameters to be perturbed, *limit* that is the maximum number of exploitations a solution allowed and scout production period (SPP) that the limit checking period and neighborhood radius (NR) for the variants that use a neighborhood topology. The values set for these parameters are given in Table 2.

All implementations were developed using Delphi 7 programming language and run on a computer with 64 bit 3.06 GHz Intel processor and 8 GB of RAM. All algorithms were run 30 times with different seed numbers and statistics of the results (the best, mean, worst and standard deviation) of 30 runs are summarized in Tables 3-11 for the versions ABCV1-ABCV9, respectively. The results of the basic ABC algorithm proposed for constrained optimization (ABCV1) are taken from the study in ref. [10]. ABCV1 is taken as the control algorithm to test the efficiency of the variants. The best result statistic can be used to test the efficiency while the mean and standard

Table 1. Characteristics of the test problems used in the experiments. D:Dimension of the problem, LI: Linear inequality, NI: Nonlinear inequality, LE: Number of linear equalities, NE: Number of nonlinear equalities, *rho*: the ratio of feasible region over the search space [17].

	D	**Type of Prob.**	ρ	**LI**	**NI**	**LE**	**NE**
g01	13	quadr.	0.0003%	9	0	0	0
g02	20	non-linear	99.9973%	1	1	0	0
g03	10	non-linear	0.0026%	0	0	0	1
g04	5	quadr.	27.0079%	0	6	0	0
g05	4	non-linear	0.0000%	2	0	0	3
g06	2	non-linear	0.0057%	0	2	0	0
g07	10	quadr.	0.0000%	3	5	0	0
g08	2	non-linear	0.8581%	0	2	0	0
g09	7	non-linear	0.5199%	0	4	0	0
g10	8	linear	0.0020%	3	3	0	0
g11	2	quadr.	0.0973%	0	0	0	1
g12	3	quadr.	4.7697%	0	9^3	0	0
g13	5	non-linear	0.0000%	0	0	1	2

Table 2. Values of the control parameters used in the experiments

CS	MCN	MR	$limit$	SPP	NR
40	6000	0.8	$CSxD$	$CSxD$	1

Table 3. The results of ABCV1 [10].

Problem	Optimum	Best	Mean	Worst	StdDev
g01	-15.000	-15.000	-15.000	-15.000	0.000
g02	0.803619	0.803611	0.795430	0.770319	0.009466
g03	1.000	1.000	1.000	1.000	0.000
g04	-30665.539	-30665.539	-30665.539	-30665.539	0.000
g05	5126.498	5126.487	5182.868	5374.430	68.584
g06	-6961.814	-6961.814	-6961.814	-6961.813	0.0004
g07	24.306	24.324	24.447	24.835	0.113
g08	0.095825	0.095825	0.095825	0.095825	0.000
g09	680.63	680.631	680.636	680.641	0.0026
g10	7049.25	7058.823	7220.106	7493.943	122.589
g11	0.75	0.75	0.75	0.75	0.000
g12	1.000	1.000	1.000	1.000	0.000
g13	0.053950	0.760	0.968	1.000	0.055

deviation can be used as an indicator for the stability and robustness of the algorithm.

The results of ABCV2 in which each parameter of a mutant solution is taken from a different neighbor are given in Table 4. When the best results are investigated, an important improvement is achieved on g13 function while the performance on g10 gets worsened. When the mean and standard deviation results are analyzed, it is seen that the stability of ABCV2 is worse than ABCV1.

ABCV2 uses a global neighborhood while ABCV3 chooses the neighbors in a local topology. It is seen that the results in Table 5 are similar to the results in Table 3. Because the genotypes of the solutions in a local neighborhood resemble each other in later cycles, choosing the parameters from different neighbors does not have significant effect compared to choosing all the parameters from the same solution.

The results of ABCV4 in Table 6 suggest that there is no significant improvement when the selection strategy is changed in the onlooker bee phase of ABC algorithm. That means when an onlooker bee performs perturbation on the best solution in a neighborhood instead of a solution chosen using roulette wheel selection does not affect the algorithm performance on constrained optimization. However, it can be said that it has positive effect in the convergence rate of the algorithm in the earlier cycles.

Table 4. The results of ABCV2 variant

Problem	Optimum	Best	Mean	Worst	StdDev
g01	-15.000	-15.000	-15.000	-15.000	0.000
g02	0.803619	0.803602	0.801538	0.792962	0.003351
g03	1.000	1.000	0.988920	0.941852	0.016025
g04	-30665.539	-30665.539	-30665.539	-30665.539	0.000
g05	5126.498	5125.225	5170.748	5363.876	56.745
g06	-6961.814	-6961.814	-6961.814	-6961.814	0.000
g07	24.306	24.404	24.578	24.971	0.149894
g08	0.095825	0.095825	0.095825	0.095825	0.000
g09	680.63	680.634	680.644	680.667	0.009027
g10	7049.25	7110.214	7325.496	7655.235	125.834
g11	0.75	0.75	0.750112	0.751575	0.000356
g12	1.000	1.000	1.000	1.000	0.000
g13	0.053950	0.071093	0.326423	0.476347	0.095829

Table 5. The results of ABCV3 variant

Problem	Optimum	Best	Mean	Worst	StdDev
g01	-15.000	-15.000	-15.000	-15.000	0.000
g02	0.803619	0.803600	0.793502	0.774616	0.007767
g03	1.000	1.000	0.998776	0.934880	0.013489
g04	-30665.539	-30665.539	-30665.539	-30665.539	0.000
g05	5126.498	5126.491	5206.871	5522.573	98.799
g06	-6961.814	-6961.813	-6961.809	-6961.792	0.005644
g07	24.306	24.351	24.476	24.781	0.106532
g08	0.095825	0.095825	0.095825	0.095825	0.000
g09	680.63	680.633	680.640	680.649	0.003598
g10	7049.25	7061.397	7235.247	7440.239	117.820
g11	0.75	0.75	0.750001	0.750016	0.000002
g12	1.000	1.000	1.000	1.000	0.000
g13	0.053950	0.774675	0.975163	1.030087	0.050736

Table 6. The results of ABCV4 variant

Problem	Optimum	Best	Mean	Worst	StdDev
g01	-15.000	-15.000	-15.000	-15.000	0.000
g02	0.803619	0.803573	0.789310	0.760181	0.012939
g03	1.000	1.000	0.985268	0.964150	0.009554
g04	-30665.539	-30665.539	-30665.539	-30665.539	0.000
g05	5126.498	5126.495	5198.656	6112.214	176.557
g06	-6961.814	-6961.796	-6961.482	-6960.889	0.223100
g07	24.306	24.328	24.497	24.989	0.122971
g08	0.095825	0.095825	0.095825	0.095825	0.000
g09	680.63	680.632	680.646	680.666	0.007796
g10	7049.25	7051.682	7249.228	7494.751	105.537
g11	0.75	0.75	0.750016	0.750193	0.000037
g12	1.000	1.000	1.000	1.000	0.000
g13	0.053950	0.654826	0.778555	0.873567	0.135475

In ABC variants, ABCV5, ABCV6 and ABCV7 the search operator of DE algorithm is integrated into employed bee, onlooker bee and both phases and the results are presented in Tables 7-9, respectively. When the best solutions are investigated, it can be seen that on twelve problems g1-g12, these three variants reach the optimum. On

Table 7. The results of ABCV5 variant

Problem	Optimum	Best	Mean	Worst	StdDev
g01	-15.000	-15.000	-14.894270	-13.000	0.409793
g02	0.803619	0.803618	0.780956	0.744360	0.016786
g03	1.000	1.000	0.998049	0.968504	0.006637
g04	-30665.539	-30665.539	-30665.539	-30665.539	0.000
g05	5126.498	5126.484	5298.683	5889.126	224.498
g06	-6961.814	-6961.814	-6961.814	-6961.814	0.000
g07	24.306	24.306	24.321	24.435	0.028042
g08	0.095825	0.095825	0.095825	0.095825	0.000
g09	680.63	680.630	680.630	680.631	0.000454
g10	7049.25	7049.253	7091.954	7242.825	65.170
g11	0.75	0.75	0.75	0.75	0.000
g12	1.000	1.000	1.000	1.000	0.000
g13	0.053950	0.079478	0.484924	0.764011	0.134548

Table 8. The results of ABCV6 variant

Problem	Optimum	Best	Mean	Worst	StdDev
g01	-15.000	-15.000	-14.866	-13.000	0.498887
g02	0.803619	0.803618	0.780261	0.712447	0.020249
g03	1.000	1.000	1.000	1.000	0.000
g04	-30665.539	-30665.539	-30665.539	-30665.539	0.000
g05	5126.498	5126.484	5327.777	5809.034	220.034
g06	-6961.814	-6961.814	-6961.814	-6961.814	0.000
g07	24.306	24.306	24.317	24.384	0.019548
g08	0.095825	0.095825	0.095825	0.095825	0.000
g09	680.63	680.630	680.630	680.632	0.000655
g10	7049.25	7049.255	7082.506	7250.971	51.227
g11	0.75	0.75	0.75	0.75	0.000
g12	1.000	1.000	1.000	1.000	0.000
g13	0.053950	0.096854	0.419242	0.911652	0.178598

Table 9. The results of ABCV7 variant

Problem	Optimum	Best	Mean	Worst	StdDev
g01	-15.000	-15.000	-14.619	-11.281	1.021
g02	0.803619	0.803591	0.644725	0.471498	0.084904
g03	1.000	1.000	1.000	1.000	0.000
g04	-30665.539	-30665.539	-30665.539	-30665.539	0.000
g05	5126.498	5126.484	5339.028	5914.850	234.484
g06	-6961.814	-6961.814	-6961.814	-6961.814	0
g07	24.306	24.306	24.372	24.760	0.110926
g08	0.095825	0.095825	0.095825	0.095825	0.000
g09	680.63	680.630	680.632	680.642	0.003779
g10	7049.25	7049.251	7098.076	7469.046	107.195
g11	0.75	0.75	0.75	0.75	0.000
g12	1.000	1.000	1.000	1.000	0.000
g13	0.053950	0.058446	0.378819	0.752359	0.157990

g13 problem, only ABCV7, in which the operator is used in both employed bee and onlooker bee phases, reaches the optimum.

The results of ABCV8 in which the global best solution is exploited are presented in Table 10. In terms of the best results in the table, the results

Table 10. The results of ABCV8 variant

Problem	Optimum	Best	Mean	Worst	StdDev
g01	-15.000	-15.000	-15.000	-15.000	0.000
g02	0.803619	0.803610	0.788472	0.681864	0.022395
g03	1.000	1.000	1.000	1.000	0
g04	-30665.539	-30665.539	-30665.539	-30665.539	0.000
g05	5126.498	5126.834	5238.826	5463.804	95.606
g06	-6961.814	-6961.806	-6961.686	-6961.393	0.095273
g07	24.306	24.327	24.462	24.714	0.109640
g08	0.095825	0.095825	0.095825	0.095825	0.000
g09	680.63	680.631	680.636	680.641	0.002814
g10	7049.25	7049.997	7139.028	7426.031	71.411
g11	0.75	0.75	0.75	0.75	0.000
g12	1.000	1.000	1.000	1.000	0.000
g13	0.053950	0.494877	0.975300	1.000	0.091426

are similar to those of ABCV1 except for g13. In addition, stability of ABCV8 is also close to the basic version.

The results of the ABC algorithm with adaptive scout behavior (ABCV9) are presented in Table 11. This modification does not provide any improvement or change in the performance of the basic algorithm.

In addition to comparing the performance of the variants with control algorithm ABCV1, an overall comparison is conducted in terms of the best results in Table 12. If an algorithm is the best among all the algorithms on a problem, it is signed with + in the table and the last row indicates the number of problems the algorithm is the best. In terms of the best results, ABC variants (ABCV5, ABCV6, ABCV7) that use DE operator in employed bee and onlooker bee phases seem to be superior over the other versions.

In order to compare the algorithms, ANOVA statistical test is conducted to determine whether there is variation within or among different variants of ABC algorithm. If ANOVA test responds as there is significant difference, multiple comparisons are performed to find out which variants differ from the control algorithm, ABCV1. α value to decide an algorithm is significantly different was 0.05. F and P values produced by ANOVA are presented in Table 13. In Table 13, if the variant is significantly better than the control algorithm based on ANOVA and multiple comparisons, it is indicated by (+), else if it is significantly worse than the control algorithm, it is indicated by (−), otherwise it is reported as none. Based on ANOVA test on g01, g04, g08, g11 and g12, there is no significant difference between the variants. On g02, ABCV7 is significantly worse than the control algorithm. On g03, ABCV4 and ABCV9 are worse than ABCV1. On g05 problem, ABCV5, ABCV6 and ABCV7 which are proposed based on DE operators, are worse than ABCV1. On g06, ABCV4 and ABCV8 perform worse compared to the control algorithm. On g07, ABCV2, ABCV5, ABCV6, ABCV7 and ABCV9 differ from the control algorithm ABCV1. Among them, ABCV2 and ABCV9 are worse than ABCV1 while ABCV5, ABCV6 and ABCV7 are better than ABCV1. Similarly, on g09, ABCV5, ABCV6 and ABCV7 are better than ABCV1 while ABCV2 and ABCV4 are worse than ABCV1. On g10 problem ABCV1 shows better performance compared to ABCV2 while ABCV5, ABCV6 and ABCV7 produc better results compared to ABCV1. On g13 problem, ABCV2, ABCV4, ABCV5, ABCV6 and ABCV7 variants are better than ABCV1.

Based on these observations, it can be noted that ABCV5, ABCV6 and ABCV7 retain stability and robustness of the basic ABC algorithm and have shown the efficiency of the DE operator. It should be noted that ABC framework and basic operator has an important effect on the stability. The most stable versions are ABCV6, ABCV2 and ABCV1, respectively. Changing neighborhood topology of the basic ABC operator or making the scouts adaptive based on the fitness does not have significant effect on the performance of the algorithm.

In terms of computational cost, because ABCV2 changes the parameters based on the information each one chosen from a different neighbor, its computational cost is slightly higher than ABCV1. In each operation of ABCV3, a distance matrix is calculated based on the distances between all solution pairs and average distance is computed from the matrix. Therefore computational cost of ABCV3 is higher than ABCV1

Table 11. The results of ABCV9 variant

Problem	Optimum	Best	Mean	Worst	StdDev
g01	-15.000	-15.000	-15.000	-15.000	0.000
g02	0.803619	0.803600	0.792384	0.762961	0.008211
g03	1.000	1.000	0.983335	0.854720	0.034182
g04	-30665.539	-30665.539	-30665.539	-30665.539	0.000
g05	5126.498	5126.485	5185.711	5563.902	86.864
g06	-6961.814	-6961.814	-6961.814	-6961.814	0.000
g07	24.306	24.337	24.517	24.986	0.164383
g08	0.095825	0.095825	0.095825	0.095825	0.000
g09	680.63	680.633	680.640	680.651	0.004974
g10	7049.25	7060.585	7247.809	7729.255	151.192
g11	0.75	0.75	0.75	0.75	0.000
g12	1.000	1.000	1.000	1.000	0.000
g13	0.053950	0.754425	0.952718	0.999837	0.064039

Table 12. An overall comparison of the algorithms in terms of the best results

Problem	ABCv1	ABCv2	ABCv3	ABCv4	ABCv5	ABCv6	ABCv7	ABCv8	ABCv9
g01	+	+	+	+	+	+	+	+	+
g02					+	+			
g03	+	+	+	+	+	+	+	+	+
g04	+	+	+	+	+	+	+	+	+
g05	+	+	+	+	+	+	+		+
g06	+	+	+		+	+	+		+
g07					+	+	+		
g08	+	+	+	+	+	+	+	+	+
g09					+	+	+		
g10					+	+	+	+	
g11	+	+	+	+	+	+	+	+	+
g12	+	+	+	+	+	+	+	+	+
g13							+		
Total	8	8	8	7	12	12	12	7	8

Table 13. ANOVA Table and multiple comparisons to evaluate the results statistically. Control Algorithm is ABCV1 and α value is 0.05.

Problem	F	P	Significantly different groups
g01	1.9602	0.0518	None
g02	178.262	3.9918e-10	ABCV7 (-)
g03	7.4307	6.4332e-009	ABCV4 (-), ABCV9(-)
g04	NaN	NaN	None
g05	8.501	2.8056e-010	ABCV5 (-), ABCV6 (-), ABCV7 (-)
g06	127.985	9.1198e-086	ABCV4 (-), ABCV8(-)
g07	23.987	1.7659e-027	ABCV2(-), ABCV5 (+), ABCV6 (+), ABCV7 (+), ABCV9 (+)
g08	NaN	NaN	None
g09	36.4943	1.6439e-038	ABCV2 (-), ABCV4 (-), ABCV5 (+), ABCV6 (+), ABCV7 (+)
g10	21.2219	9.8283e-02	ABCV2 (-), ABCV5 (+), ABCV6 (+), ABCV7 (+)
g11	1.9087	0.0590	None
g12	NaN	NaN	None
g13	201.1567	6.0648e-107	ABCV2 (+), ABCV4 (+), ABCV5 (+), ABCV6 (+), ABCV7 (+)

and ABCV2. In onlooker phase of ABCV4, in order to produce a mutant solution, the best solution in a neighborhood topology which is constructed based on distances of the solutions and a radius is employed. Its computational cost is close to ABCV3 but higher than ABCV1 and

ABCV2. ABCV5, ABCV6 and ABCV7 do not employ additional procedure compared to the basic algorithm but only replaces the new solution production equation. Hence, their computational cost is close to the basic algorithm. ABCV8 uses the best solution information in its solution production. Since the best solution information is stored in a variable in all variants, it does not introduce more computational cost. In ABCV9, the counters of the solutions are divided by their probability to leave better solutions in the populations for more iterations. It is achieved by only one division operation, so it is computational cost can be assumed to be the same with the ABCV1.

The ABC algorithm is a simple optimization algorithm that can be used for constrained optimization without requiring a priori knowledge. Another advantage of ABC algorithm is that it considers both feasible solutions and infeasible solutions in the population and this provides diversity in the population. In this study, for all variants, the selection strategy is kept as simple as possible and Deb's rules are employed as constraint handling method instead of the greedy selection proposed for unconstrained optimization. However, the performance would change with a different constraint handling method. Analyzing the effect of selection strategies remains as a future work.

5. Conclusion

In this study, ABC algorithm originally proposed for unconstrained optimization has been analyzed on constrained optimization. Different variants of the algorithm have been proposed and compared in terms of efficiency and stability. Depending on the results when DE operators were integrated into ABC algorithm's onlooker phase and the employed bee phase was retained as in ABC algorithm, an improvement in the performance was gained in terms of the best solution and stability. The food source population of ABC algorithm can have both feasible solutions and infeasible solutions, so this provides diversity in the population.

Acknowledgments

This study is supported by Erciyes University, Scientific Research Projects Unit under contract number FBA-10-2959.

References

[1] Goldberg, D. E. . *Genetic Algorithms in Search, Optimization and Machine Learning*. Addison-Wesley Longman Publishing Co., Inc., Boston, MA, USA, 1st edition, 1989.

[2] C., C. A. C. . A survey of constraint handling techniques used with evolutionary algorithms. Technical report, Laboratorio Nacional de Informtica Avanzada, 1999.

[3] Holland, J. H. . *Adaptation in Natural and Artificial Systems*. University of Michigan Press, Ann Arbor, 1975.

[4] Storn, R. and Price, K. . Tr-95-01: Differential evolution-a simple and efficient adaptive scheme for global optimization over continuous spaces. Technical report, Berkeley, CA,, 1995.

[5] M., D. , V., M. , and A., C. . Tr 91-016: Positive feedback as a search strategy. Technical report, Politecnico di Milano, Italy, 1991.

[6] Kennedy, J. and Eberhart, R. C. . Particle swarm optimization. In *1995 IEEE International Conference on Neural Networks*, volume 4, pages 1942–1948", 1995.

[7] Karaboga, D. . An idea based on honey bee swarm for numerical optimization. Technical Report TR06, Erciyes University, Engineering Faculty, Computer Engineering Department, 2005.

[8] Koziel, S. and Michalewicz, Z. . Evolutionary algorithms, homomorphous mappings, and constrained parameter optimization. *Evol. Comput.*, 7(1):19–44, 1999.

[9] Karaboga, D. and Basturk, B. . *Foundations of Fuzzy Logic and Soft Computing: 12th International Fuzzy Systems Association World Congress, IFSA 2007, Cancun, Mexico, June 18-21, 2007. Proceedings*, chapter Artificial Bee Colony (ABC) Optimization Algorithm for Solving Constrained Optimization Problems, pages 789–798. Springer Berlin Heidelberg, Berlin, Heidelberg, 2007.

[10] Karaboga, D. and Akay, B. . A modified artificial bee colony (abc) algorithm for constrained optimization problems. *Applied Soft Computing*, 11(3):3021 – 3031, 2011.

[11] Deb, K. . An efficient constraint handling method for genetic algorithms. *Computer Methods in Applied Mechanics and Engineering*, 186(2- 4):311–338, 2000.

[12] Karaboga, D. and Akay, B. . A survey: Algorithms simulating bee swarm intelligence. *Artificial Intelligence Review*, 31(1):68–55, 2009.

[13] Karaboga, D. and Gorkemli, B. . A quick artificial bee colony (qabc) algorithm and its performance on optimization problems. *Applied Soft Computing*, 23:227 – 238, 2014.

[14] Akay, B. and Karaboga, D. . A survey on the applications of artificial bee colony in signal, image, and video processing. *Signal, Image and Video Processing*, 9(4):967–990, 2015.

[15] Karaboga, D. and Basturk, B. . On the performance of artificial bee colony (abc) algorithm. *Applied Soft Computing*, 8(1):687–697, 2008.

[16] Michalewicz, Z. and Schoenauer, M. . Evolutionary algorithms for constrained parameter optimization problems. *Evolutionary Computation*, 4(1):1– 32, 1995.

[17] Mezura-Montes, E. and Coello Coello, C. . A Simple Multimembered Evolution Strategy to Solve Constrained Optimization Problems. Technical Report EVOCINV-04-2003, Evolutionary Computation Group at CINVESTAV, Sección de Computación, Departamento de Ingeniería Eléctrica, CINVESTAV-IPN, México D.F., México,

2003. Available in the Constraint Handling Techniques in Evolutionary Algorithms Repository at http://www.cs.cinvestav.mx/˜constraint/.

Bahriye Akay *completed M.Sc. and Ph.D degrees in Erciyes University, Department of Computer Engineering in 2005 and 2009, respectively and performed post-doctoral studies in the University of Birmingham, UK. Her research areas include evolutionary optimization, swarm intelligence and software engineering. She has several papers related to optimization algorithms and their applications. She has been working in Erciyes University as an associated professor since 2013.*

Dervis Karaboga *received the B.Sc. degree in 1983 from the Department of Electronics Engineering, Erciyes University, Turkey and the M.Sc. degree in 1988 from the Department of Electronics and Communication Engineering, Istanbul Technical University, Turkey, and the Ph.D degree in 1994 from Systems Engineering Department, University of Wales, College of Cardiff, UK. He is currently a Professor at the Department of Computer Engineering, Erciyes University, Turkey. His research areas include optimization, fuzzy systems, neural networks, engineering applications of intelligent methods. He has two books on intelligent optimization techniques: The first one is a coauthored book (D.T. Pham and D. Karaboga, Intelligent Optimisation Techniques, Springer-Verlag, London, Surrey, UK, 2000.) and the second one (D. Karaboga, Artificial Intelligence Optimization Algorithms, Nobel Publisher, Ankara, 2004.) is in Turkish. He has several articles published in the journals and papers presented at the conferences related with the intelligent optimization methods and their applications.*

Appendix

g01: $Minimize\ f(\vec{x}) = 5\sum_{i=1}^{4} x_i - 5\sum_{i=1}^{4} x_i^2 - \sum_{i=5}^{13} x_i$

subject to

$$
\begin{aligned}
&g_1(\vec{x}) = 2x_1 + 2x_2 + x_{10} + x_{11} - 10 \leq 0\\
&g_2(\vec{x}) = 2x_1 + 2x_3 + x_{10} + x_{12} - 10 \leq 0\\
&g_3(\vec{x}) = 2x_2 + 2x_3 + x_{11} + x_{12} - 10 \leq 0\\
&g_4(\vec{x}) = -8x_1 + x_{10} \leq 0\\
&g_5(\vec{x}) = -8x_2 + x_{11} \leq 0\\
&g_6(\vec{x}) = -8x_3 + x_{12} \leq 0\\
&g_7(\vec{x}) = -2x_4 - x_5 + x_{10} \leq 0\\
&g_8(\vec{x}) = -2x_6 - x_7 + x_{11} \leq 0\\
&g_9(\vec{x}) = -2x_8 - x_9 + x_{12} \leq 0
\end{aligned}
$$

where bounds are $0 \leq x_i \leq 1\ (i = 1, \ldots, 9, 13)$, $0 \leq x_i \leq 100\ (i = 10, 11, 12)$. The global optimum is at $x^* = (1, 1, 1, 1, 1, 1, 1, 1, 1, , 3, 3, 3, 1)$, $f(x^*) = -15$. Constraints $g_1,\ g_2,\ g_3,\ g_4,\ g_5$ and g_6 are active.

g02: $Maximize\ f(\vec{x}) = \left| \frac{\sum_{i=1}^{n} \cos^4(x_i) - 2\prod_{i=1}^{n} \cos^2(x_i)}{\sqrt{\sum_{i=1}^{n} i x_i^2}} \right|$

subject to

$$
\begin{aligned}
&g_1(\vec{x}) = 0.75 - \prod_{i=1}^{n} x_i \leq 0\\
&g_2(\vec{x}) = \sum_{i=1}^{n} x_i - 7.5n \leq 0
\end{aligned}
$$

where n=20 and $0 \leq x_i \leq 10\ (i = 1, \ldots, n)$. The known global maximum is at $x_i^* = 1/\sqrt{n}\ (i = 1, \ldots, n)$, $f(x^*) = 0.803619$. g_1 is close to being active ($g_1 = -10^{-8}$)

g03: $Maximize\ f(\vec{x}) = (\sqrt{n})^n \prod_{i=1}^{n} x_i$

subject to

$$h(\vec{x}) = \sum_{i=1}^{n} x_i^2 - 1 = 0$$

where n=10 and $0 \leq x_i \leq 1\ (1 = 1, \ldots, n)$. The global maximum is at $x_i^* = 1/\sqrt(n)\ (i = 1, \ldots, n)$ where $f(x^*) = 1$

g04: $Minimize\ f(\vec{x}) = 5.3578547x_3^2 + 0.8356891x_1x_5 + 37.293239x_1 - 40792.141$

subject to

$$
\begin{aligned}
&g_1(\vec{x}) = 85.334407 + 0.0056858x_2x_5\\
&\quad +0.0006262x_1x_4 - 0.0022053x_3x_5\\
&\quad -92 \leq 0\\
&g_2(\vec{x}) = -85.334407 - 0.0056858x_2x_5\\
&\quad -0.0006262x_1x_4 + 0.0022053x_3x_5 \leq 0\\
&g_3(\vec{x}) = 80.51249 + 0.0071317x_2x_5\\
&\quad +0.0029955x_1x_2 - 0.0021813x_3^2\\
&\quad -110 \leq 0\\
&g_4(\vec{x}) = -80.51249 - 0.0071317x2x5\\
&\quad +0.0029955x_1x_2 - 0.0021813x_3^2\\
&\quad +90 \leq 0\\
&g_5(\vec{x}) = 9.300961 - 0.0047026x_3x_5\\
&\quad -0.0012547x_1x_3 - 0.0019085x_3x_4\\
&\quad -25 \leq 0\\
&g_6(\vec{x}) = -9.300961 - 0.0047026x_3x_5\\
&\quad -0.0012547x_1x_3 - 0.0019085x_3x_4\\
&\quad +20 \leq 0
\end{aligned}
$$

where $78 \leq x_1 \leq 102,\ 33 \leq x_2 \leq 45,\ 27 \leq x_i\ \leq 45$ $(i = 3, 4, 5)$. The optimum solution is $x^* = (78, 33, 29.995256025682, 45, 36.775812905788)$, where $f(x^*) = -30665.539$. Constraints g_1 and g_6 are active.

g05: *Minimize* $f(\vec{x}) = 3x_1 + 0.000001x_1^3 + 2x_2 + \left(\frac{0.000002}{3}\right)x_2^3$

subject to

$g_1(\vec{x}) = -x4 + x3 - 0.55 \leq 0$
$g_2(\vec{x}) = -x3 + x4 - 0.55 \leq 0$
$h_1(\vec{x}) = 1000\sin(-x_3 - 0.25) + 1000\sin(-x_4 - 0.25) + 894.8 - x_1 = 0$
$h_2(\vec{x}) = 1000\sin(x_3 - 0.25) + 1000\sin(x_3 - x_4 - 0.25) + 894.8 - x_2 = 0$
$h_3(\vec{x}) = 1000\sin(x_4 - 0.25) + 1000\sin(x_4 - x_3 - 0.25) + 1294.8 = 0$

where $0 \leq x_1 \leq 1200,\ 0 \leq x_2 \leq 1200, -0.55 \leq x_3 \leq 0.55$, and $-0.55 \leq x_4 \leq 0.55$. The best known solution is $x^* = (679.9453, 1026.067, 0.1188764, -0.3962336)$, where $f(x^*) = 5126.4981$.

g06: *Minimize* $f(\vec{x}) = (x_1 - 10)^3 + (x_2 - 20)^3$

subject to

$g_1(\vec{x}) = -(x_1 - 5)^2 - (x_2 - 5)^2 + 100 \leq 0$
$g_2(\vec{x}) = (x_1 - 6)^2 + (x_2 - 5)^2 - 82.81 \leq 0$

where $13 \leq x_1 \leq 100$ and $0 \leq x_2 \leq 100$. The optimum solution is $x^* = (14.095, 0.84296)$ where $f(x^*) = -6961.81388$. Both constraints are active.

g07: *Minimize* $f(\vec{x}) = x_1^2 + x_2^2 + x_1x_2 - 14x_1 - 16x_2 + (x_3 - 10)^2 + 4(x_4 - 5)^2 + (x_5 - 3)^2 + 2(x_6 - 1)^2 + 5x_7^2 + 7(x_8 - 11)^2 + 2(x_9 - 10)^2 + (x_{10} - 7)^2 + 45$

subject to

$g_1(\vec{x}) = -105 + 4x1 + 5x2 - 3x7 + 9x8 \leq 0$
$g_2(\vec{x}) = 10x_1 - 8x_2 - 17x_7 + 2x_8 \leq 0$
$g_3(\vec{x}) = -8x_1 + 2x_2 + 5x_9 - 2x_{10} - 12 \leq 0$
$g_4(\vec{x}) = 3(x_1 - 2)^2 + 4(x_2 - 3)^2 + 2x_3^2 - 7x4 - 120 \leq 0$
$g_5(\vec{x}) = 5x_1^2 + 8x_2 + (x_3 - 6)^2 - 2x_4 - 40 \leq 0$
$g_6(\vec{x}) = x_1^2 + 2(x_2 - 2)^2 - 2x_1x_2 + 14x_5 - 6x_6 \leq 0$
$g_7(\vec{x}) = 0.5(x1 - 8)2 + 2(x2 - 4)2 + 3x_5^2 - x6 - 30 \leq 0$
$g_8(\vec{x}) = -3x_1 + 6x_2 + 12(x_9 - 8)^2 - 7x_{10} \leq 0$

where $-10 \leq x_i \leq 10\ (i = 1, \ldots, 10)$. The global optimum is
$x^* = (2.171996, 2.363683, 8.773926, 5.095984, 0.9906548, 1.430574, 1.321644, 9.828726, 8.280092, 8.375927)$,
where $f(x^*) = 24.3062091$. Constraints $g_1,\ g_2,\ g_3,\ g_4,\ g_5$ and g_6 are active.

g08: *Maximize* $f(\vec{x}) = \frac{\sin^3(2\pi x_1)\sin(2\pi x_2)}{x_1^3(x_1 + x_2)}$

subject to

$g_1(\vec{x}) = x_1^2 - x_2 + 1 \leq 0$
$g_2(\vec{x}) = 1 - x_1 + (x_2 - 4)^2 \leq 0$

where $0 \leq x_i \leq 10\ (i = 1, 2)$. The optimum solution is located at $x^* = (1.2279713, 4.2453733)$, where $f(x^*) = 0.0095825$.

g09: *Minimize* $f(\vec{x}) = (x_1 - 10)^2 + 5(x_2 - 12)^2 + x_3^4 + 3(x_4 - 11)^2 + 10x_5^6 + 7x_6^2 + x_7^4 - 4x_6x_7 - 10x_6 - 8x_7$

subject to

$g_1(\vec{x}) = -127 + 2x_1^2 + 3x_2^4 + x3 + 4x_4^2 + 5x5 \leq 0$
$g_2(\vec{x}) = -282 + 7x_2 + 3x_2 + 10x_3^2 + x_4 - x_5 \leq 0$
$g_3(\vec{x}) = -196 + 23x_1 + x_2^2 + 6x_6^2 - 8x_7 \leq 0$
$g_4(\vec{x}) = 4x_1^2 + x_2^2 - 3x_1x_2 + 2x_3^2 + 5x_6 - 11x_7 \leq 0$

where $-10 \leq x_i \leq 10,\ (i = 1, \ldots, 7)$.
The global optimum is
$x^* = (2.330499, 1.951372, -0.4775414, 4.365726, -0.6244870, 1.038131, 1.594227)$,
where $f(x^*) = 680.6300573$. g_1 and g_4 constraints are active.

g10: *Minimize* $f(\vec{x}) = x_1 + x_2 + x_3$

subject to

$g_1(\vec{x}) = -1 + 0.0025(x_4 + x_6) \leq 0$
$g_2(\vec{x}) = -1 + 0.0025(x_5 + x_7 - x_4) \leq 0$
$g_3(\vec{x}) = -1 + 0.01(x_8 - x_5) \leq 0$
$g_4(\vec{x}) = -x_1x_6 + 833.33252x_4 + 100x_1 - 83.333333 \leq 0$
$g_5(\vec{x}) = -x_2x_7 + 1250x_5 + x_2x_4 - 1250x_4 \leq 0$
$g_6(\vec{x}) = -x_3x_8 + 1250000 + x_3x_5 - 2500x_5 \leq 0$

where $100 \leq x_1 \leq 10000,\ 1000 \leq x_i \leq 10000, (i = 2, 3),\ 10 \leq x_i \leq 1000, (i = 4, \ldots, 8)$. The global optimum is
$x^* = (579.19, 1360.13, 5109.92, 182.0174, 295.5985, 217.9799, 286.40, 395.5979)$, where $f(x^*) = 7049.25$. $g_1,\ g_2$ and g_3 are active.

g11: *Minimize* $f(\vec{x}) = x_1^2 + (x_2 - 1)^2$

subject to

$h(\vec{x}) = x_2 - x_1^2 = 0$

where $-1 \leq x_1 \leq 1,\ -1 \leq x_2 \leq 1$. The optimum solution is $x^* = (\pm 1/\sqrt{(2)}, 1/2)$, where $f(x^*) = 0.75$.

g12: $Maximize\ f(\vec{x}) = \frac{100-(x_1-5)^2-(x_2-5)^2-(x_3-5)^2}{100}$

subject to

$$g_1(\vec{x}) = (x_i - p)^2 + (x_2 - q)^2 + (x_3 - r)^2 - 0.0625 \leq 0$$

where $0 \leq x_i \leq 10,\ (i = 1, 2, 3)$ and $p,\ r,\ q$=$1, \ldots, 9$. The global optimum is located at $x^* = (5, 5, 5)$, where $f(x^*) = 1$.

g13: $Minimize\ f(\vec{x}) = e^{x_1 x_2 x_3 x_4 x_5}$

subject to

$$h_1(\vec{x}) = x_1^2 + x_2^2 + x_3^2 + x_4^2 + x_5^2 = 0$$
$$h_2(\vec{x}) = x_2 x_3 - 5x_4 x_5 = 0$$
$$h_3(\vec{x}) = x_1^3 + x_2^3 + 1 = 0$$

where $-2.3 \leq x_i \leq 2.3\ (i = 1, 2)$, $-3.2 \leq x_i \leq 3.2$,$(i = 3, 4, 5)$. The global optimum is $x^* = (-1.717143, 1.5957091, -0.736413, -0.763645)$, where $f(x^*) = 0.0539498$.

An International Journal of Optimization and Control: Theories & Applications (http://ijocta.balikesir.edu.tr)

An International Journal of Optimization and Control: Theories & Applications
ISSN:2146-0957 eISSN:2146-5703
Vol.7, No.1, pp.112-116 (2017)
http://doi.org/10.11121/ijocta.01.2017.00368

RESEARCH ARTICLE

On solutions of variable-order fractional differential equations

Ali Akgül[a*], Mustafa Inc[b] and Dumitru Baleanu[c]

[a] *Department of Mathematics, Siirt University,Turkey*
[b] *Department of Mathematics, Firat University, Turkey*
[c] *Department of Mathematics, Çankaya University, Turkey*
aliakgul00727@gmail.com, minc@firat.edu.tr, dumitru@cankaya.edu.tr

ARTICLE INFO

Article History:
Received 11 July 2016
Accepted 22 November 2016
Available 20 January 2017

Keywords:
Reproducing kernel functions
Series solutions
Variable-order fractional differential equation

AMS Classification 2010:
47B32, 26A33, 46E22, 74S30

ABSTRACT

Numerical calculation of the fractional integrals and derivatives is the code to search fractional calculus and solve fractional differential equations. The exact solutions to fractional differential equations are compelling to get in real applications, due to the nonlocality and complexity of the fractional differential operators, especially for variable-order fractional differential equations. Therefore, it is significant to enhance numerical methods for fractional differential equations. In this work, we consider variable-order fractional differential equations by reproducing kernel method. There has been much attention in the use of reproducing kernels for the solutions to many problems in the recent years. We give an example to demonstrate how efficiently our theory can be implemented in practice.

1. Introduction

Fractional differential equations have been studied by many investigators in recent years. The notion of a variable order operator is a much more recent improvement. Different authors have presented different definitions of variable order differential operators. The kernel of the variable order operators is too complex for having a variable-exponent. Therefore, to get the numerical solutions of variable order fractional differential equations is quite compelling. There are few studies of variable order fractional differential equations. Coimbra [1] applied a consistent approximation with first-order accurate for the solution of variable order differential equations. Lin et al. [2] worked the stability and the convergence of an explicit finite-difference approximation for the variable-order fractional diffusion equation with a nonlinear source term. Zhuang et al. [3] acquired explicit and implicit Euler approximations for the fractional advection-diffusion nonlinear equation of variable-order. For more details see [4–6]. No one had tried to find the numerical solutions of the variable order fractional differential equations by the reproducing kernel method (RKM).

The aim of our work is to investigate the efficiency of RKM to solve variable-order fractional differential equations. Let us consider

$$ {}_{C}D_{0,\nu}^{\alpha(\nu)}u(\nu) = f(\nu), \quad 0 \leq \nu \leq T, \tag{1} $$

and subjected to the initial condition

$$ u(0) = 0, \tag{2} $$

where ${}_{C}D_{0,\nu}^{\alpha(\nu)}$ is variable order fractional derivative of Caputo sense, $f(\nu)$ is the known continuous function, $u(\nu)$ is the unknown function, $0 < \alpha_{min} \leq \alpha(\nu) \leq \alpha_{max} < 1$.

The theory of reproducing kernels was used for the first time at the beginning of the 20th century by Zaremba [7]. Reproducing kernel theory has

*Corresponding Author

considerable implementations in numerical analysis, differential equations, probability and statistics [8–11]. Some authors discussed fractional differential equations, nonlinear oscillators with discontinuity, singular nonlinear two-point periodic boundary value problems, integral equations and nonlinear partial differential equations [7, 12–21].

This paper is arranged as follows. Some definitions and properties of the variable order fractional integrals and derivatives are presented in Section 2. Section 3 shows some useful reproducing kernel functions. The representation in $W_2^2[0,1]$ and a related linear operator are given in Section 4. Section 5 gives the main results. Numerical experiments are demonstrated in Section 6. Some conclusions are given in the last section.

2. Some useful definitions

(i) Riemann-Liouville fractional integral of the first kind with order $\alpha(\nu)$ is given as [22]:

$$I_{a^+}^{\alpha(\nu)}u(\nu) = \frac{1}{\Gamma(\alpha(\nu))}\int_{a^+}^{\nu}(\nu-T)^{\alpha(\nu)-1}u(T)\mathrm{d}T, \quad x>0\ [Re(\alpha(\nu))>0].$$

(ii) Riemann-Liouville fractional derivative of the first kind with order $\alpha(\nu)$ is presented by [22]:

$$D_{a^+}^{\alpha(\nu)}u(\nu) = \frac{\mathrm{d}^m}{\Gamma(m-\alpha(\nu))\mathrm{d}\nu^m}\int_{a^+}^{\nu}\frac{u(\tau)}{(\nu-\tau)^{\alpha(\nu)-m+1}}\mathrm{d}\tau,$$

but $D_{a^+}^{\alpha(\nu)}I_{a^+}^{\alpha(\nu)}u \neq u$, $(m-1\leq\alpha(\nu)<m)$.

(iii) Caputo's fractional derivative with order $\alpha(\nu)$ is introduced with [22]:

$$D^{\alpha(\nu)}u(\nu) = \frac{1}{\Gamma(1-\alpha(\nu))}\int_{0^+}^{\nu}(\nu-\tau)^{-\alpha(\nu)}u'(\tau)\mathrm{d}\tau + \frac{(u(0^+)-u(0^-))\nu^{-\alpha(\nu)}}{\Gamma(1-\alpha(\nu))},$$

where $0<\alpha(\nu)\leq 1$. If the starting time is in a perfect situation, we obtain the definition as follows [22]:

$$D^{\alpha(\nu)}u(\nu) = \frac{1}{\Gamma(1-\alpha(\nu))}\int_{0^+}^{\nu}(\nu-\tau)^{-\alpha(\nu)}u'(\tau)\mathrm{d}\tau, \quad (0<\alpha(\nu)<1),$$

with the definition above, we obtain the following formula $(0<\alpha(\nu)\leq 1)$:

$$D_*^{\alpha(\nu)}x^\beta = \begin{cases} 0, & \beta=0, \\ \frac{\Gamma(\beta+1)}{\Gamma(\beta+1-\alpha(\nu))}x^{\beta-\alpha(\nu)}, & \beta=1,2,3,\ldots. \end{cases} \tag{3}$$

3. Reproducing kernel functions

Definition 1. *We define the space* $G_2^1[0,1]$ *by*

$$G_2^1[0,1] = \{u\in AC[0,1]:\ u'\in L^2[0,1]\},$$

where AC denotes the space of absolutely continuous functions. The inner product and the norm in $G_2^1[0,1]$ *are defined by*

$$\langle u,h\rangle_{G_2^1} = u(0)h(0)+\int_0^1 u'(\nu)h'(\nu)\mathrm{d}\nu, \quad u,h\in G_2^1[0,1]$$

and

$$\|u\|_{G_2^1} = \sqrt{\langle u,u\rangle_{G_2^1}}, \quad u\in G_2^1[0,1].$$

Lemma 1 (See [23, page 17])**.** *The space* $G_2^1[0,1]$ *is a reproducing kernel space, and its reproducing kernel function* Q_y *is given by*

$$Q_y(\nu) = \begin{cases} 1+\nu, & 0\leq\nu\leq y\leq 1, \\ 1+y, & 0\leq y<\nu\leq 1. \end{cases}$$

Definition 2. *We describe the space* $W_2^2[0,1]$ *by*

$$W_2^2[0,1] = \{u\in AC[0,1]:\ u'\in AC[0,1],\ u''\in L^2[0,1],\ u(0)=0\}.$$

The inner product and the norm in $W_2^2[0,1]$ *are defined by*

$$\langle u,h\rangle_{W_2^2} = \sum_{i=0}^{1}u^{(i)}(0)h^{(i)}(0)+\int_0^1 u''(\nu)h''(\nu)\mathrm{d}\nu, \quad u,h\in W_2^2[0,1]$$

and

$$\|u\|_{W_2^2} = \sqrt{\langle u,u\rangle_{W_2^2}}, \quad u\in W_2^2[0,1].$$

Lemma 2 (See [23, page 148])**.** *The space* $W_2^2[0,1]$ *is a reproducing kernel space, and its reproducing kernel function* R_y *is given by*

$$R_y(\nu)=\begin{cases}\nu y+\frac{1}{2}\nu^2 y-\frac{1}{6}\nu^3, & 0\le\nu\le y\le 1,\\ \\ y\nu+\frac{1}{2}y^2\nu-\frac{1}{6}y^3, & 0\le\nu<y\le 1.\end{cases}$$

4. Solution representation in $W_2^2[0,1]$

In this section, the solution of (1)–(2) is presented in the $W_2^2[0,1]$. On defining the linear operator $L: W_2^2[0,1]\to G_2^1[0,1]$ by

$$Lu=_C D_{0,\nu}^{\alpha(\nu)}u(\nu),\quad 0\le\nu\le T,\quad u\in W_2^2[0,1], \tag{4}$$

model problem (1)–(2) changes to the problem

$$\begin{cases}Lu=f(\nu), & \nu\in[0,T],\\ \\ u(0)=0.\end{cases} \tag{5}$$

Theorem 1. *The linear operator L is a bounded linear operator.*

Proof. We need to show $\|Lu\|_{G_2^1}^2\le M\|u\|_{W_2^2}^2$, where $M>0$ is a positive constant. We get

$$\|Lu\|_{G_2^1}^2=\langle Lu,Lu\rangle_{G_2^1}=[Lu(0)]^2+\int_0^1\left[Lu'(\nu)\right]^2\mathrm{d}\nu.$$

We obtain

$$u(\nu)=\langle u(\cdot),R_\nu(\cdot)\rangle_{W_2^2},$$

and

$$Lu(\nu)=\langle u(\cdot),LR_\nu(\cdot)\rangle_{W_2^2},$$

by reproducing property. Therefore, we get

$$|Lu(\nu)|\le\|u\|_{W_2^2}\|LR_\nu\|_{W_2^2}=M_1\|u\|_{W_2^2},$$

where $M_1>0$. Therefore, we get

$$[(Lu)(0)]^2\le M_1^2\|u\|_{W_2^2}^2.$$

Since

$$(Lu)'(\nu)=\left\langle u(\cdot),(LR_\nu)'(\cdot)\right\rangle_{W_2^2},$$

then

$$\left|(Lu)'(\nu)\right|\le\|u\|_{W_2^2}\left\|(LR_\nu)'\right\|_{W_2^2}=M_2\|u\|_{W_2^2},$$

where $M_2>0$. Therefore, we obtain

$$\left[(Lu)'(x)\right]^2\le M_2^2\|u\|_{W_2^2}^2,$$

and

$$\int_0^1\left[(Lu)'(\nu)\right]^2\mathrm{d}\nu\le M_2^2\|u\|_{W_2^2}^2.$$

Thus, we get

$$\begin{aligned}\|Lu\|_{G_2^1}^2 &\le [(Lu)(0)]^2+\int_0^1\left(\left[(Lu)'(\nu)\right]^2\right)\mathrm{d}\nu\\ &\le \left(M_1^2+M_2^2\right)\|u\|_{W_2^2}^2=M\|u\|_{W_2^2}^2,\end{aligned}$$

where $M=M_1^2+M_2^2>0$ is a positive constant. □

5. The main results

Put $\varphi_i(\nu)=Q_{\nu_i}(\nu)$ and $\psi_i(\nu)=L^*\varphi_i(\nu)$, where L^* is conjugate operator of L. The orthonormal system $\left\{\widehat{\Psi}_i(\nu)\right\}_{i=1}^{\infty}$ of $W_2^2[0,1]$ can be obtained from Gram-Schmidt orthogonalization process of $\{\psi_i(\nu)\}_{i=1}^{\infty}$,

$$\widehat{\psi}_i(\nu)=\sum_{k=1}^{i}\beta_{ik}\psi_k(\nu),\quad(\beta_{ii}>0,\quad i=1,2,\ldots). \tag{6}$$

Theorem 2. *Let $\{\nu_i\}_{i=1}^{\infty}$ be dense in $[0,1]$ and $\psi_i(\nu)=L_yR_\nu(y)|_{y=\nu_i}$. Then the sequence $\{\psi_i(\nu)\}_{i=1}^{\infty}$ is a complete system in $W_2^2[0,1]$.*

Proof. We obtain

$$\begin{aligned}\psi_i(\nu) &= (L^*\varphi_i)(\nu)=\langle(L^*\varphi_i)(y),R_\nu(y)\rangle\\ &= \langle(\varphi_i)(y),L_yR_\nu(y)\rangle=L_yR_\nu(y)|_{y=\nu_i}.\end{aligned}$$

Let $\langle u(\nu),\psi_i(\nu)\rangle=0$, $(i=1,2,\ldots)$, which means that,

$$\langle u(\nu),(L^*\varphi_i)(\nu)\rangle=\langle Lu(\cdot),\varphi_i(\cdot)\rangle=(Lu)(\nu_i)=0.$$

$\{\nu_i\}_{i=1}^{\infty}$ is dense in $[0,1]$. Therefore, $(Lu)(\nu)=0$. $u\equiv 0$ by L^{-1}. □

Theorem 3. *If $u(\nu)$ is the exact solution of (1), then we obtain*

$$u(\nu)=\sum_{i=1}^{\infty}\sum_{k=1}^{i}\beta_{ik}f(\nu_k)\widehat{\psi}_i(\nu). \tag{7}$$

where $\{\nu_i\}_{i=1}^{\infty}$ is dense in $[0,1]$.

Proof. We obtain

$$\begin{aligned}
u(\nu) &= \sum_{i=1}^{\infty}\Big\langle u(\nu),\widehat{\psi}_i(\nu)\Big\rangle_{W_2^2}\widehat{\psi}_i(\nu)\\
&= \sum_{i=1}^{\infty}\sum_{k=1}^{i}\beta_{ik}\left\langle u(\nu),\psi_k(\nu)\right\rangle_{W_2^2}\widehat{\psi}_i(\nu)\\
&= \sum_{i=1}^{\infty}\sum_{k=1}^{i}\beta_{ik}\left\langle u(\nu),L^{*}\varphi_k(\nu)\right\rangle_{W_2^2}\widehat{\psi}_i(\nu)\\
&= \sum_{i=1}^{\infty}\sum_{k=1}^{i}\beta_{ik}\left\langle Lu(\nu),\varphi_k(\nu)\right\rangle_{G_2^1}\widehat{\psi}_i(\nu)\\
&= \sum_{i=1}^{\infty}\sum_{k=1}^{i}\beta_{ik}\left\langle f(\nu),Q_{\nu_k}\right\rangle_{G_2^1}\widehat{\psi}_i(\nu)\\
&= \sum_{i=1}^{\infty}\sum_{k=1}^{i}\beta_{ik}f(\nu_k)\widehat{\psi}_i(\nu).
\end{aligned}$$

by (6) and uniqueness of solution of (1). This completes the proof. □

The approximate solution $u_n(\nu)$ can be acquired as:

$$u_n(\nu)=\sum_{i=1}^{n}\sum_{k=1}^{i}\beta_{ik}f(\nu_k)\widehat{\Psi}_i(\nu). \tag{8}$$

6. Numerical results

To prove the efficiency and the practicability of the RKM, we give an example and find its solution.

Example 1. *Let us consider Eq. (1) at $T=1$ with*

$$f(\nu)=\frac{3\nu^{1-\alpha(\nu)}}{\Gamma(2-\alpha(\nu))}+\frac{2\nu^{2-\alpha(\nu)}}{\Gamma(3-\alpha(\nu))} \tag{9}$$

for variable order $0<\alpha(\nu)<1$, one can obtain the exact solution as $u(\nu)=3\nu+\nu^2$. Numerical results are shown in the Table 1.

Table 1. The comparisons between the RKM and the method given in [24] at T = 1 with CPU time(s)=9.469.

$\alpha(\nu)$	ν	[24]	RKM
$\nu/2$	1/4	$5.9851e-003$	$7.36735e-005$
$\nu/2$	1/8	$1.4262e-003$	$3.35160e-006$
$\nu/2$	1/16	$3.4719e-004$	$5.83687e-005$
$\nu/2$	1/32	$8.5572e-005$	$1.44027e-004$
$\nu/2$	1/64	$2.1234e-005$	$6.39753e-004$
$sin(\nu)$	1/4	$2.4701e-002$	$3.34572e-004$
$sin(\nu)$	1/8	$5.6021e-003$	$1.54293e-005$
$sin(\nu)$	1/16	$1.3335e-003$	$9.04701e-005$
$sin(\nu)$	1/32	$3.2530e-004$	$1.70832e-004$
$sin(\nu)$	1/64	$8.0317e-005$	$6.50846e-004$

7. Conclusion

We used the reproducing kernel method to solve a class of the variable order fractional differential equation in this work. We defined the method and used it in the test example in order to prove its applicability and validity in comparison with exact and other numerical solutions. The obtained results are uniformly convergent and the operator that was used is a bounded linear operator.

References

[1] Coimbra, C. F. M. . Mechanics with variable-order differential operators. *Ann. Phys.*, 12(11-12):692–703, 2003.

[2] Lin, R. , Liu, F. , Anh, V. , and Turner, I. . Stability and convergence of a new explicit finite-difference approximation for the variable-order nonlinear fractional diffusion equation. *Appl. Math. Comput.*, 212(2):435–445, 2009.

[3] Zhuang, P. , Liu, F. , Anh, V. , and Turner, I. . Numerical methods for the variable-order fractional advection-diffusion equation with a nonlinear source term. *SIAM J. Numer. Anal.*, 47(3):1760–1781, 2009.

[4] Sun, H. , Chen, W. , and Chen, Y. Q. . Variable order fractional differential operators in anomalous diffusion modeling. *Physica A: Statistical Mechanics and its Applications*, 388(388):4586–4592, 2009.

[5] Sun, H. , Chen, W. , Li, C. , and Chen, Y. Q. . Finite difference schemes for variable-order time fractional diffusion equation. *International Journal of Bifurcation and Chaos*, 22(4)(22(4)):1250085 (16 pages), 2012.

[6] Sun, H. , Chen, W. , Wei, H. , and Chen, Y. . A comparative study of constant-order and variable-order fractional models in characterizing memory property of systems. *Eur. Phys. J. Special Topics*, 193(193):185–192, 2011.

[7] Aronszajn, N. . Theory of reproducing kernels. *Trans. Amer. Math. Soc.*, 68:337–404, 1950.
[8] Geng, F. and Cui, M. . A reproducing kernel method for solving nonlocal fractional boundary value problems. *Appl. Math. Lett.*, 25(5):818–823, 2012.
[9] Wang, Y. , Su, L. , Cao, X. , and Li, X. . Using reproducing kernel for solving a class of singularly perturbed problems. *Comput. Math. Appl.*, 61(2):421–430, 2011.
[10] Wu, B. Y. and Li, X. Y. . A new algorithm for a class of linear nonlocal boundary value problems based on the reproducing kernel method. *Appl. Math. Lett.*, 24(2):156–159, 2011.
[11] Yao, H. and Lin, Y. . Solving singular boundary-value problems of higher even-order. *J. Comput. Appl. Math.*, 223(2):703–713, 2009.
[12] Akgül, A. . A new method for approximate solutions of fractional order boundary value problems. *Neural Parallel Sci. Comput.*, 22(1-2):223–237, 2014.
[13] Akgül, A. . New reproducing kernel functions. *Math. Probl. Eng.*, pages Art. ID 158134, 10, 2015.
[14] Akgül, A. , Inc, M. , Karatas, E. , and Baleanu, D. . Numerical solutions of fractional differential equations of Lane-Emden type by an accurate technique. *Adv. Difference Equ.*, page 2015:220, 2015.
[15] Akgül, A. and Kiliçman, A. . Solving delay differential equations by an accurate method with interpolation. *Abstr. Appl. Anal.*, pages Art. ID 676939, 7, 2015.
[16] Inc, M. and Akgül, A. . Approximate solutions for MHD squeezing fluid flow by a novel method. *Bound. Value Probl.*, pages 2014:18, 17, 2014.
[17] Inc, M. and Akgül, A. . Numerical solution of seventh-order boundary value problems by a novel method. *Abstr. Appl. Anal.*, pages Art. ID 745287, 9, 2014.
[18] Inc, M. , Akgül, A. , and Kiliçman, A. . Explicit solution of telegraph equation based on reproducing kernel method. *J. Funct. Spaces Appl.*, pages Art. ID 984682, 23, 2012.
[19] Inc, M. , Akgül, A. , and Kılıçman, A. . A new application of the reproducing kernel Hilbert space method to solve MHD Jeffery-Hamel flows problem in nonparallel walls. *Abstr. Appl. Anal.*, pages Art. ID 239454, 12, 2013.
[20] Inc, M. , Akgül, A. , and Kiliçman, A. . A novel method for solving KdV equation based on reproducing kernel Hilbert space method. *Abstr. Appl. Anal.*, pages Art. ID 578942, 11, 2013.
[21] Inc, M. , Akgül, A. , and Kılıçman, A. . Numerical solutions of the second-order one-dimensional telegraph equation based on reproducing kernel Hilbert space method. *Abstr. Appl. Anal.*, pages Art. ID 768963, 13, 2013.
[22] Wang, J. , Liu, L. , Liu, L. , and Chen, Y. . Numerical solution for the variable order fractional partial differential equation with Bernstein polynomials. *International Journal of Advancements in Computing Technology(IJACT)*, pages Volume 6, Number 3, May 2014.
[23] Cui, M. and Lin, Y. . *Nonlinear numerical analysis in the reproducing kernel space*. Nova Science Publishers Inc., New York, 2009.
[24] Cao, J. and Qiu, Y. . A high order numerical scheme for variable order fractional ordinary differential equation. *Appl. Math. Lett.*, 61:88–94, 2016.

Ali Akgül *is an Associate Professor at the Department of Mathematics, Art and Science Faculty, Siirt University. He received his B. Sc. (2005) and M. Sc. (2010) degrees from Department of Mathematics, Dicle University, Turkey and Ph.D (2014) from Frat University, Turkey. His research areas includes Differential Equations and Functional Analysis.*

Mustafa Inc *is a full Professor at the Department of Mathematics, Frat University, Turkey. He received his B.Sc. (1992), M.Sc. (1997) and obtain his PhD. (2002) degrees from Department of Mathematics, Frat University, Turkey. His research areas includes differential equations, solitons and integral equations.*

Dumitru Baleanu *is a full Professor at the Department of Mathematics, Çankaya University, Turkey. He received his B.Sc. from University of Craiova, M.Sc. from University of Bucharest and obtain his PhD. from Institute of Atomic Physics, Romania. His research areas includes fractional differential equations.*

An International Journal of Optimization and Control: Theories & Applications
ISSN: 2146-0957 eISSN: 2146-5703
Vol.7, No.1, pp.117-129 (2017)
https://doi.org/10.11121/ijocta.01.2017.00373

RESEARCH ARTICLE

Optimizing the location-allocation problem of pharmacy warehouses: A case study in Gaziantep

Eren Özceylan[a *], Ayşenur Uslu[b], Mehmet Erbaş[c], Cihan Çetinkaya[a], Selçuk Kürşat İşleyen[d]

[a] *Department of Industrial Engineering, Gaziantep University, Turkey*
[b] *Department of Industrial Engineering, Başkent University, Turkey*
[c] *General Command of Mapping, Ministry of National Defense, Ankara, Turkey*
[d] *Department of Industrial Engineering, Gazi University, Turkey*
erenozceylan@gmail.com, aysenur@baskent.edu.tr, merbas55@gmail.com, cihancetinkaya@gantep.edu.tr, isleyens@gazi.edu.tr

ARTICLE INFO

Article history:
Received: 26 July 2016
Accepted: 10 January 2017
Available Online: 20 January 2017

Keywords:
P-median
P-center
Set covering
GIS
Network analysis

AMS Classification 2010:
90B90, 90B80

ABSTRACT

It is a known fact that basic health care services cannot reach the majority of the population due to poor geographical accessibility. Unless quantitative location-allocation models and geographic information systems (GIS) are used, the final decision may be made on pragmatic considerations which can result far from optimal. In this paper, current and possible (or potential) new locations of pharmacy warehouses in Gaziantep are investigated to provide optimal distribution of hospitals and pharmacies. To do so, first of all, geographic information of 10 current and 10 potential pharmacy warehouses, 231 pharmacies and 29 hospitals are gathered using GIS. Second, a set covering mathematical model is handled to determine coverage capability of current and potential pharmacy warehouses and minimize the number of warehouses to be opened. Finally, P-center and P-median mathematical models are applied to open potential warehouses and to assign pharmacies & hospitals to the opened warehouses so that the total distance and the demand's longest distance to the source are minimized. Developed integer programming (IP) models and GIS software are compared with on a case study. Computational experiments prove that our approach can find new potential pharmacy warehouses which cover wider areas than current warehouses to service pharmacies and hospitals in the city.

1. Introduction

In health care services context, pharmacies are the medicine markets that we try to reach quickly in case of any illness. Pharmacists are part of the healthcare team and provide advice to patients, case management, and benefits management. Thus, pharmacists have an important role in helping prevent medication errors and in identifying drug interactions and pharmaceutical care is an important aspect of the spectrum of healthcare.

Continuous expansions of the city, development of multi-center urban structure and changes in population density have affected the spatial distribution of needs and demand for pharmacies. The aforementioned challenges make utilization of effective health care services more difficult. Besides rural regions, urban areas may also be unable to get transportation to the nearest pharmacy due to mentioned obstacles. While the growth of Internet and mail-order pharmacies might suggest that geographical limits to access are no longer a concern, many rural and urban residents do not have the equipment, technical skills, and/or telecommunications accessibility that these services require [1].

Especially in developing countries, pharmacies play an important role, in providing information and advice on health to low-income people. However, unbalanced distribution of pharmacies with respect to population and resources (such as warehouses and hospitals) would severely limit the accessibility of pharmacy services.

Thus, one of the principal reasons for the success of a pharmacy is suitable location and number of existing pharmacies. Despite this, locations and selection of

*Corresponding author

new pharmacies are too often selected in an unscientific manner. Sometimes pharmacies suffer because they are just outside the flow of traffic [2]. Unless quantitative location-allocation models are used, the final decision may be given on pragmatic considerations which can result far from optimal. Pharmacy distribution depends greatly on geographical location; approximately 35.45% of community pharmacies are found in Istanbul (19.90%), Ankara (8.32%) and Izmir (7.23%), where 30.60% of the population lives. Table 1 indicates top 10 cities in terms of population with number of pharmacies, number of people per pharmacy and number of required pharmacies. The regulation about controlling of number of pharmacies was published in the Turkish official gazette on May 17, 2012. According to published directive, number of pharmacies is determined per 3500 people. As it can be seen from Table 1, there are 4840 pharmacies which serve all people in İstanbul while 4188 pharmacies are enough. So, 652 pharmacies in İstanbul are surplus. As opposite, 75 pharmacies are deficit in Gaziantep which is the 8th most crowded city in Turkey. Totally 1821 pharmacies are unnecessary in Turkey [3]. The most important indicator in Table 1 is that, although there are redundant pharmacies in Turkey, optimal location and allocation of existing pharmacies is lacking.

Table 1. Top 10 cities with pharmacies in Turkey [4].

Cities	No. Pharmacies	Population	No. People per Pharmacy	No. Required Pharmacies	Gap
İstanbul	4840	14657434	3029	4188	652
Ankara	2023	5270575	2606	1506	517
İzmir	1759	4168415	2370	1191	568
Bursa	828	2842547	3434	813	15
Antalya	1013	2288456	2260	654	359
Adana	653	2183167	3344	624	29
Konya	711	2130544	2997	609	102
Gaziantep	477	1931836	4050	552	**-75**
Şanlıurfa	370	1892320	5115	541	**-171**
Kocaeli	431	1780055	4131	509	**-78**
Turkey	24319	78741053	3238	22498	1821

Many factors as proximity to hospitals, proximity to pharmacy warehouses and coverage level are effective in spatial distribution of pharmacies in settlement areas. This distribution is noteworthy in urban places especially in metropolitan areas. Thus spatial distribution of pharmacies affects their accessibility and provided services which must be socially available. To give satisfactory decisions for location and allocation of pharmacies, mathematical models and GISs are the most common tools in literature and practice [5].

Considering this situation, in this paper; current and possible new locations of pharmacy warehouses in Gaziantep are investigated to provide optimal distribution of hospitals and pharmacies. To do so, a two-step approach is followed. First, geographic information of 10 current and 10 potential pharmacy warehouses, 231 pharmacies and 29 hospitals are gathered using GIS. Secondly, set covering, P-center and P-median models are applied to setup potential warehouses then assign pharmacies and hospitals to the opened warehouses so that the total transportation distance can be minimized. Then this approach is applied to an illustrative case study in Gaziantep.

The remainder of the paper is organized as follows. Next section, we provide an overview and a summary of the existing literature of mathematical location-allocation models and GIS on healthcare services. Section 3, describes and gives details about proposed location-allocation models. Section 4 contains both computational experiments and a case study, and finally Section 5 presents our conclusion.

2. Literature review

This section presents a brief review on the location-allocation models for healthcare service problems, followed by the same steps for GIS applications.

2.1. Location-allocation models on healthcare services

Location-allocation models try to determine the optimal location for facilities and assign customers to these facilities in order to meet their demands. There are many studies in the literature related to facility location problems, which attracts the researchers for more than 50 years. In this context, the studies of Daskin [6], Owen and Daskin [7], Narula [8], Arabani and Farahani [9] can be examined. The location-allocation problems can be classified generally as public location problems (e.g., school, clinics, hospital, ambulance etc.) and private location problems (e.g., retail store, industrial facilities etc.). While cost minimization is important in private location problems, it is more important to ensure the accessibility of the facility in public location problems [10].

The application of location-allocation models in healthcare services are explained in Rahman and Smith [11], Daskin and Dean [12], Rais and Viana [13] and Afshari and Peng [14]. In Rahman and Smith [11], the location-allocation models for healthcare service are gathered in 2 categories such as single level models and hierarchical models. The single level models are used for determining the most suitable places for health care system facilities. P-median, P-center, set covering and maximal covering models are evaluated in this perspective. Hierarchical models are problems in which the upper level and lower level facilities are considered together [15]. Mestre et al. [16], Farahani et al. [17] and Teixeira and Antunes [18] can be examined as examples of hierarchical models in healthcare services.

A summary of the literature related to the single-level facility location-allocation models are given in Table 2. Also, Harper et al. [28], Abdelaziz and Masmoudi [29] and Mestre et al. [30], suggested stochastic models for planning healthcare facilities. Lovejoy and Li [31], Stummer et al. [32] have proposed multi

objective approaches in the literature.

Table 2. A summary of the literature.

Source	Solution Method	Application Area
Berghmans et al. [19]	P-center and set covering models	Determining the number of new healthcare facility in Saudi Arabia
Tavakoli and Lightner [20]	Set covering model	Locating/allocating emergency vehicles in Fayetteville, NC
Jia et al. [21]	Maximal covering model	Determining the facility locations of medical supplies
Jia et al. [22]	P-median, P-center and covering models	Optimizing the locations of facilities for medical supplies in Los Angeles
Shariff et al. [23]	Capacitated maximal covering model	New healthcare facility location in Malaysia
Valipour et al. [24]	Maximal covering model and particle swarm optimization	Determining new healthcare facility locations
Jia et al. [25]	Modified P-median model	Determining three location for healthcare facility in China
Kunkel et al. [26]	P-median and capacitated facility location models	Distribution of health resources in Malawi
Guerriero et al. [27]	P-median, P-center, set covering models and mathematical formulation for network reorganization problem	Public hospital network reorganization in Italy

2.2. GIS applications on healthcare services

GIS is a computer based system that collects, stores, analyzes and displays spatial data according to their locations [33]. The most powerful aspect of GIS is performing spatial analyses for getting information in many fields. Network analysis has been used extensively to examine relationships between organizations. This type of analysis can be used to find the shortest routes or to find the service areas of facilities. GIS has become an important tool in healthcare activities such as database management, planning, emergency situations, service area problems etc.[34,35]. It is also used as a decision making system that helps the managers in better planning, utilization of available health resources and improving health care delivery [35, 36].

Lovett et al [37] examined accessibility to surgeries by GIS. High-risk emergency maps are generated by Grekousis and Photis [38]. They analyzed health emergency data and revealing relationships in GIS, in order to show where strokes are likely to occur. Geographic distribution is used to compare GP clinics and musculoskeletal health care clinics in Sanders et al. [39]. Travel distance between women with breast cancer and the nearest mammography facility is analyzed by Huang et al. [40]. Pearce et al. [41] applied GIS to calculate travel time for geographical access to health facilities. Network analysis is used to select rotary air transport or ground transport of a burn care facility by Klein et al. [42], McLafferty [36] provide timely emergency responses for ambulance services.

As it seen from the reviewed studies in above, application of mathematical modeling and GIS approaches to location and allocation problems in healthcare is still lacking. To the best of our knowledge, the proposed study which applies three different location and allocation models and GIS to pharmacy warehouses location and allocation problem is the first as a case study. The contributions of this paper are twofold and are stated as follows: (i) To apply well-known three location-allocation models to pharmacy warehouses distribution problem, and (ii) To compare IP models and GIS software. In practical side, potential pharmacies offered by the proposed model provide better service quality than the current pharmacies.

3. Location-allocation models

Pharmacy logistics is an important issue in healthcare services. Thus, determining the locations of pharmacies and pharmacy warehouses are strategic decisions. In this section, the location-allocation models -which are used in this study to ensure the optimal distribution of the pharmacy warehouses to hospitals and pharmacies-, are described.

3.1. Set covering problem

G (*N*, *A*) is a fully connected network and *N* is the set of nodes while *A* is set of edges between these nodes. *N* consists of nodes, *I* consists of customers and *K* consists of potential warehouses. There are distances identified as d_{ik} between all node pairs within the network. The set covering problem is identified as a facility location selection problem in a way to reach every cluster at least once in a predetermined time on this network. Farahani et al. [43], Caprara et al. [44] and Li et al. [45] can be examined as set covering problem examples. The formulation of the set covering problem is as follows [46]:

Decision variables:

$y_k = 1$, if potential warehouse k is opened ($\forall k \in K$); 0 otherwise

Objective function:

$$\text{Min } Z = \sum_{k \in K} y_k \quad (1)$$

s. t.

$$\sum_{k \in K} a_{ik} y_k \geq 1 \qquad \forall i \in I \quad (2)$$

$$y_k \in \{0, 1\} \qquad \forall k \in K \quad (3)$$

The objective function (1) is to minimize the number of facilities to be opened. Constraint (2) is to provide service from at least one opened warehouse to all pharmacies and hospitals within the predetermined time. Constraint (3) is the integrality constraint of the decision variable. Here, a_{ik} is 1, if can be reached from *k* to *i* in a predetermined time; 0 otherwise.

3.2. P-median problem

On the network which is defined in sub-section 3.1, positive demand identified as w_i and transportation costs per unit between all customers identified as c_{ik} are taken into consideration. The P-median problem

tries to determine *P* amount candidate facility that is to open and which customers will be assigned to each facility. The P-median problem was examined in literature for the first time by Hakimi [47]. Kariv and Hakimi [48] proved that the problem is a combinatorial NP-Hard problem. The formulation of the P-median problem is as follows [18]:

Decision variables:

$y_k = 1$, if potential warehouse k is opened ($\forall k \in K$); 0 otherwise

$x_{ik} = 1$, if customer i is assigned to potential warehouse k ($\forall i \in I, \forall k \in K$); 0 otherwise

Objective function:

$$\text{Min } Z = \sum_{i\in I}\sum_{k\in K} w_i c_{ik} x_{ik} \quad (4)$$

s. t.

$$\sum_{k\in K} x_{ik} = 1 \qquad \forall i \in I \quad (5)$$

$$x_{ik} \le y_k \qquad \forall i \in I, \forall k \in K \quad (6)$$

$$\sum_{k\in K} y_k = P \quad (7)$$

$$y_k, x_{ik} \in \{0,1\} \qquad \forall i \in I, \forall k \in K \quad (8)$$

The objective function (4) is to minimize total costs. Constraint (5) provides the assignment of each customer to a warehouse, while Constraint (6) provides the assignment of customers to the opened warehouses Constraint (7) determines the number of warehouses which should be opened. Constraint (8) is the integrality constraint of the decision variables.

3.3. P-center problem

The P-center problem tries to determine *P* amount candidate facility that is to open and which customers will be assigned to each facility while minimizing the customer's longest distance to the facility. The formulation of the P-center problem is as follows [6]:

Decision variables:

$y_k = 1$, if potential warehouse k is opened ($\forall k \in K$); 0 otherwise

$x_{ik} = 1$, if customer i is assigned to potential warehouse k ($\forall i \in I, \forall k \in K$); 0 otherwise

Objective function:

$$\text{Min } Z = \text{Max}(d_{ik} x_{ik}) \quad (9)$$

s. t.

Constraints (5) *to* (8)

For the linearization of the model the *MaxL* decision variable is added. The objective function is written as $Z = \text{MaxL}$ and $\text{MaxL} \ge d_{ik} x_{ik}$ and $\text{MaxL} \ge 0$ constraints are added to the model.

4. Computational experiments

In this section, the current and potential locations of pharmacy warehouses in the province of Gaziantep are examined and the results are discussed using mathematical models described in the previous section. Finally, GIS software results and proposed mathematical model's results are compared.

4.1. Case study

This section presents the results of implementing the proposed technique on a city-wide area. Gaziantep is the 8th most crowded city of Turkey. The city has a mean elevation of 706 meters, and in 2015, its population was 1,931,836 with a total acreage of 7,642km2. The city is an important commercial and industrial center for Turkey and it is located at 37°04′North, 37°23′East. The biggest two districts of Gaziantep, namely Şehitkamil and Şahinbey, are considered as our study area (Figure 1).

Figure 1. Location map of the study area.

Firstly, 231 pharmacies, 29 hospitals, 10 current warehouses and potential 10 pharmacy warehouses are determined with GIS then the distances are calculated. The locations of potential pharmacy warehouses are determined by Gaziantep Chamber of Pharmacies. All facilities in the case study are shown in Figures 2 and 3. The spatial positions of every facility (hospitals, pharmacies, current and potential pharmacy warehouses) are defined by geographic coordinates (longitude and latitude). ESRI ArcGIS 10.2 software as a GIS tool is used to calculate the real distances between the facilities in the network.

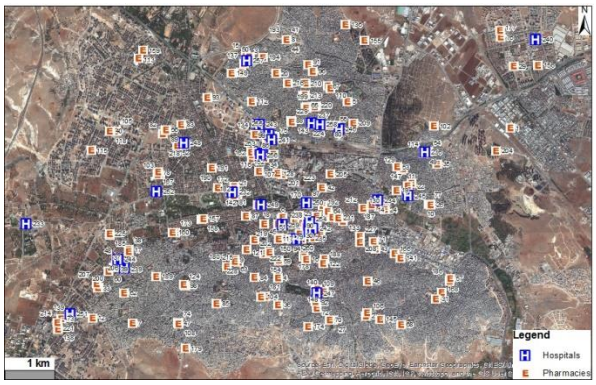

Figure 2. Considered 29 hospitals and 231 pharmacies in Gaziantep city center.

After determining the all facility locations, road network of Gaziantep is used to calculate distance between facilities rather than top view distances. For instance, Figure 4 shows the network distance between 1st current pharmacy warehouse and 190th pharmacy. While top view distance between two facilities is 2502 meters, network distance getting from the road network of Gaziantep is 2993 meters. The network distances between the all facility types' are available upon request.

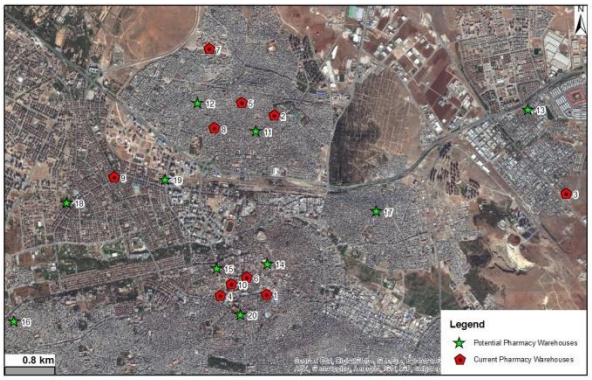

Figure 3. Considered 10 current and 10 potential pharmacy warehouses in Gaziantep city center.

Figure 4. Network distance between 1st current pharmacy warehouse and 190th pharmacy.

4.2. Application of location-allocation models

In this section, three different location-allocation models named as set covering, P-median and P-center problems are applied to different scenarios in Gaziantep city center. Generated scenarios based on locations of pharmacy warehouses are described in below:

Scenario1: This is the situation which considers 10 current pharmacy warehouses in Gaziantep city center.

Scenario2: This is the situation which considers 10 potential pharmacy warehouses instead of 10 current pharmacy warehouses in Gaziantep city center.

Scenario3: This is the situation which considers 10 current and 10 potential pharmacy warehouses together in Gaziantep city center. In other words, there are 20 pharmacy warehouses in this scenario.

Set covering, P-median and P-center models are applied to aforementioned scenarios and results are given below. It is noted that all IP runs were completed on a server with 1.8 GHz Intel Core processor and 4 GB of RAM. The computation time required to solve the model using the GAMS-CPLEX solver is less than 10 CPU seconds.

4.2.1. Solution of set covering problem

The set covering model is primarily solved with the data obtained on the basis of GIS to investigate the coverage ability of three scenarios. To do so, 6 different coverage areas in the range of 1km and 6km are examined. The results are presented in Table 3.

Table 3. Results of set covering model using IP.

Coverage area (m)	Scenarios	No. demand points in coverage area	No. demand points out of the coverage area	Opened warehouses	Number of opened warehouses
1000	Scenario1	*	*	*	*
	Scenario2	*	*	*	*
	Scenario3	*	*	*	*
2000	Scenario1	*	*	*	*
	Scenario2	*	*	*	*
	Scenario3	*	*	*	*
3000	Scenario1	*	*	*	*
	Scenario2	*	*	*	*
	Scenario3	*	*	*	*
4000	Scenario1	*	*	*	*
	Scenario2	260	0	12-13-15-16	4
	Scenario3	260	0	3-8-10-16	4
5000	Scenario1	*	*	*	*
	Scenario2	260	0	17-18	2
	Scenario3	260	0	17-18	2
6000	Scenario1	260	0	2-9	2
	Scenario2	260	0	16-17	2
	Scenario3	260	0	2-9	2

*Infeasible solution

The results given in Table 3 indicate that, IP model cannot find an optimal solution for 1km, 2km and 3km coverage areas. To make a comparison and get a detailed solution, set covering tool of ArcGIS Network Analysis tool is also applied to the problem. Network Analysis tool is based on the well-known Dijkstra's algorithm for finding shortest paths. The classic Dijkstra's algorithm solves a shortest-path problem on an undirected, nonnegative weighted graph.

Table 4. Results of set covering model using GIS.

Coverage area (m)	Scenarios	No. demand points in coverage area	No. demand points out of the coverage area	Opened warehouses	Number of opened warehouses
1000	Scenario1	105	155	1-2-4-6-7-8-9	7
	Scenario2	164	96	11-12-13-14-15-16-17-18-19-20	10
	Scenario3	174	86	1-4-7-9-11-12-13-14-15-16-17-18-19-20	14
2000	Scenario1	187	73	1-3-4-5-9	5
	Scenario2	234	26	11-12-13-14-15-16-17-18-19-20	10
	Scenario3	238	22	4-5-13-14-16-17-18-19-20	9
3000	Scenario1	225	35	1-2-3-4-9	5
	Scenario2	259	1	12-13-14-16-18-20	6
	Scenario3	259	1	1-8-9-13-16-17	6
4000	Scenario1	246	14	3-8-9-10	4
	Scenario2	260	0	12-13-15-16	4
	Scenario3	260	0	8-10-13-16	4
5000	Scenario1	254	6	3-4-5-9	4
	Scenario2	260	0	17-18	2
	Scenario3	260	0	17-18	2
6000	Scenario1	260	0	2-9	2
	Scenario2	260	0	17-18	2
	Scenario3	260	0	9-17	2

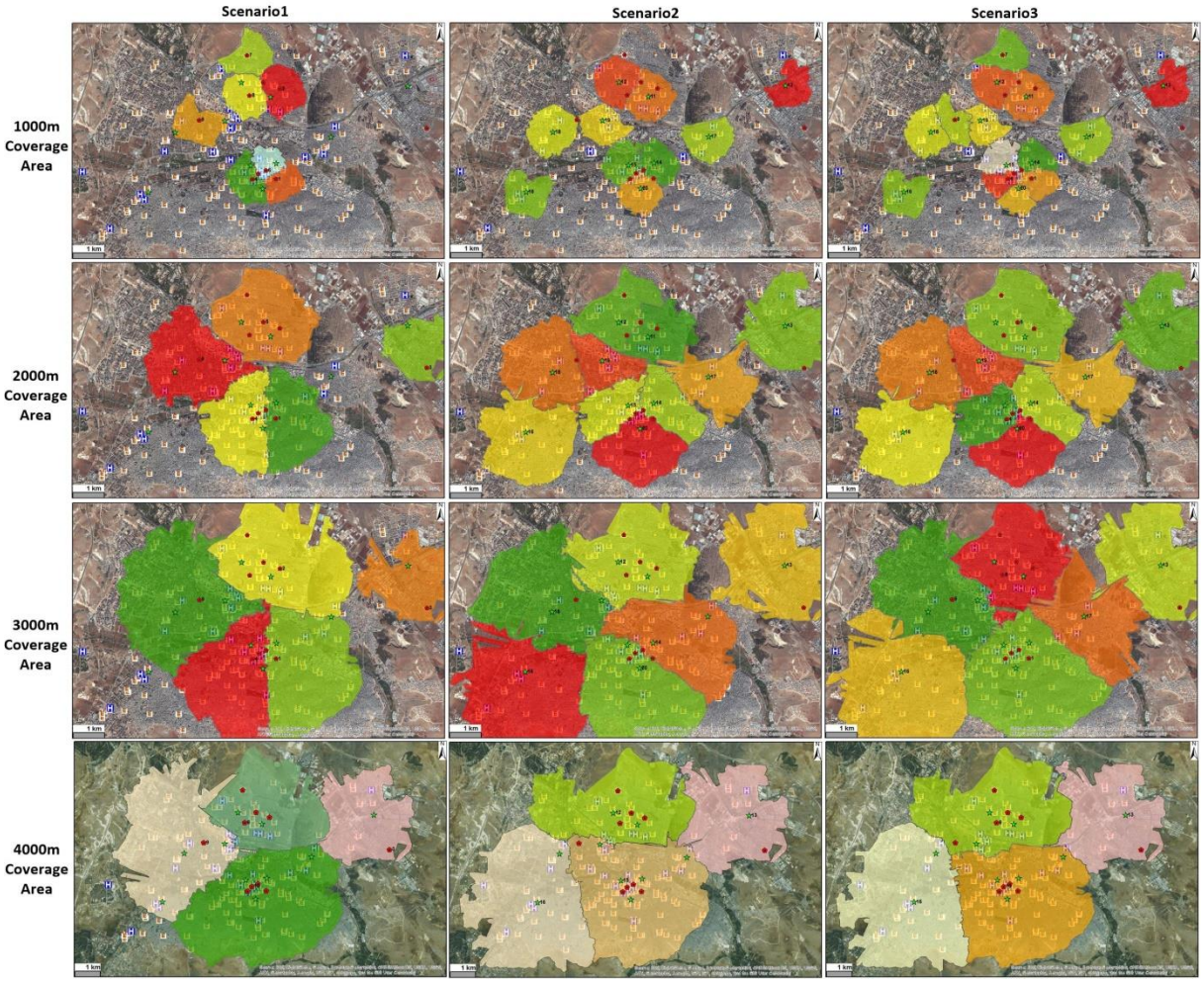

Figure 5. Set covering problem results obtained by GIS

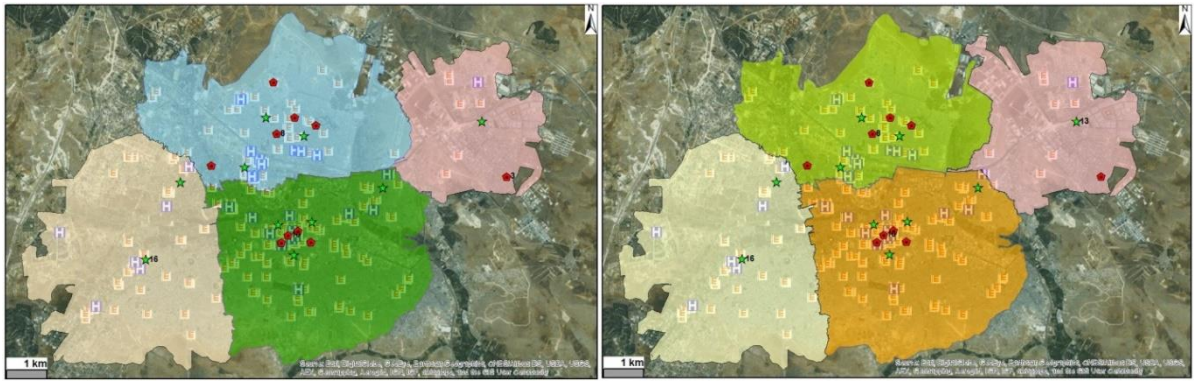

Figure 6. Comparison of IP (left) and GIS (right) for set covering problem (coverage area is 4000m for Scenario 3).

To use it within the context of real-world transportation data, this algorithm is modified to respect user settings such as one-way restrictions, turn restrictions, junction impedances, barriers, and side-of-street constraints while minimizing a user-specified cost attribute. The performance of Dijkstra's algorithm is further improved by using better data structures such as d-heaps. The d-heap is a priority queue data structure, a generalization of the binary heap in which the nodes have d children instead of 2. In additio, the algorithm needs to be able to model the locations anywhere along an edge, not just on junctions. Table 4 gives the results obtained by ArcGIS Network Analysis tool.

According to results of Tables 3 and 4, the following outcomes can be obtained:

• It is clear that Scenarios 2 and 3 have wider coverage ability than the Scenario 1 in all coverage area except in 6km. For example, while current pharmacy warehouses (Scenario 1) can cover 246 pharmacies and hospitals, Scenarios 2 and 3 can cover all the demand points in 4km coverage area. This result shows that current warehouses are not enough for supplying hospitals and pharmacies (Figure 5).

• While IP finds infeasible solutions in some coverage areas (Table 3), GIS provides detailed results for all coverage areas (Table 4). However, obtained number of demand points in and out of coverage areas is the same for both solutions.

• In some coverage areas, although IP and GIS cover all demand points, opened pharmacy warehouses can be different. For instance, while IP model opened 3rd, 8th, 10th and 16th warehouses, GIS opened 8th, 10th, 13th and 16th warehouses for 4km coverage area (Figure 6). It means that there are at least two ways on which warehouses will be opened to cover all demand points.

• As expected, increasing the coverage area also increases the covered demand points. Increasing the coverage area from 1km to 6km leads to an increment from 40% to 100% coverage percentage for current warehouses (Figure 7).

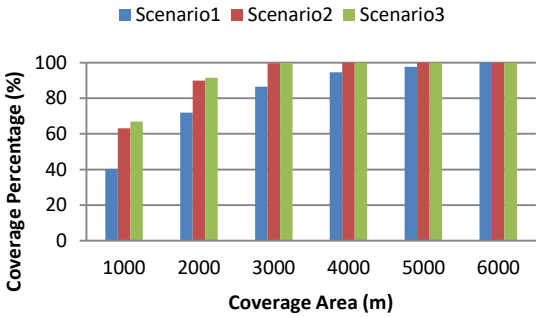

Figure 7. Coverage percentages in different coverage areas.

Table 5. Fixed costs of potential pharmacy warehouses.

	Potential pharmacy warehouses				
	1	**2**	**3**	**4**	**5**
Fixed cost (f_k)($)	8151	7736	6556	6989	5769
	6	**7**	**8**	**9**	**10**
	5942	5368	6252	7076	5360

In addition to analysis above, set covering problem with fixed costs of potential pharmacy warehouses are considered. To do so, data between 5000$ and 1000$ are generated randomly for each potential pharmacy warehouse (Table 5). A parameter (f_k) which represents the fixed cost of potential warehouse (k) is added to the objective function (Eq. 1) of set covering problem.

Table 6. Results of set covering problem with fixed costs solved by IP.

				With fixed-costs		Without fixed-costs	
Coverage area(m)	**Scenarios**	**No. demand points in coverage area**	**No. demand points out of the coverage area**	**Opened warehouses**	**Number of opened warehouses**	**Opened warehouses**	**Number of opened warehouses**
1000	**Scenario2**	*	*	*	*	*	*
	Scenario3	*	*	*	*	*	*
2000	**Scenario2**	*	*	*	*	*	*
	Scenario3	*	*	*	*	*	*
3000	**Scenario2**	*	*	*	*	*	*
	Scenario3	*	*	*	*	*	*
4000	**Scenario2**	260	0	**12-13-16-20**	4	**12-13-15-16**	4
	Scenario3	260	0	3-8-10-16	4	3-8-10-16	4
5000	**Scenario2**	260	0	17-18	2	17-18	2
	Scenario3	260	0	**3-4-5-16**	4	**17-18**	2
6000	**Scenario2**	260	0	16-17	2	16-17	2
	Scenario3	260	0	2-9	2	2-9	2

* Infeasible solution

Set covering problem with fixed cost is applied to Scenarios 2 and 3 due to consideration of potential warehouses. The results are presented in Table 6 which also shows the related part of solutions without fixed-costs. As it is seen, all demand points are also covered with fixed costs except in 1, 2 and 3km coverage areas. There are two different results which are shown in bold. While, 20th potential warehouse is opened instead of 15th potential warehouse in Scenario 2 with 4km coverage area; 3rd, 4th, 5th and 16th current and potential warehouses are chosen instead of 17th and 18th potential warehouses in Scenario 3 with 5km coverage area. As expected, considering the fixed costs of potential warehouses causes to select current warehouses instead of potential warehouses in one solution.

4.2.2. Solution of P-median problem

After showing the benefits of potential warehouses, we implement P-median and P-center models to assign current and potential warehouses to demand points (hospitals and pharmacies) so that the total transportation distance is minimized. P-median model is implemented assuming the demands are equal (w_i=1). Due to information privacy, demand data of hospitals and pharmacies cannot be obtained. We apply the P-median model for the demand points by setting 1 to 10 values for p. The results of P-median problem obtained by IP and GIS are given in Tables 7 and 8, respectively. As it can be seen from Tables 7 and 8, results are also classified based on three scenarios as set covering problem.

Table 7. Results of P-median problem using IP.

	Scenario1		Scenario2		Scenario3	
P	**Total Distance (m)**	**Opened Warehouses**	**Total Distance (m)**	**Opened Warehouses**	**Total Distance (m)**	**Opened Warehouses**
1	703648.3	10	676557.4	15	676557.4	15
2	549791.0	4-8	561416.9	15-16	549791.0	4-8
3	473911.7	5-9-10	446711.5	11-15-16	430234.3	6-8-16
4	448085.6	1-4-5-9	389665.1	12-15-16-17	374944.0	8-10-16-17
5	431530.3	1-3-4-8-9	347900.4	12-16-17-19-20	330811.2	8-9-10-16-17
6	418835.5	1-3-4-7-8-9	322475.6	12-16-17-18-19-20	311459.3	5-10-16-17-18-19
7	409915.8	1-3-4-6-7-8-9	305611.0	12-15-16-17-18-19-20	294954.5	7-10-11-16-17-18-19
8	401939.2	1-2-3-4-6-7-8-9	288979.1	11-12-15-16-17-18-19-20	278586.5	7-10-11-13-16-17-18-19
9	399889.8	1-2-3-4-6-7-8-9-10	272611.1	11-12-13-15-16-17-18-19-20	265841.8	4-6-7-11-13-16-17-18-19
10	398401.8	1-2-3-4-5-6-7-8-9-10	261275.8	11-12-13-14-15-16-17-18-19-20	257254.8	1-4-6-7-11-13-16-17-18-19

Table 8. Results of P-median problem using GIS.

	Scenario1		Scenario2		Scenario3	
P	**Total Distance (m)**	**Opened Warehouses**	**Total Distance (m)**	**Opened Warehouses**	**Total Distance (m)**	**Opened Warehouses**
1	703648.3	10	676557.4	15	676557.4	15
2	549791.0	4-8	561416.9	15-16	549791.0	4-8
3	473911.7	5-9-10	446711.5	11-15-16	430234.3	6-8-16
4	448085.6	1-4-5-9	389665.1	12-15-16-17	374944.0	8-10-16-17
5	431530.3	1-3-4-8-9	**352926.1**	12-15-16-17-18	330811.2	8-9-10-16-17
6	418835.5	1-3-4-7-8-9	322475.6	12-16-17-18-19-20	**314443.3**	8-9-10-13-16-17
7	409915.8	1-3-4-6-7-8-9	305611.0	12-15-16-17-18-19-20	**301660.6**	4-6-8-9-13-16-17
8	401939.2	1-2-3-4-6-7-8-9	288979.1	11-12-15-16-17-18-19-20	278586.5	7-10-11-13-16-17-18-19
9	399889.8	1-2-3-4-6-7-8-9-10	272611.1	11-12-13-15-16-17-18-19-20	265841.8	4-6-7-11-13-16-17-18-19
10	398401.8	1-2-3-4-5-6-7-8-9-10	261275.8	11-12-13-14-15-16-17-18-19-20	**257770.8**	4-7-11-13-14-16-17-18-19-20

According to Table 7, all P-median problems are solved optimally. Although, the results obtained by GIS seem similar with the results of IP, all solutions of GIS are not optimal (Table 8). Results which are not optimal are shown with bold in Table 8. Figure 8 indicates the optimal (obtained by IP) and non-optimal (obtained by GIS) solutions for P= 5. As expected, increasing the number of P decreases the total distance between warehouses and demand points in all solutions. Results in Figure 9 show that increasing the number of pharmacy warehouses from 1 to 10, decreases the total travelled distance by 43.38%, 61.38% and 61.98% for Scenarios 1, 2 and 3, respectively.

Another outcome can be seen from Figure 9 that potential warehouses provide shorter distance than the current warehouses in all P values except P= 2. While the gap between current and potential warehouses is 3.85% in P= 1, this gap is increased dramatically by 34.42% in P= 10 (Figure 10). On the other hand, Scenario 3 outperforms other scenarios in P-median problem.

In addition to analysis above, P-median problem is re-solved with generated demand data for three scenarios. While demand for pharmacies is randomly generated between 5 and 10 boxes of medicine, range for hospitals is determined as 20 and 30 boxes of medicine. Demand dataset is available upon request from corresponding author. The results of P-median problem with different demand data obtained by IP are given in Table 9.

According to Table 9, all P-median problems are solved optimally. As expected, increasing the number of P also decreases the total distance when different demand values exist. In fact, the case with different demand values provides less travelled distance than the case with equal demand values. Improvements (%) in travelled distance are shown in Figure 11. Results in Figure 11 show that embedding different demand values into the P-median model improve the solutions averagely by 6.68%, 8.46% and 8.71% for Scenarios 1, 2 and 3, respectively. It must be noted that changing the demand values of each pharmacy and hospital can yield different results.

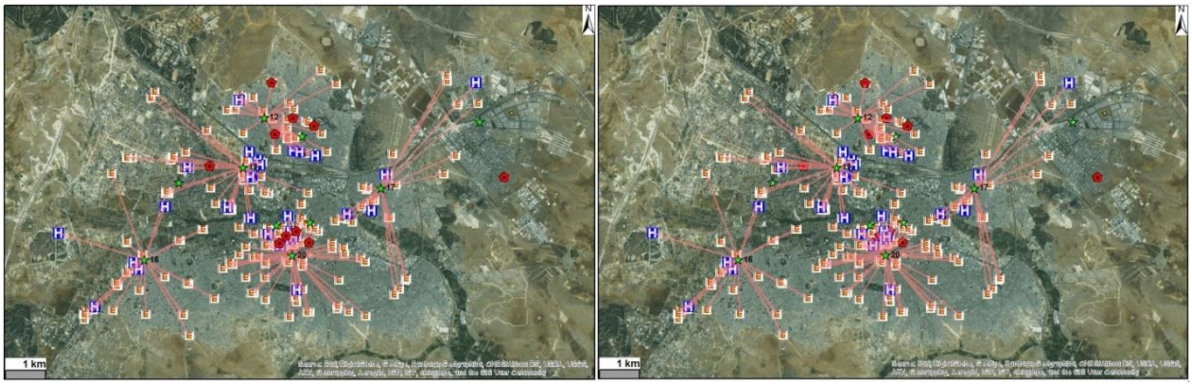

Figure 8. Comparison of mathematical model (left) and GIS (right) for P-median problem (P=5).

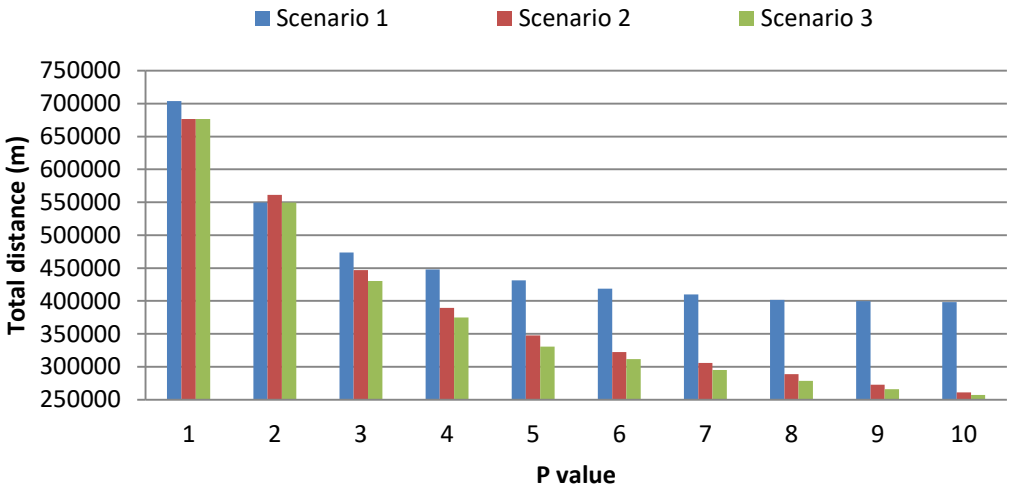

Figure 9. Comparison of total distances obtained by IP for P-median problem.

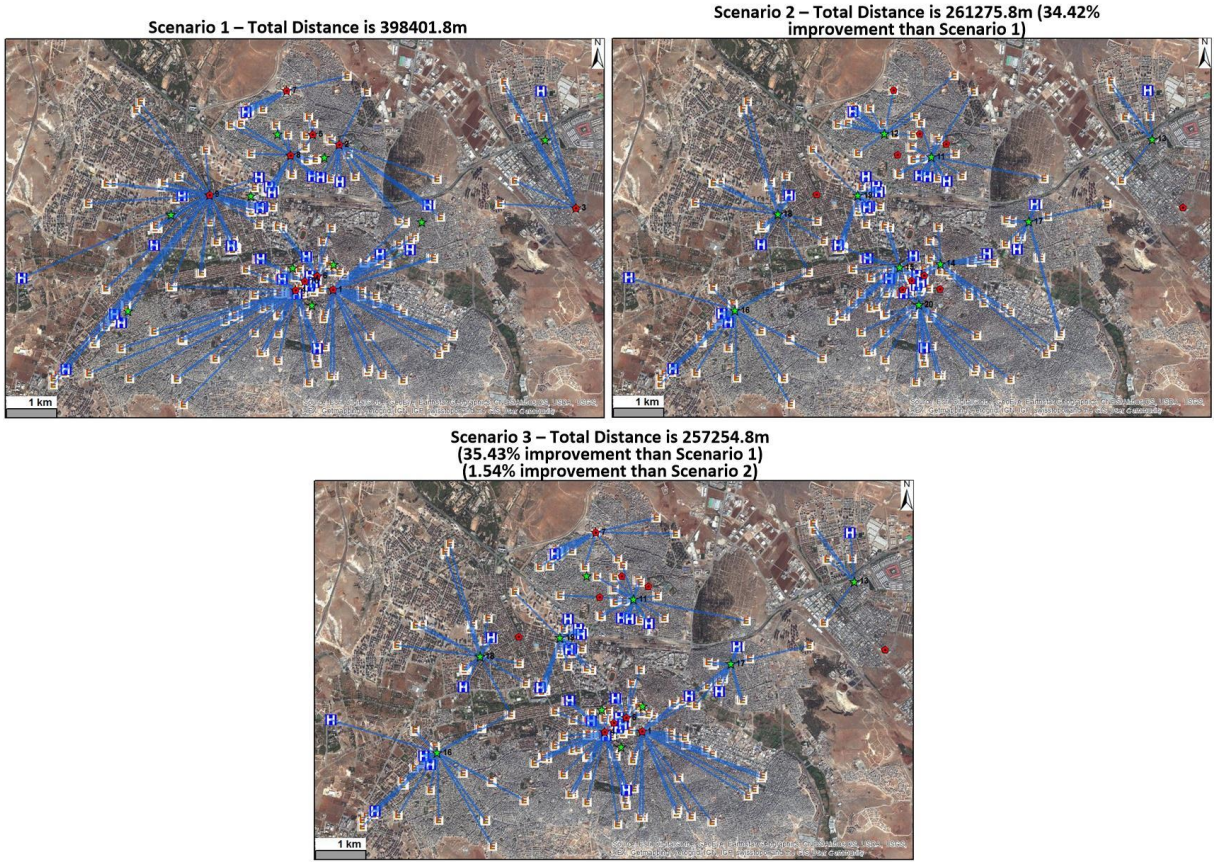

Figure 10. Results of P-median problem obtained by IP (*P*= 10).

Table 9. Results of P-median problem with demand data using IP.

	Scenario1		Scenario2		Scenario3	
P	**Total Distance (m)**	**Opened Warehouses**	**Total Distance (m)**	**Opened Warehouses**	**Total Distance (m)**	**Opened Warehouses**
1	6640359.3	10	6340796.2	15	6340796.2	15
2	5171164.4	4-8	5222308.7	15-16	5171164.4	4-8
3	4384727.3	5-6-9	4139945.6	11-15-16	3986775.3	8-10-16
4	4185826.5	4-5-6-9	3624850.3	12-15-16-17	3464420.1	8-10-16-17
5	4008892.3	3-4-6-8-9	3187588.7	11-16-17-19-20	3013817.0	8-9-10-16-17
6	3905634.2	3-4-6-7-8-9	2938938.2	11-16-17-18-19-20	2813233.8	5-10-16-17-18-19
7	3818425.7	1-3-4-6-7-8-9	2763719.7	11-12-16-17-18-19-20	2648571.2	5-10-13-16-17-18-19
8	3741018.6	1-2-3-4-6-7-8-9	2599057.0	11-12-13-16-17-18-19-20	2485439.7	7-10-11-13-16-17-18-19
9	3724589.6	1-2-3-4-6-7-8-9-10	2438867.3	11-12-13-15-16-17-18-19-20	2379573.6	4-6-7-11-13-16-17-18-19
10	3714122.3	1-2-3-4-5-6-7-8-9-10	2360164.0	11-12-13-14-15-16-17-18-19-20	2316881.7	4-6-7-11-13-16-17-18-19-20

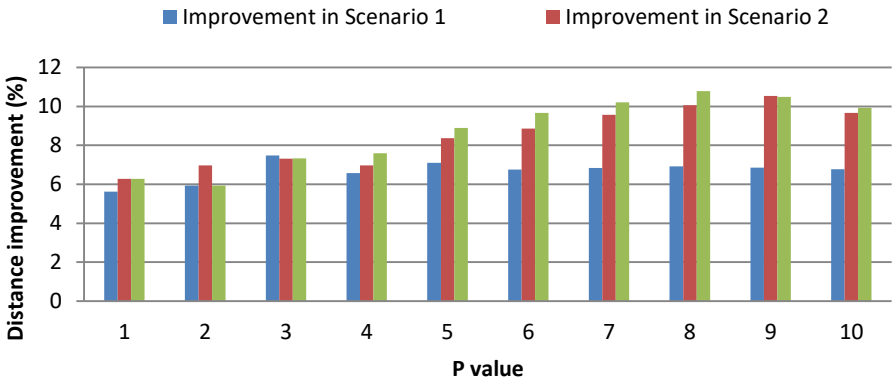

Figure 11. Distance improvements when different demand values are considered.

4.2.3. Solution of P-median problem

In addition to considered set covering and P-median problems, P-center problem is also investigated to minimize the longest distance between pharmacy warehouses and demand points. Table 10 presents the results of P-center problem obtained by IP. It is noted that P-center problem cannot be solved via GIS because of non-availability of the required tool in the software.

According to Table 10; increasing the number of warehouses to be opened, decreases the longest distance between serving warehouses and underserved pharmacy/hospitals. In the current situation (Scenario1), the longest distance between source and demand points is fixed by 5477.8m after opening three warehouses. On the other hand, the longest distance between assigned pharmacy warehouse and demand point is obtained as 3666.7m in Scenarios 2 and 3. Figure 12 illustrates the improvements in terms of longest distance for Scenarios 1 to 3. As it can be seen from Figure 12, the minimum longest distance (5477.8m) is obtained with 3 warehouses (1-3-9) in Scenario 1. On the other hand, Scenarios 2 and 3 provide the minimum longest distance (3666.7m) with 5 warehouses. Although Scenario 1 appears like successful due to succeeding the minimum longest distance with fewer warehouses, it is clear that P-center model with 5 warehouses (Scenarios 2 and 3) leads to shorter longest distance by 33.96% than the current warehouses situation (Scenario 1).

The results show that with the suggested new warehouse locations, the current coverage level of pharmacies and hospitals has increased, the total transport distance has reduced substantially and the distance to the demand node, which has the longest distance to the warehouse, has also decreased.

5. Conclusion

In this paper, current and possible new locations of pharmacy warehouses in Gaziantep are investigated to provide optimal distribution to hospitals and pharmacies. To do so, firstly geographic information of 10 current and 10 potential pharmacy warehouses, 231 pharmacies and 29 hospitals are gathered using GIS. Secondly, set covering, P-center and P-median models are applied to set up potential warehouses and assign pharmacies and hospitals to the opened warehouses so that the total transportation distance is minimized. Computational experiments on the case study prove that proposed approach can find new potential pharmacy warehouses which cover wider area than current warehouses to support pharmacies and hospitals in the city.

Table 10. Results of P-center problem using IP.

	Scenario1		Scenario2		Scenario3	
P	**Distance (m)**	**Opened warehouses**	**Distance (m)**	**Opened warehouses**	**Distance (m)**	**Opened warehouses**
1	7321.0	6	7380.1	14	7321.0	6
2	5909.1	2-9	4747.1	17-18	4747.1	17-18
3	5477.8	1-3-9	4674.0	13-17-18	4674.0	3-17-18
4	5477.8	1-3-9-10	3720.9	12-13-14-16	3720.9	1-12-13-16
5	5477.8	1-2-3-5-9	3666.7	12-13-14-16-19	3666.7	8-13-16-19-20
6	5477.8	1-2-3-4-9-10	3666.7	11-12-13-14-16-19	3666.7	9-12-13-14-15-16
7	5477.8	1-2-3-4-6-8-9	3666.7	11-12-13-14-16-18-20	3666.7	1-2-3-4-9-13-16
8	5477.8	1-2-3-4-5-7-8-9	3666.7	11-12-13-14-15-16-18-20	3666.7	1-2-3-4-5-13-16-18
9	5477.8	1-2-3-4-6-7-8-9-10	3666.7	11-12-13-14-15-16-17-18-20	3666.7	1-2-4-6-9-13-16-17-18
10	5477.8	1-2-3-4-5-6-7-8-9-10	3666.7	11-12-13-14-15-16-17-18-19-20	3666.7	1-2-4-7-8-9-11-13-16-20

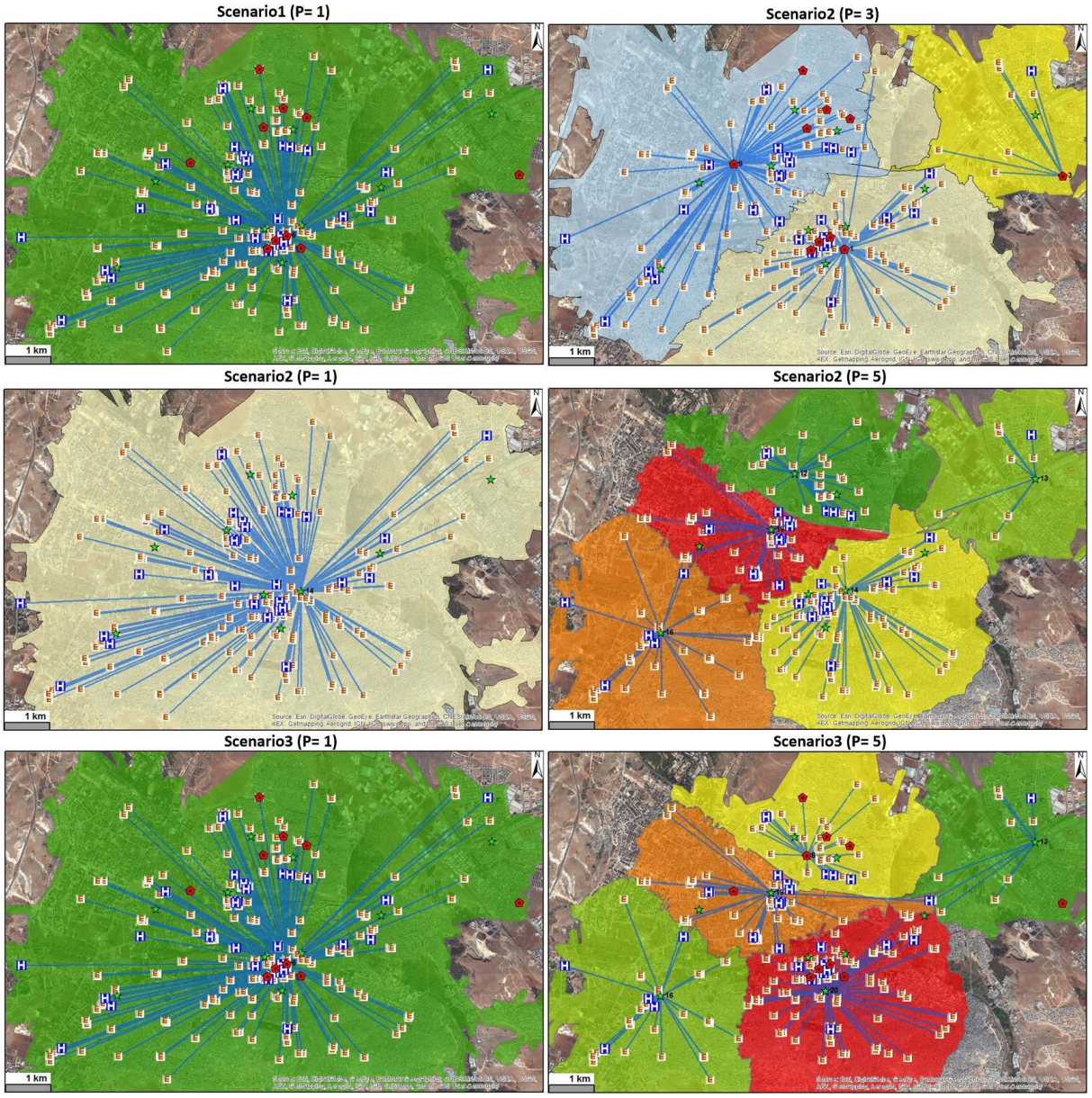

Figure 12. Results of P-center problem using IP.

Consideration of the study area as city center, testing the proposed approaches with only the hospitals and pharmacies, generalization of the proposed method and determination the locations of potential warehouses are the limitations and shortcomings of the paper. To overcome mentioned shortcomings and direct potential researchers, several extensions to our method are worth further investigation. First, a web-based GIS application can be developed. Second, community health centers can be considered as another demand points besides hospitals and pharmacies. Third, investigated area can be expanded. In this case, heuristics can be required to obtain a near optimal solution, and finally multi-criteria decision making tools can be applied to determine alternative locations.

Acknowledgments

The authors express sincere appreciation to the editor and two anonymous reviewers for their efforts to improve the quality of this paper. The authors also thank Pharmacy Chambers of Gaziantep for their help and collaboration to collect related data. First author was supported by the BAGEP Award of the Science Academy in Turkey.

References

[1] Tekiner, H., Pharmacy in Turkey : past, present, and future. Pharmazie, 69 (6):477-480 (2014).

[2] Tootelian, D.T., Wertheimer A.I., and Mikhailitchenko, A., Essentials of pharmacy management. Pharmaceutical Press (2012).

[3] Turkish Pharmacists Association, (2016) Available from:http://dergi.tebeczane.net/public_html/ARSIV-TEBHABERLER/index.html. Accessed 11 Jan 2017.

[4] Population statistics in 2015, (2016). Available

from:http://www.turkstat.gov.tr/PreHaberBultenleri .do?id=6178. Accessed 11 Jan 2017.

[5] Dokmeci, V., and Ozus, E., Spatial analysis of urban pharmacies in Istanbul. European Planning Studies, 12:585-594 (2004).

[6] Daskin, M.S., Network and discrete Locations: Models, algorithms and applications. Wiley and Sons, New York (1995).

[7] Owen, S.H., and Daskin, M.S., Strategic facility location: A review. European Journal of Operational Research, 111 (3):423-447 (1998).

[8] Narula, S.C., Minisum hierarchical location-allocation problems on a network: A survey. Annals of Operations Research, 6 (8):255-272 (1986).

[9] Arabani, A.B., and Farahani, R.Z., Facility location dynamics: An overview of classifications and applications. Computers & Industrial Engineering, 62 (1):408-420 (2012).

[10] ReVelle, C.S., and Eiselt, H.A., Location analysis: A synthesis and survey. European Journal of Operational Research, 165 (1):1-19 (2005).

[11] Rahman, S., and Smith, D.K., Use of location-allocation models in health service development planning in developing nations. European Journal of Operational Research, 123 (3):437-452 (2000).

[12] Daskin, S., and Dean, L., Location of health care facilities. Handbook of OR/MS in Health Care: A Handbook of Methods and Applications, 43–76 (2004).

[13] Rais, A., and Viana, A., Operations Research in Healthcare: a survey. International Transactions in Operational Research, 18 (1):1-31 (2011).

[14] Afshari,H., and Peng,Q., Challenges and Solutions for Location of Healthcare Facilities. Industrial Engineering & Management, 03 (02) (2014).

[15] Şahin, G., Süral, H., and Meral, S., Locational analysis for regionalization of Turkish Red Crescent blood services. Computers & Operations Research, 34 (3):692-704 (2007).

[16] Mestre, A., Oliveira, M.,D., and Barbosa-Póvoa, A., Organizing hospitals into networks: a hierarchical and multiservice model to define location, supply and referrals in planned hospital systems. OR spectrum, 34 (2):319-348 (2012).

[17] Farahani, R.Z., Hekmatfar, M., Fahimnia, B., and Kazemzadeh, N., Hierarchical facility location problem: Models, classifications, techniques, and applications. Computers & Industrial Engineering, 68:104-117 (2014).

[18] Teixeira, J.C., and Antunes, A.P., A hierarchical location model for public facility planning. European Journal of Operational Research, 185 (1):92-104 (2008).

[19] Berghmans, L., Schoovaerts, P., and Teghem, J., Implementation of Health Facilities in a New City. The Journal of the Operational Research Society, 35 (12):1047-1054 (1984).

[20] Tavakoli, A., and Lightner, C., Implementing a mathematical model for locating EMS vehicles in fayetteville, NC. Computers & Operations Research, 31 (9):1549-1563 (2004).

[21] Jia, H., Ordóñez, F., and Dessouky, M., Solution approaches for facility location of medical supplies for large-scale emergencies. Computers & Industrial Engineering, 52 (2):257-276 (2007).

[22] Jia, H., Ordóñez, F., and Dessouky, M., A modeling framework for facility location of medical services for large-scale emergencies. IIE transactions, 39 (1):41-55 (2007).

[23] Shariff, R.S.S., Moin, N.H., Omar, M., Location allocation modeling for healthcare facility planning in Malaysia. Computers & Industrial Engineering, 62 (4):1000-1010 (2012).

[24] Valipour, M.T., Nedjati, A., and Kazemi, R., Solving Health Care Facility Location Problems with New Heuristic Algorithm Method. International Journal of Modeling and Optimization,12-14 (2013).

[25] Jia, T., Tao, H., Qin, K., Wang, Y., Liu, C., and Gao, Q., Selecting the optimal healthcare centers with a modified P-median model: a visual analytic perspective. International journal of health geographics, 13 (1):1 (2014).

[26] Kunkel, A.G., Van Itallie, E.S., and Wu, D., Optimal distribution of medical backpacks and health surveillance assistants in Malawi. Health care management science (2013).

[27] Guerriero, F., Miglionico, G., and Olivito, F., Location and reorganization problems: The Calabrian health care system case. European Journal of Operational Research, 250 (3):939-954 (2016).

[28] Harper, P., Planning health services with explicit geographical considerations: a stochastic location-allocation approach. Omega, 33 (2):141-152 (2005).

[29] Abdelaziz, F.B., and Masmoudi, M., A multiobjective stochastic program for hospital bed planning. Journal of the Operational Research Society, 63 (4):530-538 (2012).

[30] Mestre, A.M., Oliveira, M.D., and Barbosa-Póvoa, A.P., Location–allocation approaches for hospital network planning under uncertainty. European Journal of Operational Research, 240 (3):791-806 (2015).

[31] Lovejoy, W.S., and Li, Y., Hospital operating room capacity expansion. Management Science, 48 (11):1369-1387 (2002).

[32] Stummer, C., Doerner, K., Focke, A., and Heidenberger, K., Determining location and size of

medical departments in a hospital network: A multiobjective decision support approach. Health care management science, 7 (1):63-71 (2004).

[33] Bansal, V.K., Application of geographic information systems in construction safety planning. International Journal of Project Management, 29 (1):66-77 (2011).

[34] Keyser, J.J., Book review. The Journal of Hand Surgery, 39 (8):1649-1650 (2014).

[35] Minutha, A., and Sannasiddanannavar, S.S., Planning for public health care services in Nanjangud Taluk a spatial analysis using GIS, Indian Streams Research Journal 4 (2):1-5 (2014).

[36] McLafferty, S.L., GIS and health care. Annual review of public health, 24 (1):25-42 (2003).

[37] Lovett, A., Haynes, R., Sünnenberg, G., and Gale, S., Car travel time and accessibility by bus to general practitioner services: a study using patient registers and GIS. Social Science & Medicine, 55 (1):97-111 (2002).

[38] Grekousis, G., and Photis, Y.N., Analyzing high-risk emergency areas with GIS and neural networks: The case of Athens, Greece. The Professional Geographer, 66 (1):124-137 (2014).

[39] Sanders, L.J., Aguilar, G.D., and Bacon, C.J., A spatial analysis of the geographic distribution of musculoskeletal and general practice healthcare clinics in Auckland, New Zealand. Applied Geography, 44:69-78 (2013).

[40] Huang, B., Dignan, M., Han, D., and Johnson, O., Does distance matter? Distance to mammography facilities and stage at diagnosis of breast cancer in Kentucky. The Journal of Rural Health, 25 (4):366-371 (2009).

[41] Pearce, J., Witten, K., Hiscock, R., and Blakely, T., Are socially disadvantaged neighbourhoods deprived of health-related community resources? International journal of epidemiology, 36 (2):348-355 (2007).

[42] Klein, M.B., Kramer, C.B., Nelson, J., Rivara, F.P., Gibran, N.S., and Concannon, T., Geographic access to burn center hospitals. JAMA, 302 (16):1774-1781 (2009).

[43] Farahani, R.Z., Asgari, N., Heidari, N., Hosseininia, M., and Goh, M., Covering problems in facility location: A review. Computers & Industrial Engineering, 62 (1):368-407 (2012).

[44] Caprara, A., Toth, P., and Fischetti, M., Algorithms for the set covering problem. Annals of Operations Research, 98 (1-4):353-371(2000).

[45] Li, X., Zhao, Z., Zhu, X., and Wyatt, T., Covering models and optimization techniques for emergency response facility location and planning: a review. Mathematical Methods of Operations Research, 74 (3):281-310 (2011).

[46] Beasley, J.E., An algorithm for set covering problem. European Journal of Operational Research, 31 (1):85-93 (1987).

[47] Hakimi, S.L.,Optimum locations of switching centers and the absolute centers and medians of a graph. Operations research, 12 (3):450-459 (1964).

[48] Kariv, O., and Hakimi, S.L., An algorithmic approach to network location problems. II: The p-medians. SIAM Journal on Applied Mathematics, 37 (3):539-560 (1979).

Eren Özceylan *is an assistant professor in Industrial Engineering Department, Gaziantep University, Gaziantep, Turkey. He received his PhD from Selçuk University, Computer Engineering in 2013. His research focuses on logistics and supply chain management.*

Ayşenur Uslu *graduated from the Industrial Engineering Department of Selçuk University, Turkey, in 2014. She received her MS in Industrial Engineering from Gazi University in 2016, Ankara, Turkey. She is research assistant at the Department of Industrial Engineering of the Başkent University, Ankara, Turkey.*

Mehmet Erbaş *is working at General Command of Mapping in Ankara. His research and teaching interests focus on the topics of the Geographic Information Systems and Remote Sensing Applications.*

Cihan Çetinkaya *has graduated from the Turkish Military Academy in 2006. He received his MS and PhD in Industrial Engineering Department of Gazi University in 2011 and 2014, respectively. He is an Assistant Professor at the Department of Industrial Engineering at Gaziantep University, Turkey.*

Selçuk Kürşat İşleyen *graduated from the Industrial Engineering Department of Gazi University, Turkey, in 2001. He received his MS and PhD in Industrial Engineering from the same university in 2004 and 2008, respectively. He is Associate Professor at the Department of Industrial Engineering of Gazi University, Turkey.*

INSTRUCTIONS FOR AUTHORS

Aims and Scope

This journal shares the research carried out through different disciplines in regards to optimization, control and their applications.

The basic fields of this journal are linear, nonlinear, stochastic, parametric, discrete and dynamic programming; heuristic algorithms in optimization, control theory, game theory and their applications. Problems such as managerial decisions, time minimization, profit maximizations and other related topics are also shared in this journal.

Besides the research articles expository papers, which are hard to express or model, conference proceedings, book reviews and announcements are also welcome.

Journal Topics

- Applied Mathematics,
- Financial Mathematics,
- Control Theory,
- Game Theory,
- Fractional Calculus,
- Fractional Control,
- Modeling of Bio-systems for Optimization and Control,
- Linear Programming,
- Nonlinear Programming,
- Stochastic Programming,
- Parametric Programming,
- Conic Programming,
- Discrete Programming,
- Dynamic Programming,
- Optimization with Artificial Intelligence,
- Operational Research in Life and Human Sciences,
- Heuristic Algorithms in Optimization,
- Applications Related to Optimization on Engineering.

Submission of Manuscripts

New Submissions

Solicited and contributed manuscripts should be submitted to IJOCTA via the journal's online submission system. You need to make registration prior to submitting a new manuscript (please click here to register and do not forget to define yourself as an "Author" in doing so). You may then click on the "New Submission" link on your User Home.

IMPORTANT: If you already have an account, please click here to login. It is likely that you will have created an account if you have reviewed or authored for the journal in the past.

On the submission page, enter data and answer questions as prompted. Click on the “Next” button on each screen to save your work and advance to the next screen. The names and contact details of at least four internationally recognized experts who can review your manuscript should be entered in the "Comments for the Editor" box.

You will be prompted to upload your files: Click on the “Browse” button and locate the file on your computer. Select the description of the file in the drop down next to the Browse button. When you have selected all files you wish to upload, click the “Upload” button. Review your submission before sending to the Editors. Click the “Submit” button when you are done reviewing. Authors are responsible for verifying all files have uploaded correctly.

You may stop a submission at any phase and save it to submit later. Acknowledgment of receipt of the manuscript by IJOCTA Online Submission System will be sent to the corresponding author, including an assigned manuscript number that should be included in all subsequent correspondence. You can also log-

on to submission web page of IJOCTA any time to check the status of your manuscript. You will receive an e-mail once a decision has been made on your manuscript.

Each manuscript must be accompanied by a statement that it has not been published elsewhere and that it has not been submitted simultaneously for publication elsewhere.

Manuscripts can be prepared using LaTeX (.tex) or MSWord (.docx). However, manuscripts with heavy mathematical content will only be accepted as LaTeX files.

Preferred first submission format (for reviewing purpose only) is Portable Document File (.pdf). Please find below the templates for first submission.

Click for download first submission Word template (.docx)

Click for download first submission LaTeX template (.tex)

Revised Manuscripts

Revised manuscripts should be submitted via IJOCTA online system to ensure that they are linked to the original submission. It is also necessary to attach a separate file in which a point-by-point explanation is given to the specific points/questions raised by the referees and the corresponding changes made in the revised version.

To upload your revised manuscript, please go to your author page and click on the related manuscript title. Navigate to the "Review" link on the top left and scroll down the page. Click on the "Choose File" button under the "Editor Decision" title, choose the revised article (in pdf format) that you want to submit, and click on the "Upload" button to upload the author version. Repeat the same steps to upload the "Responses to Reviewers/Editor" file and make sure that you click the "Upload" button again.

To avoid any delay in making the article available freely online, the authors also need to upload the source files (Word or LaTex) when submitting revised manuscripts. Files can be compressed if necessary. The two-column final submission templates are as follows:

Click for download final submission Word template (.docx)

Click for download final submission LaTeX template (.tex)

Authors are responsible for obtaining permission to reproduce copyrighted material from other sources and are required to sign an agreement for the transfer of copyright to IJOCTA.

Article Processing Charges

There are no charges for submission and/or publication.

English Editing

Papers must be in English. Both British and American spelling is acceptable, provided usage is consistent within the manuscript. Manuscripts that are written in English that is ambiguous or incomprehensible, in the opinion of the Editor, will be returned to the authors with a request to resubmit once the language issues have been improved. This policy does not imply that all papers must be written in "perfect" English, whatever that may mean. Rather, the criteria require that the intended meaning of the authors must be clearly understandable, i.e., not obscured by language problems, by referees who have agreed to review the paper.

Presentation of Papers

Manuscript style

Use a standard font of the **11-point type: Times New Roman** is preferred. It is necessary to single line space your manuscript. Normally manuscripts are expected not to exceed 25 single-spaced pages including text, tables, figures and bibliography. All illustrations, figures, and tables are placed within the text at the appropriate points, rather than at the end.

During the submission process you must enter: (1) the full title, (2) names and affiliations of all authors and (3) the full address, including email, telephone and fax of the author who is to check the proofs. Supply a brief **biography** of each author at the end of the manuscript after references.

- Include the name(s) of any **sponsor(s)** of the research contained in the paper, along with **grant number(s).**
- Enter an **abstract** of no more than 250 words for all articles.

Keywords

Authors should prepare no more than 5 keywords for their manuscript.

Maximum five **AMS Classification number** (http://www.ams.org/mathscinet/msc/msc2010.html) of the study should be specified after keywords.

Writing Abstract

An abstract is a concise summary of the whole paper, not just the conclusions. The abstract should be no more than 250 words and convey the following:

1. An introduction to the work. This should be accessible by scientists in any field and express the necessity of the experiments executed.
2. Some scientific detail regarding the background to the problem.
3. A summary of the main result.
4. The implications of the result.
5. A broader perspective of the results, once again understandable across scientific disciplines.

It is crucial that the abstract conveys the importance of the work and be understandable without reference to the rest of the manuscript to a multidisciplinary audience. Abstracts should not contain any citation to other published works.

Reference Style

Reference citations in the text should be identified by numbers in square brackets "[ ]". All references must be complete and accurate. Please ensure that every reference cited in the text is also present in the reference list (and vice versa). Online citations should include date of access. References should be listed in the following style:

Journal article

Author, A.A. and Author, B., Title of article. *Title of Journal*, Vol (issue), pages (Year).

Evans, W.A., Approaches to intelligent information retrieval. *Information Processing and Management*, 7 (2), 147–168 (1994).

Book

Author, A., *Title of book*. Publisher, Place of Publication (Year).

Mercer, P.A. and Smith, G., *Private Viewdata in the UK*. 2nd ed. Longman, London (1993).

Chapter

Author, A., Title of chapter. *In*: A. Editor and B. Editor, eds. *Title of book*. Publisher, Place

of publication, pages (Year).

Bantz, C.R., Social dimensions of software development. *In*: J.A. Anderson, ed. *Annual*

review of software management and development. CA: Sage, Newbury Park, 502–510 (1995).

Internet document

Author, A., Year. *Title of document* [online]. Source. Available from: URL [Accessed date

Month Year].

Holland, M., 2004. *Guide to citing Internet sources* [online]. Poole, Bournemouth University.

Available from:

http://www.bournemouth.ac.uk/library/using/guide_to_citing_internet_sourc.html [Accessed

4 November 2004].

Newspaper article

Author, A. (or Title of Newspaper), Title of article. *Title of Newspaper*, day Month, page, column (Year).

Independent, Picking up the bills. *Independent*, 4 June, p. 28a (1992).

Thesis

Author, A., *Title of thesis*. Type of thesis (degree). Name of University (Year).

Agutter, A.J., *The linguistic significance of current British slang*. Thesis (PhD). Edinburgh University (1995).

Illustrations

Illustrations submitted (line drawings, halftones, photos, photomicrographs, etc.) should be clean originals or digital files. Digital files are recommended for highest quality reproduction and should follow these guidelines:

- 300 dpi or higher
- Sized to fit on journal page
- TIFF or JPEG format only
- Embedded in text files and submitted as separate files (if required)

Tables and Figures

Tables and figures (illustrations) should be embedded in the text at the appropriate points, rather than at the end. A short descriptive title should appear above each table with a clear legend and any footnotes suitably identified below.

Proofs

Page proofs are sent to the designated author using IJOCTA EProof system. They must be carefully checked and returned within 48 hours of receipt.

Offprints/Reprints

Each corresponding author of an article will receive a PDF file of the article via email. This file is for personal use only and may not be copied and disseminated in any form without prior written permission from IJOCTA.

Submission Preparation Checklist

As part of the submission process, authors are required to check off their submission's compliance with all of the following items, and submissions may be returned to authors that do not adhere to these guidelines.

1. The submission has not been previously published, nor is it before another journal for consideration (or an explanation has been provided in Comments for the Editor).
2. The submission file is in Portable Document Format (.pdf).
3. Where available, URLs for the references have been provided.
4. The text is single line spaced; uses a 11-point font; employs italics, rather than underlining (except with URL addresses); and all illustrations, figures, and tables are placed within the text at the appropriate points, rather than at the end.
5. The text adheres to the stylistic and bibliographic requirements outlined in the Author Guidelines, which is found in "About the Journal".
6. Maximum five AMS Classification number (http://www.ams.org/mathscinet/msc/msc2010.html) of the study have been provided after keywords.
7. After the acceptance of manuscript (before copy editing), Word (.docx) or LaTeX (.tex) version of the paper will be presented.
8. The names and email addresses of at least four (4) possible reviewers have been indicated in "Comments for the Editor" box in Paper Submission Step 1. Please note that at least two of the recommendations should be from different countries. Avoid suggesting reviewers who are at arms-length from you or your co-authors. This includes graduate advisors, people in your current department, or any others with a conflict of interest.

Peer Review Process

All contributions, prepared according to the author guidelines and submitted via IJOCTA online submission system are evaluated according to the criteria of originality and quality of their scientific content. The corresponding author will receive a confirmation e-mail with a reference number assigned to the paper, which he/she is asked to quote in all subsequent correspondence.

All manuscripts are first checked by the Technical Editor using plagiarism detection software (iThenticate) to verify originality and ensure the quality of the written work. If the result is not satisfactory (i.e. exceeding the limit of 30% of overlapping), the submission is rejected and the author is notified.

After the plagiarism check, the manuscripts are evaluated by the Editor-in-Chief and can be rejected without reviewing if considered not of sufficient interest or novelty, too preliminary or out of the scope of the journal. If the manuscript is considered suitable for further evaluation, it is first sent to the Area Editor. Based on his/her opinion the paper is then sent to at least two independent reviewers. Each reviewer is allowed up to four weeks to return his/her feedback but this duration may be extended based on his/her availability. IJOCTA has instituted a blind peer review process where the reviewers' identities are not known to authors. When the reviews are received, the Area Editor gives a decision and lets the author know it together with the reviewer comments and any supplementary files.

Should the reviews be positive, the authors are expected to submit the revised version usually within two months the editor decision is sent (this period can be extended when the authors contact to the editor and let him/her know that they need extra time for resubmission). If a revised paper is not resubmitted within the deadline, it is considered as a new submission after all the changes requested by reviewers have been made. Authors are required to submit a new cover letter, a response to reviewers letter and the revised manuscript (which ideally shows the revisions made in a different color or highlighted). If a change in authorship (addition or removal of author) has occurred during the revision, authors are requested to clarify the reason for change, and all authors (including the removed/added ones) need to submit a written consent for the change. The revised version is evaluated by the Area editor and/or reviewers and the Editor-in-Chief brings a decision about final acceptance based on their suggestions. If necessary, further revision can be asked for to fulfil all the requirements of the reviewers.

When a manuscript is accepted for publication, an acceptance letter is sent to the corresponding author and the authors are asked to submit the source file of the manuscript conforming to the IJOCTA two-column final submission template. After that stage, changes of authors of the manuscript are not possible. The manuscript is sent to the Copyeditor and a linguistic, metrological and technical revision is made, at which stage the authors are asked to make the final corrections in no more than a week. The layout editor prepares the galleys and the authors receive the galley proof for final check before printing. The authors are expected to correct only typographical errors on the proofs and return the proofs within 48 hours. After the final check by the layout editor and the proofreader, the manuscript is assigned a DOI number, made publicly available and listed in the forthcoming journal issue. After printing the issue, the corresponding metadata and files published in this issue are sent to the databases for indexing.

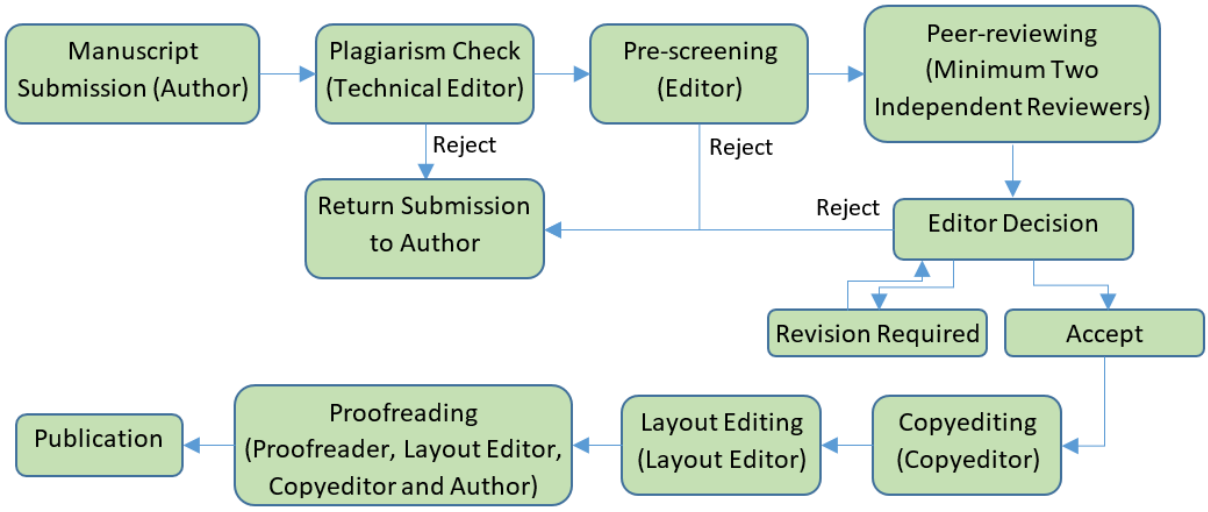

Publication Ethics and Malpractice Statement

IJOCTA is committed to ensuring ethics in publication and quality of articles. Conforming to standards of expected ethical behavior is therefore necessary for all parties (the author, the editor(s), the peer reviewer) involved in the act of publishing.

International Standards for Editors

The editors of the IJOCTA are responsible for deciding which of the articles submitted to the journal should be published considering their intellectual content without regard to race, gender, sexual orientation, religious belief, ethnic origin, citizenship, or political philosophy of the authors. The editors may be guided by the policies of the journal's editorial board and constrained by such legal requirements as shall then be in force regarding libel, copyright infringement and plagiarism. The editors may confer with other editors or reviewers in making this decision. As guardians and stewards of the research record, editors should encourage authors to strive for, and adhere themselves to, the highest standards of publication ethics. Furthermore, editors are in a unique position to indirectly foster responsible conduct of research through their policies and processes.

To achieve the maximum effect within the research community, ideally all editors should adhere to universal standards and good practices.

- Editors are accountable and should take responsibility for everything they publish.
- Editors should make fair and unbiased decisions independent from commercial consideration and ensure a fair and appropriate peer review process.
- Editors should adopt editorial policies that encourage maximum transparency and complete, honest reporting.
- Editors should guard the integrity of the published record by issuing corrections and retractions when needed and pursuing suspected or alleged research and publication misconduct.
- Editors should pursue reviewer and editorial misconduct.
- Editors should critically assess the ethical conduct of studies in humans and animals.
- Peer reviewers and authors should be told what is expected of them.
- Editors should have appropriate policies in place for handling editorial conflicts of interest.

Reference:

Kleinert S & Wager E (2011). Responsible research publication: international standards for editors. A position statement developed at the 2nd World Conference on Research Integrity, Singapore, July 22-24, 2010. Chapter 51 in: Mayer T & Steneck N (eds) Promoting Research Integrity in a Global Environment. Imperial College Press / World Scientific Publishing, Singapore (pp 317-28). (ISBN 978-981-4340-97-7) [Link].

International Standards for Authors

Publication is the final stage of research and therefore a responsibility for all researchers. Scholarly publications are expected to provide a detailed and permanent record of research. Because publications form the basis for both new research and the application of findings, they can affect not only the research community but also, indirectly, society at large. Researchers therefore have a responsibility to ensure that their publications are honest, clear, accurate, complete and balanced, and should avoid misleading, selective or ambiguous reporting. Journal editors also have responsibilities for ensuring the integrity of the research literature and these are set out in companion guidelines.

- The research being reported should have been conducted in an ethical and responsible manner and should comply with all relevant legislation.
- Researchers should present their results clearly, honestly, and without fabrication, falsification or inappropriate data manipulation.
- Researchers should strive to describe their methods clearly and unambiguously so that their findings can be confirmed by others.
- Researchers should adhere to publication requirements that submitted work is original, is not plagiarised, and has not been published elsewhere.
- Authors should take collective responsibility for submitted and published work.
- The authorship of research publications should accurately reflect individuals' contributions to the work and its reporting.

- Funding sources and relevant conflicts of interest should be disclosed.
- When an author discovers a significant error or inaccuracy in his/her own published work, it is the author's obligation to promptly notify the journal's Editor-in-Chief and cooperate with them to either retract the paper or to publish an appropriate erratum.

Reference:

Wager E & Kleinert S (2011) Responsible research publication: international standards for authors. A position statement developed at the 2nd World Conference on Research Integrity, Singapore, July 22-24, 2010. Chapter 50 in: Mayer T & Steneck N (eds) Promoting Research Integrity in a Global Environment. Imperial College Press / World Scientific Publishing, Singapore (pp 309-16). (ISBN 978-981-4340-97-7) [Link].

Basic principles to which peer reviewers should adhere

Peer review in all its forms plays an important role in ensuring the integrity of the scholarly record. The process depends to a large extent on trust and requires that everyone involved behaves responsibly and ethically. Peer reviewers play a central and critical part in the peer-review process as the peer review assists the Editors in making editorial decisions and, through the editorial communication with the author, may also assist the author in improving the manuscript.

Peer reviewers should:

- respect the confidentiality of peer review and not reveal any details of a manuscript or its review, during or after the peer-review process, beyond those that are released by the journal;
- not use information obtained during the peer-review process for their own or any other person's or organization's advantage, or to disadvantage or discredit others;
- only agree to review manuscripts for which they have the subject expertise required to carry out a proper assessment and which they can assess within a reasonable time-frame;
- declare all potential conflicting interests, seeking advice from the journal if they are unsure whether something constitutes a relevant conflict;
- not allow their reviews to be influenced by the origins of a manuscript, by the nationality, religion, political beliefs, gender or other characteristics of the authors, or by commercial considerations;
- be objective and constructive in their reviews, refraining from being hostile or inflammatory and from making libellous or derogatory personal comments;
- acknowledge that peer review is largely a reciprocal endeavour and undertake to carry out their fair share of reviewing, in a timely manner;
- provide personal and professional information that is accurate and a true representation of their expertise when creating or updating journal accounts.

Reference:

Homes I (2013). COPE Ethical Guidelines for Peer Reviewers, March 2013, v1 [Link].

Copyright Notice

An International Journal of Optimization and Control: Theories & Applications

Volume: 7 Number: 1
January 2017

IJOCTA
An International Journal of Optimization and Control: Theories & Applications
2010

CONTENTS

crossref

ISSN 2146-0957

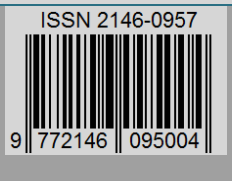

www.ijocta.com
info@ijocta.com